

Predicting the Hydraulic Influence of Hydropower Operations on Upstream Aquatic Habitat

by

Mathew Thomas Langford

A thesis submitted in partial fulfillment of the requirements for the degree of

Doctor of Philosophy

in

Water Resources Engineering

Department of Civil and Environmental Engineering  
University of Alberta

© Mathew Thomas Langford, 2016

## Abstract

---

The development of hydropower facilities greatly affects the morphology of regional water resources, as well as the physical, chemical and biological factors of upstream aquatic ecosystems. Evaluating the environmental impacts of hydropower operations is important in a regulatory context. Of particular interest is investigating fish entrainment risk, which has been identified as one of the key impacts of hydropower generation on the productivity and biodiversity of aquatic species. Entrainment results when fish of the upstream reservoir are passed through the turbines of a dam. The risk of fish entrainment at a particular facility is correlated with the effect of intake withdrawals on the flow and thermal structures of the forebay.

Developing an understanding of the upstream hydraulics at hydropower dams is a key component of studying fish entrainment risk. Deep lakes and reservoirs in northern climates have a dimictic stratification cycle and generally thermal stratification develops in later summer and fall. Some reservoirs can be approximated by a distinct two-layer stratification profile, with a sharp temperature change at the thermocline; however this is not the case for all reservoirs. The shape of the thermal profile is controlled by solar insolation as well as surficial wind mixing, a lack of which may result in a less distinct hyperbolic thermal profile. The vertical density distribution of a stratified reservoir may limit the elevation at which water is withdrawn at hydropower facilities, known as selective withdrawal.

When evaluating the physical impacts of hydropower generation on the upstream forebay (hydraulic and thermal characteristics), it is important to not only look at the direct impacts to fish, but also the impacts to the geometry of the forebay itself. The potential for sediments to deposit on the reservoir bed, or be entrained into the flow is a dynamic process that can lead to significant changes in reservoir bathymetry over time. The coarseness of the bed material also has an impact on fishes habitat use (i.e. fish fry commonly inhabit gravel beds). Determination of the wall shear stress induced by hydropower flows may dictate the bed form's dynamics upstream of a facility, the anticipated substrate size and potential habitat utilization adjacent to the intake. The objectives of this thesis are to use numerical modelling to evaluate the impact of hydropower operations on erosion and sedimentation patterns, thermal structure and flow field upstream of hydropower facilities. This knowledge can then be applied in the context of evaluating fish entrainment risk.

CFD models have been used to simulate the flow field in the forebay of Aberfeldie Dam on the Bull River, Mica Dam on the Columbia River and Revelstoke Dam on the Columbia River in British Columbia, Canada. These sites include both shallow and deep reservoirs as well as run-of-the-river and storage reservoirs. These models were verified through detailed hydroacoustic field measurements at both Aberfeldie and Mica Dams. This thesis outlines methodologies for completing CFD modelling as well as complex acoustic studies upstream of hydropower facilities.

At Aberfeldie Dam, a large scour hole has been created due to increased velocities induced by the intakes. The CFD solver shows that flow-induced bed shear stress causes a seasonally fluctuating, dynamic bed form. The modelled velocity field has been used to evaluate the

entrainment risk of mountain whitefish and westslope cutthroat trout based on swimming mechanics and life stage. CFD modelling proves to be a promising tool for evaluating fish entrainment risk and the effectiveness of potential mitigation measures and management options.

The Mica Dam CFD model evaluated the upstream hydraulics under varying discharges and reservoir levels. The results highlight how intake selection may suppress vortex formation and limit the size of the entrainment risk zone. A potential flow solution was applied to predict the velocity field induced by Mica Dam. Despite the simplicity of the solution the velocities compared well with the more complex CFD model, even with rotational flows. At Mica and Revelstoke Dams, the thermal profile has distinct impacts on the upstream flow field. The inclusion of thermal stratification greatly increases the entrainment risk volume for smaller fish, while having negligible impacts on the risk zone for larger fish. Additionally it was found that CFD modelling is effective at predicting the impact of forebay stratification on discharge temperature.

## Preface

---

Some of the research conducted for this thesis forms part of a national research collaboration by NSERC Hydronet involving the University of Alberta, Carleton University, the University of Waterloo, the Department of Fisheries and Oceans Canada and BC Hydro. Professor D.Z. Zhu was the lead collaborator at the University of Alberta.

The field measurements describe in Chapters 2, 3, and 4 of this thesis were planned by myself and executed by myself with assistance from collaborators. The modelling and data analysis discussed in this thesis are my original work with direction from my supervisor, Professor D. Z. Zhu.

Chapter 2 of this thesis has been published as Langford, M., Zhu, D., and Leake, A. (2015). "Upstream Hydraulics of a Run-of-the River Hydropower Facility for Fish Entrainment Risk Assessment." *J. Hydraul. Eng.* , 10.1061/(ASCE)HY.1943-7900.0001101 , 05015006. I was responsible for the data collection and analysis as well as the manuscript composition. D. Zhu was the supervisory author and was involved in the concept formation and manuscript composition. A. Leake provided recommendation as the apply in a hydropower context to the manuscript.

Chapter 3 of this thesis has been submitted to the IAHR Journal of Hydraulic Research as Langford, M., Zhu, D., Leake, A., and Cooke, S. "Hydropower Intake-induced Fish Entrainment Risk Zone Analysis." Manuscript ID TJHR-2015-0132.R1 and is currently under review. I was

---

responsible for the data collection and analysis as well as the manuscript composition. D. Zhu was the supervisory author and was involved in the concept formation and manuscript composition. A. Leake reviewed the recommendations of the manuscript as they apply in a hydropower operations context. S. Cooke reviewed recommendations regarding the potential biological impact of the intake-induced hydraulics on resident fish.

# Dedication

---

To my mom and dad, my biggest fans.

## Acknowledgements

---

First and foremost I would like to thank my supervisor and friend Dr. David Zhu for making my doctoral program as fun and fruitful as it was. I cannot thank David enough for all the guidance and encouragement he has given me over the years. On a daily basis he inspires me to be the best engineer and the best person I can be.

I would like to thank my parents, Rita and Graeme Langford, and my sister, Lisa Langford for the last 29 years of love, encouragement and support. Also, thanks to my best friend Casey, for your unwavering loyalty and companionship.

I would like to express a very special thanks to my research partners Beth Robertson and Md. Rashedul Islam for all of the laughs and the things you have taught me. Thank you to Perry Fedun and Chris Krath for all your help with completing my field work and ongoing technical support. Over the course of my research I was lucky to have a large number of people from the University of Alberta and BC Hydro who took time out of their busy schedules to assist me in the collection of field data, which I could not appreciate more.

Last, but certainly not least, I would like to thank all the Water Resources Professors and students and the other Hydronet researchers I have had the honour of working with over the years.

This research would not have been possible without the generous support of NSERC Hydronet, BC Hydro, Engineers Canada, Manulife Financial, and the University of Alberta Faculties of Engineering and Graduate Studies and Research.

# Table of Contents

---

Abstract.....	ii
Preface.....	v
Dedication.....	vii
Acknowledgements.....	viii
Table of Contents.....	x
List of Tables.....	xiv
List of Figures.....	xv
List of Symbols and Acronyms.....	xix
Symbols.....	xix
Acronyms.....	xxii
Chapter 1.....	1
Introduction and Objectives.....	1
1.1 Background.....	1
1.2 Literature Review.....	4
1.3 Objectives.....	11

---

---

1.4 References.....	13
Chapter 2.....	20
Upstream Hydraulics of a Run-of-the River Hydropower Facility for Fish Entrainment Risk Assessment.....	20
2.1 Abstract.....	20
2.2 Keywords.....	21
2.3 Introduction.....	21
2.4 Methodology.....	27
2.4.1 Project Site.....	27
2.4.2 Field Measurements.....	30
2.4.3 Computational Fluid Dynamic Model.....	33
2.5 Results.....	42
2.5.1 River Bathymetry and Scour Hole Development.....	42
2.5.2 Upstream Hydraulics and Fish Entrainment Risk.....	49
2.6 Concluding Remarks.....	59
2.7 Acknowledgements.....	62
2.8 References.....	64
Chapter 3.....	70
Hydropower Intake-induced Fish Entrainment Risk Zone Analysis.....	70

---

3.1 Abstract.....	70
3.2 Key Words .....	71
3.3 Introduction.....	71
3.4 Methodology.....	77
3.4.1 Field Measurements.....	79
3.4.2 Computational Fluid Dynamic Modelling.....	83
3.4.3 Model Verification.....	88
3.5 Forebay Flow Field.....	92
3.6 Fish Entrainment Risk in the Biological Context.....	106
3.7 Conclusions.....	109
3.8 Acknowledgements.....	111
3.9 References.....	112
Chapter 4.....	118
Thermal Stratification Impact on Forebay Flow Field and Fish Entrainment Risk.....	118
4.1 Introduction.....	118
4.1.1 Background.....	119
4.1.2 Objectives .....	125
4.2 Field Measurements .....	126
4.2.1 Thermal Profile .....	126

---

4.2.2 Velocity Field.....	129
4.3 Computation Fluid Dynamic Modelling.....	130
4.3.1 Model Development.....	130
4.3.2 Linear.....	134
4.3.3 Hyperbolic.....	134
4.3.4 Discrete.....	134
4.4 Results and Discussion.....	137
4.4.1 Flow Field at Mica Dam.....	137
4.4.2 Flow Field at Revelstoke Dam.....	149
4.4.3 Discharge Temperature.....	167
4.4.4 Fish Entrainment Risk.....	173
4.5 Conclusions.....	176
4.6 Acknowledgements.....	179
4.7 References.....	180
Chapter 5.....	183
Conclusions and Recommendations.....	183
5.1 General Conclusions.....	183
5.2 Recommendations for Further Research.....	187
References.....	189

## List of Tables

---

Table 1: Computational fluid dynamic model scenarios. ....	26
Table 2: Proportion of upstream transects exceeding threshold velocities.....	57
Table 3: Mica Dam model scenarios. ....	76
Table 4: Mica Dam fish entrainment risk volumes.....	103
Table 5: Mica Dam thermal stratification scenarios. ....	131
Table 6: Revelstoke Dam thermal stratification scenarios. ....	133
Table 7: Mica Dam discharge temperatures (°C). ....	167
Table 8: Revelstoke Dam discharge temperatures (°C).....	169
Table 9: Revelstoke Dam entrainment risk volumes (m <sup>3</sup> ).....	175

---

## List of Figures

---

Figure 1: (a) Site location of Aberfeldie Dam (adapted from Map Data: Google, 2015); (b) Intake layout profile looking downstream; (c) Site plan and field measurement locations (with ADCP transects) (aerial photo adapted from Map Data: Google, DigitalGlobe, 2015).....	29
Figure 2: Convergence history of the governing equations. ....	36
Figure 3: Transect 1 velocity magnitude (a) field measured; (b) CFD model.....	39
Figure 4: Field measurements of the velocity magnitude compared with the CFD predictions (a) T1.1; (b) T1.2; (c) T1.3; (d) T2.1; (e) T2.2; (f) T2.3; (g) T5.1; (h) T5.2; (i) T7.1; (j) T7.2;.....	41
Figure 5: Bed shear stress (a) field scenario headpond; (b) spring freshet scenario headpond; (c) field scenario scour hole; (d) spring freshet scenario scour hole.....	43
Figure 6: Critical shear stress for sediment mobilization. ....	45
Figure 7: Field measured bathymetry (all elevation contours are in metres). ....	47
Figure 8: Headpond profile.....	48
Figure 9: Plan contours of velocity magnitude (a) field scenario elevation 876.504 (0.5m depth); (b) spring freshet scenario elevation 876.504; (c) field scenario elevation 872.004 (5m depth); (d) spring freshet scenario elevation 872.004.....	51
Figure 10: Perpendicular profile contours of velocity magnitude (a) field scenario; (b) spring freshet scenario. ....	53
Figure 11: Headpond streamlines (a) field scenario; (b) spring freshet scenario. ....	56
Figure 12: (a) Field measurement locations; (b) CFD model extents (2.5 km upstream of dam). 78	

---

Figure 13: Field measurement setup (a) Inline mooring cage; (b) Three point anchoring system. .....	81
Figure 14: Convergence history of the governing equations. ....	86
Figure 15: Model verification - velocity magnitude at specific distance upstream of dam (a) August 8 – Transect 1, 17.4 m, (b) August 9 – Transect 1, 61.5 m, (c) August 8 – Transect 2, 24.6 m, (d) August 9 – Transect 2, 57.1 m, (e) August 8 – Transect 3, 17.4 m, (f) August 9 – Transect 3, 46.9 m, (g) August 8 – Transect 4, 62.6 m (h) August 9 – Transect 4, 18.1 m intake 3 velocity magnitude (a) August 8, 2011; (b) August 9, 2011; (c) CFD model. ....	90
Figure 16: Velocity at centre of intake elevation (692.46) (a) Scenario A; (b) Scenario B; (c) Scenario C; (d) Scenario D. ....	93
Figure 17: Velocity profile at Intake 1 (a) Scenario A; (b) Scenario B; (c) Scenario C; (d) Scenario D.....	95
Figure 18: Velocity profile at Intake 3 (a) Scenario A; (b) Scenario B; (c) Scenario C; (d) Scenario D.....	96
Figure 19: Velocity magnitude at varying distances in front of the intakes (a) Intake elevation (692.46); (b) 15 m above intake elevation (707.46); (c) 30 m above intake elevation (707.46)..	97
Figure 20: Potential flow solution versus CFD model velocity profiles (a) Scenario A; (b) Scenario B.....	99
Figure 21: Velocity magnitude profile 0, 5, 10, 25 and 50 m upstream of intake (a) Intake 1; (b) Intake 3.....	102
Figure 22: Velocity curl profile at Intake 1 (a) Scenario A; (b) Scenario B; (c) Scenario C; (d) Scenario D.....	104

---

Figure 23: Hydraulic parameters at the intake centre elevation (692.46) Scenario A (a) Velocity Curl; (b) Turbulent Kinetic Energy.....	106
Figure 24: Location plan.....	123
Figure 25: Thermistor chain location.....	127
Figure 26: Kinbasket Reservoir thermal stratification (a) May; (b) July; (c) August, (d) October (modified from Roberston, 2012). .....	128
Figure 27: Thermal stratification profiles (a) Mica Dam; (b) Revelstoke Dam. ....	136
Figure 28: Intake 3 velocities magnitudes (high head scenarios (a) MCA-1; (b) MCA-2. ....	138
Figure 29: Intake 3 velocity magnitudes (low head scenarios) (a) MCA-3; (b) MCA-4; (c) MCA-5; (d) MCA-6. ....	140
Figure 30: Velocity profiles upstream of Intake 3 for varied water surface elevations (a) MCA-1 and MCA-2 (high head); (b) MCA-3 and MCA-4 (low head). ....	142
Figure 31: Velocity profiles upstream of Intake 3 for varied thermal stratification profiles (a) 0 m upstream; (b) 5 m upstream; (c) 10 m upstream, (d) 25 m upstream; (e) 50 m upstream. ....	144
Figure 32: Thermal stratification profiles upstream of Intake 3 (a) MCA-3; (b) MCA-5; (c) MCA-6.....	146
Figure 33: Thermal profiles upstream of Intake 3 for varied thermal stratifications MCA-3, MCA-5 and MCA-6.....	147
Figure 34: Thermal profile upstream of Intake 3 for MCA-3.....	149
Figure 35: Velocity magnitude upstream of Revelstoke Dam at intake elevation (a) REV-1; (b) REV-3; (c) REV-4. ....	151
Figure 36: Intake 3 velocity magnitudes (a) REV-1; (b) REV-2; (C) REV-3; (d) REV-4.....	153

---

Figure 37: Velocity profiles for 0 – 50 m upstream of Intake 3 for varied thermal stratification profiles (a) REV-1; (b) REV-3; (c) REV-4.....	156
Figure 38: Velocity profiles for 10 – 50 m upstream of Intake 3 for varied thermal stratification profiles (a) REV-1; (b) REV-3; (c) REV-4.....	157
Figure 39: Velocity profiles upstream of Intake 3 for linear thermal stratification profiles (a) 0 – 50 m upstream; (b) 10 – 50 m upstream. ....	160
Figure 40: Velocity profiles upstream of Intake 3 for discrete thermal stratification profiles (a) 0 – 50 m upstream; (b) 10 – 50 m upstream. ....	162
Figure 41: Impact of thermal stratification profile on velocity profile upstream of Intake 3 (a) REV-5 and REV-8; (b) REV-6 and REV-9; (c) REV-7 and REV-10.....	164
Figure 42: Thermal stratification profiles at varied distance upstream of Intake 3 (a) REV-1; (b) REV-3; (c) REV-4; (d) REV-5; (e) REV-6; (f) REV-7; (g) REV-8; (h) REV-9; (i) REV-10. ..	166
Figure 43: Temperature upstream of dam face (a) Linear stratification scenarios; (b) Discrete stratification scenarios. ....	171
Figure 44: Temperature upstream of dam face (a) REV-5; (b) REV-6; (C) REV-7; (d) REV-8; (e) REV-9; (f) REV-10.....	172

## List of Symbols and Acronyms

---

### Symbols

$^{\circ}$	degrees
$^{\circ}\text{C}$	degree Celsius (a unit of temperature)
$A$	cross-sectional area
$\alpha_1$	coefficient related to the hyperbolic form of the function
$\alpha_2$	depth spanned by the thermocline,
$\alpha_3$	coefficient related to the slope of the thermocline
$\alpha_4$	temperature at the middle of the thermocline
$D_*$	non dimensional particle diameter
$d_{75}$	particle diameter at which 75 % of particle are smaller than
$d_{50}$	median particle diameter
$d_m$	scour hole depth
$\varepsilon$	eddy dissipation rate
$g_i$	force of gravity in the $i$ direction

$k$	turbulent kinetic energy
$\kappa$	von-Karman constant
K	Kelvin
kHz	kilohertz
$p$	pressure
$\rho$	density
$\rho_{ref}$	a reference density
$\rho_s$	substrate density
$Q$	flow-rate
$Q_2/Q_0$	ratio of discharge from the hypolimnion to the total discharge
$R^2$	coefficient of determination
$\delta_{ij}$	Kronecker delta
$\delta$	a distance from a boundary
$t$	time
$\tau$	bed shear stress
$\tau_{cr}$	critical shear stress

$T_e$	temperature at the epilimnion
$T_h$	temperature of the hypolimnion
$\theta$	Shields parameter
$\theta_{cr}$	critical Shields parameter
$u$	velocity in the x-direction
$U$	velocity at a distance $\delta$ from the boundary
$u_i$	velocity in the $i$ direction
$u^*$	shear velocity
$\mu$	molecular viscosity
$\mu_t$	eddy viscosity
$v$	velocity in the y-direction
$w$	velocity in the z-direction
$x_i$	distance in the $i$ direction
$Z_e$	depth to the bottom of the epilimnion
$Z_h$	depth to the top of the hypolimnion
$Z_t$	depth of the thermocline

## **Acronyms**

ABN	Aberfeldie Dam
ADCP	Acoustic Doppler Current Profiler
BC	British Columbia
CFD	Computational Fluid Dynamic
IFR	Instream Flow Requirement
MCA	Mica Dam
NSERC	Natural Sciences and Engineering Research Council
REV	Revelstoke Dam
ROR	Run of River
RMS	Root Mean Square

# Chapter 1

## Introduction and Objectives

---

### 1.1 Background

The country of Canada has over 470 hydroelectric facilities, which generate approximately 60% of the total power used by Canadians. As such, this renewable energy source is incredibly important to all Canadians. That being said, the development of hydropower facilities greatly affects the morphology of regional water resources, as well as the physical, chemical and biological factors of both upstream and downstream aquatic and riparian ecosystems.

Fish entrainment has been identified as one of the key potential impacts of hydropower operations on the productivity and biodiversity of these aquatic species. Fish entrainment deals with a scenario in which resident fish of the upstream reservoir are passed through the turbines of a dam. It is anticipated that the risk of fish entrainment at a particular dam facility is correlated with the effect of hydropower operations on the flow and thermal structures of the forebay. The assessment of fish entrainment risk at hydropower facilities is an important issue for the hydropower industry, as environmental regulations and approval requirements are becoming more stringent. The risk extends beyond the volume of fish killed by these facilities, to sustaining the viability of regional commercial, sport and first nation's fisheries, a prominent industry and food source for many people.

---

Near the intakes at a hydropower facility, the velocity of flow increases significantly, forming an acceleration, or entrainment zone. Depending on the size, swimming strength and other biological and behavioral characteristics of fish located within this zone, there may be a substantial potential for fish entrainment. The characteristics of this entrainment zone are affected by the geometry of the intakes and upstream reservoir; specifically the location of the intakes in the water column the proximity of other boundaries (such as the bed or water surface).

When evaluating the physical impacts of hydropower generation on the upstream forebay (hydraulic and thermal characteristics), it is important to not only look at the direct impacts to fish, but also the impacts to the geometry of the forebay itself. This is particularly important for hydropower facilities with sediment laden inflows and shallower reservoirs. The potential for sediments to fall out of suspension to the reservoir bed, or be entrained into the flow is a dynamic process that can lead to significant changes in reservoir bathymetry over time. The coarseness of the bed material also has an impact on fishes habitat use (i.e. fish fry commonly inhabit gravel beds). As such, determination of the wall shear stress induced by hydropower flows can not only dictate the bed form's dynamics upstream of a facility, but also the anticipated grain size and habitat utilization in close proximity to the intake. In order to understand the phenomena of fish entrainment, it is important to first address the impacts of hydropower operations on the upstream flow field, thermal regime, and bed dynamics.

Larger hydropower facilities may have deeper reservoirs that have distinctly different temperature structures over the course of the year, especially in northern climates, such as Canada. In late summer the water near the surface is substantially warmer than the underlying colder water, separated by a thermocline. The development of this thermocline is primarily due

---

to the local meteorological conditions. A system with well-developed stratification will limit the facility to withdrawing water from only the intake adjacent layer of the reservoir at lower discharges. At higher discharges, the thermocline may break allowing withdrawal from a greater portion of the reservoir.

Previous studies have focused on the downstream passage of anadromous fish, specifically attraction flows to alternative outlet structures. They have not related the impacts of hydropower operations to resident fish species. Additionally, there has not been a significant number of studies including three dimensional numerical modelling upstream of dams, much less that include thermally stratified flows and identify what impacts of thermal stratification are on fish entrainment risk. There has been a good base of knowledge developed on the mobilization shear stresses required for particles of varying diameters, but have been few studies modelling this in three dimensions upstream of dams. To assess the impacts of these facilities on upstream habitats, the scope of this research aspires to further understand these physical characteristics of forebay hydraulics by applying various aspects of hydraulic engineering including field assessment and computational fluid dynamic (CFD) modelling. The objectives of this study can generally be summarized by: increasing our understanding in using CFD modelling for assessing the potential for bed geometric dynamics in low head reservoirs, in linking the wall shear stress to the potential grain size upstream of a specific facility and what that translates to in terms of habitat usage and entrainment risk, in assessing the flow fields generated by using CFD modelling for fish entrainment risk and in CFD modelling of thermally stratified limnic flows and the implications for fish entrainment risk.

## 1.2 Literature Review

The issue of fish entrainment and fish mortality at hydropower facilities is becoming a more and more important issue for hydropower operators as environmental policies evolve and are becoming more stringent. Numerous previous studies have been completed regarding fish entrainment risk at hydropower facilities. Many of these studies have focused specifically on the passage of fish through turbines and the resulting mortality. Fish mortality can be caused by strong velocity shear, pressure gradient, turbulence, cavitation, direct impact of turbine blades, etc. (BC Hydro, 2006) and the impacts vary due to physical factors (turbine type and size, intake arrangement, discharge) and biological factors (fish size, swimming style, body orientation entering turbines, buoyancy) (Coutant and Whitney, 2000). Sale et al. (2000) identified the the U.S. Advanced Hydropower Turbine Systems program was focused on studying the biological criteria for fish mortality, followed by optimizing turbine design. Experiments done by Von Raben (1964), Monten (1985) and Solomon (1988) attempted to model the likelihood of mechanical injury to fish (primarily by blade strikes) to determine fish mortality. However it was noted by van Esch (2012) that these studies tended to overestimate the amount of mortality, as fish do not behave in a predictable manner, and may have alternate body orientations, or swimming speed (in the direction of or against the direction of flow) that were not accounted for in these studies. More recent studies completed by Turnpenny et al. (2000) and Jacobsen (2011) showed that the mortality rate of turbine blade strikes can be related to the ratio of blade edge length and fish body length. This has led to the development of “fish-friendly” turbines, or turbines with blades that have been specifically designed to minimize the probability of blade strikes as fish pass through a generating station (Francois et al. (2000), Amaral et al. (2011)).

It is fairly universal in the literature that the impact of hydropower turbines on fish mortality is a function of the fish species, size and life stage. It is also largely a function of the type of turbine that is installed at the facility (i.e., a Francis turbine results in lower fish mortality than a Pelton-wheel turbine) (Coutant and Whitney, 2000).

The normal feeding and rearing habits of fish upstream of dams commonly place them close to the intakes, at varying times during the year (Coutant and Whitney, 2000). Fish occupying habitats close to the intake may not be able to escape being entrained into the intake units when velocities exceed their swimming capabilities (EPRI, 1992). This region of high velocity is often termed the risky zone, acceleration zone or the entrainment zone. Previous work has been completed studying the use of physical, acoustic and lighting methods to repel fish from this high risk zone (NPP, 2005). To ensure the efficiency of these operational devices, prediction of near intake velocity field upstream of the dam is necessary. Water velocity, temperature, depth, acceleration, etc., affects the habitat uses in addition to the fish species present and their age classes. Hence, the upstream flow patterns at the facilities can provide valuable information on explaining fish movement.

A number of engineered systems have been developed to reduce the number of fish entrained at hydropower facilities with the ultimate goal of reducing fish mortality. Generally these mitigation measures are classified as physical barriers (i.e. mesh screen and bar racks), collections systems (which collect fish that have been entrained within the hydropower facility and return them to the upstream water body), diversion systems (which attract fish away from hydropower intakes), and behavioural deterrence's (such as strobe lights and sound deterrence's) (Amaral, et al. 2005). Though it has been shown that behavioural deterrents have been

successful, there is no research available regarding fishes adaptation to these deterrents, and thus the longevity of the solution.

Previous works on this subject have generally focused on the downstream passage of anadromous fish and the direction of these fish to alternate (turbine-free) downstream transport outlets (Johnson and Dauble, 2006). These studies have primarily focused on the attraction flow required through alternate outlets to guide fish to safer outlets. In addition to the downstream passage of anadromous fish, high levels of entrainment of resident fish can cause impacts to fish population conservation and recreational objectives (RL&L Environmental, 2000). The primary objective of this thesis is focused on the involuntary passage of resident fish downstream as opposed to the voluntary passage of anadromous fish downstream.

Shammaa et al. (2005) looked at developing an analytical potential flow solution to describe the flow upstream of orifices and sluice gates, which provides a base point for describing the flow upstream of hydropower facilities. Bryant et al. (2008) investigated flow upstream of orifices in a laboratory setting, including the impacts of multiple outlets, and proposed a revised potential flow solution. CFD numerical solvers have also been used as a flow modelling tool for about a decade. There have been several previous numerical studies completed to evaluate the flow field upstream of hydropower dam. Meselhe and Odgaard (1998) developed a numerical model to evaluate the forebay of Wanapum Dam (on the U.S. portion of the Columbia River). The study included evaluating the forebays conditions with several modifications to the fish surface attraction facility. This piece of work also included the development of a 1:16 scale physical hydraulic model. A strong correlation between the numerical and physical model data was ascertained in this study, promoting the effectiveness of CFD as modelling tool for generating

---

flows fields upstream of hydropower facilities. The study also notes that numerical modelling is generally less time consuming and thus more cost effective than physical modelling and field experimentation.

Rakowski et al. (2002, 2006, 2010, 2012) have done significant research simulating the forebay hydraulics upstream of the Bonneville powerhouse and Dalles Dam. Rakowski et al. (2006) evaluated the hydraulics of a behavioural guidance system upstream of the Dalles Dam. The simulations that were created in this study were compared to a 1:80 scale physical model and matched well. This study also evaluated the CFD model against some acoustic field measurements that were made previously. It was found that the CFD model most accurately matches the physical model, though the comparison with the field measurements matched fairly well ( $R^2 = 0.79$ ). Rakowski et al. (2002, 2010, 2012) focused on simulating the forebay flows at the Bonneville Powerhouse. The model that was developed and validated was used in these studies to determine the attraction flow of behavioural guidance systems for fish passage downstream of the facility. The studies were able to make recommendations on the efficiency of these systems by altering the turbines that are operational at the facility.

Khan et al. (2004, 2008) also used a steady state numerical model to evaluate the forebay hydraulics of Dalles Dam, and Wickelin et al. (2002) ran simulations at the Howard Hanson Dam. The model created by Khan et al. (2004, 2008) was validated using a physical model, and looked at the hydraulic impact of varying facility configuration, as well as the impact of the facility's trash racks. These were also compared against field acoustic studies. It was once again found that the CFD data more closely matched the physical model than the field measured

results. This however is anticipated, as a natural reservoir will have a more detailed geometry than is simulated in either a numerical or physical model, as well as transient flows.

Run-of-the-river facilities are (generally smaller) hydropower facilities with relatively small storage headponds and the inflow to the reservoir matches the outflow year round (i.e. the facilities discharge hydrograph matches the rivers streamflow hydrograph). This will generally result in dam operations that fluctuate greatly over the course of the year. The impact of the flow dynamics is of significance for dams with shallow headponds and sediment laden inflows as the deposition and erosion of sediments on the bed can have a great impact on the headpond geometry, which in turn affects the upstream flow field and fish entrainment risk (Csiki and Rhoads, 2010). The primary driving force effect sediment deposition/erosion is the shear stress induced by the flow on the bed.

The USDT (2005) manual states that critical (mobilizing) shear stress for non-cohesive fine grained soil ( $d_{75} < 1.3$  mm) is relatively constant and can be estimated as  $1 \text{ N/m}^2$ . In addition to these general guidelines, a procedure was developed by Shields (1936) to assess the critical shear stress at which sediment will mobilize. By non-dimensionalizing the shear stress on the bed as well as the particle diameter, Shields (1936) was able to define a relationship between shear stress and particle diameter. Soulsby (1997) expanded this by fitting Shields (1936) empirical data to an equation. Soulsby (1997) also developed a modified relationship based on additional advances at the time of his study, including additional data on finer grained sediments.

Scour holes upstream of water intakes have been studied by many researchers (Powell & Khan, 2011, Fathi-Moghadam, et al., 2010; Atkinson, 1996, Lai & Shen, 1996, Liu, et al., 2004, Shen, 1999). Longitudinal and transverse scour profiles upstream of circular orifices have been

---

successfully fit to non-dimensional equations in the laboratory setting. Equations to predict scour extent have been developed, which are dependent upon head, orifice diameter, and the nature of the bed material. A parameter has been developed to estimate the volume of a scour zone by the integration of the longitudinal and transverse laboratory scour profiles (Powell & Khan, 2011).

Though there is a general understanding of the impacts of flow on scour hole production adjacent to intakes as well as the processes of sedimentation and erosion, this concept has generally not been applied to run-of-the-river facilities. Csiki and Rhoads (2010) noted that the effects of these facilities on the upstream geomorphology (bed dynamics) and hydraulics have not been studied to any great detail, as the majority of studies focus on larger impoundment reservoirs.

These previous studies have a commonality in that they have generally modelled the upstream reservoirs as isothermal bodies of water. It is generally well known that deeper lakes and reservoirs in northern climates have dimictic stratification cycle. This results in the lakes “turning over” twice over the course of the year. Generally reservoirs will be isothermal during the winter and spring and stratification will develop in later summer and fall (Fischer et al., 1979). An ideal reservoirs stratification profile will have three distinct layers: a well-mixed epilimnion near the water surface, a relatively distinct thermocline or metalimnion, and a cooler isothermal hypolimnion below this. Some reservoirs, such as the Arrow Lakes on the Columbia River at Hugh Keenleyside, can be approximated by this distinct two-layer stratification (Robertson, 2012). Vidal et al. (2005) noted that this is not the case for all reservoirs. This is reiterated by the measurements done by Bray (2010, 2011, 2012) on the Kinbasket Reservoir upstream of Mica Dam.

The characteristics of this thermal stratification have been looked at by numerous researchers, generally noting that the temperature and depth of the epilimnion are controlled by the amount of solar insolation from the sun as well as the strength of surficial mixing by the wind, among other meteorological factors (Prigo, et al. 1995). A lack of wind mixing can result in a less distinct or more gradual thermocline (Wiegand and Chamberlain, 1987).

The vertical density distribution of a thermally stratified reservoir may limit the elevation at which water is withdrawn from. This applies directly to hydropower intakes in thermally stratified reservoirs, and is called selective withdrawal (Fischer et al. 1979). This is most distinct in reservoirs that have a very distinct thermal stratification profile (i.e. a sharp thermocline). The research of Shammaa and Zhu (2010) included a laboratory study to determine at one point the discharge through an outlet is great enough to upset the upstream thermal stratification and allow withdrawal from all layer. This is termed the critical discharge. Several other studies also look at the concept of selective withdrawal and its impacts on upstream thermal stratification. These include studies completed by Wood (2001), Casamitjana et al. (2003), Caliskan and Elci (2009), Anohin et al. (2006) and Islam and Zhu (2015). Generally, when the discharge through a facility exceeds the critical withdrawal it has been noted that there is a much greater effect on the thermal regime of the upstream reservoir. Craya (1949) provided a formula relating the vertical distance from a point sink to the thermocline to the critical discharge in a two layer stratified reservoir.

### **1.3 Objectives**

The overall objective of the proposed research is to develop a means to assess the hydraulic entrainment risk to resident fish species in reservoir upstream of hydropower dams relative to hydropower generation operations. As aforementioned, it is anticipated that the entrainment risk is attributed to both the type of facility and operational characteristics, as well as physical factors (magnitude and extents of the flow fields induced by hydropower operations and temperature) and biological factors (age, size and swimming strength as well as behavioural aspects such as utilization of the forebay for rearing, migration, predation, etc.).

In order to understand the role of physical hydraulics in assessing fish entrainment risk, this research furthers our understanding of the behaviour of limnic flows in the vicinity of hydropower facilities. Through this research the viability of acoustic field measurements upstream of hydropower facilities of various depths, geometries, water quality and operational styles was evaluated. Field measurements of extended time period temperature characteristic in close proximity to a hydropower facility were collected to analyze the thermal dynamics of its forebay. The hydraulic and thermal measurements provided as base point for three dimensional CFD modelling, providing both input data and validation data. The CFD models developed for this study were used to analyze the hydraulic and thermal characteristics upstream of hydropower facilities under varying operational (i.e. discharge), and environmental (i.e. stratified) conditions. The results produced by the CFD simulations were then analyzed to determine the hydraulic entrainment risk for various fish species as well as the potential for sediment deposition and re-entrainment (which may modify the geometry of the forebay, and thus the local hydraulics and habitat structure).

This allows hydropower utilities to complete fish entrainment risk assessments and make environmentally sound decisions regarding operations. It also allows them to focus the development of mitigation measures on areas of high risk for fish entrainment.

The current study has been divided into five chapters, each focusing on a specific aspect of the evaluation of fish entrainment risk in relation to hydropower operations. The objectives of each are as follows:

- Chapter one provides an overview of fish entrainment and the work that has been previously completed,
- Chapter two uses CFD to investigate the impact of withdrawal from a run-of-the-river dam on the induced flow field and bed shear stress throughout the headpond. This has been related to the potential for erosion and sedimentation, scour hole development and fish entrainment risk.
- Chapter three uses a CFD solver and potential flow solution to evaluate the seasonal impact of a high head, high discharge hydropower facility on the forebays hydraulics. The results of the CFD solver are compared to a potential flow solution and have been used to study the development of risk zones for fish entrainment.
- Chapter four evaluates the impact of seasonal thermal stratification on the flow field and thermal structure upstream of two hydropower dams with complex and simple geometries.
- Chapter five provides a summary of the knowledge that has been gained through this study and provides recommendations for further study.

## 1.4 References

- Amaral, S. V., Hecker, G. E., and Dixon, D. A. (2011). “Designing Leading Edges of Turbine Blades to Increase Fish Survival From Blade Strike,” *EPRI-DOE, Conference on Environmentally-Enhanced Hydropower Turbines*, WA.
- Anohin, V.V., Imberger, J., Romero, J.R., and Ivey, G.N. (2006). “Effect of long internal waves on the quality of water withdrawn from a stratified reservoir.” *Journal of Hydraulic Engineering - ASCE*, 132(11), 1134-1145.
- Atkinson, E. (1996). “The Feasibility of Flushing Sediment from Reservoirs”, Report ID 137. HR Wallingford.
- BC Hydro (2006). Fish Entrainment Risk Screening and Evaluation Methodology, BC Hydro, Report No. E478.
- Bray, K. (2010). “Kinbasket and Revelstoke Reservoirs Ecological Productivity Monitoring – Progress Report Year 1.” *Columbia River Project Water Use Plan*, BC Hydro, Revelstoke, B.C.
- Bray, K. (2011). “Kinbasket and Revelstoke Reservoirs Ecological Productivity Monitoring – Progress Report Year 2.” *Columbia River Project Water Use Plan*, BC Hydro, Revelstoke, B.C.
- Bray, K. (2012). “Kinbasket and Revelstoke Reservoirs Ecological Productivity Monitoring – Progress Report Year 3.” *Columbia River Project Water Use Plan*, BC Hydro, Revelstoke, B.C.

- Bryant, D. B., Khan, A. A., & Aziz, N. M. (2008). Investigation of Flow Upstream of Orifices. *Journal of Hydraulic Engineering*, 134(1), 98-104.
- Caliskan, A. and Elci, S. (2009). "Effects of selective withdrawal on hydrodynamics of a stratified reservoir." *Water Resources Management*, 23, 1257-1273.
- Casamitjana, X., Serra, T., Colomer, J., Baserba, C., and Perez-Losada, J. (2003). "Effects of the water withdrawal in the stratification patterns of a reservoir." *Hydrobiologia*, 504, 21-28.
- Coutant, C.C., Whitney, R.R. (2000). "Fish behaviour in relation to passage through hydropower turbines: a review". *Transactions of the American Fisheries Society*, 129(2), 351-380.
- Csiki, S., Rhoads, B.L. (2010). "Hydraulic and Geomorphological Effects of Run-of-the-River Dams." *Progress in Geomorphology*. 34(6). Pages 755-780.
- Craya, A. (1949). "Theoretical research on the flow of nonhomogenous fluids", *La Houille Blanche*, 4, 44-55.
- EPRI (1992). "Fish Entrainment and Turbine Mortality Review and Guideline, Final Report", Electric Power Research Institute, TR 101231.
- Fathi-Moghadam, M., Emamgholizadeh, S., Bina, M., Ghomeshi, M. (2010). "Physical modelling of pressure flushing for desilting of non-cohesive sediment." *Journal of Hydraulic Research*, 48(4), 509-514.

- Fischer, H.B., List, E.J., Koh, R.C.Y., Imberger, J., Brooks, N.H. (1979). "Mixing in Reservoirs." *Mixing in Inland and Coastal Waters*, Academic Press Inc., San Diego CA. p.150 – 228.
- Francois, M., Vinh, P., and Mora, P. (2000). "Fish Friendly Kaplan Turbine," "*Proceedings of the 20th IAHR Symposium on Hydraulic Machinery and Systems*", Charlotte, NC, Paper No. ENV-03.
- Islam, M.R. and Zhu, D.Z. (2015). "Selective withdrawal in two-layer stratified flows", *Journal of Hydraulic Engineering*, 141(7) , 04015009.
- Jacobson, P. (2011). "Fish Passage through Turbines: Application of Conventional Hydropower Data to Hydrokinetic Technologies," Electric Power Research Institute (EPRI), Palo Alto, CA, Final Technical Report No. 1024638.
- Johnson, G.E., Dauble, D.D. (2006). "Surface Flow Outlets to Protect Juvenile Salmonids Passing Through Hydropower Dams." *Reviews in Fisheries Science*, 14(3). Pages 213-244.
- Julien, P. (1998). "Erosion and Sedimentation". Cambridge University Press, Cambridge, UK.
- Khan, L.A., Wicklein, E.A., Rashid, M., Ebner, L.L., and Richards, N.A. (2004). "Computational fluid dynamics modeling of turbine intake hydraulics at a hydropower plant", *Journal of Hydraulic Research*, 42(1), 61-69.

Khan, L.A., Wicklein, E.A., Rashid, M., Ebner, L.L., and Richards, N.A. (2008). “Case Study of an Application of a Computational Fluid Dynamics Model to the Forebay of the Dalles Dam, Oregon.”, *Journal of Hydraulic Engineering*, 134(5), 509-519.

Lai, J.-S., & Shen, H. W. (1996). “Flushing Sediment Through Reservoirs”. *Journal of Hydraulic Research*, 34(2) , 237-255.

Liu, J., Minami, S., Otsuki, H., Liu, B., & Ashida, K. (2004). Prediction of Concerted Sediment Flushing”. *Journal of Hydraulic Engineering* , 1089-1096.

Meselhe, E.A., and Odgaard, A.J. (1998). “3D numerical flow model for fish diversion studies at Wanapum dam ”, *Journal of Hydraulic Engineering*, 124 (12), 1203-1214.

Monten, E. (1985). “Fish and Turbines: Fish Injuries During Passage Through Power Station Turbines,” Norstedts Tryckeri, Sweden, Report No. 549.

NPP (2005). “Fish Entrainment and Mortality Study”, Vol 1, Niagara Power Project, New York Power Authority.

Powell, D., & Khan, A. (2011). “Sediment Transport Upstream of Circular Orifices”. *Journal of Hydraulic Research*, 1-36.

Prigo, R.B., Manley, T.O., and Connell, B.S.H. (1995). “Linear, one-dimensional models of the surface and internal standing waves for a long and narrow lake.” *American Journal of Physics*, 64(3), 288-300.

- Rakowski, C.L., Richmond, M.C., Serkowski, J.A., Ebner, L. (2002), “Three dimensional simulation of forebay and turbine intakes flows for the Bonneville project”, *Proc., of HydroVision 2002*, Oregon.
- Rakowski, C.L., Richmond, M.C., Serkowski, G.E. Johnson (2006). “Forebay Computational Fluid Dynamics Modeling for the Dalles Dam to Support Behaviour Guidance System Siting Studies”, Pacific Northwest National Laboratory. Richland, WA.
- Rakowski, C.L., Richmond, M.C., Serkowski, (2010). “Bonneville Powerhouse 2 3D CFD for the Behavioural Guidance System”, Pacific Northwest National Laboratory. Richland, WA.
- Rakowski, C.L., Richmond, M.C., Serkowski, (2012). “Bonneville Powerhouse 2 Guidance Efficiency Studies: CFD Model of the Forebay”, Pacific Northwest National Laboratory. Richland, WA.
- RL&L Environmental (2000). “Resident Fish Entrainment: Information Review”, RL&L Environmental Services Ltd., Edmonton, AB.
- Robertson, C.B. (2012). “Forebay Thermal Dynamics at Hydropower Facilities on the Columbia River System”. M.Sc. Thesis, University of Alberta.
- Sale, M. J., Cada, G. F., Rinehart, B. N., Sommers, G. L., Brookshier, P. A., and Flynn, J. V., (2000). “Status of the US Department of Energy’s Advanced Hydropower Turbine Systems Program,” Proceedings of the 20th IAHR Symposium on Hydraulic Machinery and Systems, Charlotte, NC, Paper No. ENV-01.

Shammaa, Y., Zhu, D.Z., Rajaratnam, N. (2005) “Flow Upstream of Orifices and Sluice Gates.”

*Journal of Hydraulic Engineering.*, ASCE, 131(2), 127-133

Shammaa, Y. and Zhu, D.Z. (2010). “Experimental study on selective withdrawal in a two-layer reservoir using a temperature-control curtain.” *Journal of Hydraulic Engineering -*

*ASCE*, 136(4), 234-246.

Shen, H. W. (1999). “Flushing Sediment Through Reservoirs”. *Journal of Hydraulic Research*,

37(6) , 743-757.

Shields, I.A. (1936). *Application of Similarity Principle and Turbulence Research to Bed-Load*

*Movement*. Translated by United States Department of Agriculture Soil Conservation

Service Cooperative Laboratory, California Institute of Technology, Pasadena,

California. By: Ott, W.P. and van Uchelen, J.C.

Solomon, D. J. (1988). “Fish Passage Through Tidal Energy Barrages,” Energy Technical

Support Unit, Harwell, U.K., Report No. ETSU TID4056.

Soulsby (1997). “Dynamics of Marine Sands”, Thomas Telford Publications, Thomas Telford

Services Ltd., Heron Quay, London.

Turnpenny, A. W. H., Clough, S., Hanson, K. P., Ramsey, R., and McEwan, D. (2000). “Risk

Assessment for Fish Passage Through Small Low-Head Turbines,” Energy Technical

Support Unit, Harwell, U.K., Report No. ETSU H/06/00054/REP.

USDT (2005). “Design of Roadside Channels with Flexible Linings”, Federal Highway

Administration, United States Department of Transportation.

- Van Esch, B.P.M. (2012). “Fish Injury and Mortality During Passage Through Pumping Stations.” *Journal of Fluids Engineering*. 134(7). (9pages).
- Vidal, J., Casamitjana, X., Colomer, J., Serra, T. (2005). “The internal wave field in Sau reservoir: Observation and modeling of a third vertical mode.” *Limnology and Oceanography - ASLO*, 50(4), 1326-1333.
- Von Raben, K. (1964). “Regarding the Problem of Mutilations of Fishes by Hydraulic Turbines,” *Fisheries Research Board of Canada, Translation Series, No. 448*, [Die Wasserwirtschaft, 4 , 97-100 (1957)].
- Wicklein, E.A., Khan, L.A., Rashid, M., Deering, M.K., and Nece, R.E. (2002). “A three dimensional computational fluid dynamics model of the forebay of Howard Hanson dam”, Washington, Proc., Hydro Vision 2002, Portland, Oregon.
- Wiegand, R.C. and Chamberlain, V. (1987). “Internal waves of the second vertical mode in a stratified lake.” *Limnology and Oceanography - ASLO*, 32(1), 29- 42.
- Wood, I. R. (2001). “Extensions to the theory of selective withdrawal.” *J. Fluid Mech.*, 448, 315–333.

## Chapter 2

# Upstream Hydraulics of a Run-of-the River Hydropower Facility for Fish Entrainment Risk Assessment

---

Mathew T. Langford, David Z. Zhu, Alf Leake

### 2.1 Abstract

Run-of-the-river hydropower is a typical form of power generation in mountainous regions. This study investigates the velocity field upstream of Aberfeldie Dam, a run-of-the river facility on the Bull River near Wardner, British Columbia (BC), Canada. As is typical for these types of run-of-the river facilities, the headpond of this dam is very shallow (~1 m deep) due to long term sediment deposition. Near the facility's power intakes, a large scour hole has been created due to increased velocities induced by the intakes. This study conducted field measurements and developed a computational fluid dynamic (CFD) model to investigate the velocity field under various flow conditions. The CFD solver shows in a simplistic way that flow-induced bed shear stress likely causes a fluctuating, dynamic bed form that varies by season and the distance upstream that a consistent velocity pattern is seen across the entire headpond. The velocity field generated by the CFD solver is used to evaluate the entrainment risk of mountain whitefish and westslope cutthroat trout based on swimming mechanics and life stage. The unique habitat

conditions generated by the scour hole act as an attractant to the high risk zone, greatly increasing fish density adjacent to the intakes at this facility.

## 2.2 Keywords

Aquatic habitat; Computational fluid dynamics; Fish entrainment; Intake; Reservoir bathymetry; Scour hole.

## 2.3 Introduction

Run of the river (ROR) hydropower is a very prominent form of electricity generation in mountainous regions, such as British Columbia, Canada, due to limited storage capabilities and high elevation potentials. As a result, headpond characteristics upstream of the dam see higher velocity flows than seen at dams that maintain an upstream reservoir. For ROR facilities, sediment laden inflow may deposit or entrain sediment on/from the bed of the headpond depending on the seasonally varying flow through the facility and overall watershed stability. This develops a scenario in which the headpond bathymetry is dynamic, and may change over the course of the year. As headpond infilling with sediments may occur at many facilities, erosive forces adjacent to the power intake may form a local scour hole caused by the accelerating flow. Fragmented habitat caused by the lack of upstream passage at some ROR facilities separates upstream and downstream fish stocks, although many ROR facilities may be installed at previously impassable barriers. The combination of the provision of fish habitat created by the scour hole and the upstream velocity field generated by power intake flows may result in "fish entrainment". The term "fish entrainment" refers to the involuntary downstream passage of fish through the dam. It is anticipated that the risk of fish entrainment at a particular

dam facility is correlated with the effect of hydropower operations on the flow field of the headpond and the effects of that field on sediment erosion and deposition.

A number of studies have been completed regarding fish entrainment risk at hydropower facilities, many of which have focused specifically on the passage of fish through turbines and the resulting mortality, see the review paper by Coutant and Whitney (2000). Fish mortality due to entrainment can be caused by a number of means including: strong velocity shear, pressure gradient, turbulence, cavitation and direct impact of turbine blades (BC Hydro, 2006). The impacts vary due to physical factors (turbine type and size, intake arrangement, discharge) and biological factors (fish size, swimming style, body orientation, bulk biotic density) (Coutant and Whitney, 2000). Sale *et al.* (2000) linked the biological criteria for fish mortality to optimizing turbine design. A number of studies have also looked at innovative “fish-friendly” turbine development, specifically with the goal of minimizing the probability of blade strikes (e.g., Francois *et al.* (2000), Amaral *et al.* (2011)).

Additionally, fish mortality is a function of the fish species, size and life stage and behaviour. The normal habits of fish upstream of dams commonly place them in the vicinity of the intakes at varying times during the year (Coutant and Whitney, 2000), depending on headpond habitat attributes. Fish located adjacent to the intake may not be able to escape being entrained into the intake units when velocities exceed their swimming capabilities (EPRI, 1992) or where their feeding and rearing behaviours take them into these entrainment “risk zones”. Previous work has been completed studying the use of physical, acoustic and lighting methods to repel fish from this high risk zone (NPP, 2005). Mitigation measures including physical barriers (i.e. mesh screen and bar racks), collections systems (which collect fish that have been entrained within the

---

hydropower facility and return them to the upstream water body), diversion systems (which attract fish away from hydropower intakes), and behavioural deterrence's (such as strobe lights and sound deterrence's) have been developed to prevent entrainment (Amaral *et al.* 2011).

Though some behavioural deterrence's have been shown to be successful, biological adaptation to these deterrence's, and their effectiveness in ROR headponds is uncertain. To ensure the efficiency of these operational devices, it is necessary to simulate the near intake velocity field upstream of the dam. Water velocity, temperature, depth, acceleration, etc. affects the habitat use of the headpond based on fish species and their age classes. Hence, the upstream flow patterns at ROR facilities can provide valuable information on explaining fish movement.

CFD is becoming more and more prominent in evaluating the flow field upstream of hydropower dams. Meselhe and Odgaard (1998) developed a numerical model to evaluate the fish surface attraction facility in the forebay of the Wanapum Dam. A strong correlation between the observed and physical model data was ascertained in this study, promoting the effectiveness of CFD as modelling tool for predicting flow fields upstream of hydropower facilities. Rakowski *et al.* (2002, 2006, 2010, 2012) simulated the forebay hydraulics upstream of the Bonneville powerhouse and Dalles Dam, and evaluated the hydraulics of a behavioural guidance system upstream of the Dalles Dam against a physical model study. It was found that the CFD model most accurately matched the physical model, while the comparison with the field measurements also matched well. Khan *et al.* (2004, 2008) also used a numerical model to evaluate the forebay hydraulics of Dalles Dam, and Wicklein *et al.* (2002) at the Howard Hanson Dam. The model created by Khan was validated using a physical model, and looked at the hydraulic impact of varying facility configurations, as well as the impact of trash racks against field acoustic studies.

At ROR facilities, where headpond storage is limited, the impacts of bedform dynamics (scour hole formation as well as sedimentation and erosion) have a significant effect on the geometry and hydraulics of the headpond, as well as the fisheries habitat attributes created by operations. The main driving force for each of these phenomena relates to the velocity field generated by the outlet structures of the facility (Julien, 2008). Shammaa *et al.* (2005) and Bryant *et al.* (2008) applied a potential flow solution for predicting the velocity field upstream of an intake. Various studies have been completed to assess the flushing of sediment through dams for dam maintenance including modelling completed by Basson and Olesen (1997), Liu *et al.* (2004), Lai and Shen (1996) and Shen (1999). Powell and Khan (2012) studied scour hole formation upstream of orifices and identified the characteristics of scour hole formation induced by an orifice outlet. Powell and Khan (2015) furthered this work by investigating the flow field upstream of an orifice under fixed bed and equilibrium scour conditions across a variety of sediment sizes. The laboratory measurements of Powell and Khan (2015) were compared against a CFD model of the experiment, verifying the use of CFD for this application. Other work relating the characteristics of scour hole formation include the studies of Xue *et al.* (2013) and Guo *et al.* (2013), both of which investigated the formation of scour holes above downward oriented orifices. Though these are fundamentally different from the orifices of a typical ROR facility headpond, the contribution to the knowledge of scour hole characteristics is notable.

The evaluation of fish entrainment risk based on threshold hydraulic criteria is a relatively new concept. The use of key parameters relating fish swimming strength to induced velocity has primarily been limited to upstream fish passage evaluations (Katopodis, 1992; Katopodis and Williams, 2012), noting that fish movements are strongly effected by velocity field, hydrostatic

pressure (depth) and turbulence (Katopodis et al. 2001). Enders et al. (2012) also linked the use of a spatial velocity gradient (or accelerating flows) to fish detection of altered flow fields.

Other studies evaluated the effects of turbulence and shear strain on fish, identifying it as one of the primary physical attributes detected by fish, effecting their orientation and holding patterns (Goodwin, 2004). Together, these studies provide a basic conceptual framework for predicting fish entrainment risk in fish utilizing habitats near flow orifices.

The current study attempts to expand the knowledge of the headpond hydraulics at ROR facilities, by means of an investigatory field study, as well as computational fluid dynamic (CFD) numerical study at Aberfeldie (ABN) Dam in BC. Preliminary biological studies have identified that mountain whitefish fry and larvae and westslope cutthroat trout juveniles are at particular risk at this facility as they frequently utilize the ABN headpond (Westslope Fisheries Ltd., 2012). This includes telemetry studies identifying that 58.3 % and 57.7 % of upstream westslope cutthroat trout and mountain whitefish utilize the dams headpond to some extent during all seasons of the year (Westslope Fisheries Ltd., 2012). This includes entrainment rates of 24 % for westslope cutthroat trout and 19.2 % for mountain whitefish. Westslope cutthroat trout are a provincially blue-listed species (a vulnerable species of special concern), the population in the Upper Bull River is considered to be one of the few genetically pure populations (2 - 4 %). As the dam is a barrier to rainbow trout migration upstream, there has been no hybridization of the stock (Westslope Fisheries Ltd., 2012). The pre-screening report identifies that the highest risk to fish is typically over winter when the spillway is not active (July – April). Fish will orient themselves in the direction of flow to seek out preferred habitat, leading them to the entrainment zone adjacent to the intakes, within the local scour hole

(Westslope Fisheries Ltd., 2012). The hydraulic information can be extended to identify areas of headpond that are of particularly high risk for fish entrainment under varying flow conditions.

This chapter focuses on two different flow conditions, a fall low flow condition that was investigated in the field, as well as a spring high flow scenario during freshet. The headpond elevation and discharges through each of the facilities outlet structures are outlined in Table 1.

**Table 1: Computational fluid dynamic model scenarios.**

<b>Scenario</b>	<b>Description</b>	<b>ABN Head-pond Elevation (m)</b>	<b>ABN Power Intake Flow (m<sup>3</sup>/s)</b>	<b>Spillway Releases (m<sup>3</sup>/s)</b>
<b>Field</b>	<b>Fall - Low Flow</b>	877.004	14.711	0
<b>Spring Freshet</b>	<b>Freshet - High Flow</b>	877.482	38.5	80

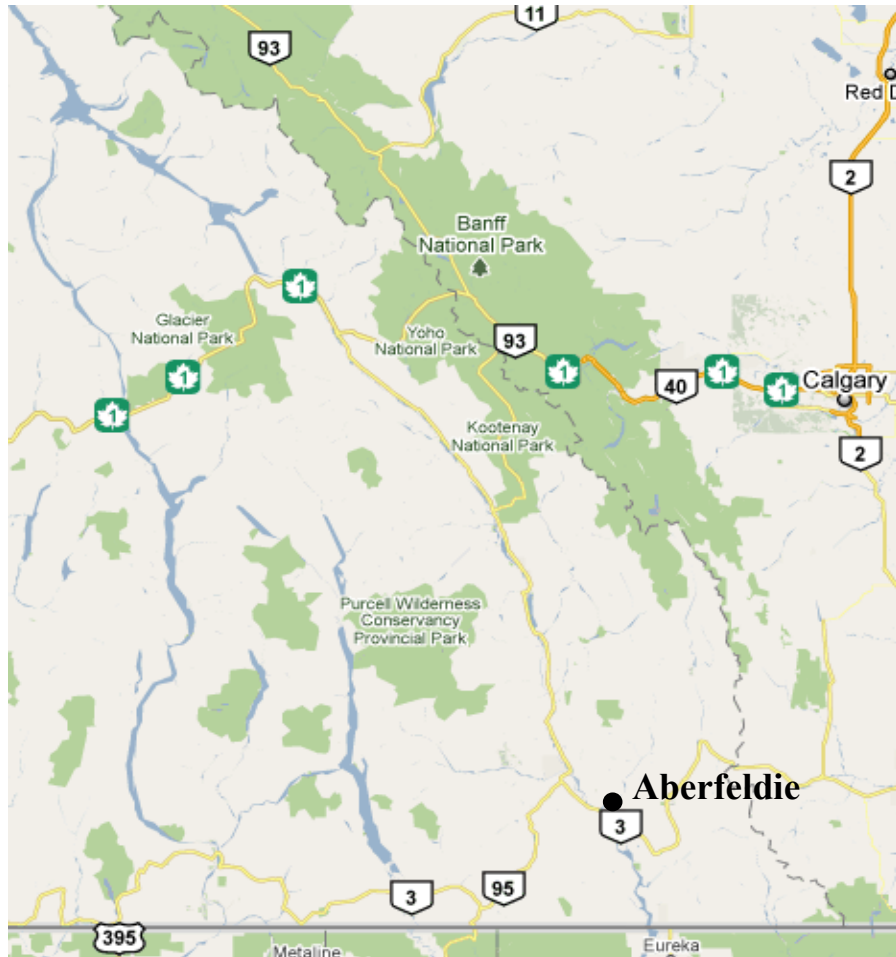
The objectives of the study are to assess the risk posed to mountain whitefish and westslope cutthroat trout during different seasons upstream of ABN using CFD modelling. The model is also used to assess the size and geometry of the local scour hole upstream of the intakes in a simplified way and to develop a concept of the depth of potential seasonal erosion of the bed upstream of the facility under different flow regimes. Having a basic knowledge of the forebay geometry is important in assessing the upstream hydraulics and its impact on resident fish. The CFD model can be used as a tool to proactively address operations planning for both sediment and habitat management. The tool can be used to assess the potential impacts of facility outages and operational changes on upstream habitat as well as planning annual dredging operations to optimize habitat availability and reduce entrainment risk.

## 2.4 Methodology

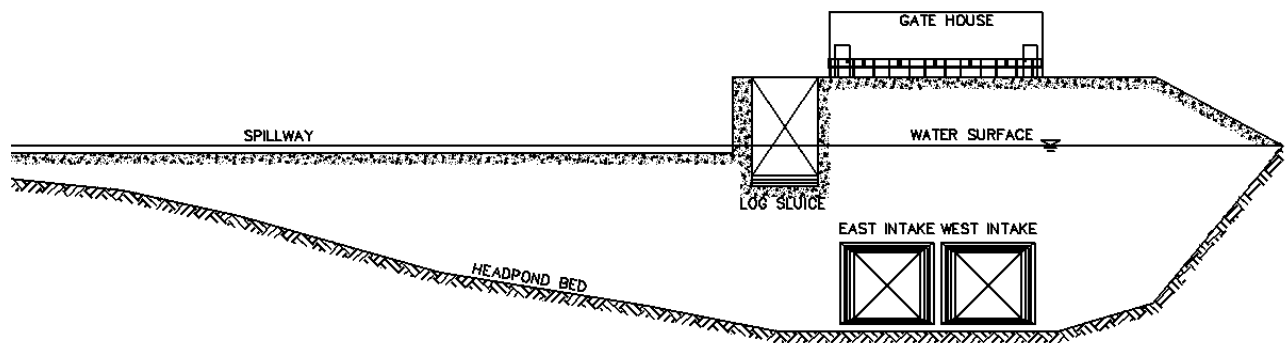
### 2.4.1 Project Site

The ABN Dam is a ROR hydropower generation station located on the Bull River, near Wardner, BC (49°29'47"N 115°21'23"W) as shown on Figure 1(a). The Bull River flows southwesterly and is approximately 117 km in length, originating at the continental divide. It is divided into four distinct sections according to facility placement and river morphology: Reach 1 is the lowest 12 km section measured from its confluence with the Kootenay River to the ABN Generating Station, Reach 2 is the 1.8 km diversion reach between the generating station and dam that sees only flow that is not generated (this portion is not accessible to fish in Reach 1 due to a series of impassible barriers); Reach 3 is the 40 km of section resident to the species of interest in this study above the dam; and Reach 4 is the portion of the river above Reach 3 that is fishless due to a barrier to fish migration. Downstream of the ABN facility exists an Environment Canada river gauging station, prior to its confluence with the Kootenay River. The discharge generally ranges from 5 – 118 m<sup>3</sup>/s. Higher flow rates are normally realized at the onset of spring freshet in mid-April, and last to early-September. The maximum turbine discharge of the ABN facility is 39 m<sup>3</sup>/s. As the dam operates as a ROR dam, any river discharge in excess of the maximum turbine capacity will be released via the spillway and instream flow requirements outlets. The Bull River supports habitat for a variety of fish species including, but not limited to: mountain whitefish (*Prosopium williamsoni*), longnose dace (*Rhinichthys cataractae*), largescale sucker (*Catostomus macrocheilus*), torrent sculpin (*Cottus rhotheus*), slimy sculpin (*C. cognatus*), westslope cutthroat trout (*Oncorhynchus clarkii lewisi*),

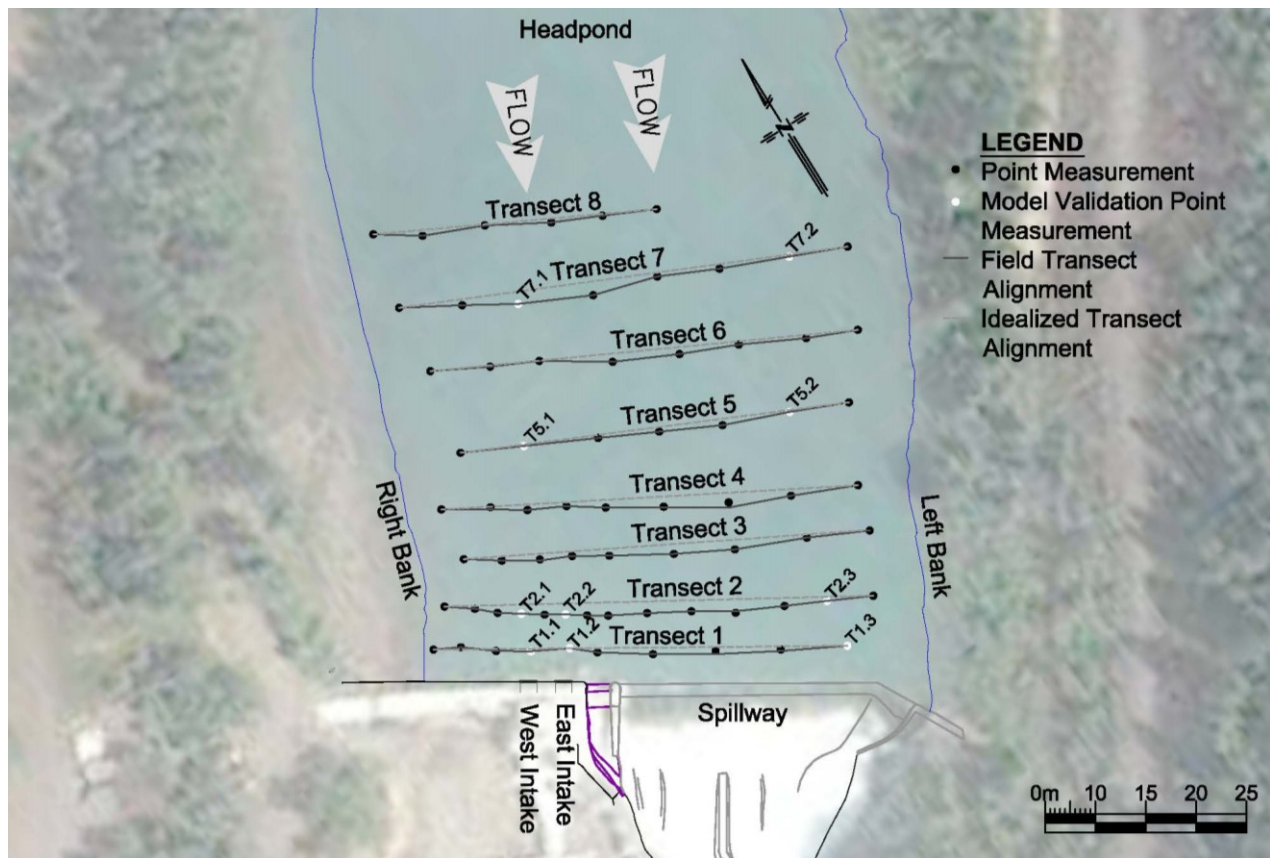
kokanee (*O. nerka*) and possibly bull trout (*Salvelinus confluentus*) (Westslope Fisheries Ltd., 2012).



(a)



(b)



(c)

**Figure 1: (a) Site location of Aberfeldie Dam (adapted from Map Data: Google, 2015); (b) Intake layout profile looking downstream; (c) Site plan and field measurement locations (with ADCP transects) (aerial photo adapted from Map Data: Google, DigitalGlobe, 2015).**

ABN Dam transects the river approximately 12 km upstream of the Kootenay River. The facility impounds a relatively small headpond, extending approximately 300 m upstream of the facility. The facility was originally constructed in 1922, with subsequent construction in 1954 and 2008, expanding the generating capacity to 25 MW. It has been estimated that the majority of the headpond volume is currently occupied by settled sediment (NHC, 2005). In recent years BC Hydro has implemented an annual sediment dredging program in early summer to reduce further infilling of the headpond.

The dam operates using a combination of two intakes (which wye to a single penstock), an ogee spillway and a log sluice unit. Each of the intakes has an outlet prior to entering the penstock to satisfy the instream flow requirements (IFR) for fish habitat downstream of the dam. The layout of the units is depicted in Figure 1 (b). The ABN headpond is generally very shallow, ranging between 0.3 and 1.5 m in depth, aside from a large, localized scour hole immediately adjacent to the intakes.

#### ***2.4.2 Field Measurements***

The bathymetry that was included in the CFD model for the ABN headpond was constructed using field measurements at the dam site. Bathymetry and velocity measurements were both completed using two models of acoustic Doppler current profiler (ADCP) on August 21 - 22, 2010 including a 600 kHz River Ray, equipped with a phased-array transducer as well as a 600 kHz Workhorse Rio Grande (with standard piston-style transducers). The River Ray measurements have an accuracy of 0.25 % of the water velocity relative to the instruments velocity, or 2 mm/s, whichever is greater. The Rio Grande has a velocity measurement accuracy of 0.25 % of the water + boat velocity, or 2.5 mm/s, whichever is greater. Both instruments have a velocity resolution of 1 mm/s.

At the time of use, each of these instruments was equipped with a Trimble R8 GNSS Model 2 real-time kinetic global positioning system (RTK GPS) affixed to the top of the ADCP, immediately above the instrument. For kinematic surveying, the RTK GPS unit has a vertical accuracy of 20 mm + 1 ppm RMS and a horizontal accuracy of 20 mm + 1 ppm RMS. The 1 ppm RMS component indicates that for every kilometre the rover is away from the receiver, an

additional error of 1 mm is anticipated. For this project, the rover was always within a relatively short range of the receiver ( $< 0.5$  km).

Over the course of the measurements completed at ABN the dam's intake discharge was held constant at  $14.711 \text{ m}^3/\text{s}$ . The maximum variation in discharge, based on hourly measurements in the powerhouse was  $0.34 \text{ m}^3/\text{s}$ , which accounts for 2 % of the total discharge through the facility. The total discharge is split evenly between each of the intakes, with the IFR discharge extracted from the flow downstream of the intakes. Based on the water surface measurements collected by the GPS during the data collection period, the water surface elevation was 877.004 m, which is below the crest of the spillway which was not operational at the time. There was no discernable variation in water surface elevation over the course of the measurements in replicate measurements completed on each day. The average difference in water surface elevation between the most upstream and downstream transects was 0.018 m, resulting in flat ( $0.00016 \text{ m/m}$ ) water surface profile through the headpond. Low inflows meant that only the power intakes were operational during the study.

The ADCPs were installed in floatable trimaran boats specifically designed to minimize the pitch and roll of the instruments during each measurement. Due to the dangers inherent to working in close proximity of a functional hydropower facility, boat access upstream of the facility and spillway was not permitted. As such, the ADCP trimarans were tethered to a nylon rope guideline stretching across the forebay and were moved from the west to east banks and upstream and downstream by the field research team. A total of eight transects were collected over the course of two days, with a total of 71 points measured. The location of these points is depicted on Figure 1 (c). The spacing between each measurement point was approximately 10

m. A smaller distance (approximately 5 m) was used for transects nearest the dam face for points in close proximity to the intakes. Each of the ADCP measurements was completed for a duration of five minutes and subsequently time-averaged to reduce error in the measurements. Over the measurement period the River Ray collected between 358 and 666 ensembles at each point (an average of 466 measurements were collected per point and time-averaged). The Rio Grande, which was used for transects 3 and 4 collected between 33 and 46 measurements at each point, averaging 41 ensembles per point measurement.

It was found that in general the River Ray measured higher transect discharges (3.2 – 6.7 %) than measured in the generating station and the Rio Grande measured lower discharges (4.2 – 12.1 %). The measurements herein have been linearly adjusted based on the measured discharges through the generating station to account for differences in instrument calibration. Functionally, the use of two ADCP units allowed real-time data collection in the zone nearest the dam face as the River Ray has Bluetooth capabilities. The Rio Grande allowed for self-contained autonomous measurements in the locations further upstream where remote connection capabilities were infeasible. This method for collecting field data upstream of a functional facility is feasible for smaller facilities, where the guideline can easily be controlled and tension applied at each measurement point. Longer length guidelines (exceeding 50-100 m) are difficult to suspend, and may cause significant drag depending on the velocity of the waterbody.

Correlation is one of the key quality control parameters in completing flow field measurements with acoustic devices. A high correlation value ensures that high quality data is being obtained, and a low correlation value increases the potential error in the measurements. Both of these instruments use a manufacturer specific linear correlation scale from 0 to 255. Low correlation

is obtained in pure waters, with little seeding available, which hinders acoustic performance.

The manufacturer's manual suggests that low, or unacceptable correlations are those with a correlation value less than 64. The correlation of the averaged ADCP data ranged from approximately 120 to 255 over the course of field measurements at ABN.

The Rio Grande has a beam angle of  $20^\circ$  and the River Ray has a beam angle of  $30^\circ$ . The beam angle restricts the horizontal position from the dam at which the measurements can be taken. The beam angle also increases the sampling (and averaging) volume of the instrument with depth. For these reasons a narrow beam angle is preferred for deeper applications, and it is anticipated that the data quality is highest near the surface. As the ABN headpond is relatively shallow, the effects of increased sampling volume due to the beam angle are less pronounced as compared to deeper limnic flow measurements.

Environmental factors exist that contribute to the potential error in ADCP measurements. Error may be introduced into the measurements due to wave movement, the units setting within its buoyant frame (trimaran) or the buoyancy balancing of the frame itself. This is reflected in the pitch and the roll of the measurements. The pitch was in the order of  $2.6^\circ$  and the roll was in the order of  $1.5^\circ$  for all measurements completed at ABN.

#### ***2.4.3 Computational Fluid Dynamic Model***

The numerical model domain extends up to approximately 100 m upstream of the dam headwall. A 7 m deep scour hole is observed immediately upstream of the intake, and at approximately 30 m upstream, the channel is found to be very shallow. The headpond morphology has been created by long-term sediment deposition in the forebay area and was measured during the field study.

---

The CFD solver solves the three-dimensional Reynolds-Averaged Navier-Stokes equations, with the  $k - \varepsilon$  turbulence model to assess the eddy viscosity. The  $k - \varepsilon$  model was utilized for its robustness and numerical stability, and as there was not inferred to be severe pressure gradients within the headpond. The governing equations are as follows (CFX, 2009),

$$\frac{\partial \rho}{\partial t} + \frac{\partial \rho u_j}{\partial x_j} = 0$$

$$\frac{\partial \rho u_i}{\partial t} + \frac{\partial \rho u_j u_i}{\partial x_j} = -\frac{\partial p}{\partial x_i} + \frac{\partial}{\partial x_j} \left\{ (\mu + \mu_t) \left( \frac{\partial u_i}{\partial x_j} + \frac{\partial u_j}{\partial x_i} \right) - \frac{2}{3} \rho k \delta_{ij} \right\} - (\rho - \rho_{ref}) g_i \quad \text{Equation 1}$$

where,  $x_i$  is a distance in the  $i$  direction,  $u_i$  is a velocity in the  $i$  direction,  $t$  is time,  $\rho$  is the density,  $k$  is the turbulent kinetic energy,  $\delta_{ij}$  is the Kronecker delta,  $p$  is the pressure,  $\mu$  is the molecular viscosity,  $\mu_t$  is the eddy viscosity,  $\rho_{ref}$  is the reference density,  $g_i$  is the force of gravity in the  $i$  direction. Equation 1 presents a system of equations where subscript  $i$  refers to the  $x$ ,  $y$ , or  $z$  directions in Cartesian coordinates.

To compute the eddy viscosity, the standard  $k - \varepsilon$  turbulence model was used. The governing equations for the  $k - \varepsilon$  turbulence model are,

$$\frac{\partial \rho k}{\partial t} + \frac{\partial \rho k u_j}{\partial x_j} = \frac{\partial}{\partial x_j} \left\{ \left( \mu + \frac{\mu_t}{\sigma_k} \right) \frac{\partial k}{\partial x_j} \right\} + \mu_t \left( \frac{\partial u_i}{\partial x_j} + \frac{\partial u_j}{\partial x_i} \right) \frac{\partial u_i}{\partial x_j} - \rho \varepsilon$$

$$\frac{\partial \rho \varepsilon}{\partial t} + \frac{\partial \rho \varepsilon u_j}{\partial x_j} = \frac{\partial}{\partial x_j} \left\{ \left( \mu + \frac{\mu_t}{\sigma_\varepsilon} \right) \frac{\partial \varepsilon}{\partial x_j} \right\} + C_1 \frac{\varepsilon}{k} P_k - C_2 \rho \frac{\varepsilon^2}{k}$$

$$\mu_t = \rho C_\mu \frac{k^2}{\varepsilon} \quad \text{Equation 2}$$

The constants in the model include:  $C_1 = 1.44$ ,  $C_2 = 1.92$ ,  $\sigma_k = 1.0$ ,  $\sigma_\tau = 1.3$ , and  $C_\mu = 0.09$ . At the no-slip wall, the CFX solver uses a no-flux boundary condition for the kinetic energy equation. For the dissipation ( $\varepsilon$ ) equation, the following equation is used,

$$\varepsilon = \frac{\rho u^* C_\mu^{3/4} k^{3/2}}{\mu \kappa \tilde{y}^*} \quad \text{Equation 3}$$

where,  $\kappa$  is the von-Karman constant,  $\tilde{y}^*$  is  $\rho u^* \Delta y / \mu$  or 11.06, whichever is larger,  $\Delta y$  is the distance of the first grid point from the wall, and  $u^*$  is computed by,

$$u^* = C_\mu^{1/4} k^{1/2} \quad \text{Equation 4}$$

The solution for the model used a high resolution advection scheme and high resolution solution for turbulence numerics. The convergence criteria for the model were set such that the root mean square (RMS) of the residual is below  $10^{-5}$  in all the simulations carried out. The pressure and velocity interpolation schemes were specified as trilinear with a geometric shape function option. Velocity pressure coupling was included with a fourth order Rhie Chow option. Figure 2 shows a typical convergence history for the momentum and the pressure equations, demonstrating excellent convergence.

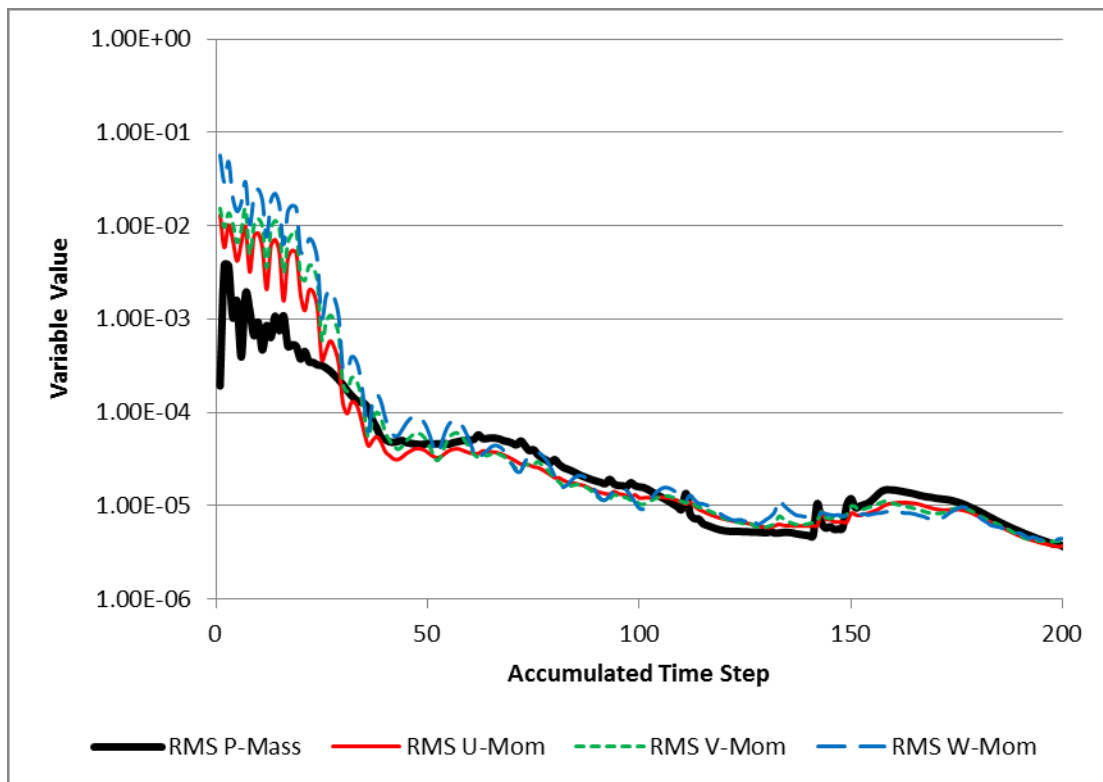


**Figure 2: Convergence history of the governing equations.**

A free slip boundary was used to model the free surface, while other walls were modelled as no slip walls. For the flow conditions that were modelled, the Froude number of the headpond was between 0.11 and 0.38. Additionally, based on the field measurements, there was a very small (0.0016 m/m) free surface gradient. This indicates that the flow through the headpond can be simulated using free surface modelling. The outlet discharge for each of the intakes and the spillway was provided as boundary conditions for the model, and a pressure regulated open boundary was modelled as the upstream boundary.

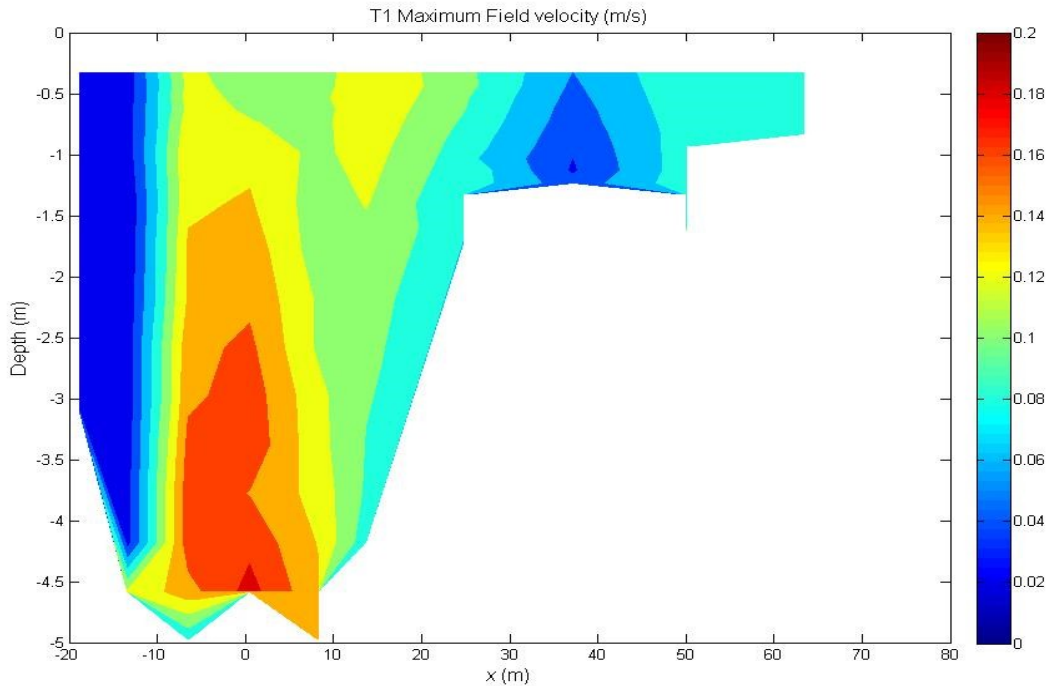
In the model, a rough, non-slip boundary with a roughness height of 0.2 mm was used. The sediment size was noted by NHC (2005) as the mean sediment size measured in a previous

sedimentation investigation report for the facility. The concrete structures including the dam face and the inside of the intake were modelled as smooth non-slip walls as they were constructed of smoothed concrete with minimal surface roughness. Bed material sampling was included in the field measurements of this study, however it was limited to stream bed samples taken adjacent to the western bank of the forebay, in a zone with a relatively shallow, low velocity flow due to lack of access to the main channel for safety reasons. This indicates that the grain size in the middle of the channel is likely larger than what was measured in the current study ( $d_{50} = 0.013$  mm) and the channel bed is predominantly composed of silts near the banks, although the main channel is likely comprised of coarser material ranging in size from silts-sands. The streambed sampling also noted a relatively high ( $>5$ ) coefficient of uniformity for the upstream sediment at ABN suggesting the sediment is relatively non-uniform and that significant gradation is present.

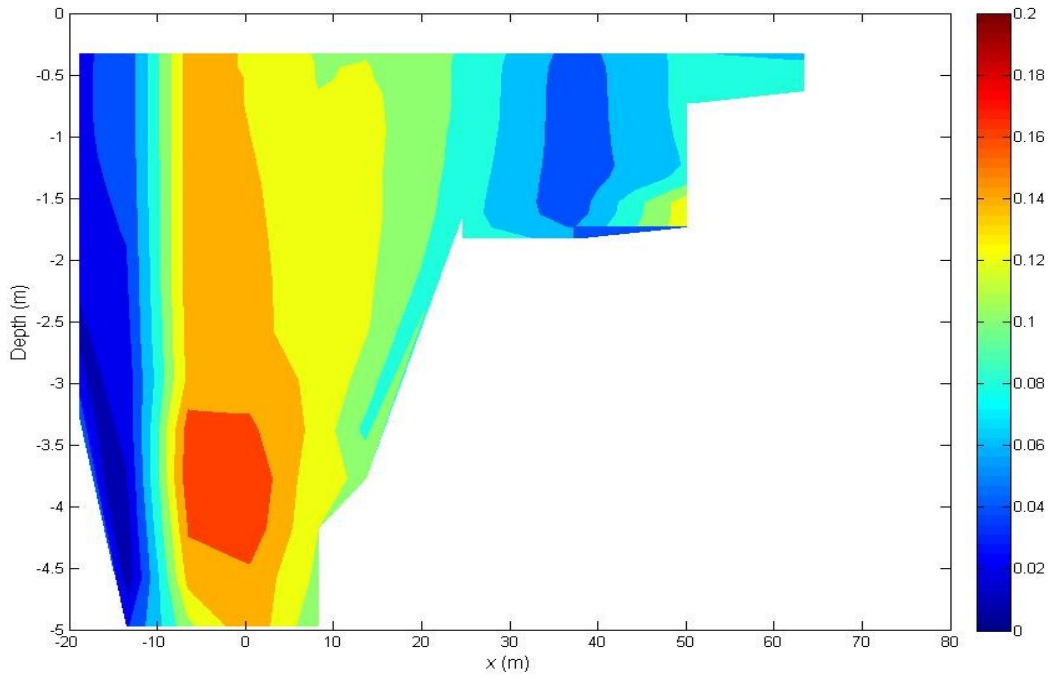
An unstructured tetrahedral mesh has been used in the numerical simulations, with local refinement provided adjacent to the outlets. Throughout the headpond a mesh element size of 0.1 - 0.5 m was specified. Near the intakes (within 20 m or 5 times the equivalent diameter of the intake) a mesh size of 0.05 - 0.1 m was used. A fine mesh which was developed using 1/2 the element size as the coarse mesh was used to investigate the impact of mesh size on the derived results from the CFD model. The fine mesh had an element size of 0.05 - 0.25 m in the upstream headpond, and 0.025 - 0.05 m within the refinement region (20 m of the outlets). The velocity results of the field simulation using the coarse mesh and refined mesh were compared at each of the vertical profiles indicated on Figure 1 (c). For the locations within the refinement region (T1.1, T1.2, T2.1, T2.2) the results using the coarse and fine mesh were within 0.8 % of one

another. For the remaining comparison locations (T1.3, T2.3, T5.1, T5.2, T7.1, T7.2) the results using the coarse and fine mesh were within 1.3 % of one another. As both the coarse and fine mesh yielded similar results, demonstrating mesh independence, the coarser, 1.6 million node mesh was used in the numerical simulations presented herein.

The CFD model was validated using results from the field measurements (Scenario 1 in Table 1). The field measured ADCP velocity profiles throughout the headpond were evaluated against the CFD simulated results. Figure 3(a) and (b) show the field and modelled velocity magnitudes respectively for Transect 1. As the ADCP does not measure velocities all the way to the bed due to backscatter, the cross-section in Figure 3(a) only shows the portion of the transect where data was measured.



(a)



(b)

**Figure 3: Transect 1 velocity magnitude (a) field measured; (b) CFD model.**

In comparing the field measured results with the modelled results it was noted that generally the results match well. The maximum difference in velocity magnitude for transects 1 and 2 was 0.06 m/s, which corresponds to a maximum discrepancy of 20 %. The magnitude of the downstream, transverse and vertical components as well as the trends identified in each of these transects matched well between the model and the field results, with maximum differences of 0.05 m/s, 0.02 m/s and 0.03m/s in each direction respectively. The largest differences, of up to 0.08 m/s were seen in the velocity magnitude at locations adjacent the shorelines in the further upstream transects, which are a greater distance from the intakes. At this distance upstream, the flow is relatively steady, and uniform for a natural stream. The magnitude of the peak was well

predicted by the model, however the location is not. The discrepancy may be due to the fact that the flow is quite shallow in this location, and the wall effects of bathymetry are more pronounced. The model may be improved by the inclusion of more detailed bathymetry throughout the domain. It is also noted that the blanking distance, at the top and bottom of the ADCP profiles is large in comparison to the depth at these points, so a relatively large portion of the transect was not measured in these areas due to instrument limitations.

Vertical profiles of velocity magnitude at locations throughout the headpond are included in Figure 4 for each of the model validation locations shown on Figure 1 (c). On average the field measured velocity magnitudes were 0.02 m/s higher than that modelled velocities using CFD. In some locations, such as those measurements within the scour hole at T1.1 and T1.2 a larger blanking distance was noted in the ADCP measurement due to the proximity of the measurement to a vertical surface (including the dam headwall and scour hole sides). As the ADCP was unable to measure the near-bed velocity, field measurements of the flow field adjacent to the bed were not obtained. There is less certainty of the near bed velocity field that was simulated by the CFD model as field measurements were not obtained. However, based on the comparison between the field measured and CFD simulated flow field, the CFD model accurately describes the flow field that is generated upstream of ABN dam.

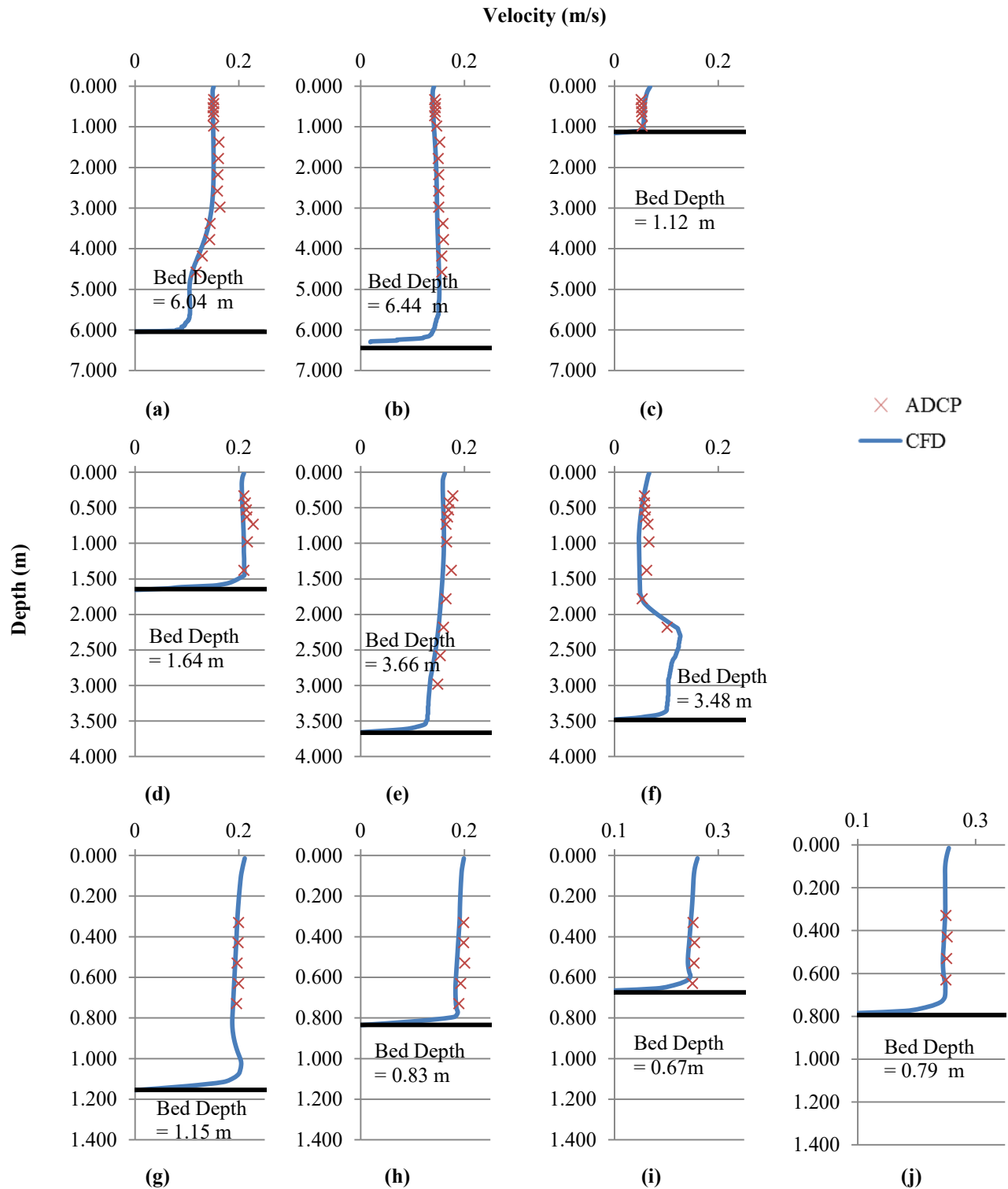


**Figure 4: Field measurements of the velocity magnitude compared with the CFD predictions (a) T1.1; (b) T1.2; (c) T1.3; (d) T2.1; (e) T2.2; (f) T2.3; (g) T5.1; (h) T5.2; (i) T7.1; (j) T7.2;**

## 2.5 Results

### 2.5.1 River Bathymetry and Scour Hole Development

In order to assess the upstream hydraulics of the facility for the purpose of evaluating fish entrainment risk under varied flow conditions, it is important to understand the geometry of the upstream reservoir and potential changes that may occur. The flow velocity field upstream of the ROR facilities is influenced by the sedimentation and erosion processes as well as the seasonally varying stream flows. It is anticipated that annually the bed of the headpond is relatively dynamic, with both sedimentation and scouring happening under varying flow conditions. The analysis completed herein is simplified, with the intention of giving a generalized sense of upstream bed dynamics. Bed shear stress in the CFD model is developed using a “Log-Law of the Wall” iterative procedure computed by (CFX, 2009),

$$\frac{U}{u^*} = \frac{1}{K} \times \ln\left(\frac{\delta u^*}{v}\right) \quad \text{Equation 5}$$

where  $U$  is the velocity at a distance  $\delta$  from the boundary and  $u^*$  is the shear velocity, calculated as  $u_* = \sqrt{\tau/\rho}$ , where  $\tau$  is bed shear stress. Figure 5(a) depicts the modelled bed shear stress for the field scenario. Figure 5(b) shows the wall shear stress distribution for higher flow spring freshet scenario. Figure 5(c) and (d) show the modelled bed shear stress in the vicinity of the intakes, within the scour holes for the field and spring freshet scenarios respectively.

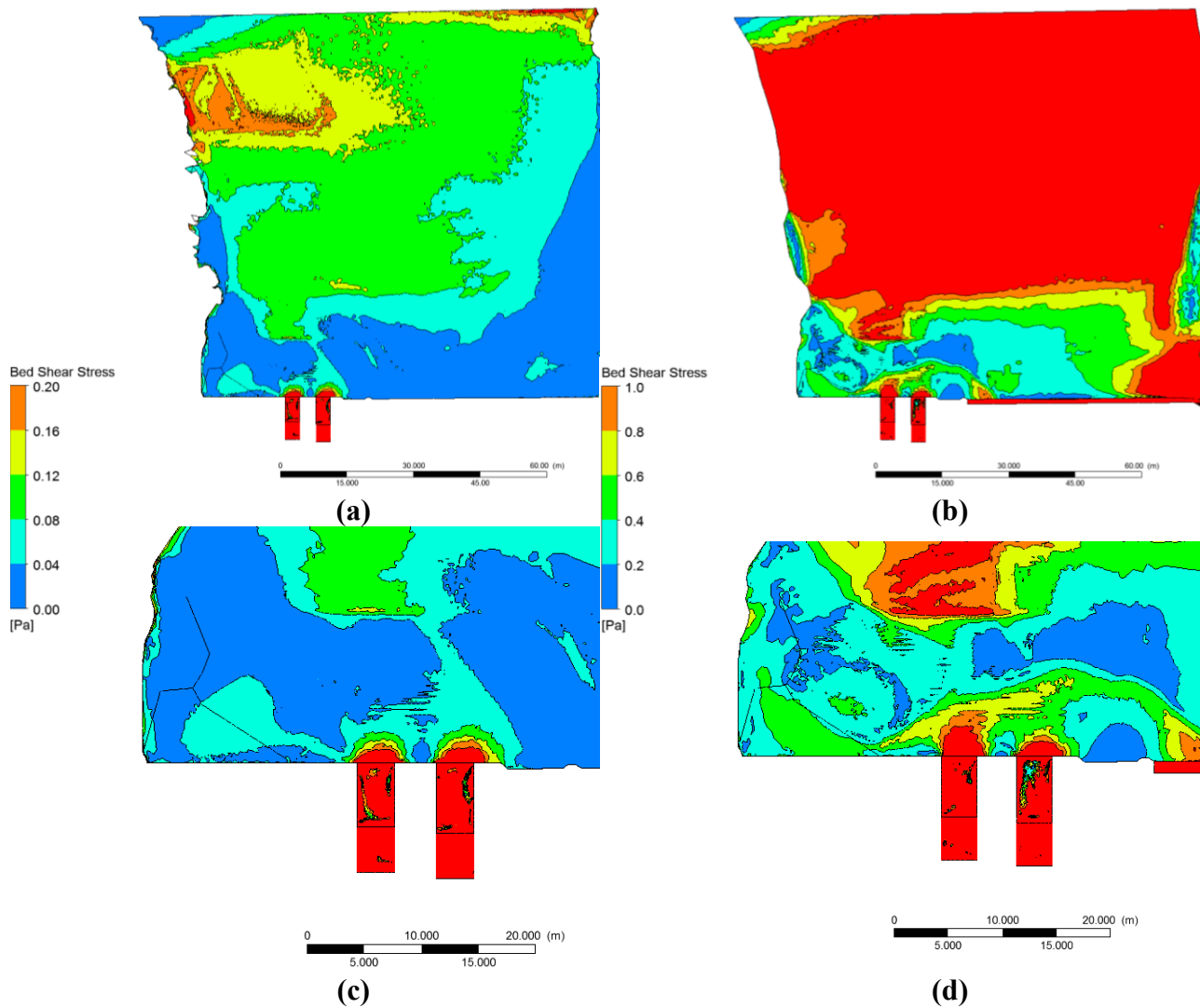


**Figure 5: Bed shear stress (a) field scenario headpond; (b) spring freshet scenario headpond; (c) field scenario scour hole; (d) spring freshet scenario scour hole.**

The USDT (2005) manual states that critical shear stress for non-cohesive fine grained soil ( $D_{75} < 1.3 \text{ mm}$ ) is relatively constant and can be estimated as  $1 \text{ N/m}^2$ . In addition to these guidelines, a procedure has been developed to assess the critical shear stress at which sediment will mobilize. This process can be used to infer what size of sediment particles will be mobilized

under different operational scenarios. When the bed shear exceeds the critical shear stress the sediments will mobilize, while bed shear stresses below critical will allow deposition. In order to assess the critical shear stress for various size sediments, Shields (1936) method and the Soulsby (1997) adaptation have been used. These methods are applicable throughout the flat portions of the headpond, upstream of the scour hole, where the slope of the bed ranges from 0.0079 - 0.0093 m/m. For these methods the critical Shields parameter, a non-dimensional shear stress is defined as,

$$\theta_{cr} = \frac{\tau_{cr}}{d_{50} \times g \times (\rho_s - \rho)} \quad \text{Equation 6}$$

where  $\theta_{cr}$  is the critical Shields parameter,  $\tau_{cr}$ , is the critical shear stress and  $\rho_s$  is the density of the substrate.

A non-dimensional particle diameter was also developed as,

$$D_* = d_{50} \times \left( \frac{g \rho_s}{\rho_w v^2} \right)^{1/3} \quad \text{Equation 7}$$

Soulsby (1997) developed an equation to fit the work previously done by Shields, as well as a modified equation to suit more advanced experiments on fine particles for  $D_*$  ranging from 0.1 – 10 in current driven flows, which is similar to the situation at ABN. The equation developed by Soulsby is as follows:

$$\theta_{cr} = \frac{0.30}{1+1.2D_*} + 0.055(1 - \exp(-0.020 \times D_*)) \quad \text{Equation 8}$$

A plot has been developed to relate the critical, mobilizing bed shear stress for varying particle sizes, see Figure 6.

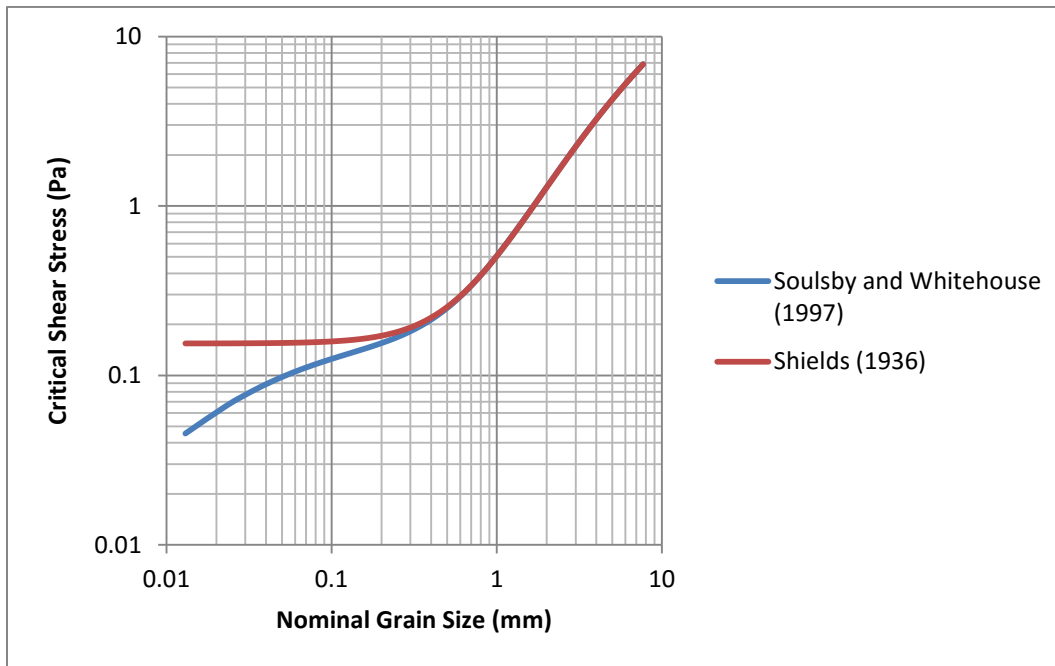


**Figure 6: Critical shear stress for sediment mobilization.**

From the modelled scenarios, it was observed that for freshet scenarios, the bed shear stress varies from 1 – 2 Pa, while at the fall scenario, the wall shear stress is less than 0.8 Pa, which was the established equilibrium shear stress at the time of field measurement. Hence, freshet scenarios (from April to August) are susceptible to sediment erosion as the wall shear stress is above the critical shear stress for particles in the size range of the ABN headpond bed. However, low velocities in winter and outage scenarios may cause deposition of sediments.

In order to assess the depth of the potential headpond erosion in the higher flow freshet scenarios (Scenario 2 in Table 1), the CFD model was re-modelled for varying bed depths. The purpose of this exercise was to investigate at what bed scour depth was the shear stress in the highest flow scenario in the same range as the shear stress in the lowest flow scenarios. It is assumed that the bed depth observed during the field measurements (a lower flow scenario, with a lower wall

shear stress) can be used as a control to identify the actual critical wall shear stress for the sediment present at the ABN facility. By using a threshold value of 0.8 Pa and reducing the elevation of the bed, the potential seasonal bed scour in the spring freshet scenarios can be identified. The method is not exhaustive, as it evaluates the bed shear stress based on a uniform reduction in bed elevation across the entire headpond, which is simplistic. The analysis has however been successful in identifying an approximation of the uniform scour depth that can be anticipated seasonally. By reducing the elevation of the entire headpond by 0.20 m in Scenario 2, an average shear stress across the entire headpond of 0.8 Pa was achieved. Thus, approximately 0.20 m of uniform scour is anticipated to occur seasonally at the ABN facility.

The bathymetry that was measured during the field study at the site in the summer of 2010 is included as Figure 7. The scour hole that was measured during the field measurements is similar to that developed by NHC (2005), though the two studies were fundamentally different. The intake induced scour hole is centred around the intake outlets, and are skewed upstream towards the channel thalweg.

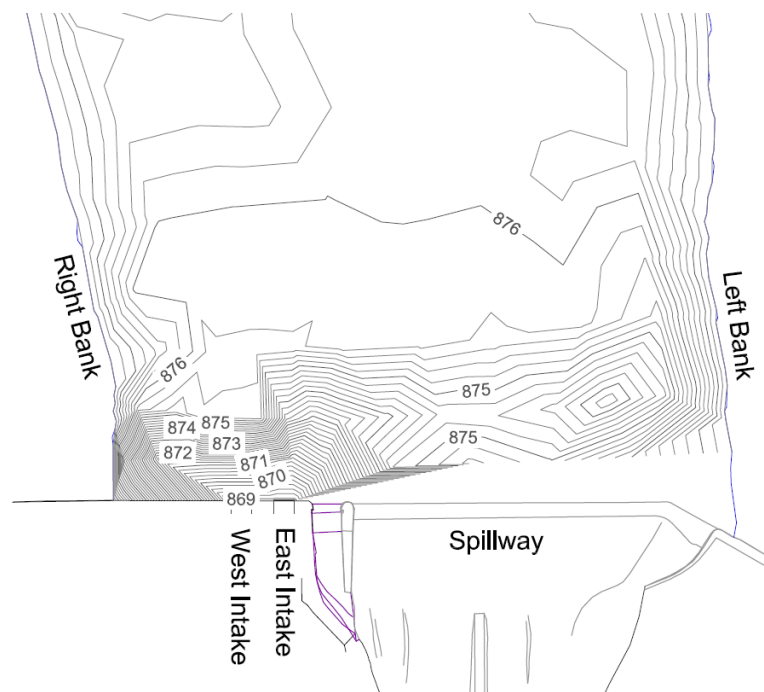


**Figure 7: Field measured bathymetry (all elevation contours are in metres).**

The scour hole side slopes were observed to range from  $15^{\circ}$  –  $26^{\circ}$  in the field. Figure 8 depicts the angle of the scour hole measured at the ABN facility for the west and east intakes. For the west intake the scour hole side slope is  $26^{\circ}$ . The corresponding numbers for the east intake are  $15^{\circ}$ . The results presented in Powell and Khan (2012) in a laboratory study produced a ratio of scour hole length ( $L$ ) to scour hole depth ( $d_m$ ) ranging from 2.78 to 3.45 across the sediment sizes and head scenarios evaluated. This corresponds to an overall average scour hole slope ranging from  $16^{\circ}$  -  $20^{\circ}$ , an envelope that has also been included on Figure 8. Though the Powell and Khan (2012) measured scour holes developed below intakes on a flat bed, the slope of the scour hole that was measured in the field is similar to those measured in the laboratory by Powell and Khan (2012). The consistency of these results might indicate that the score hole shape is less sensitive to the flow field.

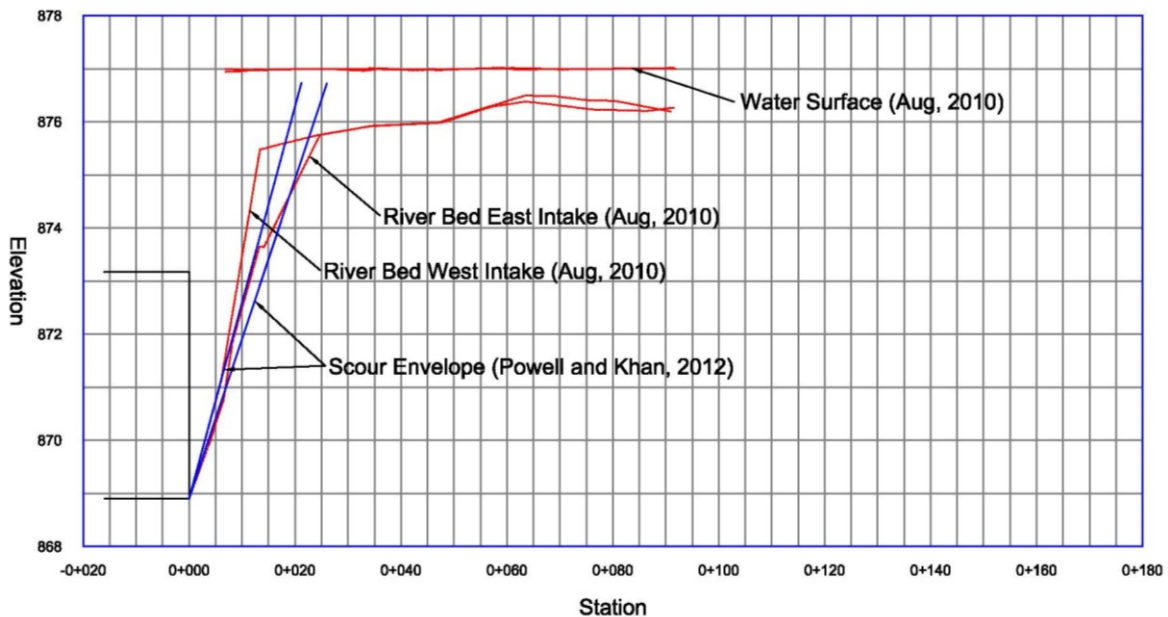


**Figure 8: Headpond profile.**

The angle of repose for wetted sand size sediments is typically in the range of  $26^{\circ}$  -  $34^{\circ}$  (Julian, 2008). Guo *et al.* (2013) also noted the development of side slopes ranging from  $25^{\circ}$  –  $40^{\circ}$  in their laboratory experiments. This suggests that for the west intake, which is nearest the bank the scour hole side slope is at or near the sediments angle of repose. This is adjacent to the local recirculation zone that develops west of the intake and indicates that sedimentation here is gravity driven. The east intake scour hole side slope, which has a shallower slope and extends further towards the channel thalweg however is well below the anticipated angle of repose. Towards the channel centre the form of the scour holes is strongly affected by the bed shear stresses generated by the facilities operations.

The scour hole geometry that was measured in the field, was included in the CFD model. The bed shear stress of the scour hole, as simulated by the CFD model developed for ABN is

depicted in Figure 5 (c) and (d) for the field and freshet condition respectively. It can be noted that the shear stress induced by the flow under both conditions within the scour hole result in a similar shear stress between each of the intakes in both scenarios, despite the difference in slope. In the lower flow field scenario, a shear stress of approximately 0.06 Pa was simulated within the scour hole. For the higher flow freshet scenario bed shear stresses are an order of magnitude greater at 0.4 Pa. It can also be noted that the shear stress throughout the scour hole is more uniform in the field scenario. It is anticipated that increased discharge through the dam will mobilize fine sediments occupying the scour hole in low flow conditions, increasing the size of the scour hole. Under these high flow conditions, it is anticipated that the scour hole size will continue to increase due to erosion until an equilibrium shear stress in the range of 0.06 Pa is generated by the flow field. The shear stress generated by the flow is the primary physical factor in determining the shape of the scour hole upstream of the intake at the ABN facility. Using CFD to analyze the shear stress within the scour hole under varying operating conditions for different geometries provides a means of assessing the size and extent of scour hole development.

### ***2.5.2 Upstream Hydraulics and Fish Entrainment Risk***

The CFD model that was developed for the current study was subsequently used to simulate forebay hydraulics at the ABN Dam under the field scenario, which is a low flow scenario, and a spring freshet scenario (Table 1). The model inputs, including the outlet discharge and headpond surface elevation are outlined in Table 1. Under each of these scenarios the flow stream lines, and velocities were modelled.

Figure 9 (a) and (b) depict the simulated velocity contours within the headpond of the ABN facility for the field and spring freshet scenarios respectively at an elevation of 876.504 (0.5 m depth in Scenario 1 Table 1, 0.9 m depth in Scenario 2 Table 1). Figure 9 (c) and (d) describe the simulated velocity field at an elevation of 872.004 (5.0 m depth in Scenario 1 Table 1, 5.4 m depth in Scenario 2 Table 1), within the scour hole for the field and freshet scenarios respectively. In the lower flow scenarios, which reflect the facilities operations in the fall and winter seasons, the water velocity magnitude throughout the headpond is relatively small, and does not exceed 0.3 m/s, except when the spillway is operational. As the spillway is not operational during low flow conditions, a low velocity zone ( $< 0.1$  m/s) is noticed extending from the scour hole to the eastern bank of the headpond. Conversely, in higher flow scenarios, high velocity currents are present throughout the headpond, specifically as the headpond shallows approximately 80 m upstream of the dam headwall, as the headpond inlet is approached.

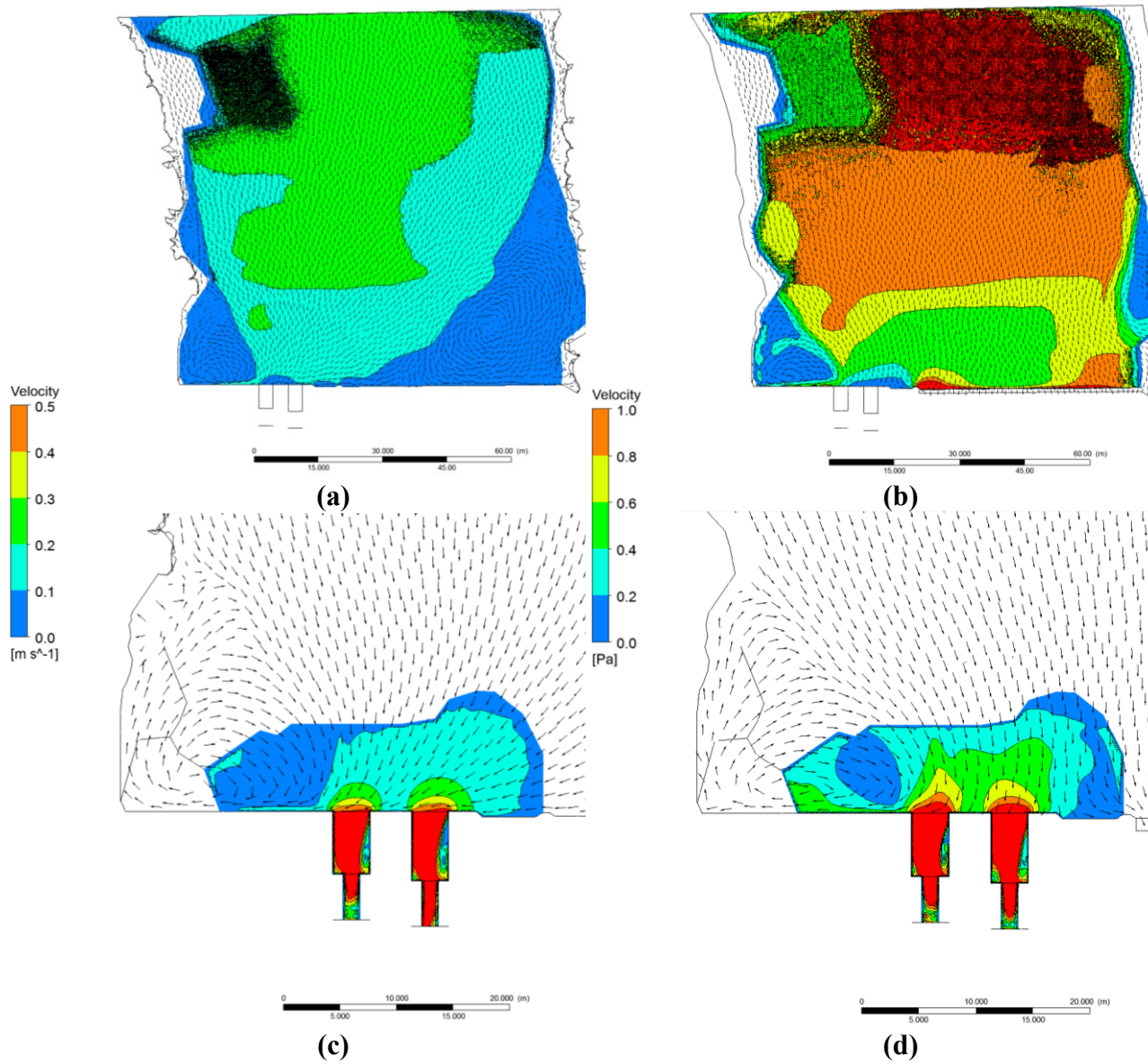


**Figure 9: Plan contours of velocity magnitude (a) field scenario elevation 876.504 (0.5m depth); (b) spring freshet scenario elevation 876.504; (c) field scenario elevation 872.004 (5m depth); (d) spring freshet scenario elevation 872.004.**

Figure 10 shows the velocity contours at two longitudinal sections perpendicular to the dam head wall for (a) the field and (b) spring freshet scenarios. The first section is located at the centre of

the East intake, and the second section is located 45 m east of the first section. In the lower flow field scenario, the acceleration zone developed by the intake is local to the intake and is completely contained within the scour hole. As such, direct entrainment of fish will only occur for fish utilizing habitat within the scour hole. Approximately 40 m upstream of the intake larger velocities, exceeding 0.2 m/s are simulated due to the shallowness of the channel. For the freshet scenario, the velocity 40 m upstream of the dam head wall is greater than 0.7 m/s. Hence, during freshet scenarios, fish may have a higher risk of entrainment. It is noteworthy that the velocity 80 m upstream of the dam head wall is always greater than the velocity at the 40 m transect, as water depth is shallower at the 80 m transect compared to the 40 m transect. It is observed that the velocity at the 80 m transect is greater than 0.1 m/s in all the scenarios. As fish's swimming speed depends on its body length (RL&L 2000), large adult fish (> 300 mm) may not be susceptible to entrainment during winter and fall scenarios. However, small and/or juvenile fish may be at risk of entrainment year round. It was also observed that the velocity in the main channel at >30 m upstream of the dam headwall is fairly uniform and can be approximated by  $Q/A$ , where  $Q$  is the total flow-rate and  $A$  is the cross-sectional area.

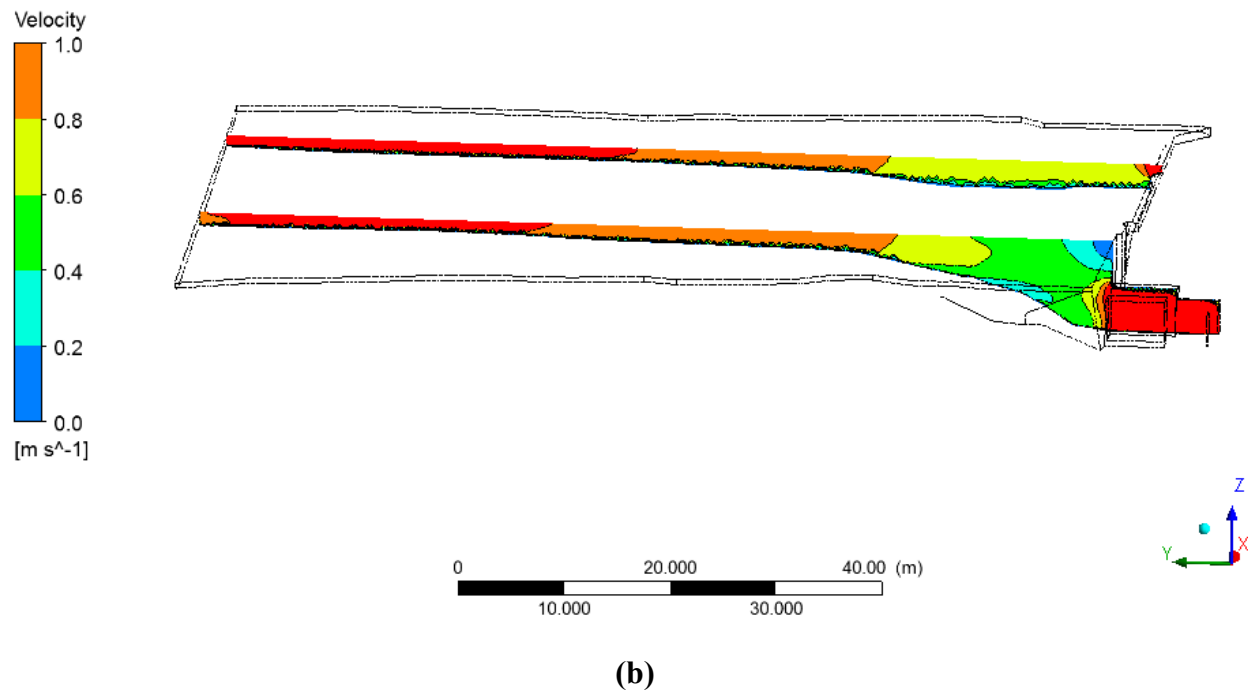
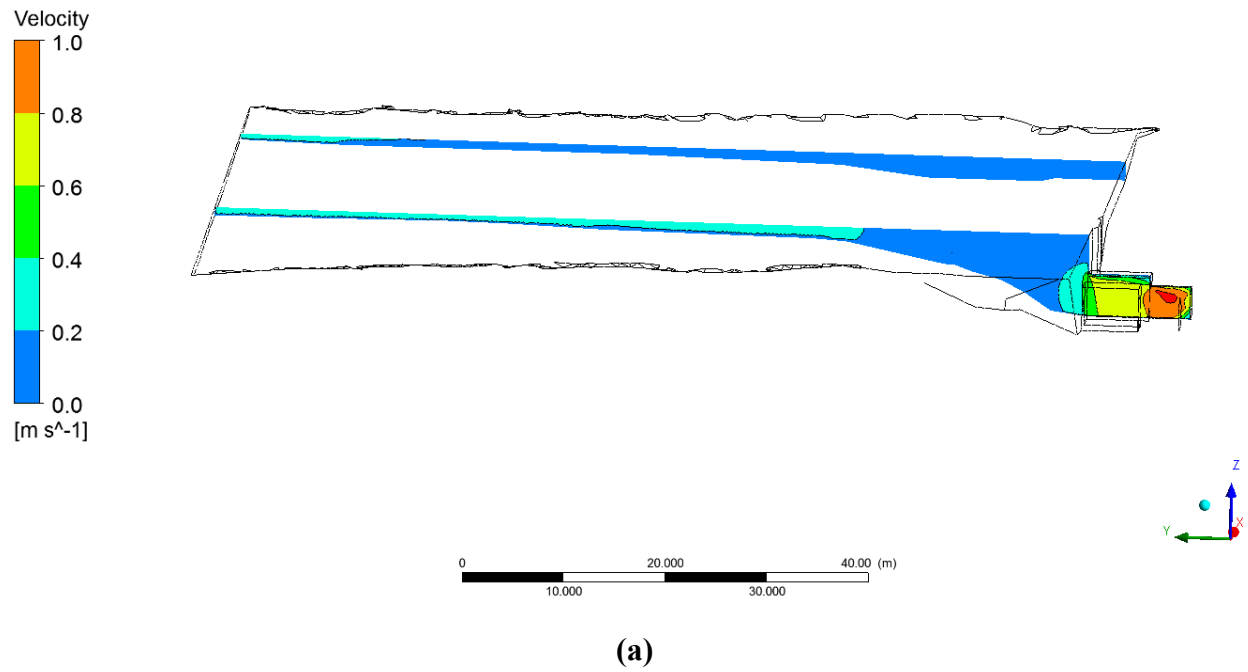
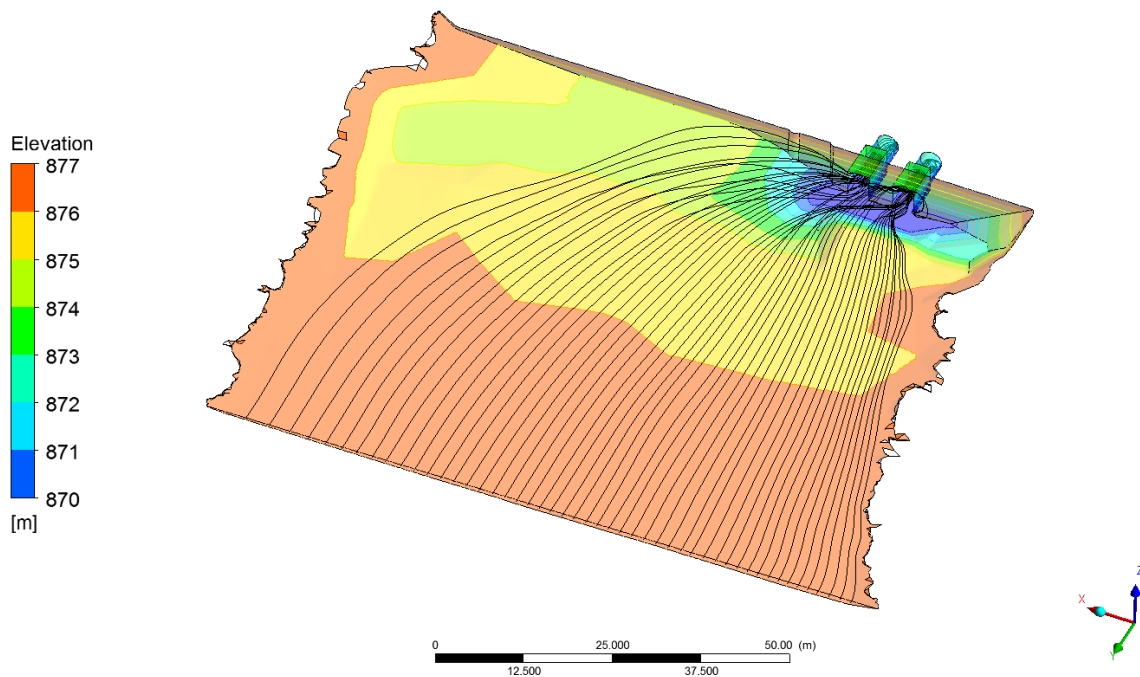


**Figure 10: Perpendicular profile contours of velocity magnitude (a) field scenario; (b) spring freshet scenario.**

Velocity distribution across the channel in the local scour section (<30 m) from the dam is characterized by the greatest velocities extending from the intakes towards the channel centres. Relatively low velocity zones occupy the shallow littoral zone near the left and right banks, extending approximately 8 m from the East bank, and into the scour hole on the West bank. It is evident from the CFD modelling that the hydraulics of the ABN headpond has a direct impact on the size and geometry of the scour hole, which in turn has an impact on the evaluation of fish entrainment risk in this acceleration or “risky” zone. Within the scour hole, adjacent to the intakes a slower moving recirculation zone is present in all the simulated conditions west of the west intake. The recirculation zone, which is present at all depths within the reservoir may provide a haven for fish occupying the scour hole.

Stream lines were generated for each of the model scenarios showing flow paths through the headpond. For the field scenario, the stream lines are depicted as Figure 11(a). Figure 11(b) shows the stream line plot for a high flow spring freshet scenario (Scenario 2). The streamlines depicted in Figure 11 are three-dimensional streamlines, originating at the upstream boundary. At this water surface elevation, it can be shown that the bathymetry does not affect the flow pattern, and stream lines are parallel throughout the flow domain. Alternatively, the stream lines in the shallower field scenario show prominent bathymetry effects. In the CFD model, the sand bar located upstream of the intakes is found to deflect the stream lines, and flow enters the intake obliquely as observed in Figure 11(a). The deflection in the stream lines upstream of the spillway is possibly caused by a 1 m deep pool located close to the east bank. Similar effects are also shown in other scenarios, for shallow flows, when the spillway is not active. The regions where the stream lines are deflected are areas that are occupied by recirculation zones. Figure 9

(c) and (d) shows an example of such a recirculation zone close to the intakes. These recirculation zones, which are not occupied by streamlines, occur at both the East and West banks, and cause the slow moving zones occupying the littoral zones adjacent to the dam structure. As mentioned earlier, these circulation zones are not seen upstream where the headpond shallows (>30 m upstream of the dam face).



(a)

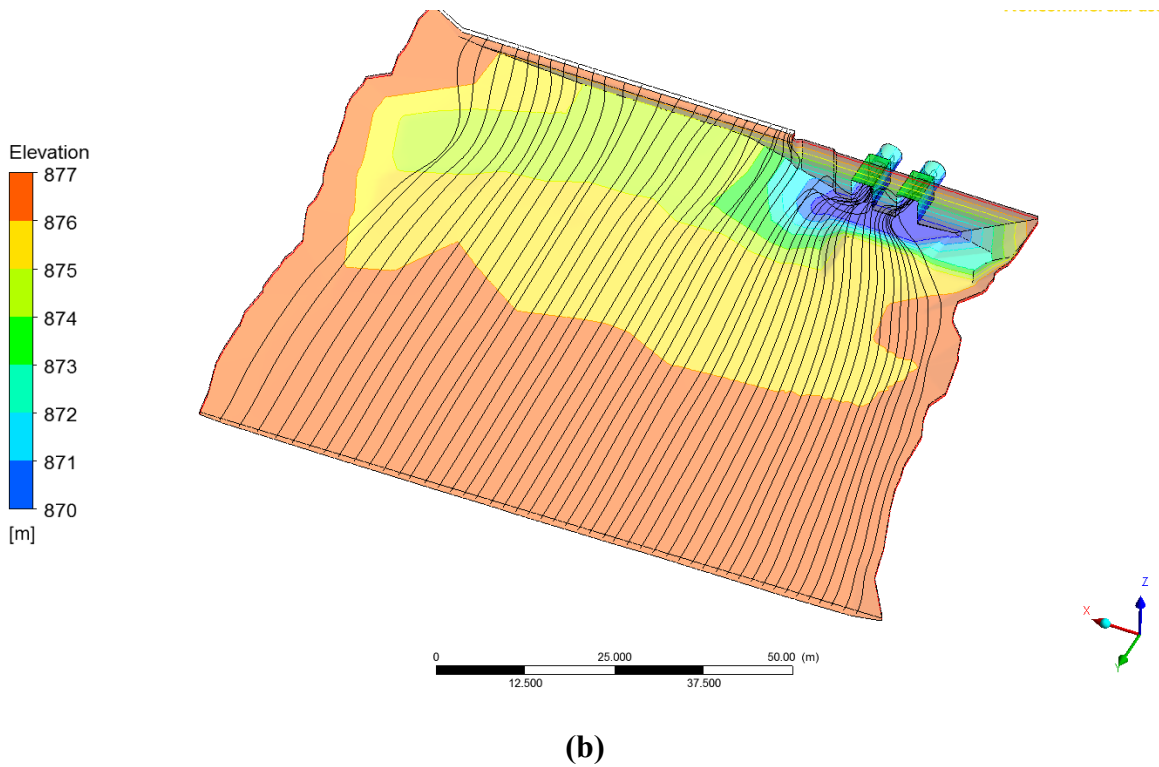


**Figure 11: Headpond streamlines (a) field scenario; (b) spring freshet scenario.**

At the time of field investigation, adult salmonids (primarily westslope cutthroat trout with body lengths of approximately 300 mm) were visually noted to be occupying the scour hole at ABN. The headpond is used by both westslope cutthroat trout and mountain whitefish during all seasons. It has been noted that 58.3% of westslope cutthroat trout and 57.7% of mountain whitefish upstream of the dam use the headpond at some point over the course of the year. The scour hole adjacent to the intake is particularly heavily utilized by overwintering fish with 40.9% of westslope cutthroat trout and 43% of mountain whitefish in the Upper Bull River System overwintering in the headpond of the facility. The formation of the local scour hole is an attractant to sub-adult and adult fish during all seasons due to the foraging afforded by diverting nutrient rich flows through the intakes. Mountain whitefish are of particularly high risk, with a

large proportion of fish spending overwintering as well as spawning periods adjacent to the intakes (Westslope Fisheries Ltd., 2012).

In order to assess the portion of the scour hole that is of high entrainment risk for fish occupying the scour hole the proportion of the lateral transects, parallel to the dam, located 1 m, 2 m and 5m upstream of the dam exceeding threshold velocities of 0.1 m/s and 0.5 m/s were tabulated in Table 2.

**Table 2: Proportion of upstream transects exceeding threshold velocities.**

<b>Scenario</b>	<b>Transect Distance (m)</b>	<b>Proportion Exceeding 0.1 m/s</b>	<b>Proportion Exceeding 0.5 m/s</b>
<b>Field</b>	<b>1</b>	44%	0%
	<b>2</b>	48%	0%
	<b>5</b>	51%	0%
<b>Spring Freshet</b>	<b>1</b>	99%	39%
	<b>2</b>	90%	37%
	<b>5</b>	94%	41%

As noted in Table 2, within the scour hole, typically the distance upstream does not have a significant impact on the extents of the entrainment zone. The threshold values presented here are based on the swimming distance curves developed for 200 mm body length anguilliform (locomotion achieved through lateral oscillation of the entire body) mode swimmers (0.1 m/s) and subcarangiform (locomotion achieved through lateral oscillation of the rear 2/3 of the body, with minimal head movement to reduce drag) mode swimmers (0.5 m/s) (Katopodis, 1992). Of the species of interest at the ABN facility, both westslope cutthroat trout and mountain whitefish

exhibit subcarangiform swimming modes. Fraley and Sheppard's (2005) observations of westslope cutthroat trout identified that in a sample of 843 individuals, fish below the age of 3-4 are likely to be below the 200 mm body length noted by Katopodis (1992). A similar study by McPhail and Troffee (1998) on mountain whitefish identified that age zero fish (young of year) generally fall below the 200 mm threshold, while much larger fish exist within the Columbia River basin. Mature fish of both species exhibit similar body lengths based on the Fraley and Sheppard (2005) and McPhail and Toffee (1998) studies. Thus, in low flow scenarios, juvenile and/or age zero fish may be at high entrainment risk for these areas adjacent to the dam structure, especially within the scour hole. During high flow scenarios, entrainment of juvenile and/or age zero fish is likely in all areas adjacent to the dam. This includes entrainment via both the spillway and the intakes. Additionally, larger fish may also be entrained in these higher flow scenarios.

Mitigating fish entrainment at ABN and other facilities is of high importance for hydropower operators. At the ABN facility, fish entrainment risk is primarily due to the infilling of the headpond with sediments and the formation of the scour hole adjacent to the intakes. The shallow upstream headpond, which has little cover from predators, and an increased velocity (generally greater than 2 times the velocity of the deeper scour region), restricts the habitat available for summer holding and overwintering. One of the primary options available for mitigating fish entrainment is to establish holding and overwintering habitat that is not directly adjacent to the hydropower intakes. This can be done by revising the annual dredging program to provide suitable, deeper, lower velocity habitat away from the intakes. The program has in previous years focused on expanding the depth of scour hole (SEC, 2014). Extending the scour

hole east along the spillway would expand the suitable habitat available for fish species. It also reduces the amount of sediment that is drawn through the hydropower facility annually and the associated wear-and-tear on the turbomachinery. Dredging provides a means of modifying the upstream geometry and flow field of the headpond without introducing nets that cause dam safety issues. It also provides a means to reduce fish density and the associated entrainment risk adjacent to the intakes by increasing habitat availability.

The CFD modelling that was completed through the current study indicated the geometry of the forebay resulted in establishing slow-moving recirculation zones, which are ideal fish habitat. The incorporation of built-in groins in the headpond may provide additional habitat. The orientation of the groins could be designed to reduce in-filling the recirculation zones with sediment.

During seasons where higher fish densities are expected or noted adjacent to the intakes, the operator may modify operations to mitigate entrainment risk. Available options include decreasing the discharge, modifying the amount of discharge through each outlet structure, or complete shutdowns if necessary. The CFD model provides a tool to evaluate the impacts of these operational modifications on upstream fish entrainment risk.

## **2.6 Concluding Remarks**

The current study analyzed the flow-field and wall shear stress in the forebay area of the ABN hydropower generating facility. The ABN Dam is a ROR facility, which has a shallow-depth forebay area. A 7 m deep scour hole has been created in close proximity to the intakes due to the high velocity created by the intakes. A field study was completed upstream of the facility to

investigate flow fields and to measure bathymetry. This information was used to validate a numerical model of the forebay. Two flow conditions have been analyzed using the CFD model: low flow field condition and the high flow freshet condition.

The wall shear stress generated by the CFD model is found to exceed the critical shear stress during freshet scenarios, which may cause sediment erosion throughout the headpond. During the winter and fall scenarios, the shear stress is below the critical shear stress, and clear water conditions should prevail. However, low velocities in these scenarios, may cause deposition of silts at the forebay area. The headpond is anticipated to be dynamic and fluctuate over the course of the year. A bed shear stress of 0.8 Pa is the dynamic equilibrium stress present in the fall at the facility. Using this as a threshold value and varying the bed elevation in higher flow scenarios determined a potential annual uniform fluctuation of approximately 0.20 m is anticipated ABN. The analysis presented is simplified, with the intention of describing the scale of bed form dynamics, as it affects the upstream flow structure of the headpond.

The scour hole adjacent to the intakes at ABN has sidewall angles below the anticipated angle of repose for the local substrate. The scour hole developed at the ABN facility has a similar slope as those produced by Powell and Khan (2012), demonstrating a similarity between scour holes developed below intakes on a flat-bed (as in the laboratory) and those formed with upstream beds extending above the intakes (as in the field). The variability in the flow conditions studied by Powell and Khan (2012) and the current study and the similarity of the results may indicate that the form of the scour hole is not sensitive to the flow field. The use of CFD is a promising analytical tool for assessing the probability and magnitude of scour hole deformation, if used to

analyze wall shear stress for different scour geometries. The inclusion of morphodynamics in the CFD model may provide more detailed results, while being less computationally efficient.

At distances greater than 30 m upstream of the dam head wall, the headpond shallows, and the velocity distribution is nearly uniform over the cross-section. During freshet scenarios, the mean velocity can exceed 50 cm/s and fish may be susceptible to entrainment. However, recirculation zones close to the intakes and banks may provide a haven for the fish to escape from entrainment. Due to the headpond's shallowness, the velocity at a distance 80 m upstream of the dam head wall is greater than 0.1 m/s at all times of the year. Therefore, small and/or juvenile fish may be at risk of entrainment under all scenarios. Fast moving flow mimics the nature of riverine flows and may result in fish orienting themselves in the direction of the flowing water, leading them into the intakes (Westslope Fisheries Ltd., 2012).

By combining the knowledge gained through both detailed telemetry and hydraulic modelling studies at the ABN headpond, it is evident that the entrainment rates of 24 % and 19.2 % of westslope cutthroat trout and mountain whitefish respectively is affected by both the dam's impacts on the upstream hydraulics as well as on the upstream reservoir morphology. The formation of a sediment infilled headpond, with a local scour hole creates the unique conditions in which upstream riverine fish are oriented toward to the optimal habitat created by the scour hole. Within the scour hole, deeper overwintering habitat and foraging opportunities attract both these species to the scour hole, which is partially occupied by a fast moving risky zone. The fish attraction to this zone, greatly increases the fish density adjacent to the intakes, which perhaps has the greatest impact on entrainment risk, as opposed to swimming capability. Reducing fish density by providing alternate habitat through dredging sediments in locations not adjacent to the

intakes would be an effective means to reduce entrainment risk. Alternatively, establishing additional recirculation zones, by targeted dredging and/or installing built in-groins also would reduce fish density adjacent to the intakes.

The current research investigates the role of CFD modelling in environmental management and habitat management, which can be extended to larger facilities, with different geometric and operational configurations. The completion of field work to measure the upstream headpond hydraulics of a hydropower facility under vary operational conditions may be cost prohibitive. The completion of a numerical modelling study is a more cost effective approach; as simulations can be rapidly run for vary operational scenarios. From these results engineers, planners and biologists can make inferences on the impact of the dam on upstream fish (individuals and populations), providing a proactive measurement for habitat management for the hydropower facility. CFD may also be used to analyze retrofitting schemes to establish low velocity zones within the forebay for habitat management (such as dredging and built in groins). Additionally, the CFD modelling of flow induced bed shear stresses can be used to assess the likelihood of sediment deposition and sediment re-entrainment into the headpond's flow. This may allow the utility to forecast the rate of sedimentation, if there is a point at which the headpond bed form will reach a dynamic equilibrium and assist in evaluating requirements for sediment removal (dredging, flushing, etc.).

## **2.7 Acknowledgements**

The authors would like to thank Paul Higgins of BC Hydro for providing information used in the completion of the current study. Additionally the authors would like to thank Teal Moffat, Emily (Xue) Chen and Gregory Courtice for assistance in the collection of field data and Kurt

Morrison for analyzing the sediment samples. Funding for this research was provided by the Natural Sciences and Engineering Research Council of Canada (NSERC) and NSERC Hydronet.

## 2.8 References

- Amaral, S. V., Hecker, G. E., and Dixon, D. A. (2011). "Designing leading edges of turbine blades to increase fish survival from blade strike," *EPRI-DOE, Conference on Environmentally-Enhanced Hydropower Turbines*, WA. Pages 2-39 to 2-48.
- Basson, G. R., & Olesen, K. W. (1997). "Modelling flood flushing". *International Water Power & Dam Construction*, 49(6), 40-41.
- BC Hydro (2006). "Fish entrainment risk screening and evaluation methodology", BC Hydro, Report No. E478. 101 pages.
- Bryant, D. B., Khan, A. A., & Aziz, N. M. (2008). "Investigation of flow upstream of orifices". *Journal of Hydraulic Engineering*, 134(1), 98-104.
- CFX (2009). "ANSYS CFX solver theory guide", Release 12.0, ANSYS Inc., PA 15317.
- Coutant, C.C., Whitney, R.R. (2000). "Fish behaviour in relation to passage through hydropower turbines: a review". *Transactions of the American Fisheries Society*, 129(2), 351-380.
- Enders, E.C., Gessel, M.H., Anderson, J.J., & Williams, J.G. (2012). "Effects of decelerating and accelerating flows on juvenile salmonid behavior", *Transactions of the American Fisheries Society*, 141(2), 357-364.
- EPRI (1992). Fish entrainment and turbine mortality review and guidelines. Stone & Webster Environmental Service, Boston, Massachusetts. 285 pages.

- Fraley, J., Sheppard, B. (2005). "Age, growth, and movements of westslope cutthroat trout, *Oncorhynchus clarki lewisi*, inhabiting the headwaters of a wilderness river". *Journal of Northwest Science*, 79(1), 12-21.
- Francois, M., Vinh, P., and Mora, P. (2000). "Fish friendly kaplan turbine," "*Proceedings of the 20th IAHR Symposium on Hydraulic Machinery and Systems*", Charlotte, NC, Paper No. ENV-03.
- Goodwin, R.A. (2004). "Hydrodynamics and juvenile salmon movement behavior at Lower Granite Dam: decoding the relationship using 3-D space-time (Cel Agent IBM) simulation". Ph.D. Thesis, Cornell University. 213 pages.
- Google. (2015). Google Maps, <<http://www.maps.google.com>> (August 29, 2015).
- Guo, S., Shao, Y., Zhang, T.Q., Zhu, D.Z., Zhang, Y.P., (2013). "Physical modeling on sand erosion around defective sewer pipes under the influence of groundwater", *Journal of Hydraulic Engineering*, 139(12), 1247–1257.
- Julien, P. (2008). "Erosion and sedimentation". Cambridge University Press, Cambridge, UK.
- Katapodis, C. (1992). "Introduction to fishway design". Freshwater Institute, Central and Arctic Region, Department of Fisheries and Oceans Canada, Winnipeg, Manitoba. 70 pages.
- Katapodis, C., Kells, J.A., Acharya, M. (2001). "Nature-like and conventional fishways: alternative concepts?", *Canadian Water Resources Journal*, 26(2), 211-232.
- Katapodis, C., Williams, J.G. (2012). "The development of fish passage research in a historical context". *Ecological Engineering*, 48, 8-18.
-

Khan, L.A., Wicklein, E.A., Rashid, M., Ebner, L.L., and Richards, N.A. (2004).

“Computational fluid dynamics modeling of turbine intake hydraulics at a hydropower plant”, *Journal of Hydraulic Research*, 42(1), 61-69.

Khan, L.A., Wicklein, E.A., Rashid, M., Ebner, L.L., and Richards, N.A. (2008). “Case study of an application of a computational fluid dynamics model to the forebay of the Dalles Dam, Oregon.”, *Journal of Hydraulic Engineering*, 134(5), 509-519.

Lai, J.-S., & Shen, H. W. (1996). “Flushing sediment through reservoirs”. *Journal of Hydraulic Research*, 34(2) , 237-255.

Liu, J., Minami, S., Otsuki, H., Liu, B., & Ashida, K. (2004). “Prediction of concerted sediment flushing”. *Journal of Hydraulic Engineering* , 130(11), 1089-1096.

McPhail, J.D., Troffee, P.M. (1998). “The mountain whitefish (*Prosopium williamsoni*): a potential indicator species for the Fraser system”, Department of Zoology, University of British Columbia, Vancouver, BC. Prepared for: Environment Canada, Report No. DOE FRAP 1998-16. 71 pages.

Meselhe, E.A., and Odgaard, A.J. (1998). “3D numerical flow model for fish diversion studies at Wanapum dam”, *Journal of Hydraulic Engineering*, 124 (12), 1203-1214.

NHC (2005). “Aberfeldie redevelopment project, hydraulic model study, final report”, Northwest Hydraulic Consultants, 2005. Prepared for BC Hydro. 92 pages.

NPP (2005). “Fish entrainment and mortality study, Vol 1, Niagara Power Project”, New York Power Authority. 162 pages.

Powell, D.N, Khan, A. (2012). “Scour upstream of a circular orifice under constant head”.

*Journal of Hydraulic Research*, 50(1), 28-34.

Powell, D.N., Khan, A. (2015). “Flow Field Upstream of an Orifice under Fixed Bed and Equilibrium Scour Conditions”, *Journal of Hydraulic Engineering*, 141(2), 04014076 1-8

Rakowski, C.L., Richmond, M.C., Serkowski, J.A., Ebner, L. (2002). “Three dimensional simulation of forebay and turbine intakes flows for the Bonneville project”, *Proc., of HydroVision 2002*, Oregon. Paper No. 137

Rakowski, C.L., Richmond, M.C., Serkowski, G.E. Johnson (2006). “Forebay computational fluid dynamics modeling for the Dalles Dam to support behaviour guidance system siting studies”, Pacific Northwest National Laboratory. Richland, WA. 37 pages.

Rakowski, C.L., Richmond, M.C., Serkowski, (2010). “Bonneville powerhouse 2 3D CFD for the behavioural guidance system”, Pacific Northwest National Laboratory. Richland, WA. 39 pages.

Rakowski, C.L., Richmond, M.C., Serkowski, (2012). “Bonneville Powerhouse 2 guidance efficiency studies: CFD model of the forebay”, Pacific Northwest National Laboratory. Richland, WA. 104 pages.

RL&L (2000). “Resident fish entrainment information review”, RL&L Information Services Ltd.

Sale, M. J., Cada, G. F., Rinehart, B. N., Sommers, G. L., Brookshier, P. A., and Flynn, J. V. (2000). “Status of the US Department of Energy’s advanced hydropower turbine

systems program,” Proceedings of the 20th IAHR Symposium on Hydraulic Machinery and Systems, Charlotte, NC, Paper No. ENV-01. 10 pages.

SEC (2014). “Routine Maintenance Dredging: Aberfeldie Dam, Bull Rive, B.C.”, SEC Project No. 003-04.1, 19 pages.

Shammaa, Y., Zhu, D.Z., Rajaratnam, N. (2005). “Flow upstream of orifices and sluice gates.” *Journal of Hydraulic Engineering*, 131(2), 127-133

Shen, H. W. (1999). Flushing sediment through reservoirs”. *Journal of Hydraulic Research*, 37(6), 743-757.

Shields, I.A. (1936). “Application of similarity principle and turbulence research to bed-load movement”. Translated by United States Department of Agriculture Soil Conservation Service Cooperative Laboratory, California Institute of Technology, Pasadena, California. By: Ott, W.P. and van Uchelen, J.C. 27 pages.

Soulsby (1997). “Dynamics of marine sands”, Thomas Telford Publications, Thomas Telford Services Ltd., Heron Quay, London.

USDT (2005). “Design of roadside channels with flexible linings”, Federal Highway Administration, United States Department of Transportation. 154 pages.

Westslope Fisheries Ltd. (2012). BC Hydro Aberfeldie dam fish entrainment strategy Bull River fish entrainment – telemetry study. Prepared for BC Hydro. 94 pages.

Wicklein, E.A., Khan, L.A., Rashid, M., Deering, M.K., and Nece, R.E. (2002). “A three dimensional computational fluid dynamics model of the forebay of Howard Hanson dam”, Washington, Proc., Hydro Vision 2002, Portland, Oregon.

Xue, W., Huai, W., Li, Z., Zeng, Y., Qian, Z., Yang, Z. (2013). “Numerical simulation of scouring funnel in front of bottom orifice,” *Journal of Hydrodynamics*, 25(3), 471-480.

## Chapter 3

# Hydropower Intake-induced Fish Entrainment

## Risk Zone Analysis

---

Mathew T. Langford, David Z. Zhu, Alf Leake, Steven J. Cooke

### 3.1 Abstract

Evaluating the impacts of hydropower intake operations on upstream aquatic habitat is important for the development of environmentally sustainable sources of energy and flood protection. A computational fluid dynamic model was used to simulate the flow field in the forebay of a high dam, Mica Dam in British Columbia, Canada. The model evaluated the upstream hydraulics under varying operational conditions and reservoir levels. This model, which was verified by a novel means of collecting acoustic Doppler current profiler field measurements, highlights how intake selection may suppress vortex formation and limit the volume of the forebay occupied by the entrainment risk zone. Additionally, a potential flow solution was applied to predict the velocity field induced by Mica Dam and the limitation of the potential flow solution was assessed. By linking the detailed knowledge developed of the forebays hydraulics to fish behaviour, the impact of fish habitat use on the entrainment risk zone is also discussed in the context of hydropower optimization.

### **3.2 Key Words**

Computational Fluid Dynamics; CFD Model Verification; Fish Entrainment; Hydraulic Engineering; Hydraulic Models; Intake; Reservoir Forebay; Thermal Stratification

### **3.3 Introduction**

The construction of high head dams around the globe for flood protection and hydropower production has resulted in the impoundment of large rivers and thus the creation of deep reservoirs. Reservoirs create different thermal and flow characteristics relative to pre-impoundment riverine conditions that may lead to changes in fish assemblage as lotic-adapted species are replaced by lentic species. Nonetheless, many reservoirs support vibrant recreational, commercial and subsistence fisheries which contribute to livelihoods, economic development and food security. For high head dams, where bi-directional fish passage is technically challenging or not feasible, upstream and downstream fish populations have limited connectivity (Schilt, 2007). The normal feeding and rearing habits and basic movement ecology of fish upstream of dams may place them close to hydropower intakes at varying times during the year, thus influencing entrainment risk (Coutant and Whitney, 2000; Martins et al. 2013). Fish that become entrained – irrespective of fate – are removed from the reservoir population.

Fish entrainment has been identified as one of the key potential impacts of hydropower operations on the productivity and biodiversity of these aquatic species (Schilt, 2007; Barnhouse 2013). Fish entrainment deals with a scenario in which fish in the upstream reservoir are involuntary passed through water intakes structures. Migratory fish are particularly susceptible to entrainment during downstream migration, but entrainment can also occur among resident fish using the habitat near the intakes (Coutant and Whitney, 2000). It is anticipated that the risk of

fish entrainment at a particular dam facility is associated with the effect of hydropower operations on the flow and thermal structure of the forebay as well as the biology of the resident fish population. Close to the intake, velocity becomes high, potentially exceeding the velocity at which fish are able to escape the flow field. This results in entrainment into the intake units (EPRI, 1992). This region is often termed the acceleration zone or the entrainment risk zone and its size can vary by species and life stage, which relate to swimming ability. Entrained fish mortality can be caused by shear stresses, pressure gradient, turbulence, cavitation or direct impact of turbine blades (Marcy et al. 1978; BC Hydro, 2006a). Previous work has examined the use of physical, acoustic and lighting methods to repel fish from this high risk zone (NPP, 2005). To assess the efficiency of these operational devices, prediction of the near-intake velocity field upstream of the dam is necessary. Factors such as water velocity, temperature, depth, and acceleration affect the behaviour and distribution of fish with the specific effects further varying with biotic factors such as life-stage, reproductive stage, body size, and species. Hence, the flow pattern in the forebay area can provide valuable information on explaining fish movement and entrainment risk (Goodwin, et al., 2006; Martins et al. 2014).

In order to assess the extents of the risk zone induced by the dam's intakes, it is important that the upstream hydraulics are accurately characterized. Shammaa et al. (2005) explored developing an analytical potential flow solution to describe the flow upstream of orifices and sluice gates, which provides a base point for describing the flow upstream of hydropower facilities. Bryant et al. (2008) investigated flow upstream of orifices in a laboratory setting, including the impacts of multiple outlets, and proposed a modified potential flow solution. Huang et al. (2014) used a potential flow solution in combination with a physical model and

Computational Fluid Dynamic (CFD) solver to investigate flow upstream of the Baihetan dam, a high head dam in China. CFD solvers have been used for about a decade to generate flow fields upstream of hydropower facilities. Among them, the CFD studies of the Wanapum dam (Meselhe and Odgaard, 1998), Dalles dam (Khan et al. 2004), Bonneville powerhouse (Rakowski et al., 2002), and Howard Hanson dam (Wicklein et al., 2002) are notable. On several occasions, CFD data was compared with physical model data and its reliability was ascertained (Meselhe and Odgaard, 1998). The field measured flow field was used to calibrate the model, which can be used to identify the fish entrainment zone.

Larger hydropower facilities may have deeper reservoirs (>10 m) that have distinctly different thermal characteristics over the course of the year. The vertical density distribution of a thermally stratified reservoir may limit the elevation at which water is withdrawn from. This applies directly to hydropower intakes in thermally stratified reservoirs, and is called selective withdrawal (Fischer et al. 1979, Imberger 1980). Selective withdrawal is most common in reservoirs that have a very distinct thermal stratification profile (i.e. a sharp thermocline). The research of Shammaa and Zhu (2010) included a laboratory component to determine how the total discharge through an orifice affects the proportion of withdrawal from each layer of a stratified water body. Several other studies also consider the concept of selective withdrawal and its impacts on upstream thermal stratification (Casajitjana et al. 2003; Caliskan and Elci 2009; Anohin et al. 2006; Islam and Zhu, 2015).

Mica Dam, located on the Columbia River in British Columbia (BC), Canada is currently undergoing an expansion project. This project involved expanding the generating capacity of the facility by installing two additional turbines, for a total of six. The intakes at Mica dam are

located at a geodetic elevation of 692.46 m. The expansion will also increase the discharge through the facility at peak hours. There is an immediate need to assess fish entrainment risk at this facility due to this expansion. BC Hydro has an ongoing ecological productivity monitoring program for a number of its large reservoirs including Kinbasket Reservoir (impounded by Mica dam) in which fish population and thermal stratification are monitored (Bray, 2013). Previous work completed by BC Hydro (2006b) indicates that the average fish density of Kokanee Salmon (*Oncorhynchus nerka*) is approximately 400 fish/ha in the vicinity of Mica dam, and that the distribution of fish in late summer ranges from 710 – 750 m geodetic elevation, with the majority of fish detections in the 730 - 735 m range. Kokanee salmon is the most abundant sportfish species in Kinbasket Reservoir. This risk screening report identified that all life stage of Kokanee are at high risk for entrainment due to the fish density in the vicinity of the intakes. Additionally, Bull Trout (*Salvenius confluentus*), which prey on kokanee during their sub-adult and adult life phases, have been identified to be at risk of entrainment late in the year, when they make more frequent use of the forebay area just upstream of the powerhouse (Martins et al. 2013). As such, the fish entrainment risk assessment for Bull Trout will be related to late fall and winter operational scenarios, when the reservoir is isothermal.

To assess the entrainment risk to fish posed by the operation of the Mica facility, we conducted a study to analyze the upstream flow field of the reservoir under varying operational conditions. This was completed through a combination of acoustic Doppler current profiler (ADCP) measurements and CFD modelling. The CFD modelling component of the study was conducted to simulate the flow field upstream of Mica under the field measurement scenario for model verification. The model was subsequently used to evaluate the reservoir flow field during

varying operational scenarios, a useful approach to assess the relationship between fish behaviour and various flow parameters. Both near-intake (within 50 m) and far-intake (1 km) flow fields were analyzed. The near-intake flow field is useful for demarcating the risk zone. The far-intake flow field may help to establish relationships between fish behaviour and characteristics of the flow field. The results also assist the hydropower producer in optimizing the operation of the facility to reduce entrainment related fish mortality. In addition to the field scenario, four additional scenarios were evaluated using the CFD model with varying operational scenarios (outlined in Table 3). Each of these operational scenarios occur when the reservoir is isothermal as this is the timeframe which is of particular interest for fish entrainment, as Bull Trout entrainment has been noted to be most significant during this period (Martins, et al., 2014), and it is anticipated Kokanee entrainment is also greatest in these conditions (BC Hydro, 2006b). The scenarios have been specifically selected to investigate two objectives. The first objective is to investigate the effect of reservoir surface elevation on the flow field upstream of the dam. As the Kinbasket Reservoir water surface annually fluctuates by approximately 25 m, the flow field upstream of the dam changes significantly seasonally. Scenarios A and B evaluate how the expanded facility (6 turbines) operations impact the forebay hydraulics at a low pool elevation (Scenario A) vs. a high pool elevation (Scenario B). The second important objective that is investigated is how the number of intakes operational affects the upstream hydraulics. Scenarios A, C and D demonstrate the impacts of 6, 4 and 1 operational turbine at the dam respectively. The number of operational intakes affects the total discharge through the facility as well as the extent of impacts on the upstream flow field.

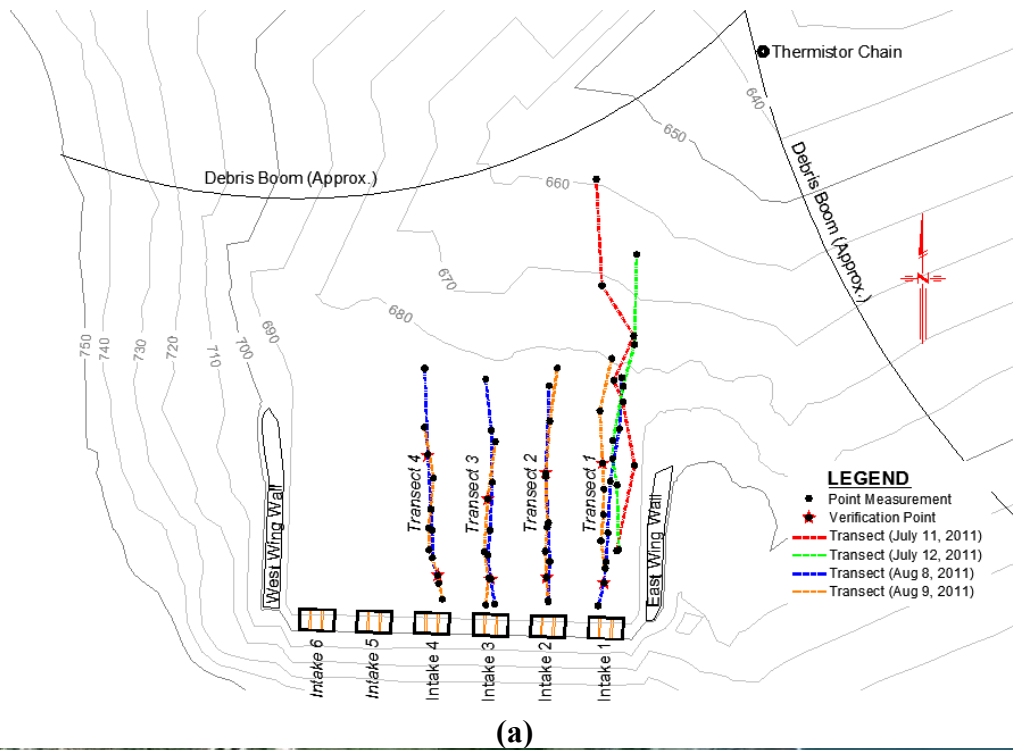
**Table 3: Mica Dam model scenarios.**

<b>Scenario</b>	<b>Description</b>	<b>Intake 1 (m<sup>3</sup>/s)</b>	<b>Intake 2 (m<sup>3</sup>/s)</b>	<b>Intake 3 (m<sup>3</sup>/s)</b>	<b>Intake 4 (m<sup>3</sup>/s)</b>	<b>Intake 5 (m<sup>3</sup>/s)</b>	<b>Intake 6 (m<sup>3</sup>/s)</b>	<b>Total Q (m<sup>3</sup>/s)</b>	<b>Water Surface Elevation (m)</b>
<b>Field</b>	<b>Field Scenario</b>	267	267	270	268	0.00	0.00	1072	752.98
<b>A</b>	<b>Low Head, 6 Turbines</b>	224	224	224	224	224	224	1344	726.55
<b>B</b>	<b>High Head, 6 Turbines</b>	224	224	224	224	224	224	1344	749.77
<b>C</b>	<b>Low Head, 4 Turbines</b>	215	217	235	234	0	0	901	726.55
<b>D</b>	<b>Low Head, 1 Turbine</b>	0	0	217	0	0	0	217	725.49

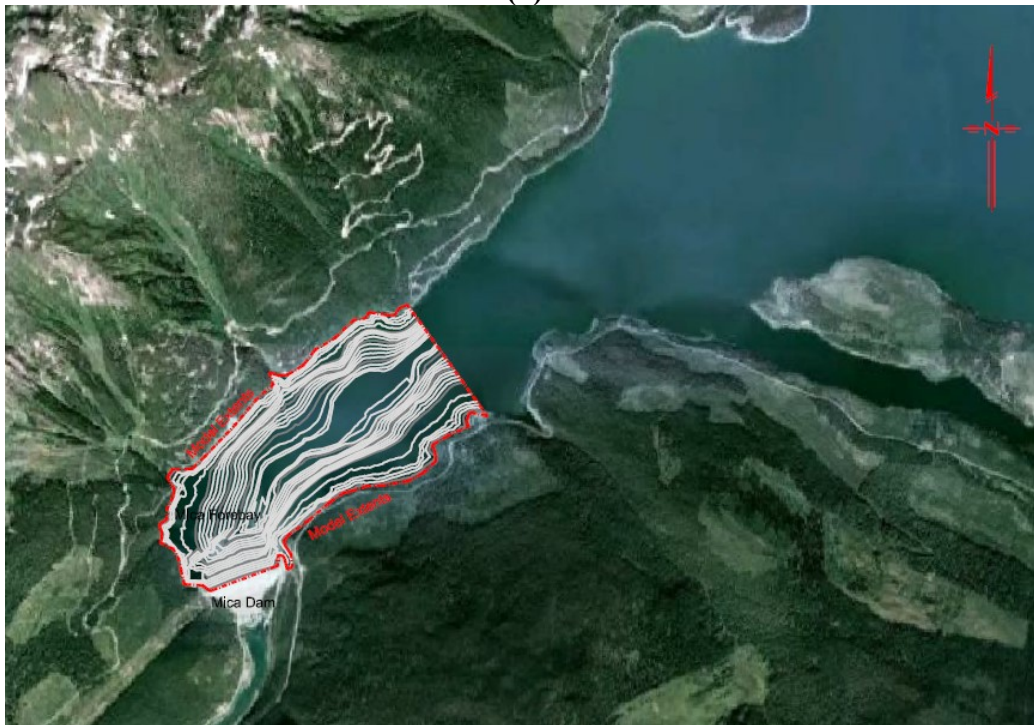
This study will demonstrate a successful technique of completing challenging ADCP measurements in a deep, low velocity, lentic environment, investigate the impact of water surface elevation and intake withdrawal scenarios on the upstream hydraulics of the facility, identify the extent of the risk zone under varying operational conditions and relate the knowledge gained about the forebay hydraulics to the potential for entrainment of resident fish. Additionally this study evaluates the capabilities and limitations of CFD modeling and potential flow analysis in evaluating the upstream hydraulics at hydropower facilities.

### 3.4 Methodology

The current study focuses on Mica dam upstream of the Columbia River, one of BC Hydro's largest generation facilities. The dam is a 244 m high concrete and earth filled structure, located upstream of the Town of Revelstoke. The Mica dam was built primarily for flood protection as part of the Columbia River Treaty, however it is also a major producer of hydroelectric power. The dam, which currently utilizes four Francis turbines, having a combined maximum generating capacity of 1740 MW, is undergoing expansion to include an additional two turbines. Each of the six intakes is 12.7 m wide by 13.6 m tall at the dam's head wall and is separated by 21.4 m (centre to centre). Intake 1 is the easternmost intake and Intake 6 is the westernmost intake (Figure 12(a)). There are concrete wing walls located a distance of 8.9 m on either side of Intakes 1 and 6 (measured from the edge of the intake to the wing wall). The wing walls are both 12.2 m tall. Currently only Intakes 1 through 4 are operational, and Intakes 5 and 6 are part of the Mica hydropower expansion project. The hydropower reservoir impounded by Mica, Kinbasket reservoir, has a level that seasonally fluctuates depending on dam operations. The dam is licensed to operate in a manner that allows the upstream water level to fluctuate by up to 47 m annually. In general the reservoir level fluctuates by approximately 25 m annually. Typically the reservoir is lowest in May and is highest in September. The 2008 - 2010 ecological productivity monitoring programs confirm that in the summer months there is significant thermal stratification throughout the reservoir (Bray, 2013). Generally the epilimnion is shallow and not distinct and the metalimnion of the reservoir is deep extending approximately from the surface to the intakes depth. The temperature profile with respect to depth throughout the metalimnion is approximately linear.



(a)



(b)

Figure 12: (a) Field measurement locations; (b) CFD model extents (2.5 km upstream of dam).

### ***3.4.1 Field Measurements***

Continuous temperature profile measurements were taken from May 13, 2011 to November 3, 2011 using a fabricated thermistor chain installed in the forebay close to the dam face, as shown in Figure 12(a). The Onset Tidbit v2 thermistors have an accuracy of 0.2 °C over the range of temperatures measured in this study, and read to a resolution of 0.02 °C. A total of 36 thermistors were spaced at approximately 2 m intervals along the depth of the chain. Each of the thermistors collected data at 5 min intervals. The thermistor measurements have been used to establish a thermal profile for the CFD model in this study.

Flow profiles were measured during the two weeks of on-site field studies from July 11 – 13 and August 8 – 10, 2011 using an acoustic Doppler current profiler (ADCP) from a boat in the forebay. The Teledyne RD Instruments Workhorse Sentinel 600 kHz (Sentinel) was used, utilizing the equipment's self-contained measurement feature. The locations of the ADCP measurements are shown in Figure 12(a). In terms of velocity measurement, the Sentinel has an accuracy of 0.3 % of the water velocity relative to the instruments, or 3.0 mm/s and a resolution of 1 mm/s. The Sentinel has a beam angle of 20 ° which restricts the approach distance the measurements can be made from the dam face. Flow profiles in the immediate forebay were recorded when the dam spilling rates were held relatively constant throughout each measurement set (i.e. one or four transects). Several different discharges (63 m<sup>3</sup>/s – 274 m<sup>3</sup>/s) and two different operational scenarios (one intake vs. all four intakes) were occurring during these measurement sets. During the July 2011 on-site field work, measurements in front of Intake 1 were taken at discharges of 63 m<sup>3</sup>/s and 221 m<sup>3</sup>/s. During the August 2011 on-site field work, measurements in front of Intakes 1 – 4 were taken at discharges of 240, 245, 270, 269 m<sup>3</sup>/s,

respectively, the first day and 252, 269, 274, 266 m<sup>3</sup>/s, respectively, the second day. ADCP measurements were particularly difficult at this facility due to the depth of the forebay in the late summer, and access restriction to the banks or the forebay.

The reservoir level was approximately 61 m and 67 m above the intakes during the 2011 July and August on-site field studies, respectively. As the intakes are located at the base of the dam face, far from the water surface, it was determined that velocities are likely only significant close to the intakes and are of little significance high above the intakes. Therefore, in order to collect a more detailed view of the area of interest, the Sentinel was placed in a mooring cage and submerged between 20 – 35 m using the boats hydraulic winch system, as shown in Figure 13(a). This allowed the instrument to have a 0.5 m bin size while still reaching the bottom of the reservoir, where the intakes are located. Velocity measurement sets included either one (July measurements) or four transects (August measurements), approximately perpendicular to each operating intake on the dam face. Measurements were collected for a duration of about 5 min at each point of interest. This allowed for time averaging during the post processing of the data in order to reduce the error inherent to measuring relatively low velocity flow fields. The ADCP was tested in the field prior to collecting measurement to determine that 5 min allowed enough ensembles to be measured such that the time-averaged value of the measurements was not impacted by the number of ensembles.



(a)



(b)

**Figure 13: Field measurement setup (a) Inline mooring cage; (b) Three point anchoring system.**

The physical location of each measurement was determined using a real-time kinematic global positioning system (RTK GPS), a Trimble R8 GNSS (Model 2). For stationary measurements, the rover was fixed on a tri-maran boat which was floating directly above the submerged ADCP transducer head. A base station was set up on top of the left bank, using a self-established benchmark. The location of this benchmark was checked against several bench marks that were located on the dam structure (GCM #73C091, BM2500 – 2503, BM2248 - 2251). For kinematic surveying, this unit has a vertical accuracy of 20 mm and a horizontal accuracy of 20 mm.

There are a number of environmental factors that contribute to the potential error in ADCP measurements. Error may be introduced into the measurements by data obtained using an ADCP that is not perfectly horizontal, which may occur due to boat or internal wave movement. This is reflected in the pitch and the roll of the measurements. In general, minimizing the pitch and roll of the instrument is required for higher quality data. This is particularly difficult in lakes and reservoirs where larger waves are anticipated. During field measurements at Mica the water was relatively calm and the absolute pitch was maintained below  $0.9^\circ$  and the absolute roll below  $1.1^\circ$  (based on averaged data). On average, the pitch was approximately  $0.3^\circ$  and the roll was approximately  $0.5^\circ$ .

An environmental condition, specific to lake and reservoir environments, which contributes to potential flow field measurement error, is the relatively low velocity of the flow (as compares to riverine and estuarine environments). This requires averaging of stationary measurements. The ADCP can drift over the course of each stationary measurement, which is difficult to control. This drifting contributes to error in the measurements during post-processing. During the July field trip, only two anchoring lines were used to secure the boat. This resulted in substantial drift

during velocity measurements. Therefore, for the August field trip, the data collection procedures were revised to include a third anchoring line, which greatly reduced the drift of the ADCP as shown in Figure 13(b). For the measurements in July, each stationary point had a horizontal drift contained to an average radius of 3.9 m. Measurements in August were much more stationary, with horizontal drift contained to an average radius of 0.4 m for each point. Due to the increased potential for error in the July field measurements, detailed analysis of the July measurements was not completed.

The relatively low velocity of the flow in reservoir and lake environments creates a system that is relatively dynamic, in both the magnitude and direction of flow at any given point may vary on a second to second basis. It is important that this is considered when reviewing and interpreting the field results herein. As previously mentioned each measurement was recorded for approximately 5 min collecting about 150 velocity profiles and averaging them in an attempt to reduce the error due to this dynamic behaviour.

### ***3.4.2 Computational Fluid Dynamic Modelling***

CFD modelling for this study was complete using a commercially available solver, Ansys CFX. The extents of the CFD model of the Mica forebay cover the forebay extending from the dam face to approximately 2.5 km upstream as shown in Figure 12(b). The CFD solver uses the three-dimensional Reynolds-averaged Navier-Stokes equations, with the k- $\epsilon$  turbulence model to assess eddy viscosity. The k- $\epsilon$  model was selected for its robustness and excellent numerical stability in addition to the fact the severe pressure gradients were not anticipated. Alternative turbulence models, including Reynold's stress models were also investigated, but displayed numerical instability for the current study and were not included in the analysis herein. To

compute temperature transport, a full buoyancy model was chosen. Density profiles for the computed temperature profiles were determined using an equation of state. The computed density was then substituted into the Navier-Stokes equations to compute the buoyancy source term as outlined in this Chapter.

The model boundaries were constructed using a patch conforming tetrahedral mesh. The model's bathymetry was created using topographic information provided by BC Hydro. The upstream bathymetry is generally constructed from pre-flooding contours of the upstream river basin, dated 1954. The contours have a spacing of 30.48 m (100 ft). The banks (for geodetic elevations great than 714.5 m), have some bathymetry refinement, based on information dated as 2002. This information is stereophotographic information and has a general lateral spacing of 15 m x 15 m. The hydropower intakes, wing walls, upstream apron and other dam details were constructed utilizing record drawings dated 1989.

Mesh independence was investigated using three different mesh sizes. The edge length of the coarse mesh (Mesh 1) was the default length determined by the meshing software (Ansys Meshing). Two finer meshes were constructed by systematically reducing the edge length of the elements in the mesh. The second intermediate mesh (Mesh 2) had an edge length of 0.5 times the edge length of Mesh 1. The finest mesh (Mesh 3) had an edge length of 0.5 times the edge length of Mesh 2. Meshes 1, 2 and 3 had a total of 1.8 million, 4.6 million and 12.8 million nodes respectively. In evaluating the performance of each mesh it was determined that the average discrepancy between Mesh 1 and Mesh 2 was 5.4%, with a maximum discrepancy of 10.3%. The average discrepancy between Mesh 2 and Mesh 3 was 0.6%, with a maximum discrepancy of 1.9%. It was determined that Mesh 2 was the appropriate mesh to use for the

completion of this study, which minimizes uncertainty due to mesh size, while maximizing computational efficiency.

In total, the entire model domain includes 4.6 million nodes for the chosen mesh size (Mesh 2), arranged in an unstructured tetrahedral mesh. Some local refinement of the computational mesh was required in close proximity to the intakes. This allows for more detailed modeling in this zone, which has higher velocity gradients, and is particularly important for fish entrainment risk assessment. This zone extends spherically from the intake centre to a radius of 200 m, extending beyond the debris boom. Within the refinement zone a minimum element edge length of 1 m is specified, which expands to 4.6 m at the edge of the refinement zone. The coarse mesh throughout the model domain has face sizes ranging from 4.6 – 50 m depending on the location and proximity to boundaries. The mesh was developed using a three-step adaptive meshing procedure, which introduces additional elements in regions within the domain with higher numerical instability.

A free-slip wall boundary was used at the reservoirs free surface, while other walls were modelled using no-slip conditions, where the standard wall function was used. At the Mica intakes, mass-flow rate boundary conditions were provided. At the upstream boundary, an ‘opening’ boundary was provided. This allows both inflow and outflow across the boundary.

The convergence criteria for the model were set such that the root mean square (RMS) of the residual is below  $10^{-4}$  in all the simulations carried out. The solution for the model used a blended advection scheme, with a blend factor of 0.90 and high resolution solution for turbulence numerics. The pressure and velocity interpolation schemes were specified as trilinear with a geometric shape function option. Velocity pressure coupling was included with a fourth order

---

Rhie Chow option. Figure 14 shows a typical convergence history for the momentum and the pressure equations, demonstrating excellent convergence.

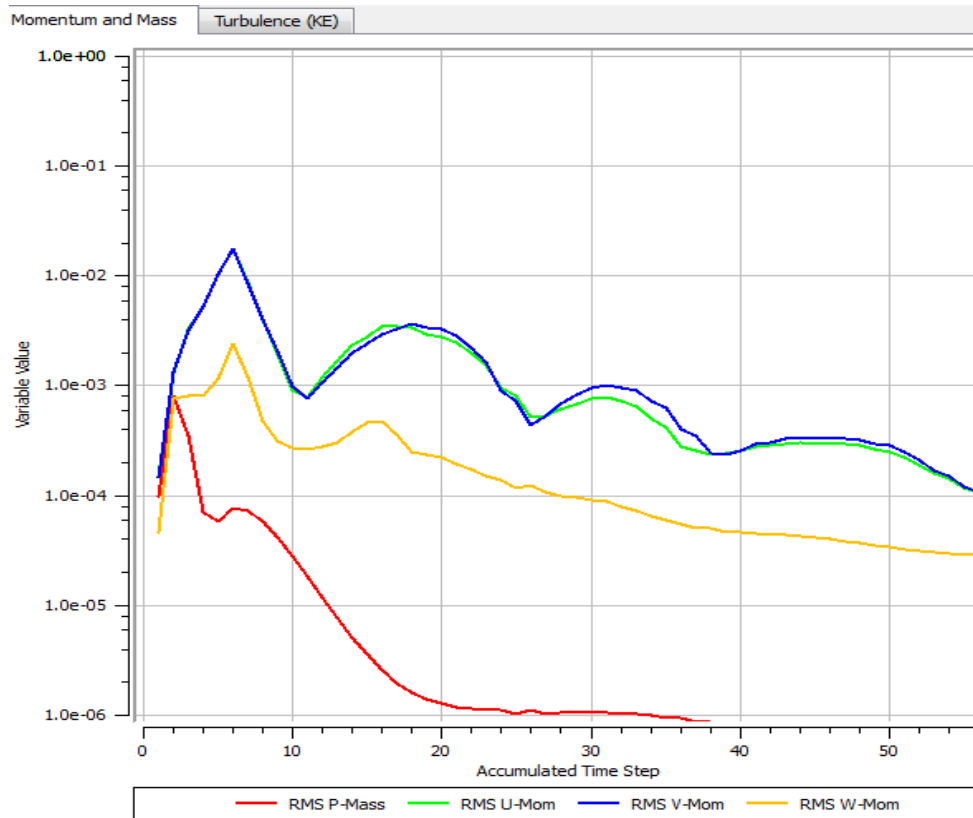


**Figure 14: Convergence history of the governing equations.**

During the field measurements collected at Mica, the forebay was found to be thermally stratified. The water temperature varied gradually to a depth of 62 m, where it became isothermal. In order to reflect this in the verification run for the CFD model, the measured temperature profile of the reservoir was fit to an empirical equation. The temperatures that were fit to the equation were the average values measured at each depth over the course of the three days of velocity measurements (August 8 to 10, 2011). In this empirical equation, temperature T

(°C) at a given geodetic elevation  $Z$  (m) can be represented as a function of water depth  $D$  (m), where  $D=752.98-Z$  with 752.98 being the average geodetic elevation of the water surface,

$$T(Z) = \begin{cases} 2.3521E^{-6}D^4 - 3.0628E^{-4}D^3 + 1.3796E^{-2}D^2 - 4.621E^{-1}D + 18.374 & D < 62 \\ 4.47116 & D \geq 62 \end{cases} \quad \text{Equation 9}$$

The fitted curve has been separated into a piece-wise function, with the upper portion representing the gradually varying thermal stratification of the forebay and the lower portion representing the isothermal layer below this. From the fitted temperature profile, density was computed based on the fluid properties of freshwater in the practical temperature range for Canadian waters (4 °C to 30 °C). It was observed that the density-temperature variation can be fitted by the following equation:

$$\rho = -0.0057T^2 + 0.0234T - 999.87 \quad \text{Equation 10}$$

where  $\rho$  (kg/m<sup>3</sup>) is the density at a given point. This equation was supplied as the ‘equation of state’ in the CFX solver to get the density from the simulated temperature distribution.

At the upstream boundary, it was required to calculate the static pressure for the given density profile. This was achieved by solving the following integration:

$$\int dP = \int (\rho - \rho_{ref})g dZ \quad \text{Equation 11}$$

where  $P$  is the static pressure (Pa),  $\rho_{ref}$  (kg/m<sup>3</sup>) is the density of water at surface, and  $g$  is -9.81 m/s<sup>2</sup>. Solving the integration, and substituting  $P = 0$  at  $D = 0$ , one obtained:

$$P = \begin{cases} 0.1154D^2 + 9797.5D - 10.378 & D < 62 \\ 9808.7D - 271.31 & D \geq 62 \end{cases} \quad \text{Equation 12}$$

This pressure profile was input at the upstream boundary, as well as the initialization pressure throughout the entire model domain.

In addition to the field scenario, which was used to compare the models performance to the field measurements, various other scenarios were developed corresponding to operations in which tagged fish were in close proximity to the dams intakes. The scenarios generally ranged in both discharge and water surface level, based on the time of year. Four scenarios, capturing a broad range of operational scenarios in which fish entrainment is probable are outlined in Table 3. Each of these scenarios are isothermal, representing the operational scenarios that are most relevant for fish entrainment risk assessment. The potential effects of temperature stratification are investigated in Chapter 4.

### ***3.4.3 Model Verification***

Due to the potential errors in both the models geometry as well as in the field measurements, model calibration was not completed. The results generated by the CFD model for the field scenario were compared against the field ADCP measurements conducted during the August field trip to verify the CFD model. Each of the velocity measurements completed at Mica were completed in duplicate, on separate days. The maximum difference measured between the two days was 0.43 m/s with average differences limited to 0.08 m/s across the domain where field measurements were completed. The model verification included comparing the CFD simulations to the field measurements by evaluating each of the three velocity components (two lateral components and one vertical component) as well as the velocity magnitude for each of the field measurements. Vertical velocity magnitude profiles for each of the measurements (noted by a star on Figure 12(a)), is included as Figure 15. This includes two measurements along each transect, one for each of the two days that field measurements were conducted (for a total of eight comparisons on each transect). In general, the velocity magnitude ( $\sqrt{u^2 + v^2 + w^2}$ ), x-

velocity (toward to dam face), and z-velocity (vertical) were fastest where the intakes are located.

For the field measured velocities, the maximum velocity magnitude was about 0.5 m/s for the measurements located 15 m from the intakes. Transects 2 and 3 had faster velocities further from the intakes, which was due to the interaction of adjacent intakes. This trend is also seen in the x-velocity measurements, where the maximum velocity was about -0.5 m/s (i.e. toward the dam face). Z-velocity contours had a maximum velocity of about -0.15 m/s (i.e. downward), but were in general much smaller than the x-velocity contours.

Y-velocity (parallel to the dam face) followed the same trend on both sets of measurements. The y-velocity was generally moving towards the left bank, and getting progressively larger when moving from Transect 1 to 4. At Transect 1, the velocity was mostly negative (maximum 0.1 m/s) and generally flowing towards the right bank. Transect 4 had the largest y-velocities, with a maximum of 0.25 m/s. These trends indicate a counter clockwise recirculation pattern at the right bank.

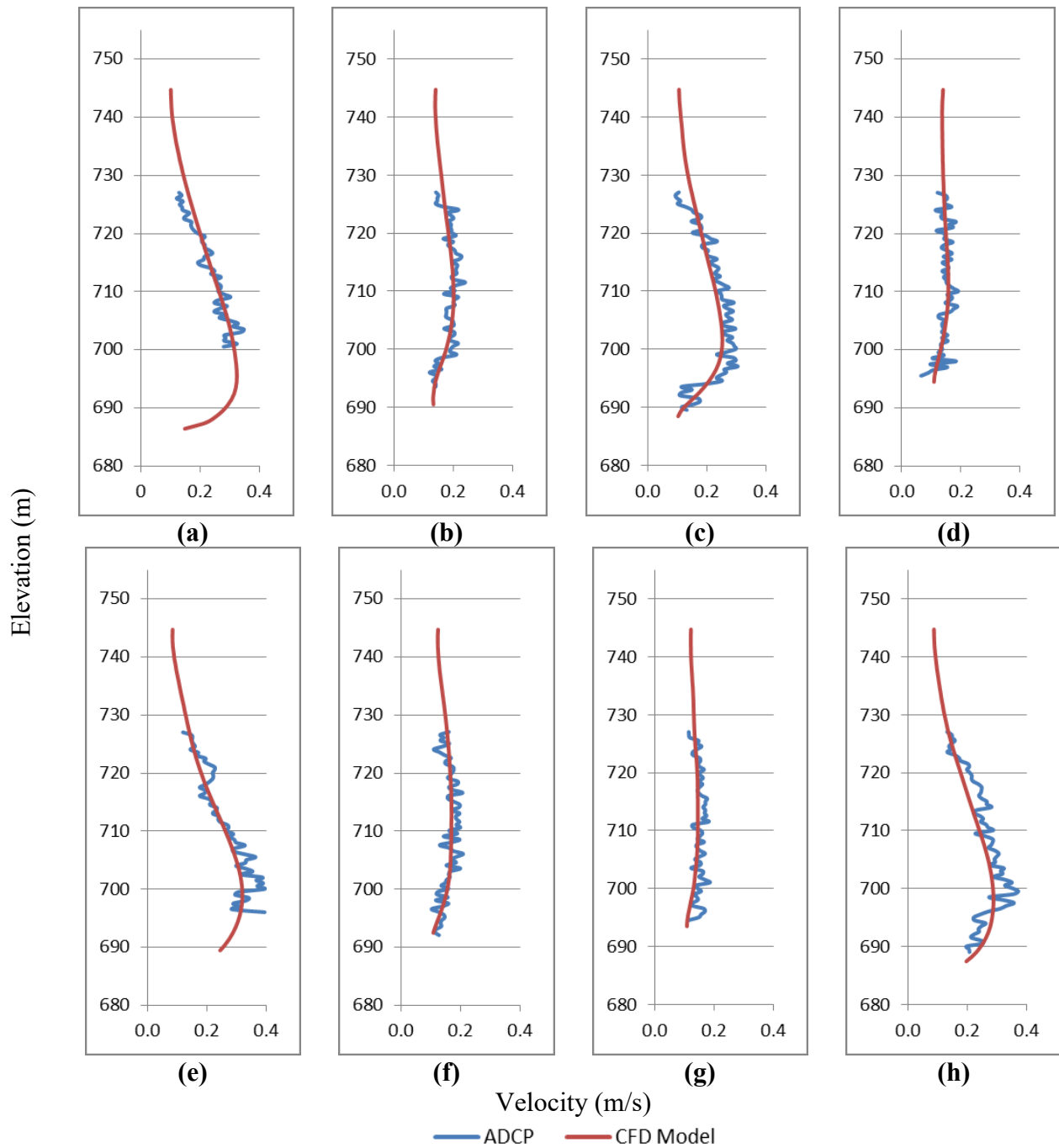


**Figure 15: Model verification - velocity magnitude at specific distance upstream of dam (a) August 8 – Transect 1, 17.4 m, (b) August 9 – Transect 1, 61.5 m, (c) August 8 – Transect 2, 24.6 m, (d) August 9 – Transect 2, 57.1 m, (e) August 8 – Transect 3, 17.4 m, (f) August 9 – Transect 3, 46.9 m, (g) August 8 – Transect 4, 62.6 m (h) August 9 – Transect 4, 18.1 m**ntake 3 velocity magnitude (a) August 8, 2011; (b) August 9, 2011; (c) CFD model.

In general the velocity magnitude and lateral velocity components (u and v) are predicted well by the model, with maximum discrepancies of 0.14 m/s perpendicular to the dam (x-direction), 0.12 m/s parallel to the dam (y-direction) and 0.16 m/s for overall velocity magnitude. The absolute mean discrepancy between the field measurements and the CFD model were 0.03 m/s (x-direction, perpendicular to dam face), 0.04 m/s (y-direction, parallel to dam face), 0.03 m/s (z-direction, upward) and 0.06 m/s (velocity magnitude). Both the pattern and the magnitude of these parameters match the measurements well. An example of the CFD simulated velocity magnitude profiles, compared to the field measured profiles is included as Figure 15. It can be noted that the location of the peak velocity, matches well between the numerical simulation and the field measurements, although there is some discrepancy upstream of the zone of high velocity. The greatest discrepancy with the modelled results was consistently noted in the vertical velocity, in which the model over-predicts the downward velocity of water, compared to the field measurements. The maximum discrepancy in this direction was 0.11 m/s, which is of similar magnitude to the two lateral directions; however the magnitude of the downward velocity is much lower than the lateral components, making the discrepancy comparatively larger.

This discrepancy is likely due to the field measurement uncertainties given the large depth of the intakes and the relative low flow velocity away from the intakes. Despite the fact that the ADCP was lowered to a depth of 20-35 m below the water surface, the size of the sampling volume was about 20 m wide at the bottom of the water column as the ADCP has a beam angle of 20°. We believe a relative error of 30% is acceptable as it indicates the reliability of both the measurements and the CFD modelling.

### **3.5 Forebay Flow Field**

The CFD model of the Mica forebay was then used to evaluate the impacts of varying operation on the upstream flow field. Specifically, hydraulic parameters that have been previously noted to potentially affect entrainment were investigated including velocity, turbulent kinetic energy, shear strain rate and velocity curl (BC Hydro 2006a; Coutant and Whitney, 2000; Goodwin, 2004; Langford, et al., 2015).

The velocity field that develops upstream of the intakes is shown in plan view (at the intake midline elevation) in Figure 16. It can be noted that the zone of influence of the dam extends much further upstream of the dam depending on the number of intakes that are operational. In comparing the low pool scenarios (A, C, D), the velocity contours in Scenario A, when six turbines are operational, become parallel to the dam face within about 10 m of the dam face. Beyond this the velocity field spans the entire width of the forebay in this location and the dam begins to act as a line sink, as opposed to series of point sinks. In Scenario D, where a single unit is operational, the velocity contours are ellipsoidal in shape, extending away from the intake. In this scenario, the single operational intake acts as a point sink.

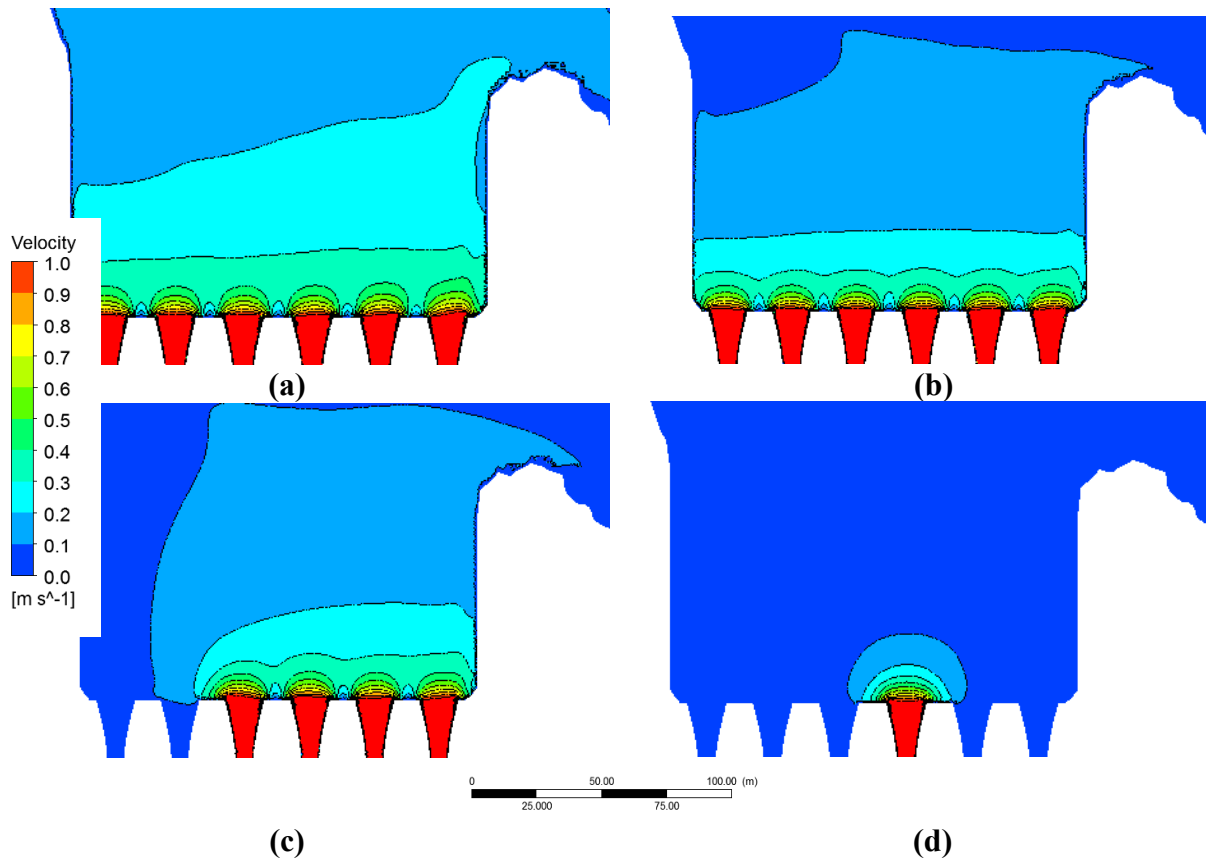


**Figure 16: Velocity at centre of intake elevation (692.46) (a) Scenario A; (b) Scenario B; (c) Scenario C; (d) Scenario D.**

When evaluating the impact of depth on the velocity field it is noted that in the low pool scenario (A) the velocity field extends further upstream than in the high pool scenario (B). Fish that are occupying the forebay during low pool (late-winter to spring) at a depth close to the intakes could be exposed to higher velocities due to the difference in cross sectional area approaching the intakes. It can be noted that generally the portion of the forebay that is impacted by higher velocities ( $>0.5$  m/s) is localized around each intake in each scenario. There is, however, a distinct difference in the portion of the forebay a lower threshold, such as 0.1 m/s, which may have implications for juvenile, anguilliform swimmers (Katopodis, 1992). The volume of the

forebay exceeding 0.1 m/s increases substantially with the number of intakes operational as well as when the water surface elevation is lower. The threshold velocity for entrainment risk is largely dependent on the species of fish present in the reservoir and their life stage.

It is also of interest to evaluate the flow field generated by the dam in profile view. Velocity profiles extending perpendicularly into the forebay upstream of Intakes 1 and 3 are shown for each of the four scenarios in Figures 17 and 18 respectively. The velocity field upstream of Intake 1 demonstrate contours with a near-vertical orientation in the low pool scenarios where 6 and 4 turbines are active (Scenarios A and C). In these scenarios, fish may be exposed to higher velocities regardless of swimming depth during low pool in late winter and early spring. It can also be noted that there is a strong velocity field oriented directly above Intake 1 in these scenarios, where a vortex is generated, which is discussed further below. This phenomenon is not apparent in the high pool scenario (B), despite there being a large discharge through the dam. In this scenario the contours are ellipsoidal in shape. The impacts of the wing wall that is adjacent to Intake 1 and other boundaries that may drive vortex formation, and increase fish entrainment risk are reduced in high pool scenarios. At Intake 3, which is operational in all four scenarios and is depicted in Figure 18, the velocity field has more ellipsoidal contours in all scenarios. As noted previously, the higher flow scenarios do result in increased velocities being generated further upstream in the higher flow scenarios where more intakes are active. This is especially prevalent in the scenarios with lower water surface elevation.

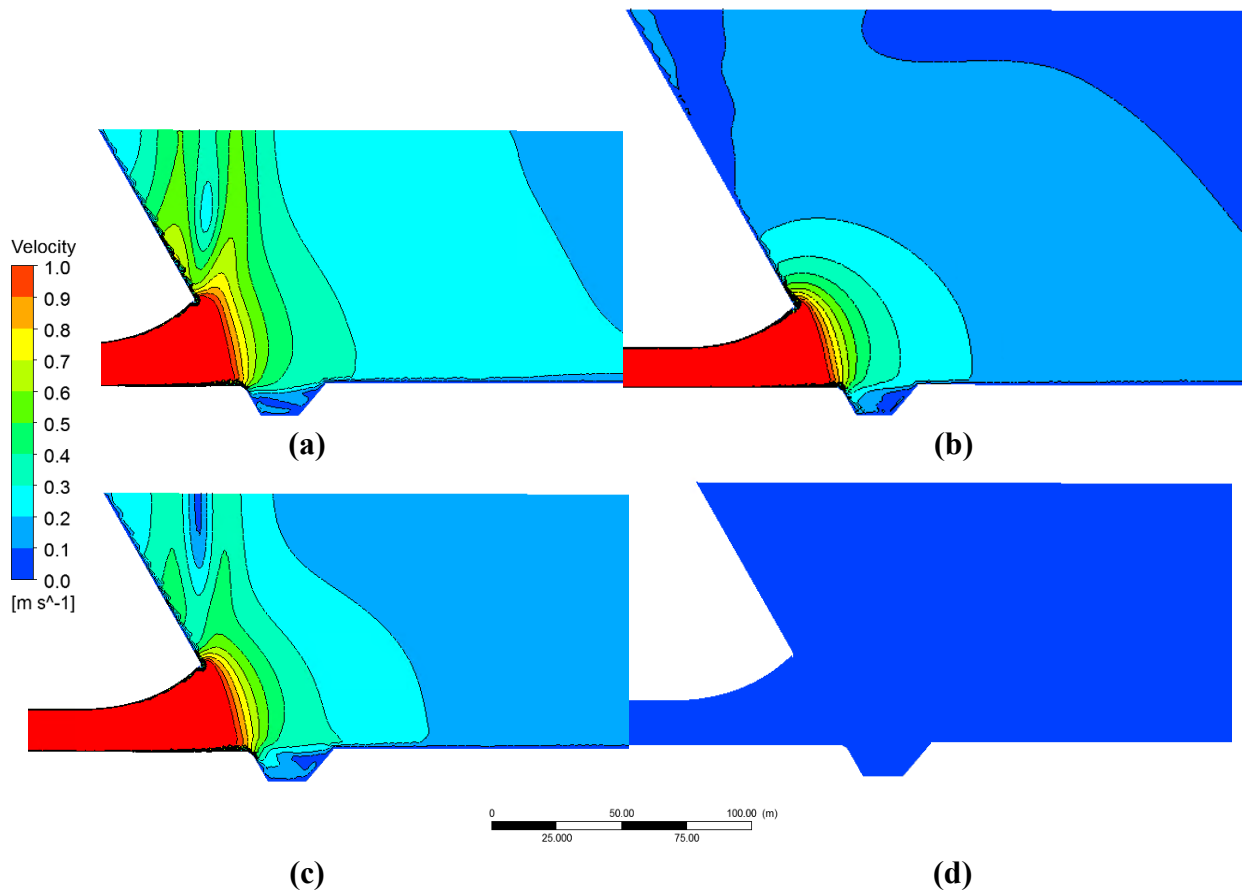


**Figure 17: Velocity profile at Intake 1 (a) Scenario A; (b) Scenario B; (c) Scenario C; (d) Scenario D.**

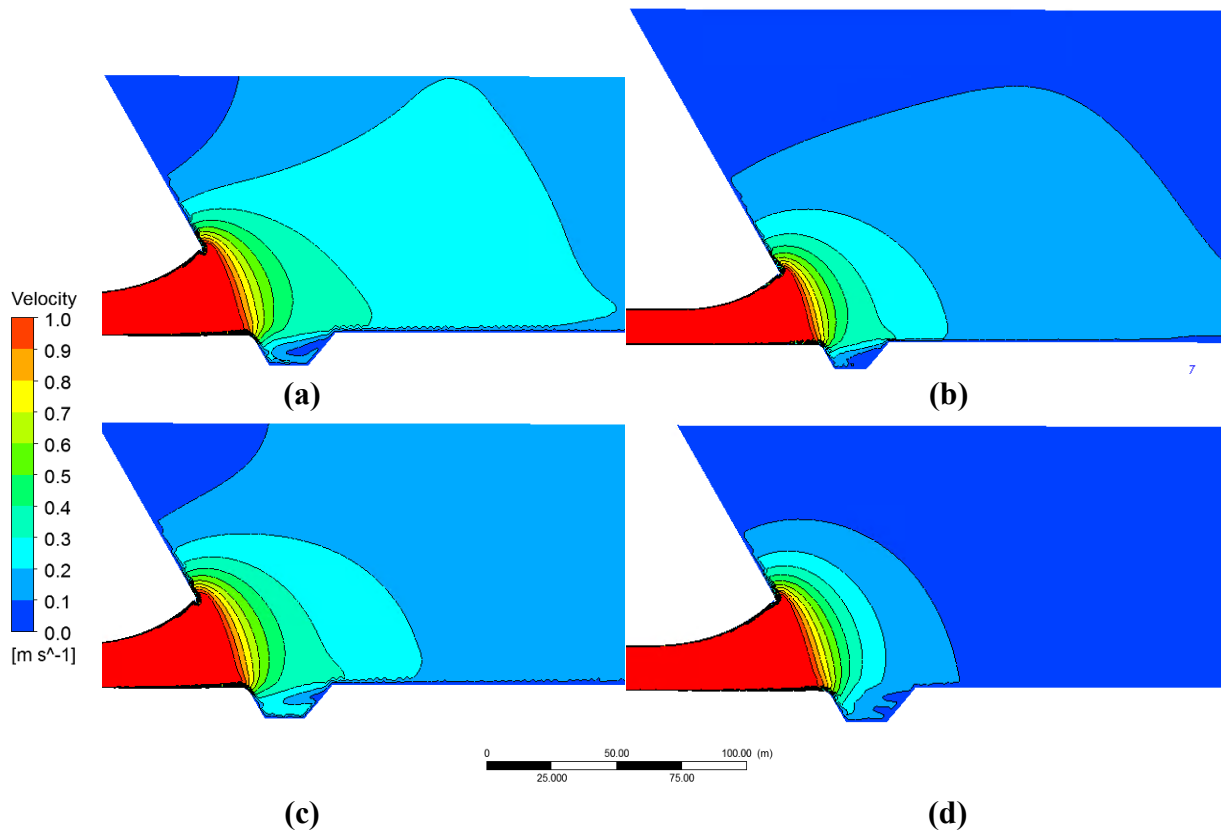
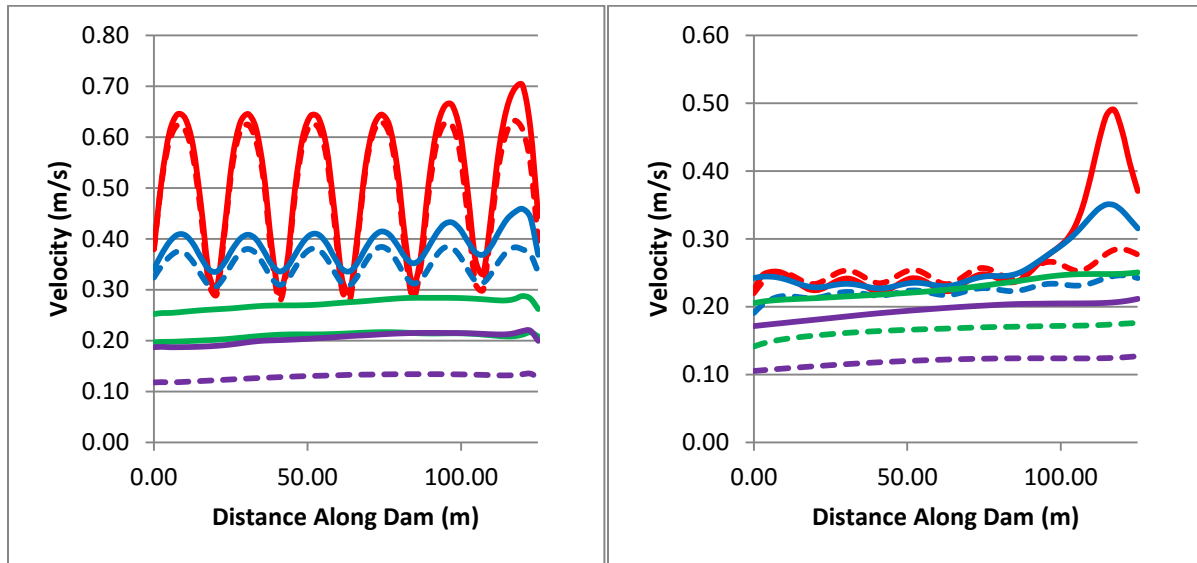


**Figure 18: Velocity profile at Intake 3 (a) Scenario A; (b) Scenario B; (c) Scenario C; (d) Scenario D.**

In scenarios A and B, where all intakes (including the two expansion intakes) are operational, it was noted that the velocity field contour become parallel to the dam face a certain distance upstream, a point at which the flow field can be approximated as a line sink instead of a series of point sinks. Figure 19 (a), (b) and (c) show the velocity field degradation with distance at the intakes elevation, as well as 15 m and 30 m above the intake elevation respectively. At the intakes elevation (Figure 19(a)) it can be noted that all distance upstream, higher velocities are generated in the low pool scenario versus the high pool scenario. The difference in velocity between each of these scenarios becomes more distinct as distance from the intakes is increased,

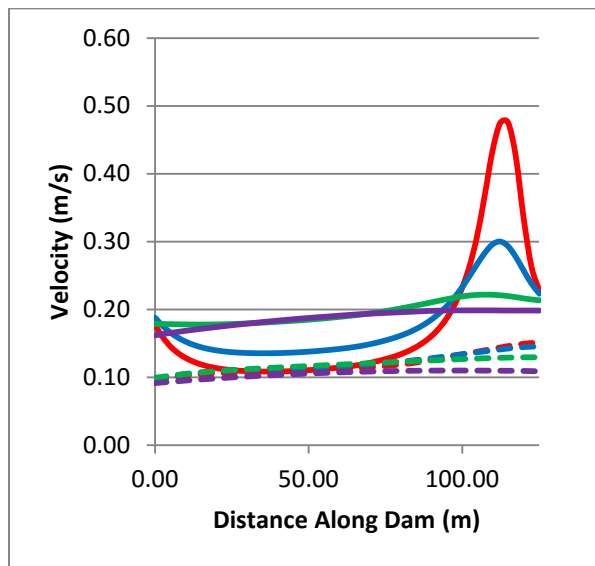
with almost two times the velocity simulated 50 m (4D) upstream of the intakes in the low pool scenario (A).



(a)

(b)

- 5 m Scenario A
- - - 5 m Scenario B
- 10 m Scenario A
- - - 10 m Scenario B
- 25 m Scenario A
- - - 25 m Scenario B
- 50 m Scenario A
- - - 50 m Scenario B



(c)

**Figure 19: Velocity magnitude at varying distances in front of the intakes (a) Intake elevation (692.46); (b) 15 m above intake elevation (707.46); (c) 30 m above intake elevation (707.46).**

The velocity field also undergoes a distinct transition from having an undulating nature, with distinct velocity difference at various distances across the dam face, to a more stable nature further away from the dam. This happens at approximately 15 m (1.25D) upstream of the dam face. At an elevation 15 m (1.25D) above the intake elevation this same transition is still apparent. The increased velocity caused by the vortex is also noted within 10 m of the intakes for the low pool scenario (A). 30 m (2.5D) above the intakes the same pattern is still apparent. It can be noted that the velocity induced by the vortex in scenario A is not diminished with distance above the intake. This creates a scenario in which the area located above Intake 1 is of high risk for fish entrainment in all low pool scenarios where that intake is active.

The results of scenarios A and B were also compared with the potential flow solution following the approach of Huang et al. (2014). The potential flow solution was developed by superimposing the flow field generated by a series of single intakes to determine the flow field generated by 6 operational intakes. The reservoir bottom, side walls and water surface were included in the potential flow solution by the inclusion of image intakes to simulate the impact of these boundaries. In the solution, 20 images were included for both the side walls, as well as the water surface. To simulate the reservoir bottom, intakes of 2 times the actual vertical dimension and flow rate were used. Only the upper half of the potential flow solution was analyzed, which allows application of potential flow theory, despite the intakes being located adjacent to a boundary. The advantages of applying potential flow theory are that it is less computationally intensive than developing a CFD model. The potential flow solution, which treats the forebay as a rectangular reservoir of infinite length and the dam headwall as vertical, can be used to provide a rough estimate of the flow field upstream of the operational dam. The potential flow solution

is compared to the averaged CFD model output upstream of each intake for scenarios A and B in Figure 20(a) and (b) respectively.

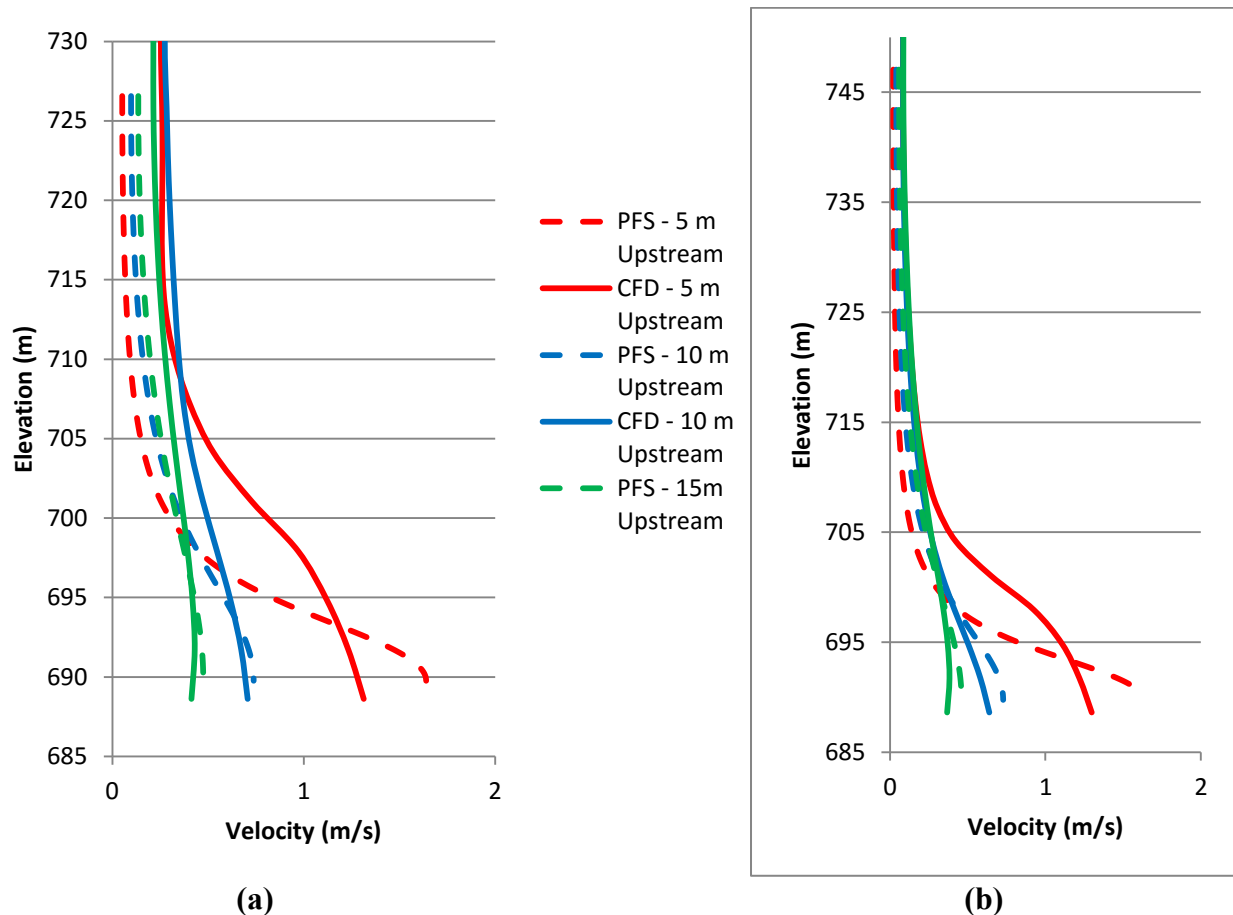


**Figure 20: Potential flow solution versus CFD model velocity profiles (a) Scenario A; (b) Scenario B.**

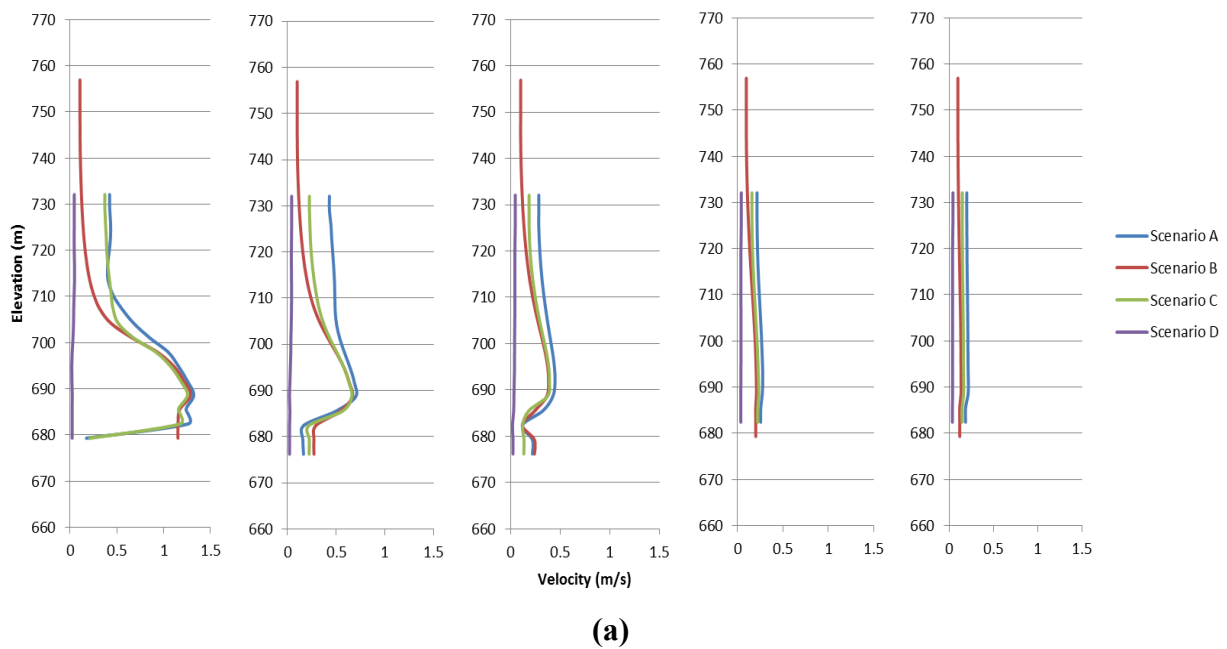
It appears that the potential flow solution overestimates the magnitude of the peak velocities near the intakes. The potential flow solution describes the peak velocities directly in front of the intakes well for locations greater than 10 m upstream of the intakes. There is a greater discrepancy between this solution and the simulated flow field near the water surface, which is due to the fact that additional images of the intakes were not included in the potential flow

solution at the water surface. As such, the potential flow solution near the water surface more closely matches the CFD output for the deep reservoir scenario, as the mean velocity throughout the forebay in this scenario is lower. The potential flow solution also matches the CFD simulation better as distance upstream of the intakes increases. This is because the potential flow solution does not take into account the unique hydraulic phenomena that were simulated near the dam face by the CFD model including vortex formation. The rectangular geometry used in the potential flow solution does not accurately predict the impacts of the complex geometry near the dam structure. As the potential flow solution is less computationally and time intensive than the numerical solution, this does provide valuable information of the forebay's flow characteristics for less detail-intensive applications.

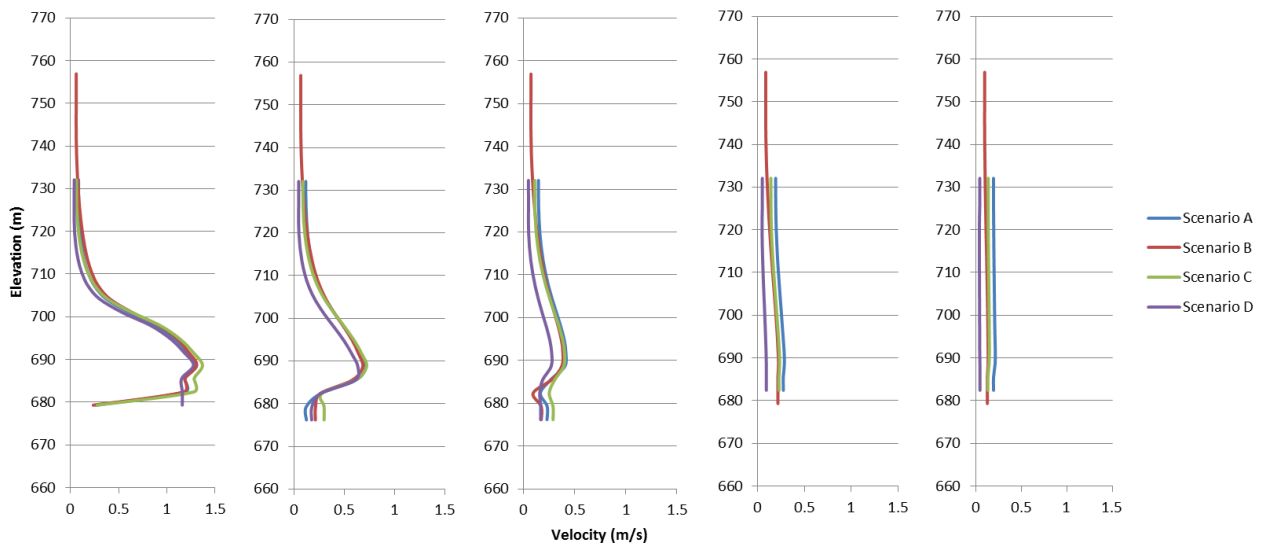
The potential flow solution does provide insight into the distance upstream of the dam headwall where velocity becomes uniform with depth. For the purpose of this analysis the distance upstream of the dam where uniformity is achieved is  $D_n$  where  $n$  is the ratio between the maximum velocity and the mean velocity of the profile. The non-dimensional distance upstream of intakes where uniformity is achieved is  $D^* = H/D_n = 1.22 n$ , where  $H$  is the depth of the forebay. The coefficient, 1.22 has been validated for  $n$  values between 1.125 and 2 with a maximum error of 6.9 % based on the potential flow solution developed.

The velocity profile upstream of the dam differs from intake to intake. Figure 21 identifies the change in velocity profile at varying distance upstream of Intakes 1 and 3 simulated by the CFD model. In all scenarios there is a distinct peak in velocity oriented at the intakes elevation in the water column at distances within 15 m of the intakes. This peak is most distinct in the high pool scenario, which indicated a great velocity gradient with depth. Upstream of 15 m the velocity

field become uniform with depth in all scenarios. As noted previously, in the low pool scenarios where Intake 1 is actively discharging water from the reservoir, much high velocities (greater than 0.5 m/s) exist all the way to the water surface. It is also of interest to note that despite the presence of vortices above Intake 1, the potential flow analysis still yields satisfactory predictions, particularly regarding the location and magnitude of the peak velocity. This is not seen in front of Intake 3 which is further from the wing wall.



(a)



(b)  
**Figure 21: Velocity magnitude profile 0, 5, 10, 25 and 50 m upstream of intake (a) Intake 1; (b) Intake 3.**

Isovolumes were produced using CFD to determine the volume of the forebay that exceed certain threshold velocities, which can be compared against fish swimming capabilities. The threshold limits that are evaluated in this study include 1.0, 0.5, 0.25 and 0.15 m/s. The volume of the forebay, upstream of the dam headwall that is occupied by each of these isovolumes is presented in Table 4. In comparing the volume of water above the 0.15 m/s and 0.25 m/s threshold, it is apparent that both discharge through the dam and the water surface elevation play a prominent role in determining flow field upstream of the dam, and thus, the risk-volumes. The higher threshold, 0.5 m/s and 1.0 m/s are less dependent on water surface elevation and generally are impacted by the volume of water passing the intakes.

**Table 4: Mica Dam fish entrainment risk volumes.**

<b>Threshold Velocity (cm/s)</b>	<b>Scenario A (m<sup>3</sup>)</b>	<b>Scenario B (m<sup>3</sup>)</b>	<b>Scenario C (m<sup>3</sup>)</b>	<b>Scenario D (m<sup>3</sup>)</b>
<b>15</b>	558,481	151,223	171,214	6,370
<b>25</b>	86,833	48,418	36,558	2,065
<b>50</b>	10,171	8,622	5,281	19
<b>100</b>	2,840	3,033	1,389	0

BC Hydro operators have noted a consistent surface oriented vortex generated above Intake 1 during low pool. The velocity curl, or vorticity about the vertical axis that is generated by the boundaries is investigated in Figure 22, which looks at the velocity curl on horizontally oriented planes extending perpendicularly into the forebay from Intake 1. In scenarios A and C, when Intake 1 is active and the water surface elevation is low a directly vertical core of high vorticity is generated. This also causes the swirling flow and downward velocity that has been discussed previously. When the water level is higher, despite having a high discharge, this vertical core is less apparent, and the peak values of velocity curl are less intense, and are oriented against the dam face as opposed to vertically. Vorticity generation at each of the other intakes is less distinct, and vortices are generated adjacent to the boundaries, however a vortex core does not develop. This indicates that the proximity of Intake 1 to the east wing wall is the primary driving force in the development of the vortex core.

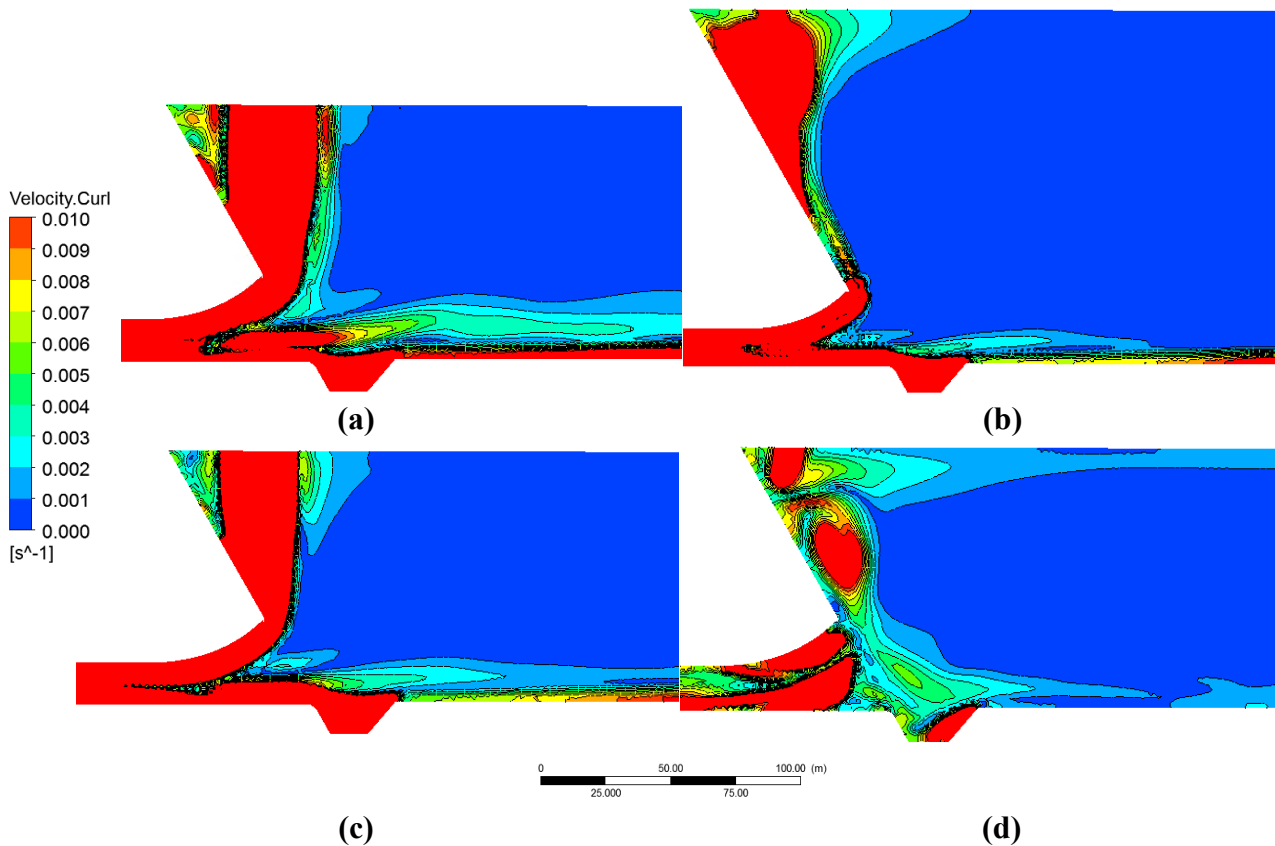


**Figure 22: Velocity curl profile at Intake 1 (a) Scenario A; (b) Scenario B; (c) Scenario C; (d) Scenario D.**

Other hydraulic parameters that have been noted to affect fish behaviour have also been simulated using the CFD model. In order to rigorously assess fish entrainment risk, the patterns of velocity curl and turbulent kinetic energy have been evaluated for Scenario A, which has the largest risk zone. Figure 23(a) shows the velocity curl in a plane at the intake midline elevation for Scenario A. At the intake level velocity curl develops a fairly consistent pattern in all of the operational scenarios, with the highest values forming within the operational intakes and adjacent to the boundaries through vortices generation. At a level of 15 m above the intakes there is consistent velocity curl due to vortex formation oriented above Intake 1, adjacent to the wing wall in all operational scenarios. The highest values are generally noted in low head

scenarios, with high flow rates, however there is consistent vortex formation in all scenarios. This indicates that the geometry of the forebay, specifically the presence of the wing wall adjacent to Intake 1, has a very significant impact on the formation of vortices in the forebay. The turbulent kinetic energy obtained from the modeled  $k-\varepsilon$  transport equation for each of the scenarios adjacent to the intakes was similar in all scenarios. As anticipated, the strongest turbulence occurs near the walls and within the intakes; however there is a sharp turbulence gradient upstream of the intakes as is demonstrated in Figure 23(b) for Scenario A. Turbulent kinetic energy within the forebay is in the range of  $3 \times 10^{-6} \text{ m}^2\text{s}^{-2}$ , with a sharp gradient occurring at the dam headwall as flow enters the intakes. Compared to the average velocity in the region, the turbulence is in the scale of 0.3 – 1.2 % of the mean velocity. The turbulence upstream of the orifices is quite low as is expected for lake environments. It is important to note that though the potential flow solution does not take into account the effects of viscosity and turbulence, it still provides acceptable results for this flow. This is similar to the conclusions of other researchers (Islam and Zhu, 2011). This is due to the fact that near the intakes the momentum flux increases by the same scale as the decrease in the pressure integral, which results in the Reynold's stresses, viscous forces and wall shear having very little impact on the momentum flux (compared to the pressure integral) (Islam and Zhu, 2011). Therefore it is expected that turbulence would have a very minor impact on the flow field upstream of the intakes at Mica Dam. Turbulence in the forebay is area is low (much less than a riverine environment) and is unlikely to deter fish from entering the forebay. At this level of turbulence, fish may respond to the flow field with controlled and volitional movements, as opposed to getting pulled along by the flow (Coutant

and Whitney, 2000). This parameter was not evaluated in great detail as it does not appear to impact fish entrainment risk.

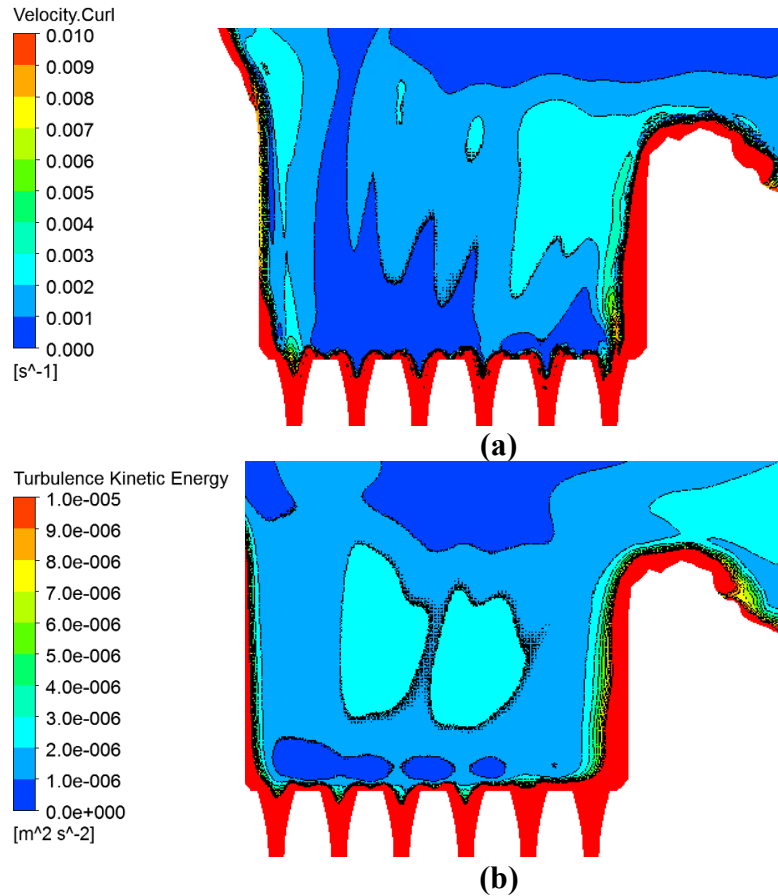


**Figure 23: Hydraulic parameters at the intake centre elevation (692.46) Scenario A (a) Velocity Curl; (b) Turbulent Kinetic Energy.**

### 3.6 Fish Entrainment Risk in the Biological Context

The high risk volume for fish entrainment increases exponentially with decreasing threshold swimming speed. Thus the high risk volume for weaker swimmers and thus, smaller and younger fish located in the forebay adjacent to the intakes is much greater than that of larger fish with greater swimming capabilities. Fish swimming capability at various life stages is likely the

primary biological characteristic that impacts fish entrainment at hydropower facilities once fish are in the vicinity of turbine intakes. The work done by Katopodis and Gervais (1991) suggests that swimming capability is largely a function of fish size and body form/swimming style. Typically salmonids, which exhibit subcarangiform swimming, have sustained swimming capabilities of between 0.5 – 1.0 m/s depending on body length. Juvenile fish, with body lengths less than 200 mm may also be at risk at velocities below 0.5 m/s. As kokanee and bull trout both exhibit subcarangiform swimming style, the swimming capability of adult fish generally exceeds the threshold capabilities presented in this manuscript. The swimming curve developed by Katopodis and Gervais (1991) suggest that for Kinbasket Kokanee, which are generally 200-300 mm in length at maturity (Bray, et al., 2013), and are subcarangiform swimmers, translate to swimming burst distances ranging from 2 - 5 m in water velocities greater than 1 m/s, which may not be sufficient to escape the entrainment zone. Velocities below 0.5 m/s however can be sustained by the species for a long period of time for these adult fish. The threshold for younger fish has yet to be established but will most certainly be lower than the value for adult fish which may suggest that early life stages of kokanee could be at particular risk of entrainment if they encounter the forebay region.

The simulated results of the theoretical high risk zone for fish entrainment indicate that fish are of the highest risk during low pool, as the volume of the forebay exceeding specific velocity thresholds is higher. However, the majority of entrainment events recorded for adult bull trout through Mica dam occurred late in the year during when the reservoir was at high pool and drafting (Martins et al 2013). This indicates that the actual entrainment of fish through hydropower turbines involves both the physical hydraulics and well as behavioural biology,

which is species specific. Indeed, fine-scale tracking of adult bull trout within 350 m of the powerhouse revealed that these fish resided for longer in the forebay and more closely approached the intakes late in the year (Martins et al 2014). Kokanee have also been observed being entrained through Mica dam (Alf Leake, Personal Observation) but there is currently no data on the magnitude and seasonal patterns of entrainment.

Each of these species maintains a certain depth in the water column by controlling their buoyance using swim bladders. The depth that fish such as bull trout occupy in the water column varies seasonally to some extent (Martin, *et al.*, 2014), as the water surface elevation varies drastically over the year, fish are oriented closer to the peak velocities generated by the intakes in low pool scenarios (later winter and early spring). There is comparatively less known about the seasonal depth distribution of kokanee in Kinbasket Reservoir. In the face of changes in pressure, juvenile kokanee have been shown to orient their body upwards and increase the rate of movement of their pectoral fins while mature fish have been noted to move laterally as well as vertically under increased pressure conditions (Harvey and Bothern, 1972). These results indicate that younger kokanee are likely to have less awareness of downward movement in the water column due to dam operations, making this life stage of the species potentially the most susceptible to entrainment.

The velocities that are generated by the dam are relatively low when compared to the theoretical swimming ability of some species and life stages. For example, even juvenile bull trout (110 to 190 mm) have mean critical swimming speeds  $>0.48$  m/s (Mesa et al. 2004). As absolute swimming speeds are correlated with body size, adults ( $> 300$  mm) would have much greater swimming speeds than the water speeds they may experience in the Mica forebay (Scott and

Crossman 1998). Juvenile fish of other species such as kokanee may, however, be at risk for entrainment, as well as adult fish that are unable to detect the relatively rapid acceleration introduced by the swirling flow in the vortex core. The high risk zones for fish entrainment at Mica include areas directly adjacent to the intakes, as well as the area adjacent to the wing wall above Intake 1. Compared to the forebay area considered as the theoretical “risk” zone in Martins et al. (2013, 2014), the actual risk zone based on this hydraulic analysis is much smaller. Fish would have to be very close to the powerhouse to experience such flows that would exceed swimming ability and presumably lead to entrainment.

Collectively these findings reveal that the entrainment risk zone is relatively small representing the areas immediately adjacent to the intakes. Although water velocities certainly accelerate in this area, they likely do not exceed the swimming ability of larger fish species. However, smaller fish, earlier life-stages of large fish and poor swimmers may be at risk of entrainment. When the water is at low pool, and is still drafting, the velocities in the forebay are at the highest suggesting that entrainment risk varies seasonally. Such observations complement those derived from parallel fish telemetry studies (i.e., Martins et al. 2013, 2014).

### **3.7 Conclusions**

A field ADCP and CFD study was completed for the forebay of Mica Dam, located on the Columbia River in BC, Canada. The study was used to evaluate the impact of dam operation on the upstream flow field, to gain insight as to the risk of fish entrainment upstream of the facility. This study presents novel approach to collecting ADCP measurements in a reservoir environment by suspended and ADCP below and anchored boat. Additionally, a complex CFD model was used to simulate the forebays hydraulics and relates both fish habitat use and

behavioural characteristic to potential for entrainment risk. The study demonstrates how CFD modelling can be used to establish the high-risk zone for fish entrainment which can be related to the fish species, age and life history. A potential flow solution was also applied to the flow field upstream of the facility, and it was determined that despite though the potential flow solution neglects viscosity, vorticity and turbulence effects, the solution still performs adequately.

The first objective of this study was to evaluate the impact of water surface elevation on the flow field, as the reservoir level of Mica Dam fluctuates greatly over the course of the year. The results indicate there is a great seasonal variation in the forebay flow field generated by the dam. When the water is at low pool, and is still drafting, the velocities in the forebay are at the highest. In these discharge scenarios there is also a consistent vortex formed above Intake 1, which generates a high velocity swirling flow at all elevations. In general, the turbulent kinetic energy of the forebay was low, average about 1% of the mean flow velocity, indicating turbulence effects are likely negligible in intake-induced flows. Turbulence is also not likely to be a deterrent to fish presence near the intakes.

The second objective of the study was to look at the distance upstream of the dam that hydraulic influences are seen depending on the intakes operational. The velocity field that is generated by the dam shows distinct variation with depth as well as distance along the dam face for the zone within 15 m, or approximately twice the equivalent diameter of the intakes, of the dam in all operational scenarios. Peak velocities occur in front of each of the operational intakes, at the intake elevation, with reduced velocities between each intake and above the intakes elevation. Beyond 15 m the velocity profile becomes uniform at all depths and distances along the dam face. Within 15 m of the dam face the flow is best represented as a series of point sinks along

the dam face. Beyond this the flow field can be represented as a line sink. There was no significant variation in this distance upstream depending on the number operational intakes.

It is important to link fish species and fish biology in interpreting fish entrainment risk analysis.

While the low water level in the spring indicates a high entrainment risk, the turbines are rarely operated during this season and bull trout (at least) barely use the forebay at this time or they stay close to the water surface where water velocities are negligible. On the other hand, significant fish entrainment was reported in the fall season as bull trout start using the forebay more and approach the intakes. An integration of hydraulic engineering with fish biology is needed in assessing fish entrainment risk.

### **3.8 Acknowledgements**

The authors would like to thank the late Mr. Paul Higgins of BC Hydro for providing information used in the completion of this study. We would like to thank Mr. Eduardo Martins for his valuable review of this chapter. Additionally we would like to thank Ms. C. Beth Robertson, Mr. Chris Krath, Mr. Pierre Bourget and Ms. Beth Manson for assistance in the collection of field data. Funding for this research was provided by the Natural Sciences and Engineering Research Council of Canada (NSERC), NSERC Hydronet as well as Engineers Canada and Manulife Financial.

### 3.9 References

- Amaral, S. V., Hecker, G. E., and Dixon, D. A. (2011). “Designing leading edges of turbine blades to increase fish survival from blade strike,” EPRI-DOE, Conference on Environmentally-Enhanced Hydropower Turbines, WA.
- Anohin, V.V., Imberger, J., Romero, J.R., and Ivey, G.N. (2006). “Effect of long internal waves on the quality of water withdrawn from a stratified reservoir.” *Journal of Hydraulic Engineering - ASCE*, 132(11), 1134-1145.
- Barnthouse, L.W. (2013). “Impacts of entrainment and impingement on fish populations: A review of the scientific evidence”. *Environ. Sci. Policy* 31: 149–156. Elsevier Ltd. doi: 10.1016/j.envsci.2013.03.001.
- BC Hydro (2006a). “Fish entrainment risk screening and evaluation methodology”, BC Hydro, Report No. E478.
- BC Hydro (2006b). “Mica Dam Entrainment Risk Screening”, BC Hydro, Report No. E487.
- Bray, K., Sebastian, D., Weir, T., Pieters, R., Harris, S., Brandt, D., Vidmanic, L. (2013). “Kinbasket and Revelstoke Reservoirs Ecological Productivity and Kokanee Population Monitoring 2008 – 2010 Synthesis Report. BC Hydro Reference No. CLBMON-2 and CLBMON-3.
- Bryant, D. B., Khan, A. A., & Aziz, N. M. (2008). “Investigation of flow upstream of orifices”. *Journal of Hydraulic Engineering*, 134(1), 98-104.

- Caliskan, A. and Elci, S. (2009). "Effects of selective withdrawal on hydrodynamics of a stratified reservoir." *Water Resources Management*, 23, 1257-1273.
- Casamitjana, X., Serra, T., Colomer, J., Baserba, C., and Perez-Losada, J. (2003). "Effects of the water withdrawal in the stratification patterns of a reservoir." *Hydrobiologia*, 504, 21-28.
- CFX (2009), "ANSYS CFX solver theory guide", Release 12.0, ANSYS Inc., PA 15317.
- Craya, A. (1949). "Theoretical research on the flow of nonhomogenous fluids", *La Houille Blanche*, 4, 44-55.
- Coutant, C.C., Whitney, R.R. (2000). "Fish behaviour in relation to passage through hydropower turbines: a review". *Transactions of the American Fisheries Society*, 129(2), 351-380.
- Enders, E.C., Gessel, M.H., Anderson, J.J., & Williams, J.G. (2012). "Effects of decelerating and accelerating flows on juvenile salmonid behavior", *Transactions of the American Fisheries Society*, 141(2), 357-364.
- EPRI (1992). *Fish entrainment and turbine mortality review and guidelines*. Stone & Webster Environmental Service, Boston, Massachusetts.
- Fischer, H.B., List, E.J., Koh, R.C.Y., Imberger, J., Brooks, N.H. (1979). "Mixing in Reservoirs." *Mixing in Inland and Coastal Waters*, Academic Press Inc., San Diego CA. p.150 – 228.

Francois, M., Vinh, P., and Mora, P. (2000). "Fish friendly kaplan turbine," "Proceedings of the 20th IAHR Symposium on Hydraulic Machinery and Systems", Charlotte, NC, Paper No. ENV-03.

Goodwin, R.A. (2004). "Hydrodynamics and juvenile salmon movement behavior at Lower Granite Dam: decoding the relationship using 3-D space-time (Cel Agent IBM) simulation". Ph.D. Thesis, Cornell University.

Goodwin, R.A., Nestler, J.M., Anderson, J.J., Weber, L.J., and Loucks, D.P. (2006). "Forecasting 3-D fish movement behavior using a Eulerian–Lagrangian–agent method (ELAM)". *Ecol. Modell.* 192: 197–223. doi: 10.1016/j.ecolmodel.2005.08.004.

Harvey, H.H., Bothern, C.R. (1972). "Compensatory swimming in the kokanee and sockeye salmon *Oncorhynchus nerka* (Walbaum)", *Journal of Fish Biology*, 4, 237-247

Huang, B., Zhu., D.Z., Shao, W., Fu, J.J., Rui, J.L. (2014). "Forebay Hydraulics and Fish Entrainment Risk Assessment Upstream of a High Head Dam in China", *Journal of Hydro-environment Research*, in press, DOI: 10.1016/j.jher.2014.03.002

Islam, M. and Zhu, D.Z. (2011). "Flow Upstream of Two-Dimensional Intakes." *J. Hydraul. Eng.*, 10.1061/(ASCE)HY.1943-7900.0000284, 129-134.

Islam, M. and Zhu, D.Z. (2015). "Selective Withdrawal of Two-Layer Stratified Flows with a Point Sink." *J. Hydraul. Eng.*, 10.1061/(ASCE)HY.1943-7900.0001007, 04015009.

Katapodis, C., Gervais, R. (1991). "Ichthyomechanics". Freshwater Institute, Central and Atlantic Region, Department of Fisheries and Oceans, Winnipeg, MB.

Khan, L.A., Wicklein, E.A., Rashid, M., Ebner, L.L., and Richards, N.A. (2004). "Computational fluid dynamics modeling of turbine intake hydraulics at a hydropower plant", *Journal of Hydraulic Research*, 42(1), 61-69.

Khan, L.A., Wicklein, E.A., Rashid, M., Ebner, L.L., and Richards, N.A. (2008). "Case study of an application of a computational fluid dynamics model to the forebay of the Dalles Dam, Oregon", *Journal of Hydraulic Engineering*, 134(5), 509-519.

Langford, M., Zhu, D.Z., and Leake, A. (2015). "Upstream Hydraulics of a Run-of-the River Hydropower Facility for Fish Entrainment Risk Assessment." *J. Hydraul. Eng.*, 10.1061/(ASCE)HY.1943-7900.0001101, 05015006.

Marcy, B.C., Jr., A.D. Beck and R.E. Ulanowicz. (1978). Effects and impacts of physical stress on entrained organisms. pp. 135-188. In: J.R. Schubel and B.C. Marcy, Jr., (eds.). *Power Plant Entrainment: A Biological Assessment*. Academic Press, NY.

Martins, E. G., Gutowsky, L. F., Harrison, P. M., Patterson, D. A., Power, M., Zhu, D. Z., Cooke, S. J. (2013). "Forebay use and entrainment rates of resident adult fish in a large hydropower reservoir". *AQUATIC BIOLOGY*, 19(3), 253-263.

Martins, E. G., Gutowsky, L. F., Harrison, P. M., Flemming, J. E. M., Jonsen, I. D., Zhu, D. Z., Cooke, S. J. (2014). "Behavioral attributes of turbine entrainment risk for adult resident fish revealed by acoustic telemetry and state-space modeling". *Animal Biotelemetry*, 2(1), 13.

- Mesa, M.G., Welland, L.K., and Zydlewski, G.B. (2004). "Critical swimming speeds of wild bull trout". *Northwest Sci.* 78: 59–65.
- Meselhe, E.A., and Odgaard, A.J. (1998) "3D numerical flow model for fish diversion studies at Wanapum dam", *Journal of Hydraulic Engineering*, 124 (12), 1203-1214.
- Monten, E. (1985). "Fish and Turbines: Fish Injuries During Passage Through Power Station Turbines," Norstedts Tryckeri, Sweden, Report No. 549.
- NPP (2005). "Fish entrainment and mortality study, Vol 1, Niagara Power Project", New York Power Authority.
- Rakowski, C.L., Richmond, M.C., Serkowski, J.A., Ebner, L. (2002). "Three dimensional simulation of forebay and turbine intakes flows for the Bonneville project", Proc., of HydroVision 2002, Oregon.
- RL&L (2000). "Resident fish entrainment information review", RL&L Information Services Ltd.
- Sale, M. J., Cada, G. F., Rinehart, B. N., Sommers, G. L., Brookshier, P. A., and Flynn, J. V. (2000). "Status of the US Department of Energy's advanced hydropower turbine systems program," Proceedings of the 20th IAHR Symposium on Hydraulic Machinery and Systems, Charlotte, NC, Paper No. ENV-01.
- Schilt, C. R. (2007). Developing fish passage and protection at hydropower dams. *Applied Animal Behaviour Science*, 104(3), 295-325.
- Scott WB, Crossman EJ. (1998). *Freshwater fishes of Canada*. Galt House Publications, Oakville, ON
-

Shammaa, Y., Zhu, D.Z., Rajaratnam, N. (2005). "Flow upstream of orifices and sluice gates."

Journal of Hydraulic Engineering, 131(2), 127-133

Solomon, D. J. (1988). "Fish Passage Through Tidal Energy Barrages," Energy Technical

Support Unit, Harwell, U.K., Report No. ETSU TID4056.

Turnpenny, A. W. H., Clough, S., Hanson, K. P., Ramsey, R., and McEwan, D. (2000). "Risk

Assessment for Fish Passage Through Small Low-Head Turbines," Energy Technical

Support Unit, Harwell, U.K., Report No. ETSU H/06/00054/REP.

Von Raben, K. (1964). "Regarding the Problem of Mutilations of Fishes by Hydraulic Turbines,"

Fisheries Research Board of Canada, Translation Series, No. 448, [Die

Wasserwirtschaft, 4, 97-100 (1957)].

Wicklein, E.A., Khan, L.A., Rashid, M., Deering, M.K., and Nece, R.E. (2002). "A three

dimensional computational fluid dynamics model of the forebay of Howard Hanson

dam", Washington, Proc., Hydro Vision 2002, Portland, Oregon.

## Chapter 4

# Thermal Stratification Impact on Forebay Flow Field and Fish Entrainment Risk

---

### 4.1 Introduction

In this chapter the model that was developed for the Mica Dam forebay (Chapter 3) has been extended to investigate the impact of seasonal thermal stratification on the flow field and thermal structure of the Kinbasket forebay. Additionally, a computational fluid dynamic (CFD) model has been developed for the downstream facility on the Columbia River, Revelstoke Dam, which has mid-depth oriented intakes, as opposed to the bottom oriented intakes at Mica Dam. The Revelstoke model has also been used to evaluate the impact of seasonal thermal stratification on the simulated flow field and thermal structure of the forebay.

Mica and Revelstoke are both large hydropower facilities that have varying temperature stratification profiles over the course of the year. In late summer a thermocline develops and the surficial layer of water is substantially warmer than the underlying colder water. The development of this thermocline is primarily due to the local meteorological conditions. In

typical conditions, a reservoir with well-developed stratification will limit the facility to withdrawing water from only the intake-adjacent layer of the reservoir at lower discharges, known as selective withdrawal. At higher discharges, water may be pulled from all layers of the reservoir. Selective withdrawal scenarios not only have an impact on the discharge temperature, and the overall thermal structure of the forebay, they also distinctly impact the flow field developed upstream of the dam. This may have implication for fish entrainment as the risk zone induced by the dam will have seasonal variation with both operations and thermal profile.

#### ***4.1.1 Background***

It is generally well known that deeper lakes and reservoirs in northern climates have dimictic stratification cycle, in which the lakes “turn over” twice each year. Generally reservoirs are isothermal during the winter and spring and stratification develops in later summer and fall (Fischer et al., 1979). A typical reservoir’s stratification profile will have three distinct layers: a well-mixed epilimnion near the water surface, a relatively distinct thermocline or metalimnion, and a lower temperature hypolimnion below this. Some reservoirs, such as the Arrow Lakes at Hugh Keenleyside, downstream of Kinbasket and Revelstoke Reservoirs on the Columbia River, can be approximated by this distinct two-layer stratification. Vidal, et al., (2005), among others have noted that this is not the case for all reservoirs. Seasonal changes in the forebay thermal structure at Kinbasket have been identified by Bray, et al., (2013) and were investigated by Robertson (2012). These studies identified that Kinbasket Reservoir has a more linear thermal stratification profile with a non-distinct thermocline. Additionally, Robertson (2012) identified the presence of internal seiching within Kinbasket Reservoir and related it to geometric control boundaries throughout the reservoir through completing a spectral frequency analysis. The work

completed by Robertson (2012) focused on dynamic fine scale changes in measured thermocline depth upstream of Mica Dam. Typically the seiching was in the order of days, whereas operational changes at Mica Dam are in the order of hours, so this was not included in the modelling. Modelling internal seiching would require transient simulations with very fine time steps and extended run times. The current study focuses on simulating thermally stratified flows under steady state conditions, which approximate the measured thermal profile at Mica Dam.

The characteristics of thermal stratification have previously been studied by numerous researchers, generally noting that the temperature and depth of the epilimnion are controlled by regional meteorological characteristics including the amount of solar insolation from the sun as well as the strength of surficial mixing by the wind (Prigo, et al. 1995). A lack of wind mixing may result in a less distinct or more gradual thermocline, such as the thermal profile noted in Kinbasket Reservoir (Wiegand and Chamberlain, 1987).

The vertical density distribution and corresponding pressure distribution of a thermally stratified reservoir may limit the elevation at which water is withdrawn from. This is most distinct in reservoirs that have a very distinct thermal stratification profile such as two-layer, or well developed hyperbolic profile thermal stratifications. Shammaa and Zhu (2010) investigated thermal stratification in the laboratory and determined that at a certain point the discharge through an outlet is great enough to upset the upstream thermal stratification and allow withdrawal from all layers of the reservoir. This is termed the critical discharge. Several other studies also look at the concept of selective withdrawal and its impacts on upstream thermal stratification. These include studies completed by Wood (2001), Casamitjana et al. (2003), Caliskan and Elci (2009), Anohin et al. (2006) and Islam and Zhu (2015). Generally, when the

discharge through a facility exceeds the critical withdrawal it has been noted that withdrawals have a much greater impact on the thermal regime of the upstream reservoir. Craya (1949) provided a formula relating the vertical distance from a point sink to the thermocline to the critical discharge in a two-layer stratified reservoir.

There have been several previous studies that have been completed at the Arrow Lakes on the Columbia River in BC, assessing thermal stratification that have generally focused on the impact on temperatures downstream of the Hugh Keenleyside Dam. In 1993, water temperature profiles were measured in the dam's forebay, which were used as input to a SELECT model to predict the temperature of flow through both the spill ways and low level outlets (RL&L Environmental, 1997). It was found that the modelled temperature downstream of the facility (which predicted cooler temperatures from the low level outlets and warmer temperatures from the spill ways) was not verified by the measured field data. Field studies found that regardless of which mode of operation the dam was using, the temperature measured directly downstream was relatively constant. This led to the hypothesis that there is significant vertical mixing immediately upstream of the facility that was not identified by the model. This explained the similarity of the withdrawal temperatures regardless of intake elevation (RL&L Environmental, 1997).

Subsequent modelling, using the DYRESM model by the National Water Research Institute demonstrated that the thermal stratification in the lake is relatively sensitive and continually changing due to weather disturbances (BC Hydro Report, 1997a).

BC Hydro's Mica Dam impounds the upstream Kinbasket Reservoir as discussed in Chapter 3. The Kinbasket Reservoir has a level that rapidly fluctuates over the course of the year depending on dam operations. The dam is licensed to operate in a manner that maintains the reservoir level

between 707 and 754 m geodetic elevation at all times. Historically the reservoir level has fluctuated by approximately 42 m with water surfaces recorded between 712 and 754 m, however annual fluctuation is generally lower. In general the reservoir level fluctuates by approximately 25 m annually. Typically the reservoir is lowest in May and is highest in September. The facility controls the reservoir level through four intakes (currently being expanded to six intakes) as well as several non-power outlets. The Kinbasket Reservoir has a linear thermal stratification profile from the atmospheric temperature at the water surface to approximately 4 °C at the intakes elevation throughout the reservoir (Bray, 2013). As the thermal profile of the upstream reservoir has a distinct difference on the flow field established upstream of outlet structures, it is important to understand the impact thermal stratification on the flow field. Mica Dam has bottom oriented outlets that are flanked on either side by wing walls. This complex geometry results in a more complicated flow throughout the forebay of the dam as studied in Chapter 3.

The downstream reservoir on the Columbia River, The Revelstoke Reservoir, impounded by Revelstoke Dam has the same number of intakes with similar capacity. The location of the Revelstoke Dam relative to Mica Dam on the Columbia River is included as Figure 24. BC Hydro operates the Revelstoke and Mica facilities in sync with each other, and typically the total discharge through Mica matches the total discharge through Revelstoke. As such, the Revelstoke Reservoir operates in a somewhat steady-state condition. Compared to Mica Dam, the Revelstoke Dam has a more simplistic geometry, consisting of six intakes located approximately 25 m below the water surface. The bed of the reservoir is an additional 100 m below the intakes. Additionally the Revelstoke intakes have no adjacent wing walls or other

structures. The Revelstoke Dam is a large run-of-the-river hydropower project, and there is not significant annual fluctuation in the reservoir level. A previous CFD modelling study was completed by Bhuyian and Zhu (2009) for the Mica and Revelstoke forebays. This study evaluated the flow field upstream of the dams in isothermal conditions only. One of the recommendations of the previous CFD study was that there would be value in evaluating the flow field upstream of Revelstoke in thermally stratified conditions. For this study CFD models have been developed to simulate similar thermal stratification scenarios for each of the dams.

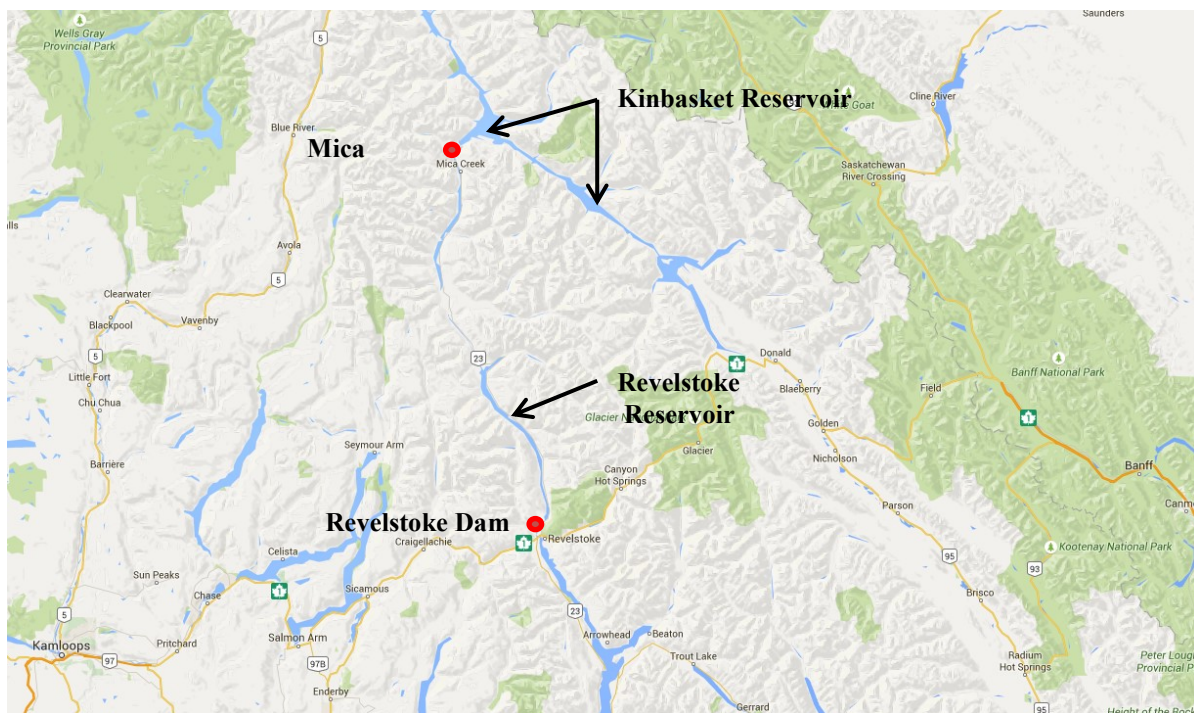


Figure 24: Location plan.

Previous studies have identified that Bull trout (*Savelinus confluentus*) and Kokanee salmon (*Oncorhynchus nerka*) are of particular risk for entrainment at the Mica facility (BC Hydro, 2006a). As Kokanee salmon are a pelagic fish species that are reliant on plankton as food during early life stages, they are generally more likely to be located in higher velocity flows adjacent to

the intakes. Additionally, they exhibit diurnal feeding habits which place them deeper in the water column (25-80 m deep) during the day when the highest discharges through the dam are seen (BC Hydro, 2006a). Bull trout, which prey on Kokanee salmon, exhibit similar feeding cycles. In addition to Kokanee salmon and Bull trout, the following fish species have been historically observed in Kinbasket: Rainbow trout (*Oncorhynchus mykiss*), Cutthroat trout (*Oncorhynchus clarki*), Brook trout (*Salvelinus fontinalis*), Mountain Whitefish (*Prosopium williamsoni*), Burbot (*Lota lota*), Longnose sucker (*Catostomus catostomus*), Largescale sucker (*Catostomus macrocheilus*), Redside shiner (*Richardsonius balteatus*), Peamouth (*Myclocheilus caurinus*), Northern pikeminnow (*Ptchocheilus oregonensis*), Pygmy whitefish (*Prosopium coulteri*), Longnose dace (*Rhinichthys cataractae*), Prickly sculpin (*Cottus asper*), Torrent sculpin (*Cottus rhotheus*) and Mottled sculpin (*Cottus bairdi*) (BC Hydro, 2006a).

The Revelstoke Dam has been noted to pose an entrainment risk to Kokanee salmon and potentially their predators, Bull trout as well (Biosonics, 2011). Biosonics, 2011, noted that near the dam face, Kokanee that were young of the year were typically surface oriented, with the greatest density at depth less than 25 m, placing them above the intakes. Large fish, age 1 and above were present throughout the water column, but were most dense at approximately 25 m depth, adjacent to the intakes. Other fish that have been noted in the Revelstoke Reservoir include Rainbow trout, Mountain Whitefish, Burbot, Largescale sucker, Longnose sucker, Peamouth, Northern pikeminnow, Redside shiner and Prickly sculpin (BC Hydro, 2006b). Of these species Kokanee salmon and Bull trout were noted to be of highest risk for entrainment due to their life history and presence in the reservoir adjacent to the dam.

#### **4.1.2 Objectives**

The objectives of this study are to provide a comparison in the difference between thermally stratified and isothermal conditions at Mica Dam and Revelstoke Dam to study the impacts of seasonal thermal stratification on the flow field. The Mica scenarios investigate the impact of thermal stratification at a dam with bottom oriented outlets and a complex geometry. The Revelstoke scenarios further investigate the impacts of thermal stratification on the flow field and thermal structure in a more idealized setting. This reservoir is distinctly different than Mica as the geometry is much simpler, and the lateral and vertical boundaries are much further away from the intakes. The objectives of this chapter include:

- analyzing the impact of water depth (and thus distance of the water surface from the intakes) on the upstream hydraulics at Mica Dam (under thermally stratified and isothermal scenarios).
- Exploring the effects of modifying operational conditions at the dam on the upstream flow field (under thermally stratified and isothermal scenarios).
- Provide a comparison as to the difference (and scale of difference) between using different thermal stratification profiles (linear, hyperbolic, two-layer discrete),
- Analyzing the impact of splitting discharge between different combinations of intakes on the flow field and thermal structure upstream of the dam,
- Developing a clear view of what the implication of thermal stratification is for fish entrainment risk,
- Investigate the impact of thermal stratification on outlet discharge temperature which has an impact on both fish attraction to the risky zone as well as on downstream habitat, and

- Evaluating how the results from the more complex geometry (bottom-oriented outlets and wing walls) relate to those of a simplified geometry (mid-depth oriented outlets with no adjacent structures).

This study involves completing both field measurements at the Mica Dam facility as well as CFD modelling. Field measurements of seasonal thermal stratification in Kinbasket Reservoir and the flow field adjacent to the intakes were measured. These measurements were used to understand the seasonal thermal structure of the reservoir and to validate a CFD model of the forebay. The CFD model was then used to simulate the flow field for different operational configurations, reservoir levels and thermal profiles. The study completed at Revelstoke Dam used CFD only, using the same methodology developed for the Mica study.

## **4.2 Field Measurements**

### ***4.2.1 Thermal Profile***

Continuous temperature profile measurements were taken autonomously from May 13, 2011 to November 3, 2011 using a thermistor chain installed in the forebay close to the dam face, as shown in Figure 25. The Onset Tidbit v2 thermistors that were used have an accuracy of 0.2 °C over the range of temperatures measured in this study and a resolution of 0.02 °C. All thermistors were recording at 5 min intervals, and were physically spaced at approximately 2 m intervals. The thermistor measurements have been used to establish a thermal profile for the CFD model in this study. The measurements collected were analyzed in detail by Robertson, (2012). The focus of Robertson, (2012) was to provide a detailed assessment of the seasonal thermal stratification characteristics. The current study extends this analysis by utilizing these

measurements in the CFD model for Mica Dam established in Chapter 3. A summary of the thermal measurements is as follows:

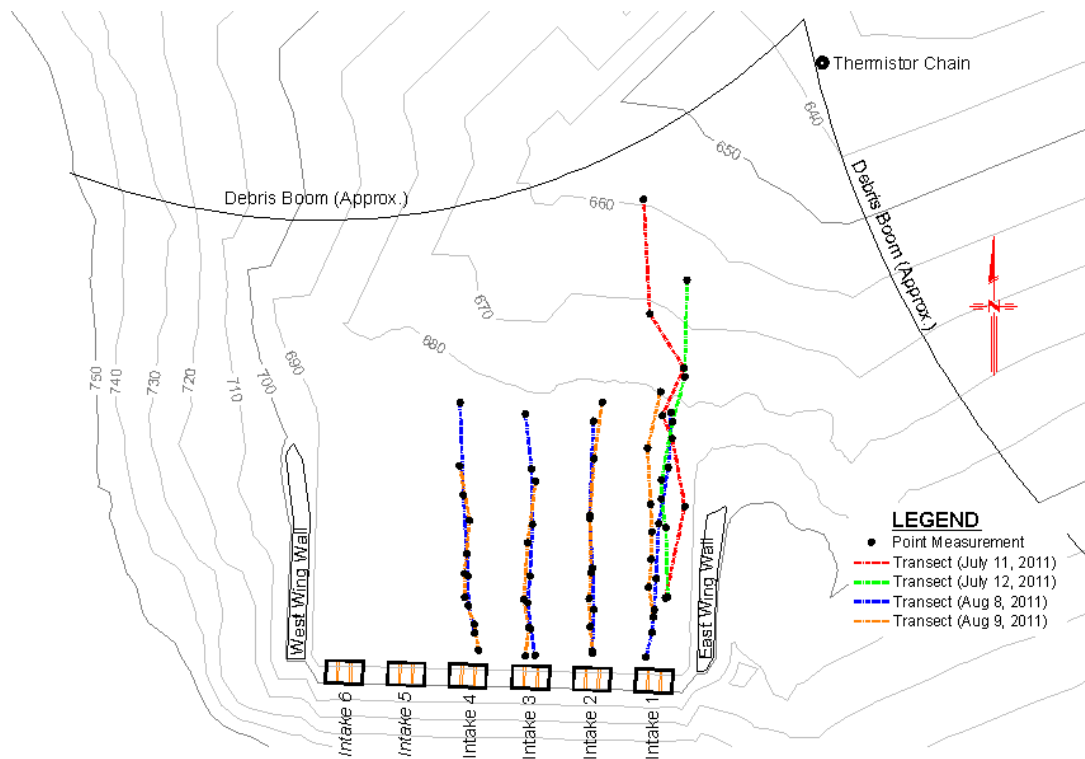


**Figure 25: Thermistor chain location.**

In spring the reservoir was relatively isothermal, with very little variation in water temperature with depth. In early June, the reservoir started experiencing its first “turn-over”, the surface of the reservoir began to warm up due to thermal isolation from the sun in the summer months. Over the months of June and July the thermal profile of the reservoir rapidly changed as the reservoir became fully stratified. The reservoir remained fully stratified for the duration of August and first half of September at which time its second cycle of “turning-over” began. The reservoir was once again isothermal by the end of October. Over the span of time that the thermistors were installed at Kinbasket, temperature measurement within the forebay ranged

from 3.72 to 20.44 °C, with the coldest temperature measured at the bottom of the thermistor chain (approximate depth = 63 m). Alternatively, the warmest temperatures were measured in the summer at the water surface. There were significant differences in the typical temperature profiles from month to month. In general, the stratification was somewhat linear from the surface to the bottom of the thermistor chain. The development of the thermal stratification profile at Kinbasket Reservoir over the summer months of 2011 is included as Figure 26.

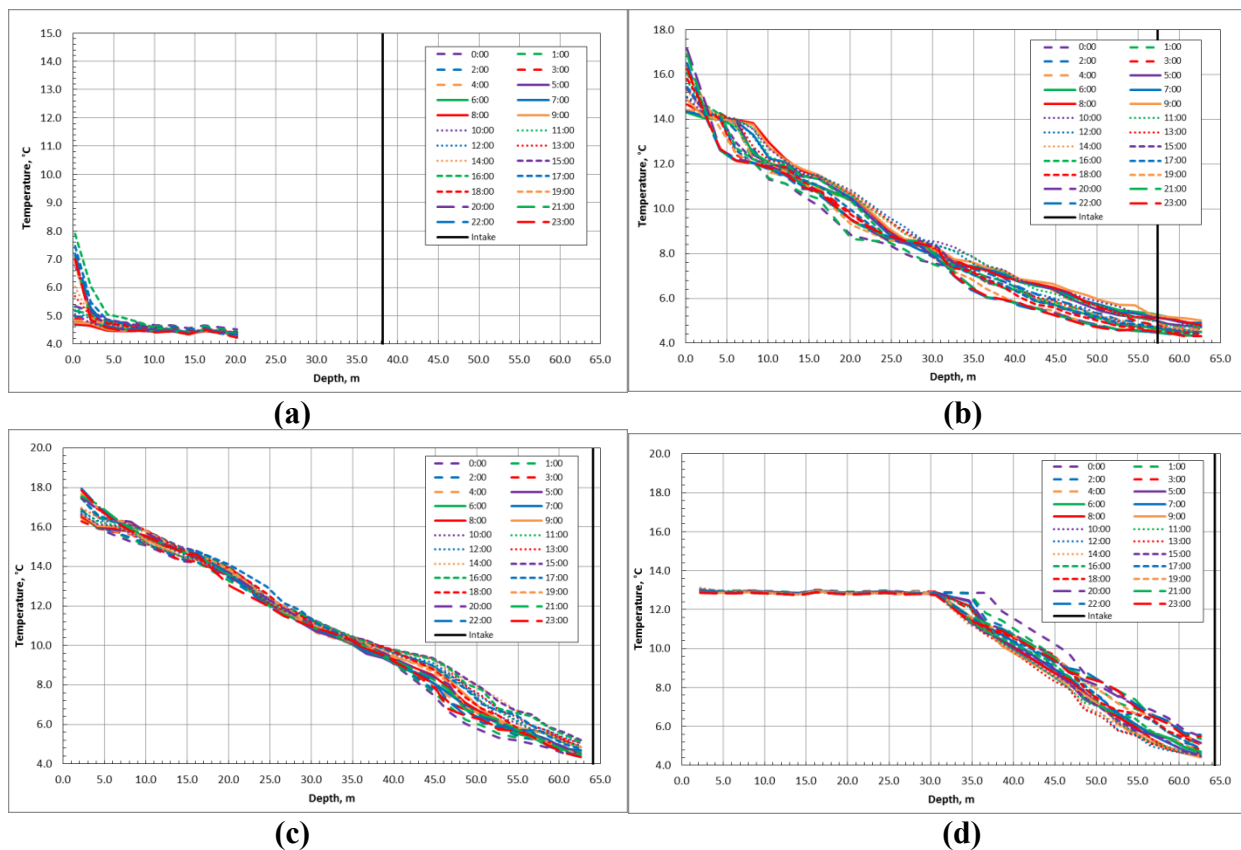


**Figure 26: Kinbasket Reservoir thermal stratification (a) May; (b) July; (c) August, (d) October (modified from Roberston, 2012).**

Water temperature profiles in the month of August, at the time of hydraulic field measurements by ADCP (previously discussed in Chapter 3), were fairly uniform. A typical profile is shown in Figure 26(c) for August 28, 2011. For the month of August, the water surface temperature ranged from 12.9 to 19.6 °C with an average temperature of 16.0 °C. As anticipated, at the deepest thermistor there was a much smaller fluctuation in water temperatures as the magnitude of the diurnal variation in temperature is decreased further from the water surface. At the lowest thermistor, the temperature range measured over the month of August ranged from 3.9 to 6.3 °C, averaging 4.6 °C. The monthly temperature measured at the surface were warmer in August, than the previous month, however there was little variation in water temperature at the bottom of the thermistor chain between July and August.

#### ***4.2.2 Velocity Field***

Flow profiles were measured during August 8 – 10, 2011 using an acoustic Doppler current profiler (ADCP) from a boat in the forebay. The Teledyne RD Instruments Workhorse Sentinel 600 kHz (Sentinel) was used, utilizing the equipment's self-contained measurement feature. The locations of the ADCP measurements are shown in Figure 25. In terms of velocity measurement, the Sentinel has an accuracy of 0.3 % of the water velocity relative to the instruments, or 3.0 mm/s and a resolution of 1 mm/s. The Sentinel has a beam angle of 20° which restricts the approach distance the measurements can be made from the dam face. Flow profiles in the immediate forebay were recorded when the dam spilling rates were held relatively constant throughout each set of measurements. During the field work, measurements in front of Intakes 1 – 4 were taken at discharges of 240, 245, 270, 269 m<sup>3</sup>/s, respectively, the first day and 252, 269, 274, 266 m<sup>3</sup>/s, respectively, the second day. ADCP measurements were particularly

difficult at this facility due to the depth of the forebay in the late summer, and restricted access to the banks or the forebay. Details on the hydraulics field measurement completed using the ADCP are included in Chapter 3.

### **4.3 Computation Fluid Dynamic Modelling**

#### ***4.3.1 Model Development***

The extents of the CFD model of the Mica forebay cover the forebay extending from the dam face to approximately 2.5 km upstream as shown in Figure 12(b) of Chapter 3. The CFD solver uses the three-dimensional Reynolds-averaged Navier-Stokes equations, with the  $k - \varepsilon$  turbulence model to assess eddy viscosity. To compute temperature transport, a full buoyancy model was chosen. Density profiles for the computed temperature profiles were determined using an equation of state. The computed density was then substituted into the Navier-Stokes equations to compute the buoyancy source term. Details of the CFD model, as well the model validation are included in Chapter 3. In the current study, the model scenarios have been expanded specifically to look at the impact of thermal stratification modelling on the upstream hydraulics at Mica dam.

In addition to the field scenario at Mica dam, which was used to compare the models performance to the field measurements, various other scenarios were developed in order to determine the impact of thermal stratification on the upstream flow field at Mica. The scenarios generally ranged in both discharge and water surface level, and thermal stratification profile. Ten select scenarios, capturing a broad variety of operations, reservoir levels and thermal profiles that were analyzed for Mica Dam are outlined in Table 5.

**Table 5: Mica Dam thermal stratification scenarios.**

Scenario	Turbines Active	Discharge per Turbine (m <sup>3</sup> /s)	Discharge Total (m <sup>3</sup> /s)	Head Description	Water Surface Elevation (m)	Stratification Profile
MCA-1	6	223.76	1342.56	High	749.77	Linear
MCA-2	6	223.76	1342.56	High	749.77	Isothermal
MCA-3	6	223.76	1342.56	Low	726.55	Linear
MCA-4	6	223.76	1342.56	Low	726.55	Isothermal
MCA-5	6	223.76	1342.56	Low	726.55	Hyperbolic
MCA-6	6	223.76	1342.56	Low	726.55	Discrete
MCA-7	4	223.76	895.04	Low	726.55	Linear
MCA-8	4	223.76	895.04	Low	726.55	Isothermal
MCA-9	1	223.76	223.76	Low	726.55	Linear
MCA-10	1	223.76	223.76	Low	726.55	Isothermal

The geometry of the intakes at Revelstoke Dam was developed based on record drawings dated 1976 and 1989. At Revelstoke, the dam headwall is vertical and the intakes are circular with a diameter of 7.9 m. Similar to the Mica model, the Revelstoke model extends 2.5 km upstream of the dam's headwall. The headwall of Revelstoke Dam is vertical. As the intakes are located > 100 m above the bottom of the reservoir and sidewalls, a simplified geometry of a rectangular open channel was incorporated into the model as the bottom and side variations are assumed to have an insignificant effect on the hydraulics of the forebay adjacent to the intakes. The water surface elevation of the Revelstoke Reservoir has fluctuations limited to approximately 1 m. A steady water surface elevation was used for the modelling in this chapter. The geodetic elevation of the water surface at Revelstoke is 536.0 m. A similar procedure was adopted by Bhuyian and Zhu (2009) in preliminary modelling of the Revelstoke Reservoir. This simplification to the model geometry allows for additional computational efficiency as the mesh adjacent to the sidewalls will be simplified. The Revelstoke model was developed using a similar methodology to the MCA model. Mesh independence was investigated using three different mesh sizes. The

edge length of the coarse mesh (Mesh 1) was the default length determined by the meshing software (Ansys Meshing). Two finer meshes were constructed by systematically reducing the edge length of the elements in the mesh by a factor of 0.5. Meshes 1 (coarse), 2 (intermediate) and 3 (fine) had a total of 1.2 million, 4.1 million and 10.8 million nodes respectively. In evaluating the performance of each mesh it was determined that the average discrepancy between Mesh 1 and Mesh 2 was 0.8%, with a maximum discrepancy of 2.1%. The average discrepancy between Mesh 2 and Mesh 3 was 0.3%, with a maximum discrepancy of 1.4%. It was determined that Mesh 1 provided an adequate solution, while maximizing the efficiency of the computations.

The convergence criteria for the model were set such that the root mean square (RMS) of the residual is below  $10^{-4}$  in all the simulations carried out. The solution for the model used a blended advection scheme, with a blend factor of 0.90 and high resolution solution for turbulence numerics. The pressure and velocity interpolation schemes were specified as trilinear with a geometric shape function option. Velocity pressure coupling was included with a fourth order Rhie Chow option.

A total of 10 operational scenarios have been simulated using the Revelstoke model. The first four scenarios (REV-1 through REV-4) simulate the dam operating at maximum capacity for four different thermal stratification scenarios (linear, isothermal, hyperbolic and discrete), similar to the development of the Mica model. The impact of discharge allotment through each of the intake structures is analyzed in more detail through the remaining six scenarios (REV-5 through REV-10), in which the difference between having a single unit operating at maximum capacity is compared against splitting the discharge between four and six units for both the linear and

discrete thermal stratification profiles. A summary of each of the scenarios that were developed for Revelstoke is included in Table 6.

**Table 6: Revelstoke Dam thermal stratification scenarios.**

Scenario	Turbines Active	Discharge per Turbine (m <sup>3</sup> /s)	Discharge Total (m <sup>3</sup> /s)	Water Surface Elevation (m)	Stratification Profile
REV-1	6	223.76	1342.56	536.00	Linear
REV-2	6	223.76	1342.56	536.00	Isothermal
REV-3	6	223.76	1342.56	536.00	Hyperbolic
REV-4	6	223.76	1342.56	536.00	Discrete
REV-5	6	37.29	223.76	536.00	Linear
REV-6	4	55.94	223.76	536.00	Linear
REV-7	1	223.76	223.76	536.00	Linear
REV-8	6	37.29	223.76	536.00	Discrete
REV-9	4	55.94	223.76	536.00	Discrete
REV-10	1	223.76	223.76	536.00	Discrete

The development of the stratification profile for each of the scenarios was based on the following equations. The derivation of the density versus depth and pressure versus depth profiles for the CFD model used the same procedure previously described for the field scenario, which is discussed in detail in Chapter 3. The thermal stratification profile was used to calculate the density profile, which in turn was integrated over depth to develop the pressure profile, which account for minor changes in water pressure with depth in the reservoir. This was supplied in the CFD model as the initialization condition throughout the reservoir, as well as at the upstream boundary.

Four different stratification profiles are analyzed in this study. These include Isothermal (constant temperature (4 °C) at all depths), Linear, Hyperbolic and Discrete (two-layer). These are respectively described by the equations below.

#### 4.3.2 Linear

$$T = \left\{ \begin{array}{l} T_e \\ T_e + (T_h + T_e) \frac{(Z-Z_e)}{(Z_h-Z_e)} \\ T_h \end{array} \middle| \begin{array}{l} Z < Z_e \\ Z_e < Z < Z_h \\ Z > Z_h \end{array} \right\} \quad \text{Equation 13}$$

Where  $T_e$  is the temperature at the epilimnion,  $T_h$  is the temperature of the hypolimnion,  $Z_e$  is the depth to the bottom of the epilimnion and  $Z_h$  is the depth to the top of the hypolimnion. For the model values of 16, 4, 10 and 30 were respectively used for each of the low head scenarios (MCA-3, MCA-7 and MCA-9). An adjustment to the variables was made for the high head scenario (MCA-1) to reflect the increase in water depth.

#### 4.3.3 Hyperbolic

$$T = \frac{\alpha_1(Z-\alpha_2)}{\sqrt{\alpha_3+(Z-\alpha_2)^2}} + \alpha_4 \quad \text{Equation 14}$$

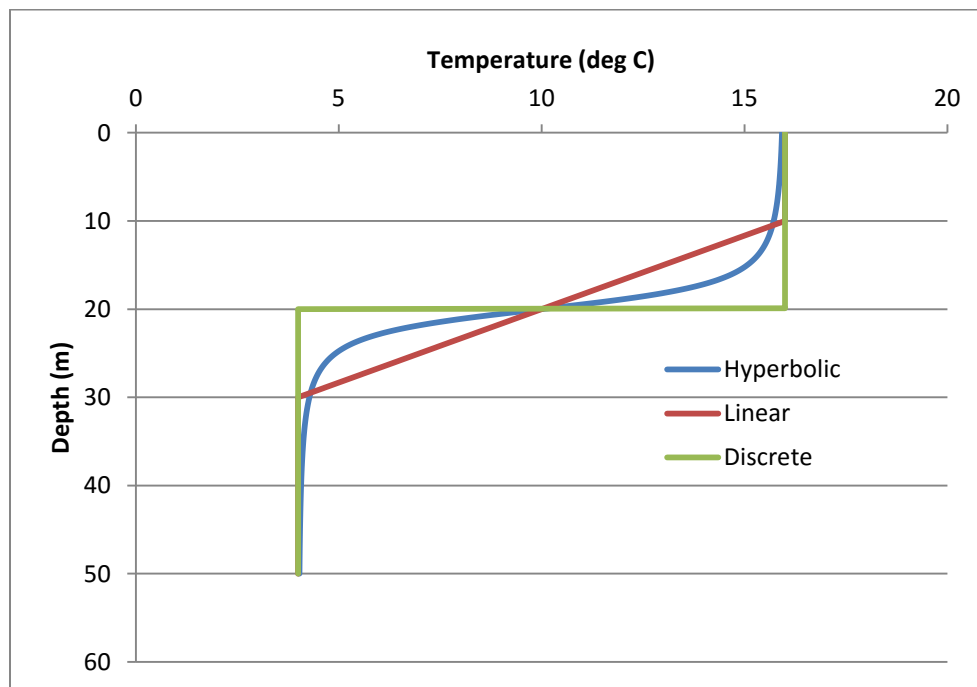
Where  $\alpha_1$  is a coefficient related to the hyperbolic form of the function (approximately  $-0.5(T_e - T_h)$ ),  $\alpha_2$  is the elevation depth spanned by the thermocline,  $\alpha_3$  is a coefficient related to the slope of the thermocline and,  $\alpha_4$  is the temperature at the middle of the thermocline (the average temperature between  $T_e$  and  $T_h$ ). For the model values of -6, 20, 10 and 10 were respectively used.

#### 4.3.4 Discrete

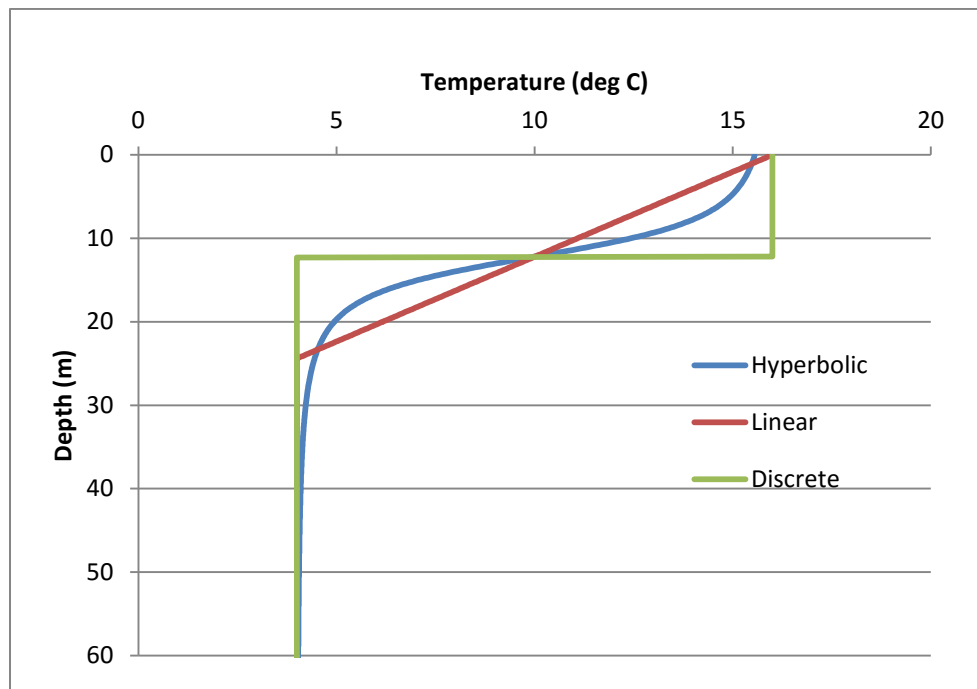
$$T = \left\{ \left\{ \begin{array}{l} T_e \\ T_h \end{array} \middle| \begin{array}{l} Z < Z_e \\ Z > Z_t \end{array} \right\} \right\} \quad \text{Equation 15}$$

Where  $Z_t$  is the depth of the thermocline. For the model this depth was 20 m for Mica Dam and 12.2 m for Revelstoke Dam.

The standard values for the coefficient that were used in the model that are presented above outline the model parameters that were used in the model scenario at low head (MCA-3 through MCA-10), such that a direct comparison was available between the varied thermal profiles. For the high head profile (MCA-1) and adjustment to the coefficients in the linear profile were made to accommodate the increased water depth. The thermocline for the Revelstoke model was simulated 12.2 m below the water surface, 1/2 of the distance from the middle of the intake to the water surface. Adjustments were made to the coefficients of Equations 13, 14 and 15 above to demonstrate this difference. The thermal profiles for Mica and Revelstoke are included as Figure 27. The profiles used are based on typical late summer field measurements throughout the reservoirs completed by BC Hydro, (Bray, et al. 2013).



(a)



(b)

Figure 27: Thermal stratification profiles (a) Mica Dam; (b) Revelstoke Dam.

The boundary conditions for the Mica and Revelstoke models include the following:

- Water surface is simulated as a fixed, free-slip surface,
- The dams headwall and intake sidewalls are specified as smooth no-slip surfaces,
- The reservoir sidewalls and bottom are specified as rough no-slip surfaces with a roughness height of 0.3 m due to the riprap apron,
- Each of the intakes are simulated as outlets with a specified mass flow rate (refer to Tables 5 and 6). Despite the minor changes in density due to temperature, mass flow rates have been calculated as discharge multiplied by the density of water at 4 °C (1000 kg/m<sup>3</sup>),

- The upstream boundary was specified as an opening which allows water to flow in and out, and
- The temperature profile and corresponding density and pressure profiles were specified as the initialization conditions throughout the reservoir as well as fixed at the upstream boundary.

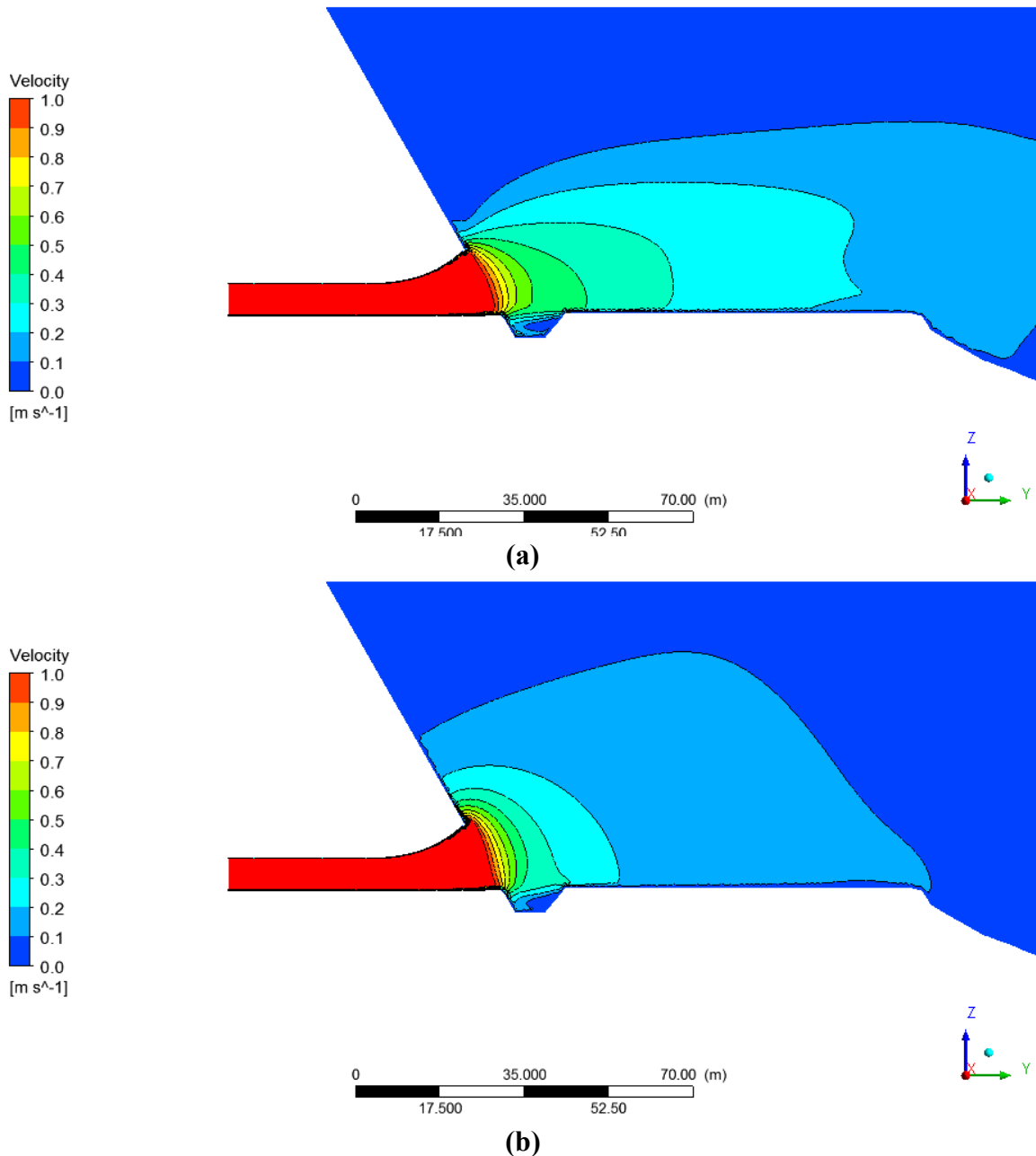
#### **4.4 Results and Discussion**

The CFD model that was developed for the study was used to simulate each of the operational scenarios outlined in Tables 5 and 6. The results consistently demonstrated that the inclusion of thermal stratification into the model simulation results in a distinctly different velocity profile upstream of the intakes. The results of the model study were applied to determine the fish entrainment risk for the facilities following the procedure that was been previously used for Aberfeldie by Langford et al (2015) and Mica Dams in Chapters 2 and 3.

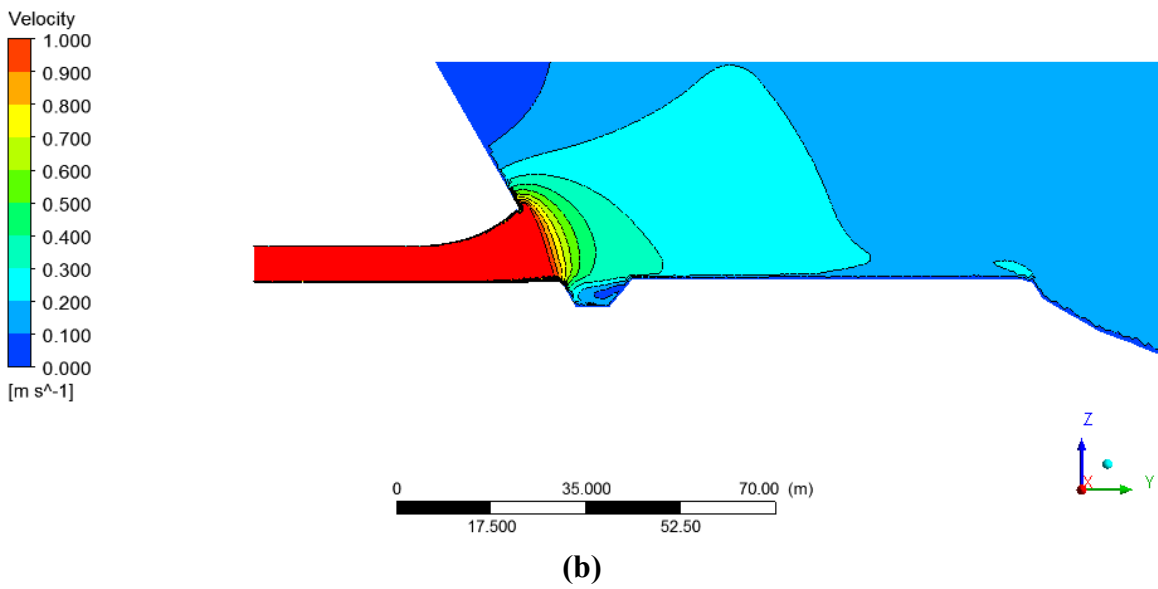
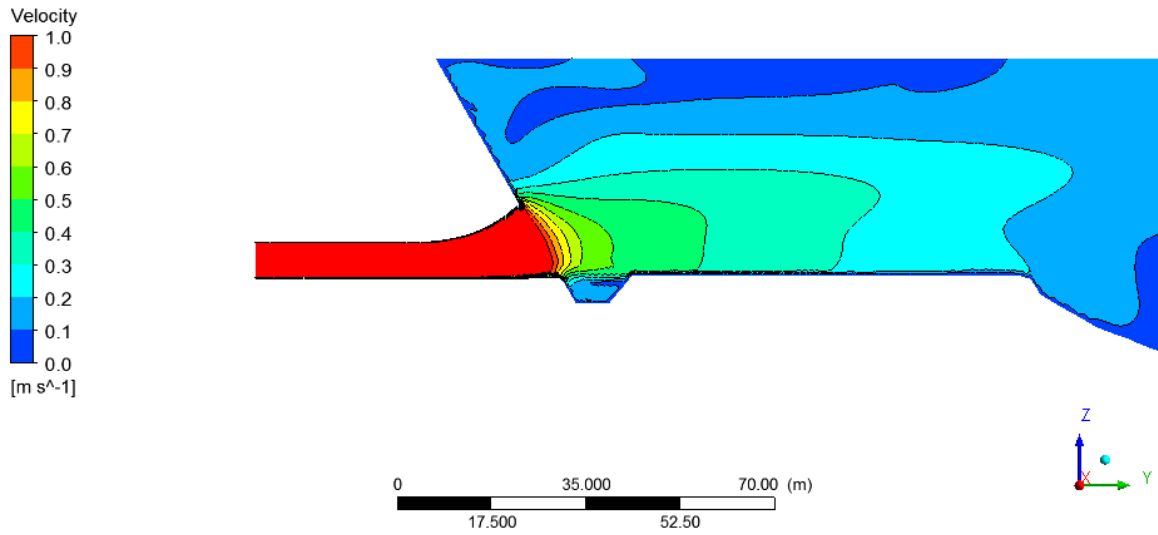
##### ***4.4.1 Flow Field at Mica Dam***

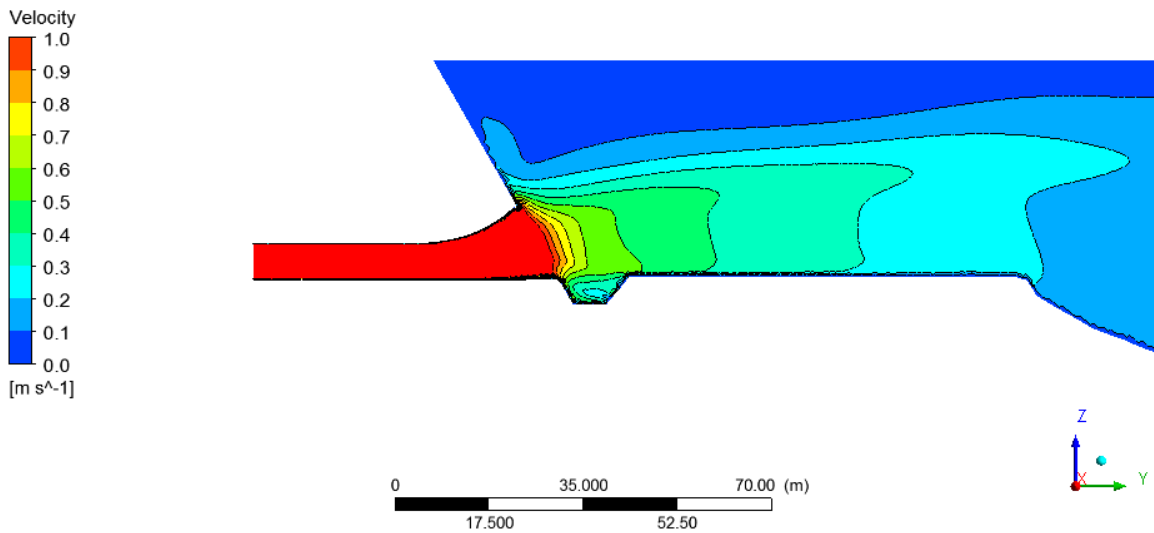
Comparisons between the velocity magnitude upstream of Intake 3 for the MCA-1 and MCA-2 scenarios are included in Figure 28. Similar plots for the low head scenarios, MCA-3, MCA-4, MCA-5 and MCA-6 are included as Figure 29. There is very little difference in the contours for the highest velocity zones ( $> 0.8$  m/s), however, in the thermally stratified scenario, MCA-1, it takes a much greater upstream distance for the velocity to become uniform with depth. Similarly in the low head scenarios (Figure 29) there is not a substantial difference in the contours generated for the high velocity zone adjacent to the intakes. The most substantial difference that can be noted is that in each of the thermally stratified scenarios, the low velocity contours extend a much greater distance upstream. In all scenarios it can be noted that the water adjacent to the

water surface is much slower moving in the thermally stratified scenarios as the majority of water drawn through the dam is from lower elevations. Thermal stratification in all scenarios develops a velocity gradient that is much larger with respect to depth in the summer months than winter (isothermal) months.

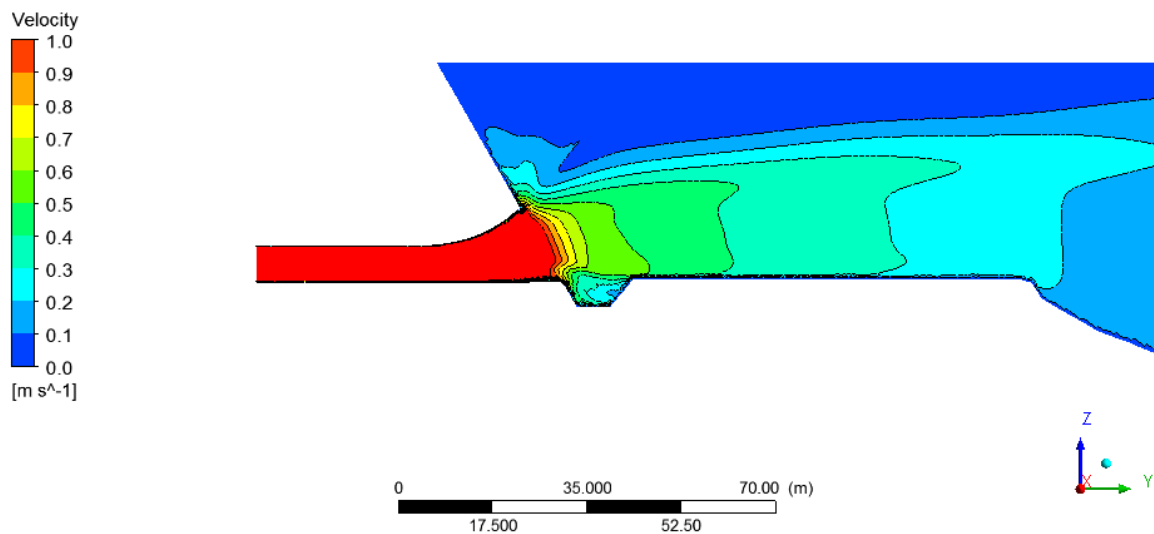


**Figure 28: Intake 3 velocities magnitudes (high head scenarios (a) MCA-1; (b) MCA-2.**





(c)



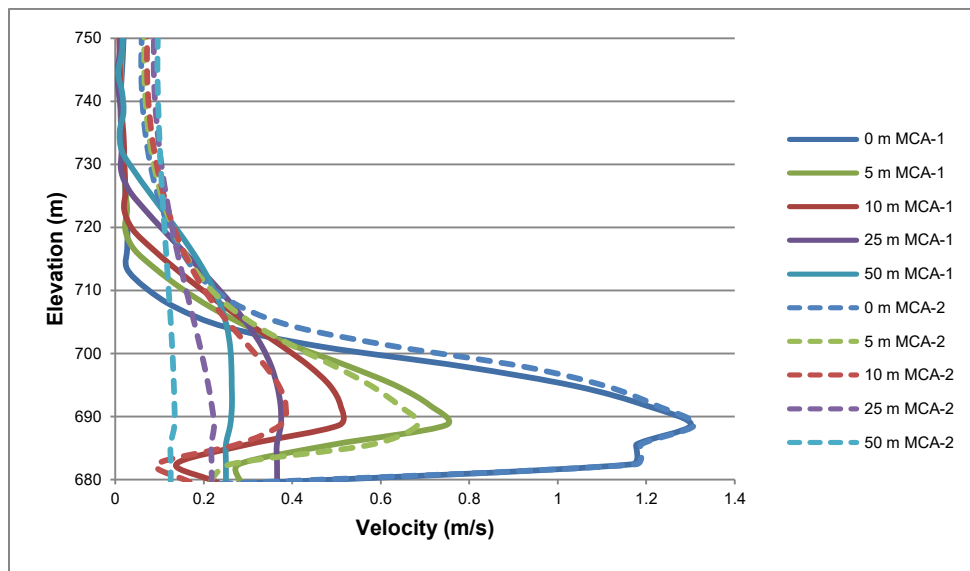
(d)

**Figure 29: Intake 3 velocity magnitudes (low head scenarios) (a) MCA-3; (b) MCA-4; (c) MCA-5; (d) MCA-6.**

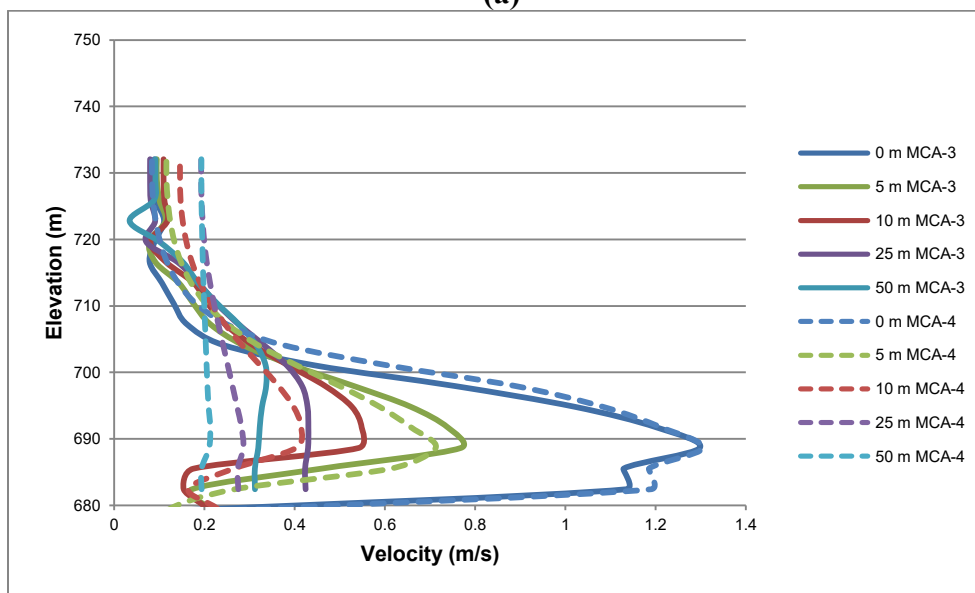
The flow field that is induced upstream of the dam in the hyperbolic and discrete thermal stratification profiles (MCA-5 and MCA-6) which as shown as Figure 29 (c) and (d) respectively, generated very similar velocity profiles for the coefficients of the equations that

were used in this study. This indicates that the hyperbolic profile, which is a more common thermal profile found in natural flows, is well represented by a discrete thermal stratification, which has previously been studied in both analytically (Craya, 1949), numerically (Islam and Zhu, 2015) and in a laboratory setting (Shammaa and Zhu, 2010).

It is also noted that generally, the acceleration zone adjacent to the intakes is confined to a decreased range of depth due to the presence of thermal stratification. This in turn results in high velocities adjacent to the intakes and lower velocities above the intakes. Figure 30 identifies the impact of thermal stratification on the upstream velocity profile at distances of 0, 5, 10, 25 and 50 m upstream of intake three in both the high head scenarios (MCA-1 and MCA-2) as well as the low head scenarios (MCA-3 and MCA-4). It is evident that the discrepancy between isothermal and thermally stratified scenarios increases with distance upstream of the intakes. Typically at the intakes (0 m) there is little to no difference between the isothermal and thermally stratified scenarios, whereas at distances of greater than 10 m (approximately 1 x the intakes equivalent diameter) upstream of the intakes, the peak velocity for thermally stratified flows is 1.5 – 2.1 times greater than the isothermal scenario. At all distances upstream of the intakes, the velocity simulated near the water surface, at depths shallower than approximately 1.5 times the intakes equivalent diameter above the intake centreline, the simulated velocities are greater in isothermal conditions.



(a)



(b)

**Figure 30: Velocity profiles upstream of Intake 3 for varied water surface elevations (a) MCA-1 and MCA-2 (high head); (b) MCA-3 and MCA-4 (low head).**

As noted the impact of thermal stratification is most prominent at locations greater than 10 m upstream of the dam headwall. Figure 31 identifies the impact of thermal stratification profile on the velocity field development as it approaches the dam face. As previously noted, at the intake

there is little difference between each of the simulations. The further the distance upstream of the dam face there is a much more notable discrepancy between the thermally stratified scenarios (MCA-3, -5 and -6) compared to the isothermal scenario (MCA-4). The distance upstream that the velocity profile becomes uniform with depth in the stratified scenarios is approximately 200 m, which is much greater than the isothermal scenario which is relative uniform (maximum variation from average of less than 10 %) at a distance of 50 m upstream of the dam face. It is also noted on Figure 31 that though the velocity profiles are similar in each of the stratified scenarios, they most closely match for the discrete and hyperbolic stratification profiles (MCA-5 and MCA-6).

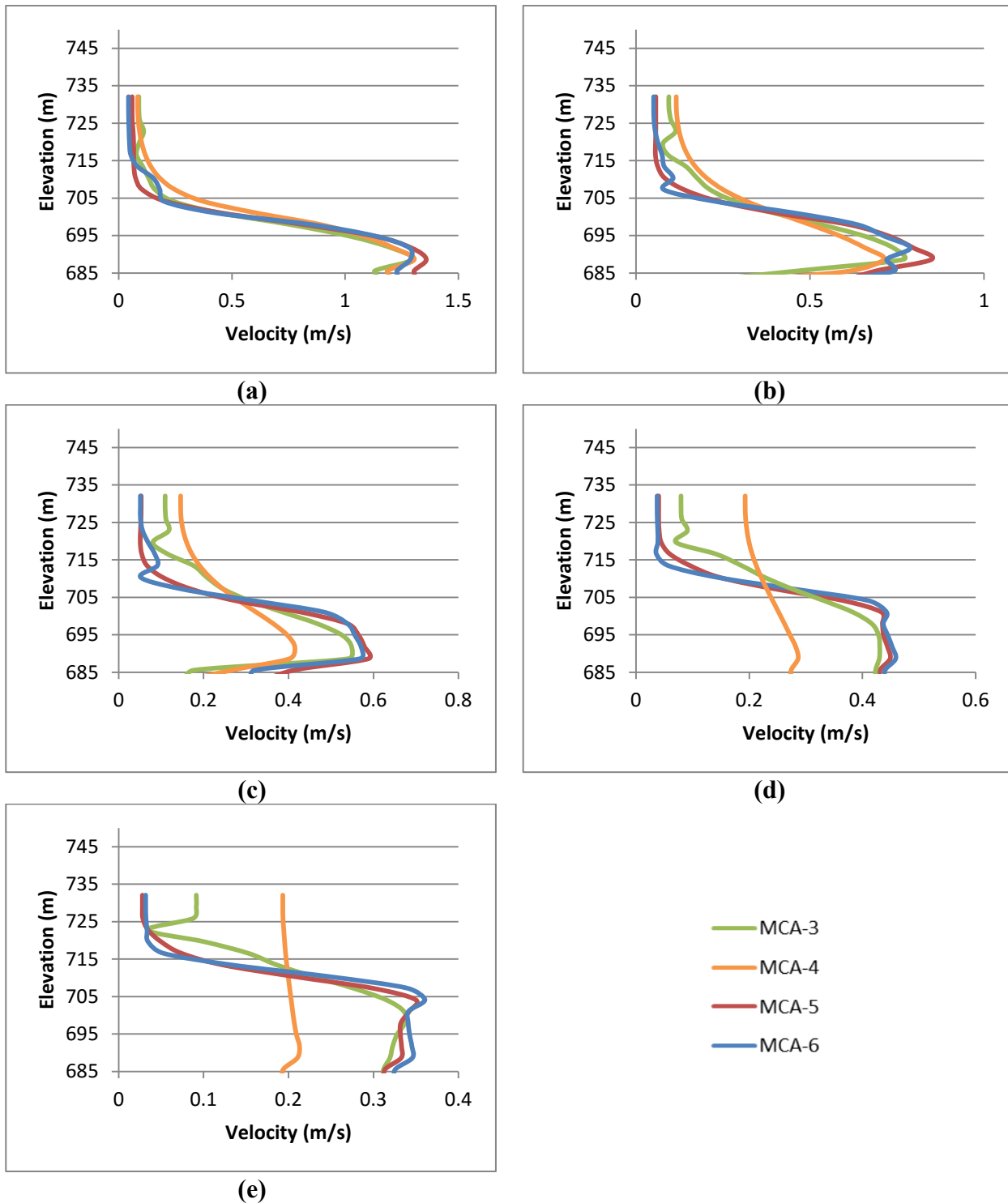


**Figure 31: Velocity profiles upstream of Intake 3 for varied thermal stratification profiles (a) 0 m upstream; (b) 5 m upstream; (c) 10 m upstream, (d) 25 m upstream; (e) 50 m upstream.**

The impact of operational changes on the thermal structure of the reservoir in the vicinity of the dam is also important as the water temperature impacts habitat utilization. Fish will have a tendency to stay in warmer temperature waters as it reduces the impact of cold torpor (stress) on their swimming capability. As warmer water is drawn down towards the intakes, fish may be drawn closer to the entrainment risk zone.

Withdrawing water from the reservoir upstream of Mica Dam also has a distinct impact on the thermal stratification of the waterbody in the vicinity of the dam. In this study, the impact of varying the thermal regime upstream was completed. Regardless of the thermal regime (linear, hyperbolic or discrete) the model simulations indicated that the thermocline was drawn deeper, closer to the intakes in all scenarios. Figure 32 shows the impact of the dams withdrawal on the upstream thermal stratification profile for distances 0, 5, 10 25 and 50 m upstream of the intakes.

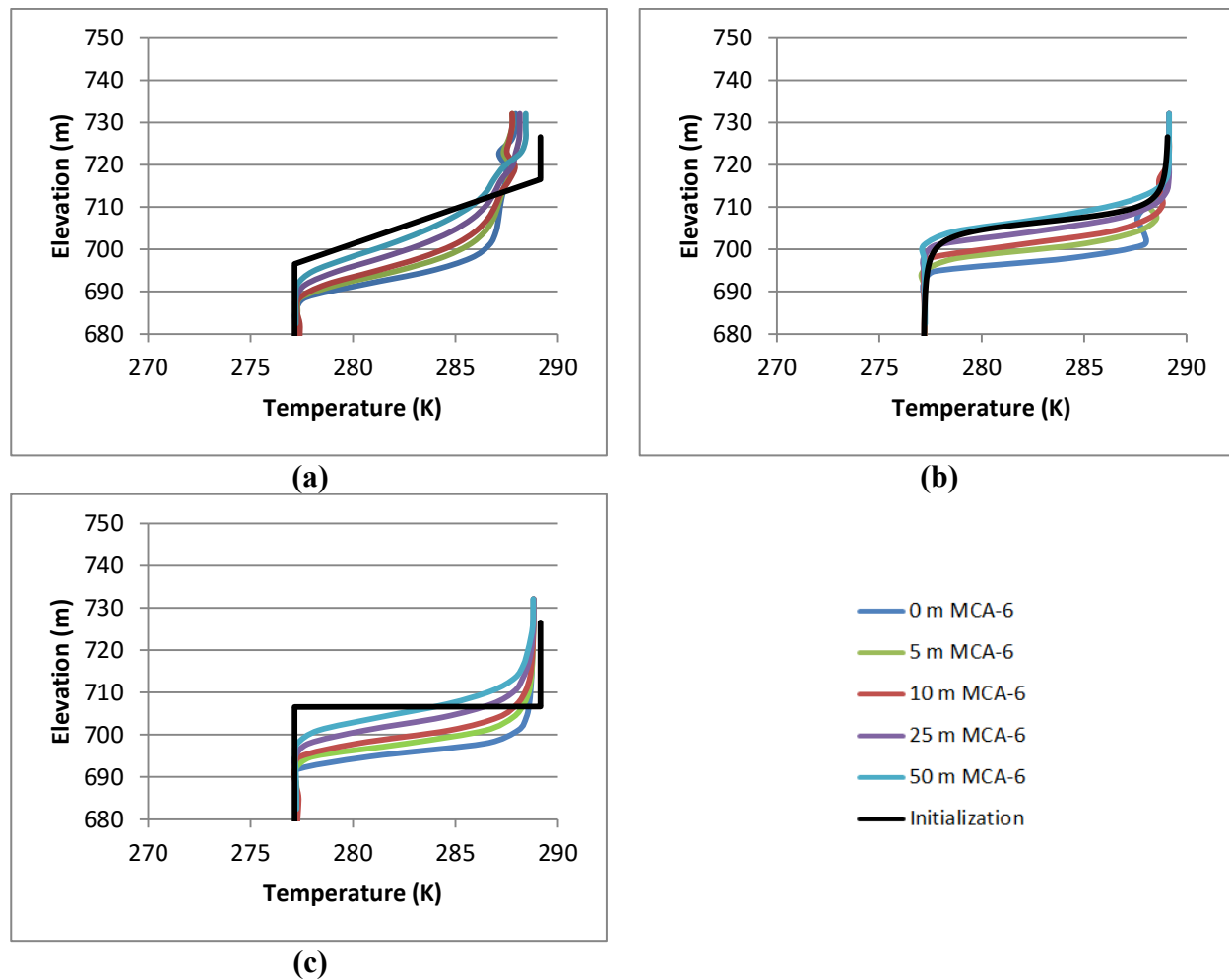


**Figure 32: Thermal stratification profiles upstream of Intake 3 (a) MCA-3; (b) MCA-5; (c) MCA-6.**

It is noted that the hyperbolic profile, was well represented by the discrete, two-layer stratification in this study. There was a discrepancy of up to 1.4 °C in locations where there is a sharp thermal gradient (i.e. the thermocline), however the depth of thermocline was simulated to be within 1 m at all distances upstream of the dam. In both the hyperbolic (MCA-5) and discrete (MCA-6) scenarios, there was not a significant change in the form of the stratification profile upstream of the dam. The main impact of the withdrawal on the thermal profile was the

thermocline depth. This is different than the simulated results of the linear thermal stratification scenario (MCA-3). In this scenario it was noted that the thermal profile transitions from relatively linear at 50 m upstream of the dam face, to hyperbolic in shape adjacent to the intakes. The difference in thermal profile upstream of Intake 3 for scenarios MCA-3, MCA-5 and MCA-6 are outlined on Figure 33. Based on these results, simulating a linearly thermally stratified reservoir (as many hydropower reservoirs are) as having a discrete two-layer, or hyperbolic stratification regime is not valid.

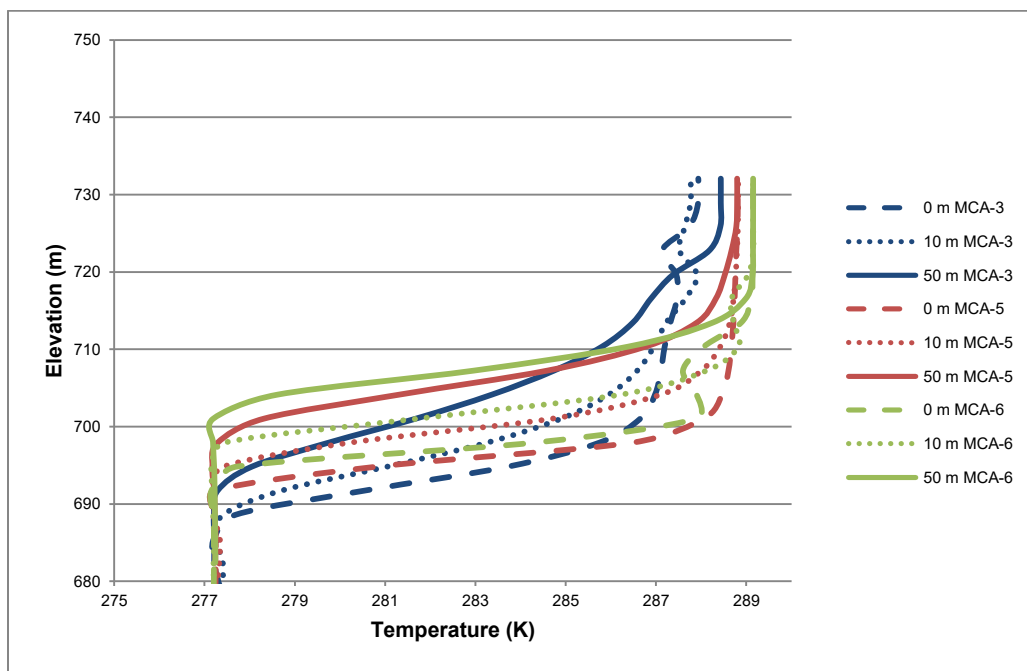


**Figure 33: Thermal profiles upstream of Intake 3 for varied thermal stratifications MCA-3, MCA-5 and MCA-6.**

In general the flow field that was generated by the model in each of the scenarios is comparable between each of the three thermal stratification profiles with maximum discrepancies of 0.11, 0.28, 0.16, 0.08 and 0.06 m/s for distances 0, 5 10, 25 and 50 m upstream of the dam headwall

respectively. It however is important to note that the temperatures throughout the forebay simulated by the model have larger discrepancies than the velocities. The maximum discrepancy between MCA-3, MCA-5 and MCA-6 simulated in the model were 6.01, 5.44, 5.82, 5.48 and 4.74 K for distances 0, 5, 10, 25 and 50 m upstream of the dam headwall respectively. Typically the largest discrepancies always occurred in the vicinity of the thermocline due to the sharp temperature gradient with respect to depth. In addition to having an impact on the flow field, inclusion of thermal stratification in the model has a distinct impact on the thermal structure of the forebay as shown on Figure 34 which can impact fish use of the forebay. As such, for studies, where temperature is of primary importance, such as fisheries studies, it is prudent that the proper temperature stratification is used in the model. In these cases preliminary sampling of the thermal stratification of the reservoir is required in order to obtain accurate model outputs. In studies where the temperature outputs of the model are of less importance, the reservoir can likely be simulated as a two-layer stratified reservoir and the stratification profile may be estimated based on meteorological parameters (air temperature, wind speed etc.) without completing field measurements of thermal stratification.

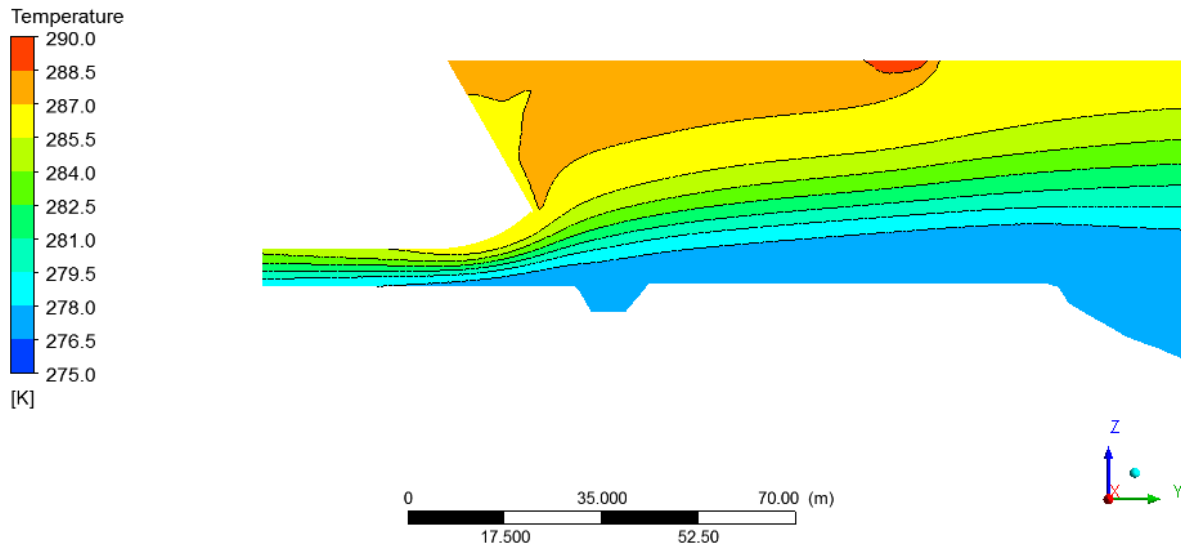
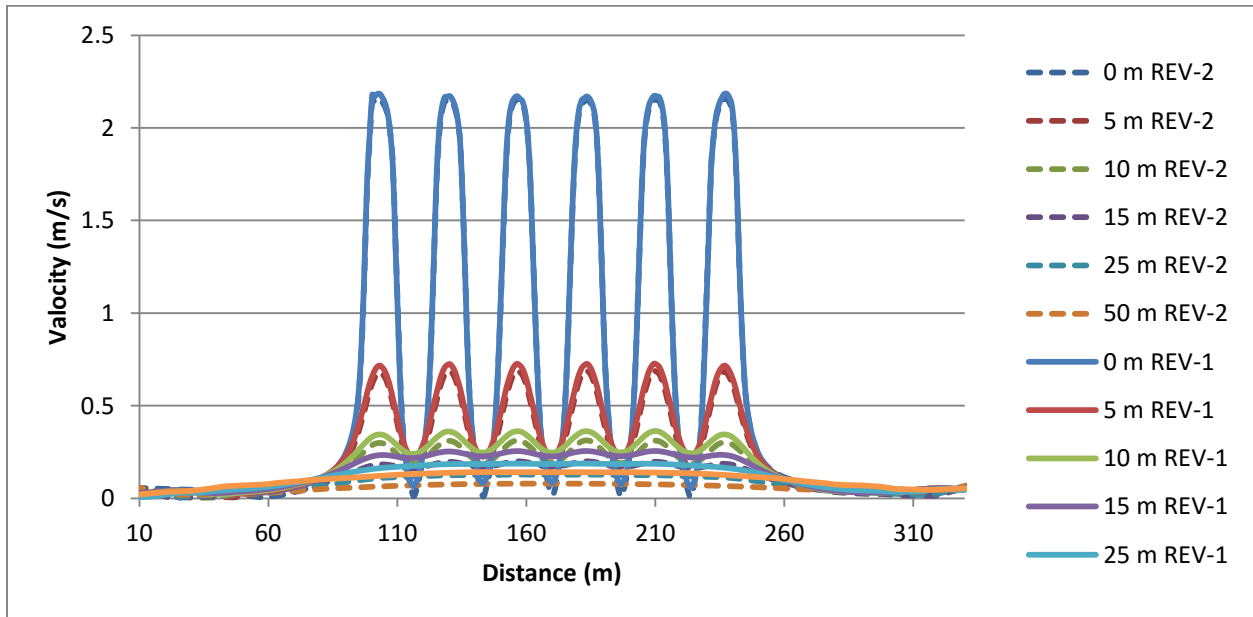


**Figure 34: Thermal profile upstream of Intake 3 for MCA-3.**

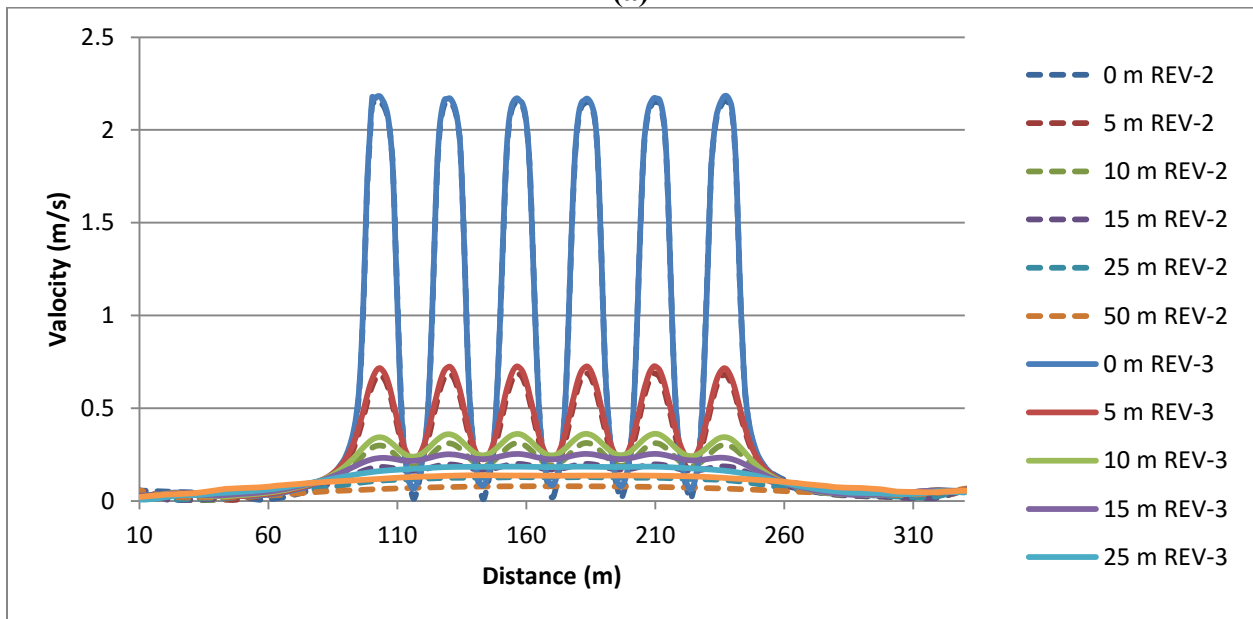
#### ***4.4.2 Flow Field at Revelstoke Dam***

The velocity field that was simulated for Revelstoke again indicates a distinct difference between the thermally stratified scenarios when compared against isothermal conditions. The velocity field that is generated in front of the intakes, at the intakes elevations is shown for the linear, hyperbolic and discrete thermal profiles in Figure 35. It can be noted at this scale there is not a distinct difference in the upstream velocity field for each of these thermal profiles. What can be noted however is that consistently the impacts of thermal stratification are most notable as the distance away from the dam headwall increases. There is little to no difference in the simulated velocity field, compared to the isothermal scenario (REV-2) for distances 0 and 5 m upstream of the dam face. The differences begin to be noticeable at a distance of 10 m and greater upstream of the dam. As noted in Chapter 3 with Mica Dam, the intakes begin to act as a line sink as opposed to a series of point sinks at distances greater than 15 m upstream of the dam. At this

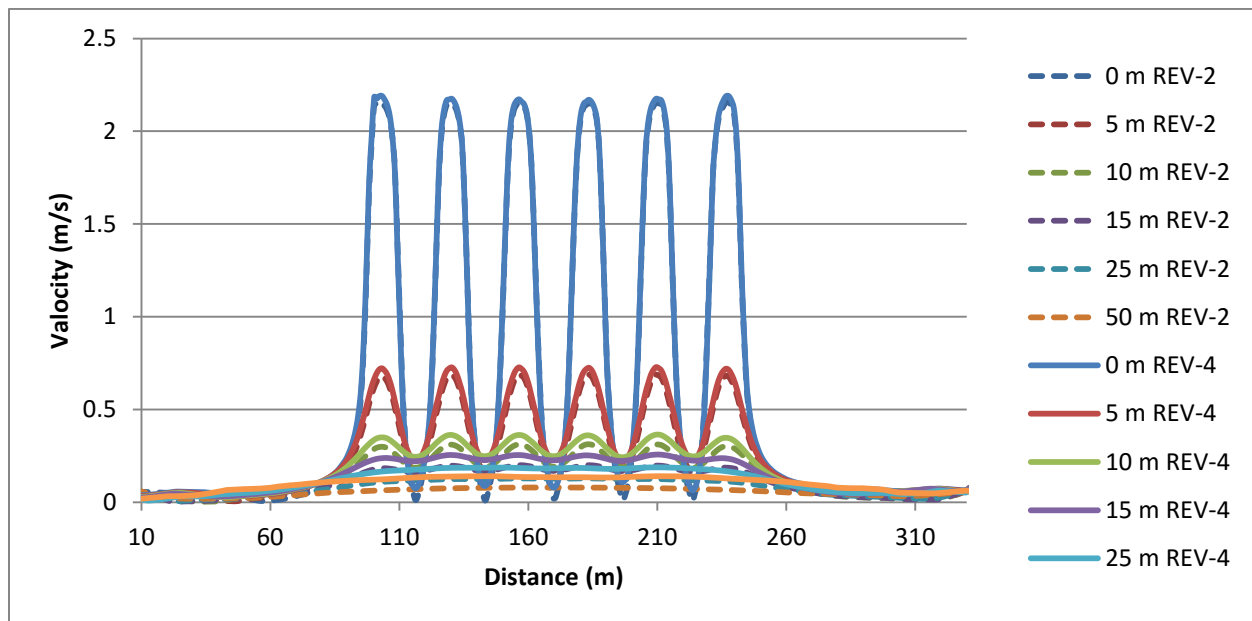
point the summation of superposition for each of the intakes is of the same scale as the velocity generated by a single intake.



(a)



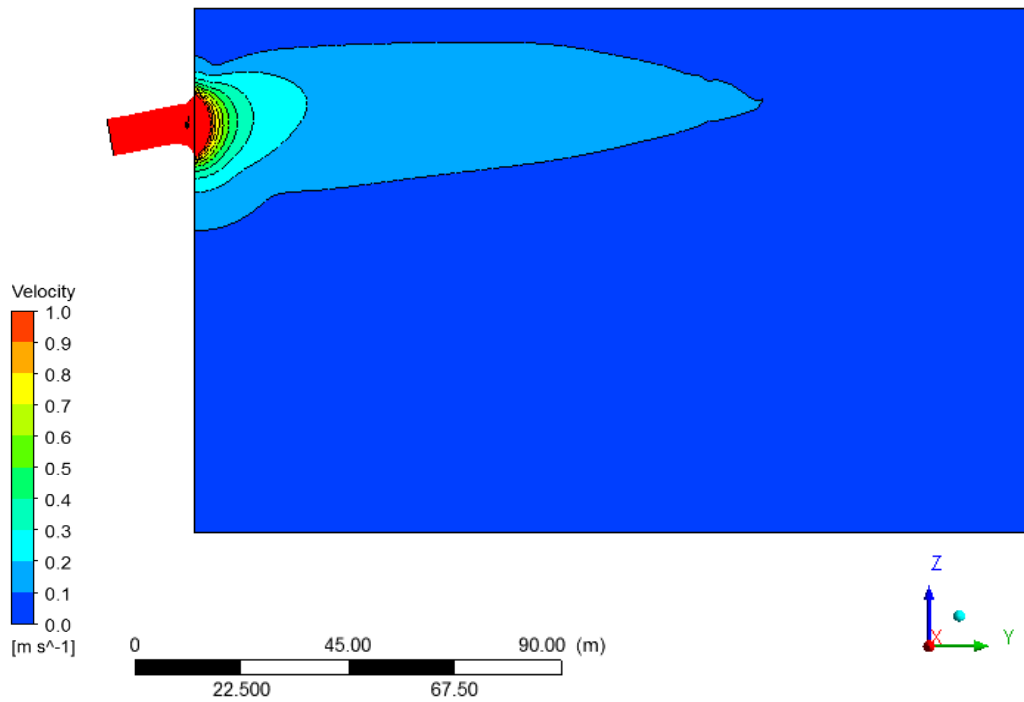
(b)



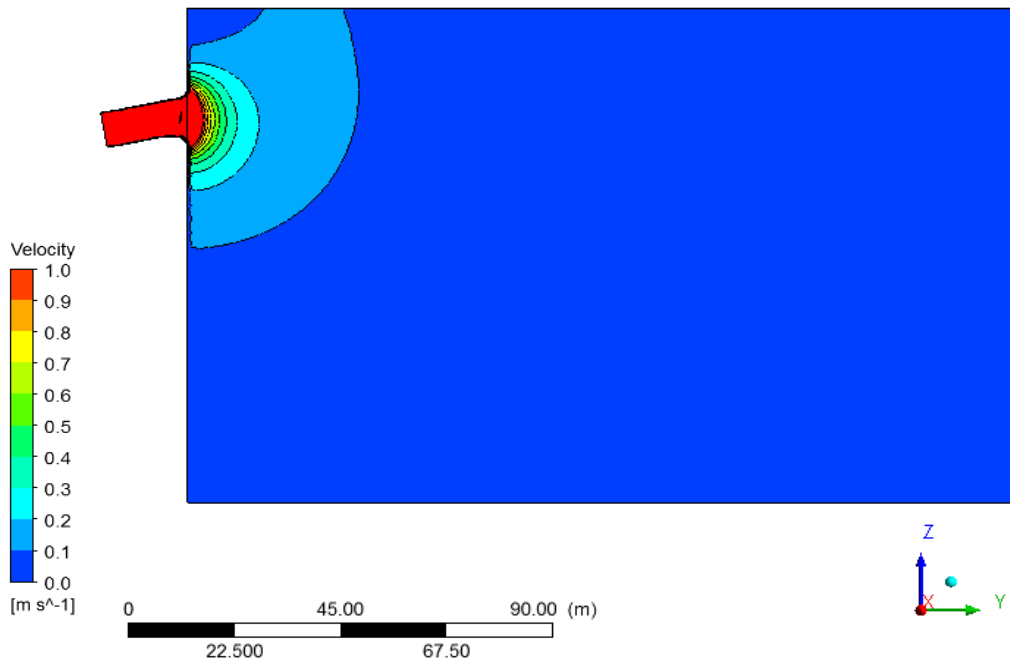
(c)

**Figure 35: Velocity magnitude upstream of Revelstoke Dam at intake elevation (a) REV-1; (b) REV-3; (c) REV-4.**

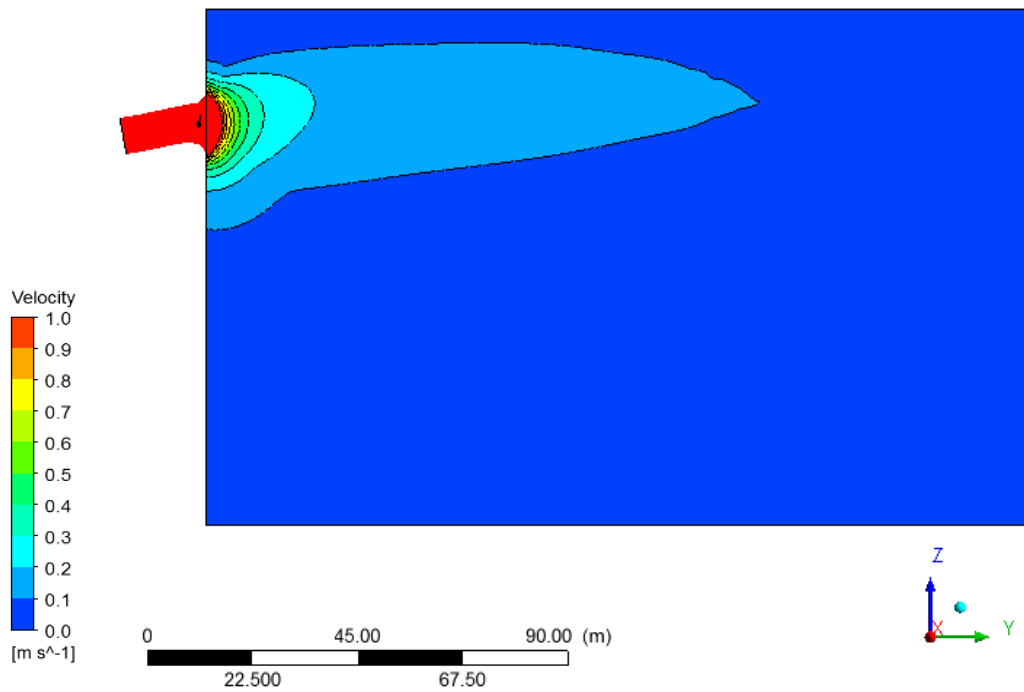
Contours of the simulated velocity upstream of Revelstoke Dam for REV-1, REV-2, REV-3 and REV-4 are included in Figure 36. Similar to the Mica facility, at Revelstoke the simulated velocity contours under thermally stratified conditions (REV-1, REV-3 and REV-4) have an elongated ellipsoidal shape compared to the more circular ellipsoid established in the isothermal scenario (REV-2). Near the water surface, approximately 1 times the intake diameter above the level of the intakes, the velocity is generally higher in isothermal conditions, as in the Mica simulations. Again, at this scale, the velocity fields generated by the linear, hyperbolic and discrete thermal profiles seem to generate similar flow fields upstream of the dam.



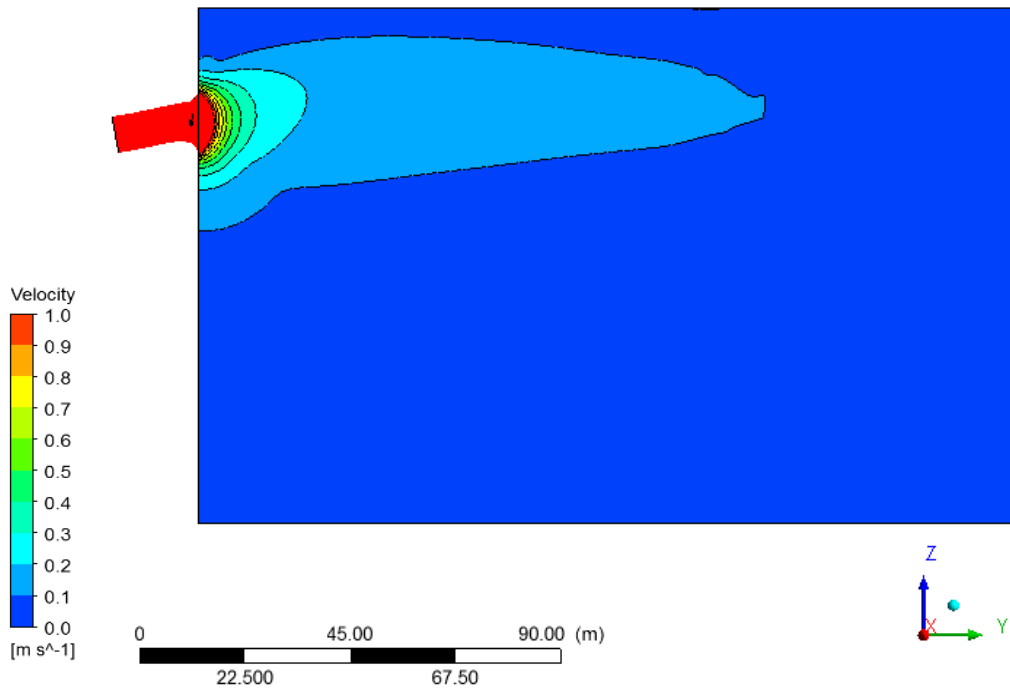
(a)



(b)



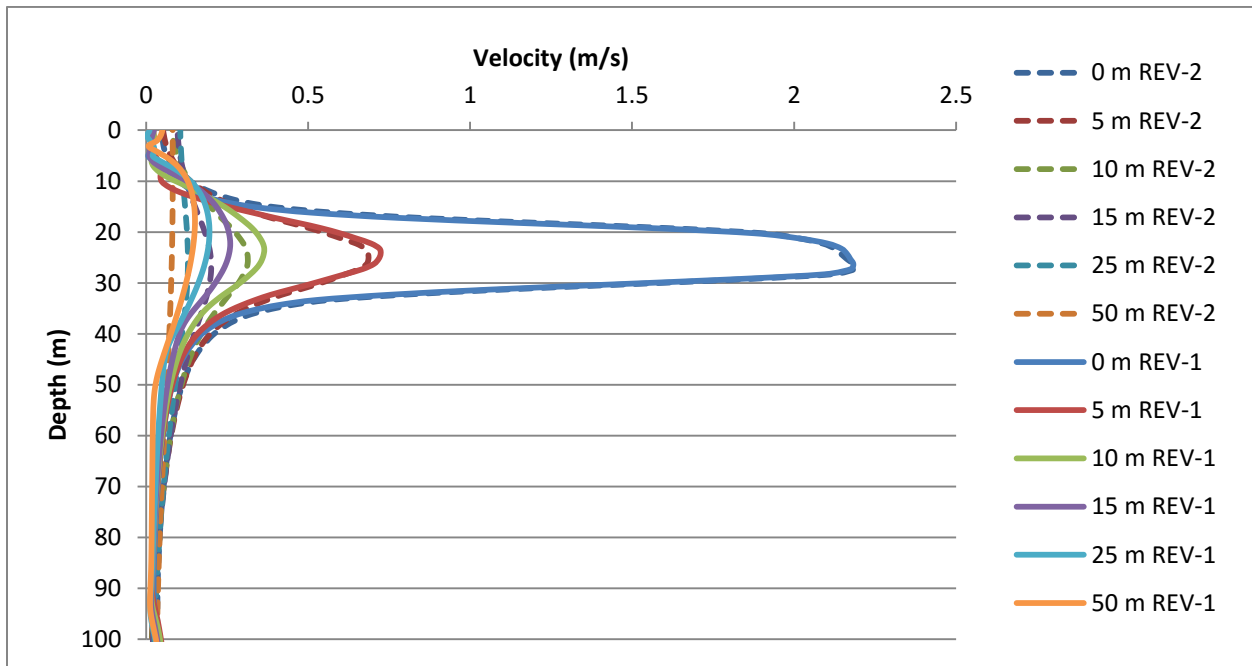
(c)



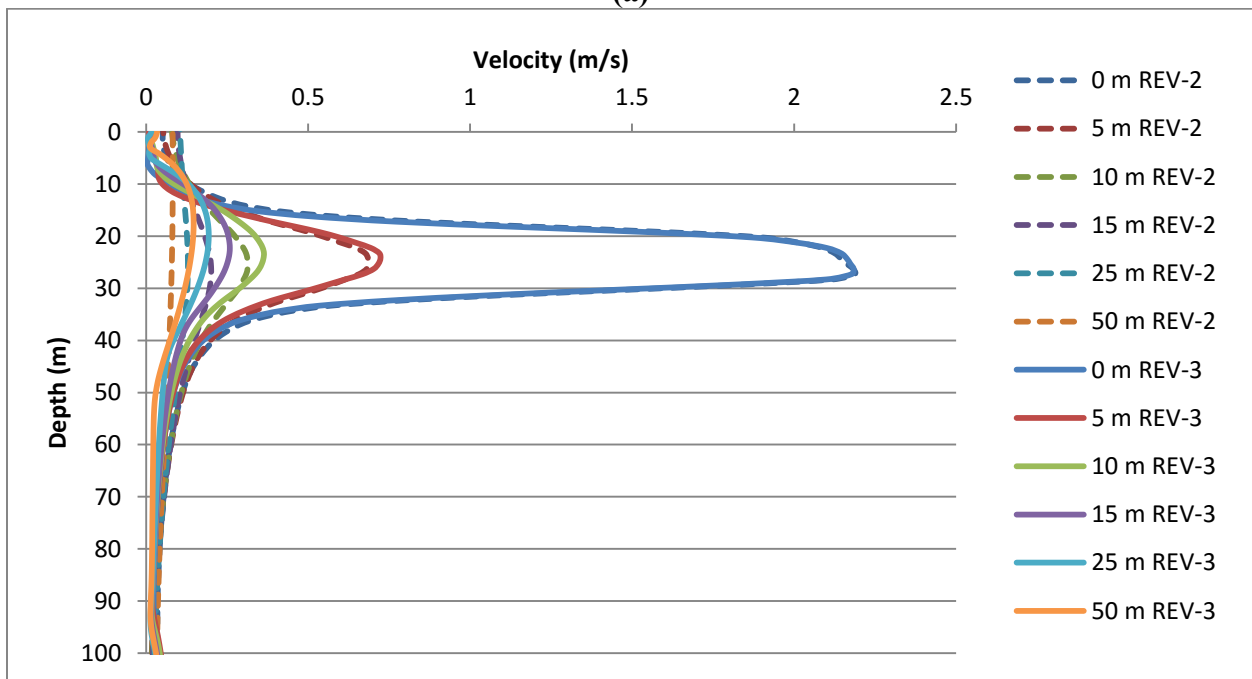
(d)

Figure 36: Intake 3 velocity magnitudes (a) REV-1; (b) REV-2; (C) REV-3; (d) REV-4.

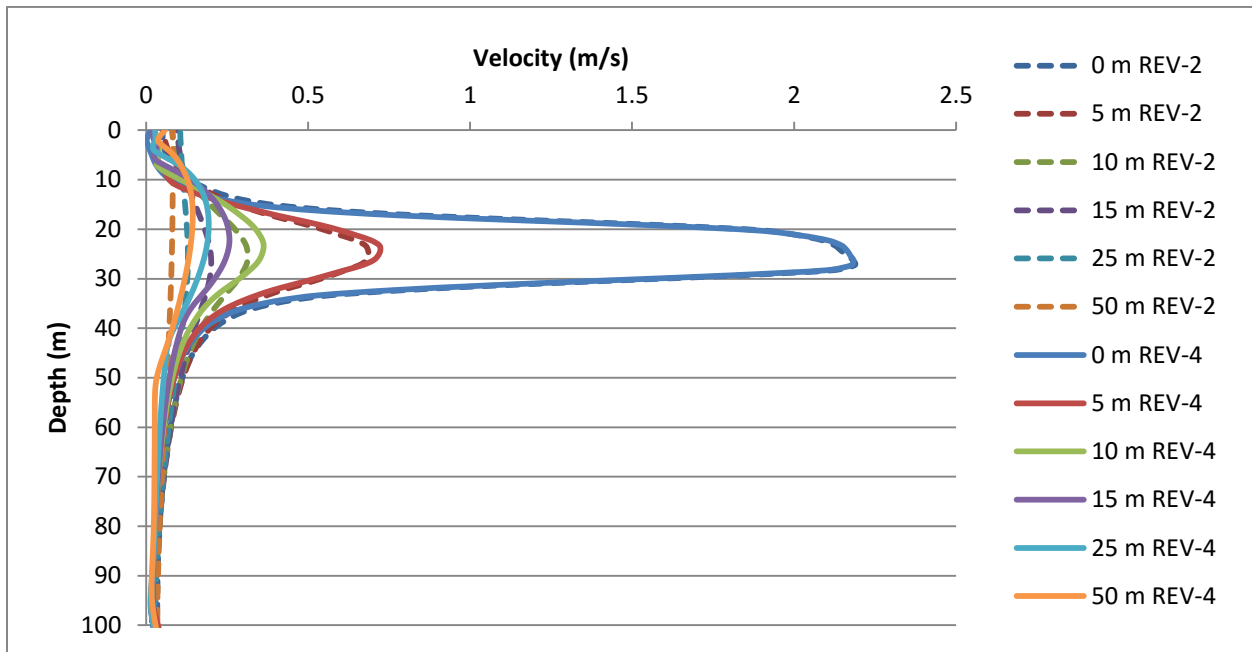
In order to determine the impact of varying the thermal profile on the upstream hydraulics at Revelstoke, the generated velocity field upstream of Intake 3 has been looked at in closer detail in Figures 37 and 38. Figure 37 again identifies that at location near the dam face, there is little impact on the flow field between thermally stratified and no stratified scenarios. The discrepancies are most distinct further away from the dam face, at distances of greater than 1 times the intakes diameter and greater away from the intakes. Figure 38 provides insight as to how this velocity field changes at greater distances upstream of the dam. The peak velocity is skewed towards the water surface in the thermally stratified scenarios as distance upstream of the dam increases. In general, peak velocities are simulated 2.4 m shallower 10 m upstream, 4.9 m shallower at 15 m upstream and 5.6 m shallower at 25 m upstream of the dam. At 50 m upstream the velocity field simulated in isothermal conditions also skews upward as noted on the contours in Figure 36. These results are similar to those simulated at Mica Dam. As the Revelstoke intakes are located in the middle of the water column as opposed to adjacent to the bed, the difference between the isothermal and thermally stratified scenarios is less significant as the acceleration zone is not impacted by an adjacent boundary. The difference between the peak velocities in the thermally stratified simulation is between 0.4 - 1.8 times the peak velocity simulated in the isothermal scenario.



(a)

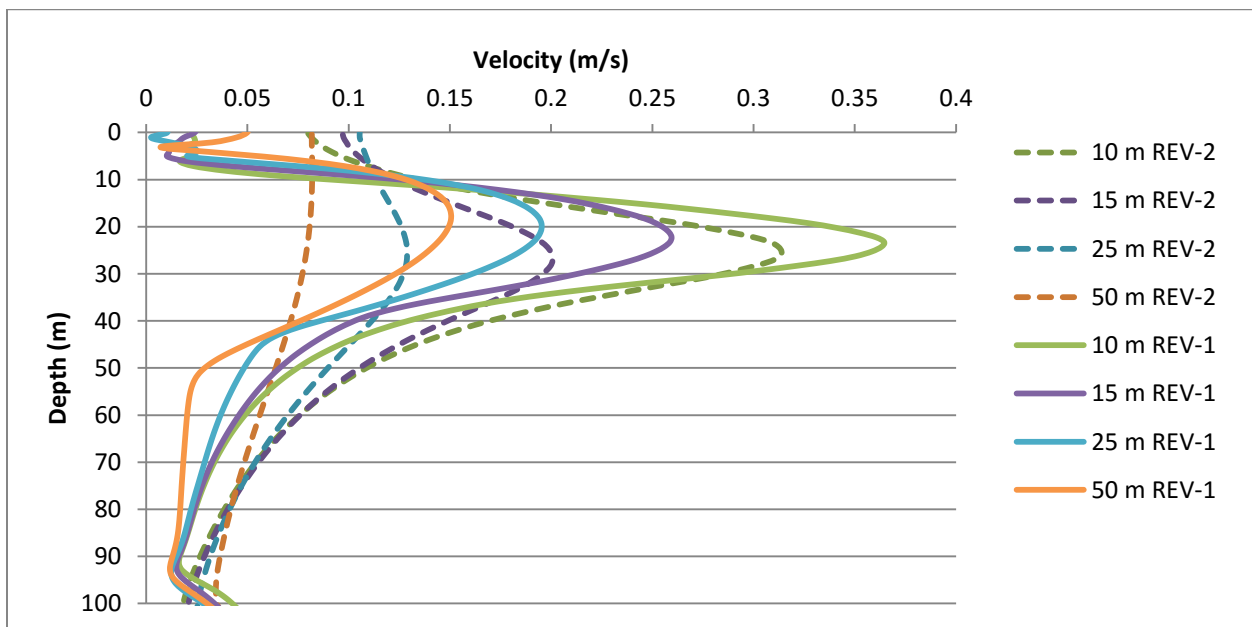


(b)

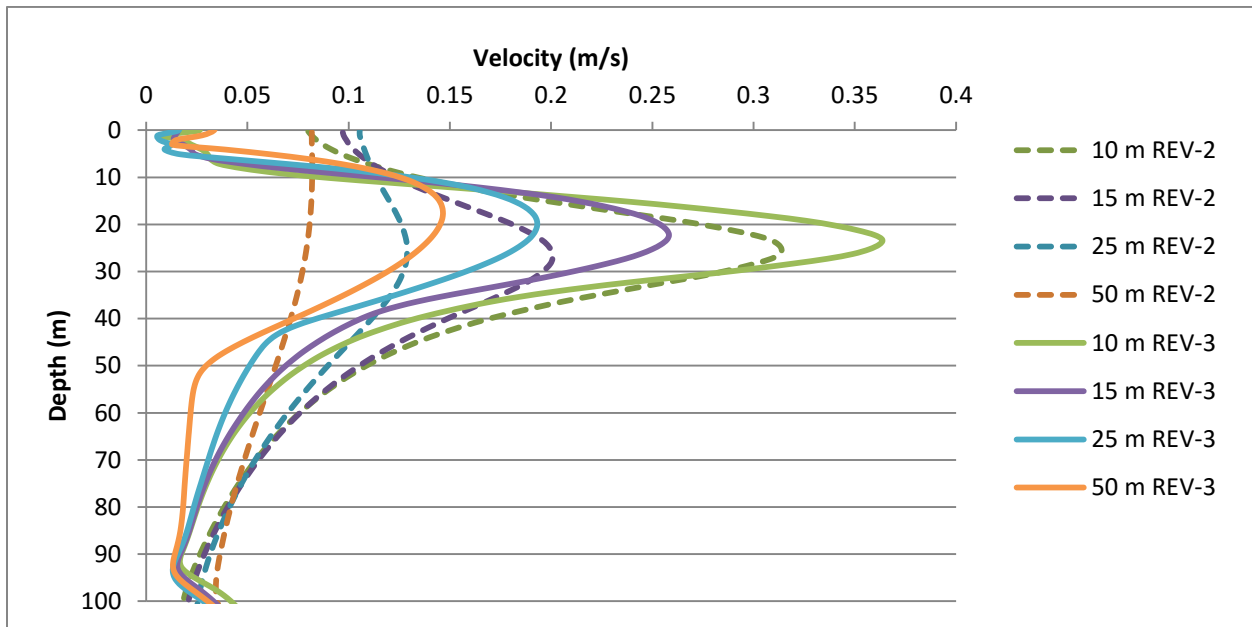


(c)

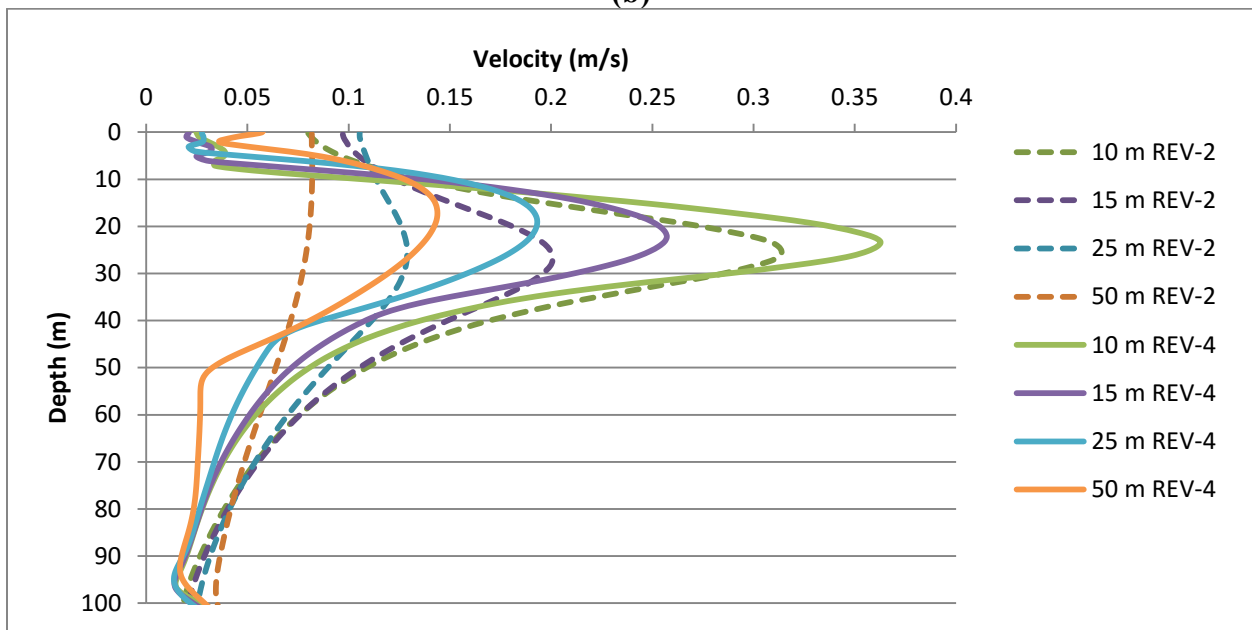
Figure 37: Velocity profiles for 0 – 50 m upstream of Intake 3 for varied thermal stratification profiles (a) REV-1; (b) REV-3; (c) REV-4.



(a)



(b)

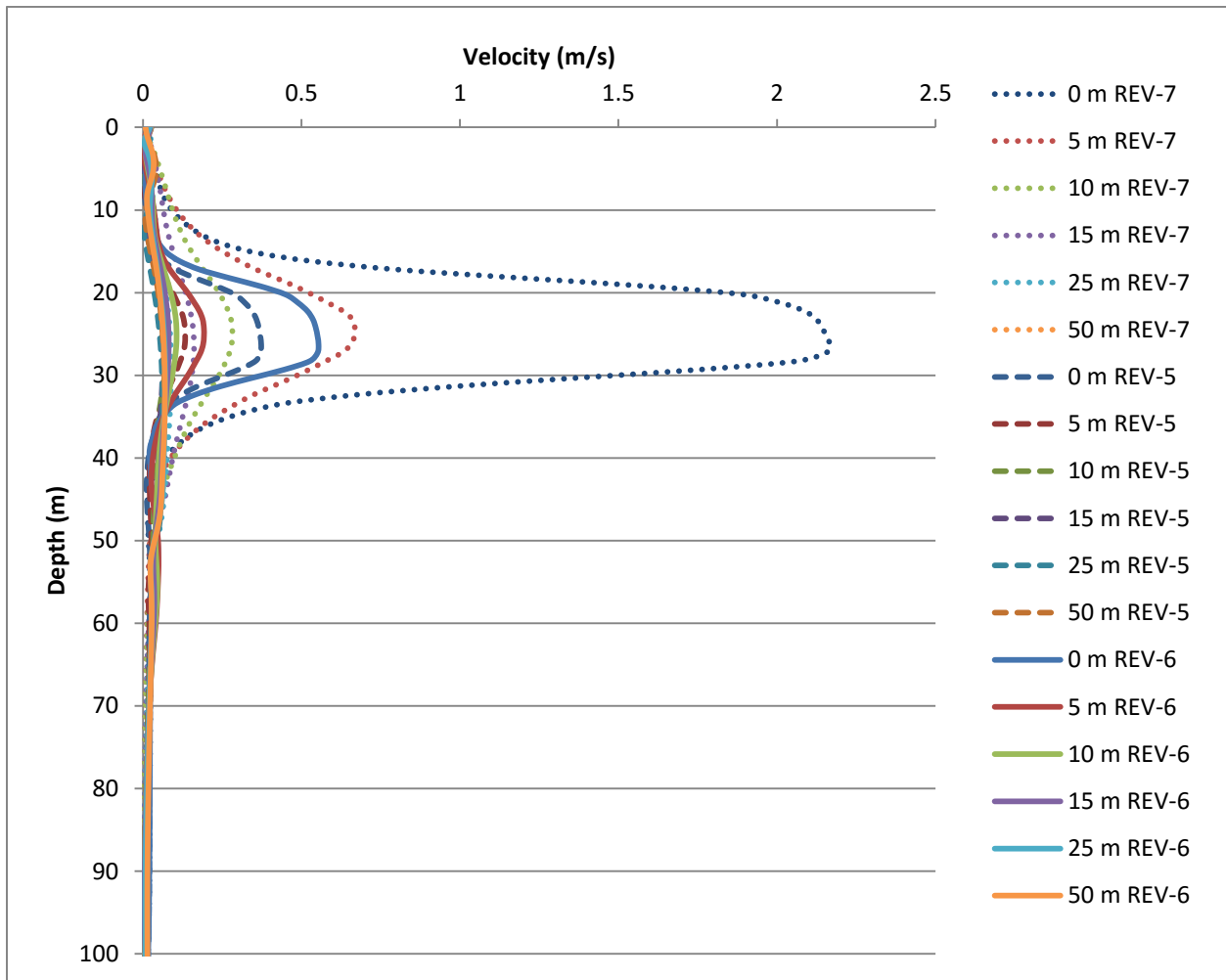


(c)

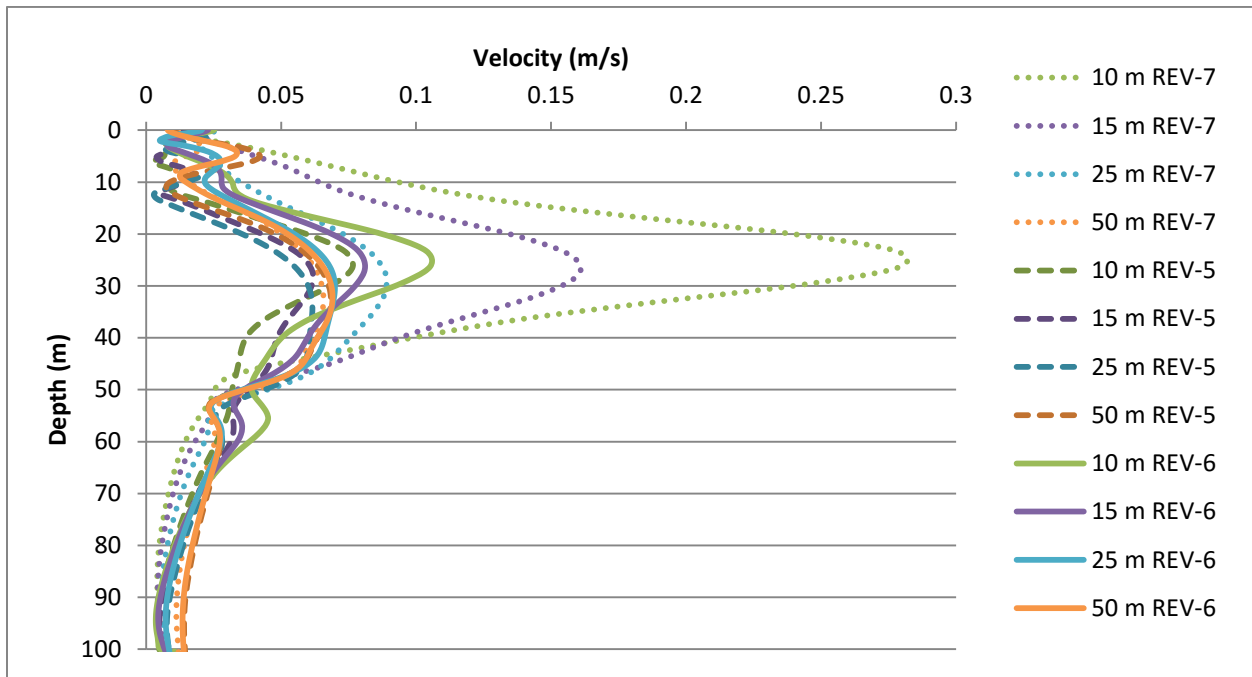
**Figure 38: Velocity profiles for 10 – 50 m upstream of Intake 3 for varied thermal stratification profiles (a) REV-1; (b) REV-3; (c) REV-4.**

In order to optimize operations of the hydropower facility to mitigate fish entrainment, the utility operator may consider altering the flow distribution between different intakes. For example,

there may be environmental benefits to splitting the discharge through the facility through multiple units operating at a reduced capacity compared to the single unit operating at full capacity. The velocity profiles simulated upstream of Intake 3 for the linear stratification scenarios (REV-5, REV-6 and REV-7) are included as Figure 39. Similar profiles for the discrete stratification scenarios (REV-8, REV-9 and REV-10) are included as Figure 40. As anticipated the peak velocity upstream of the dam face occurs when a single unit is operating at full capacity. This peak velocity is 4.3 times greater than the peak velocity when the flow is split between 4 intakes and 7.3 times greater than the peak velocity when flow is split between 6 intakes at the dam face. The peak velocities are most skewed toward the surface when flow is split between all 6 intakes, with the depth of the peak velocity simulated up to 9 m shallower when multiple intakes are operational as opposed to a single intake.

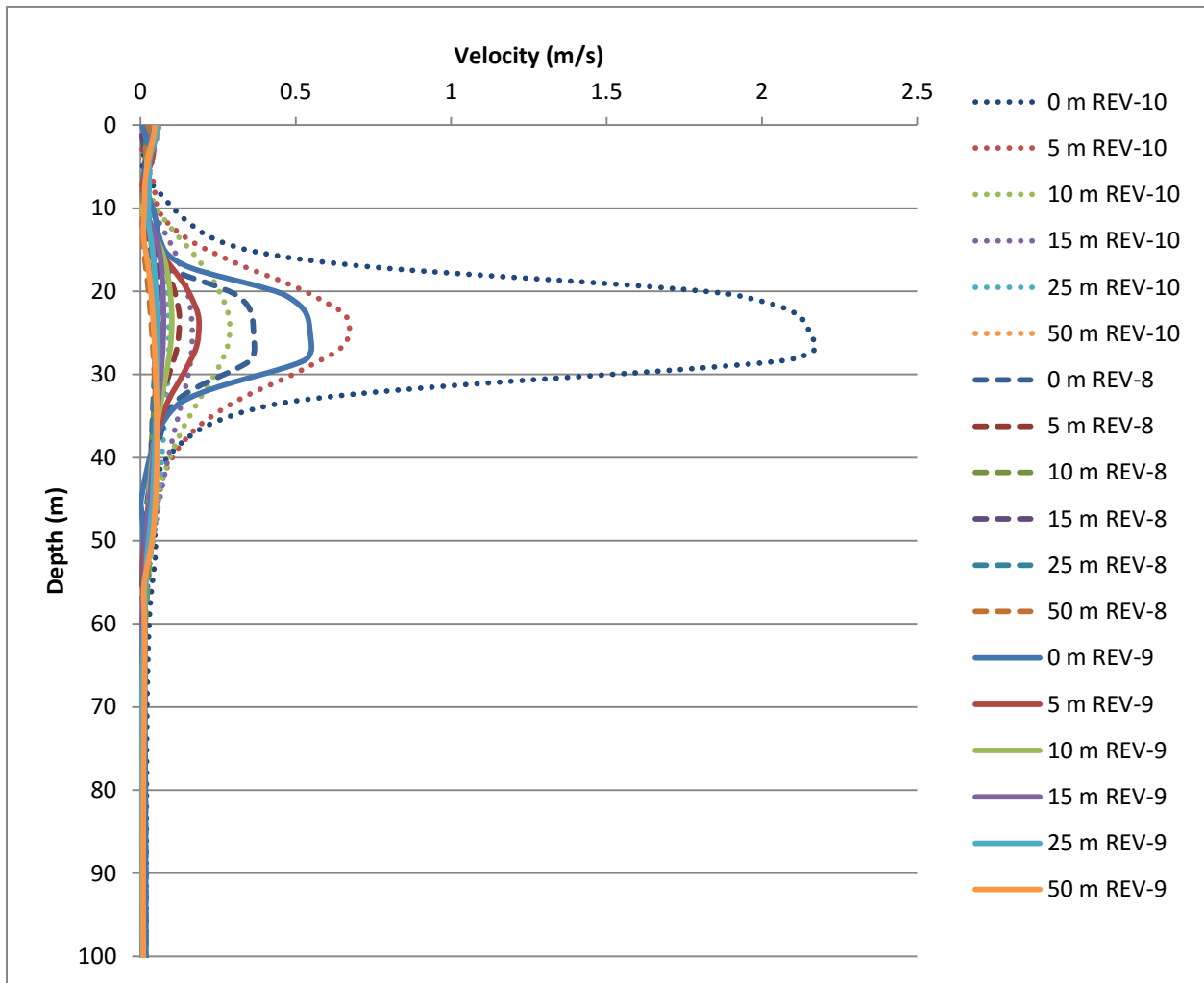


(a)

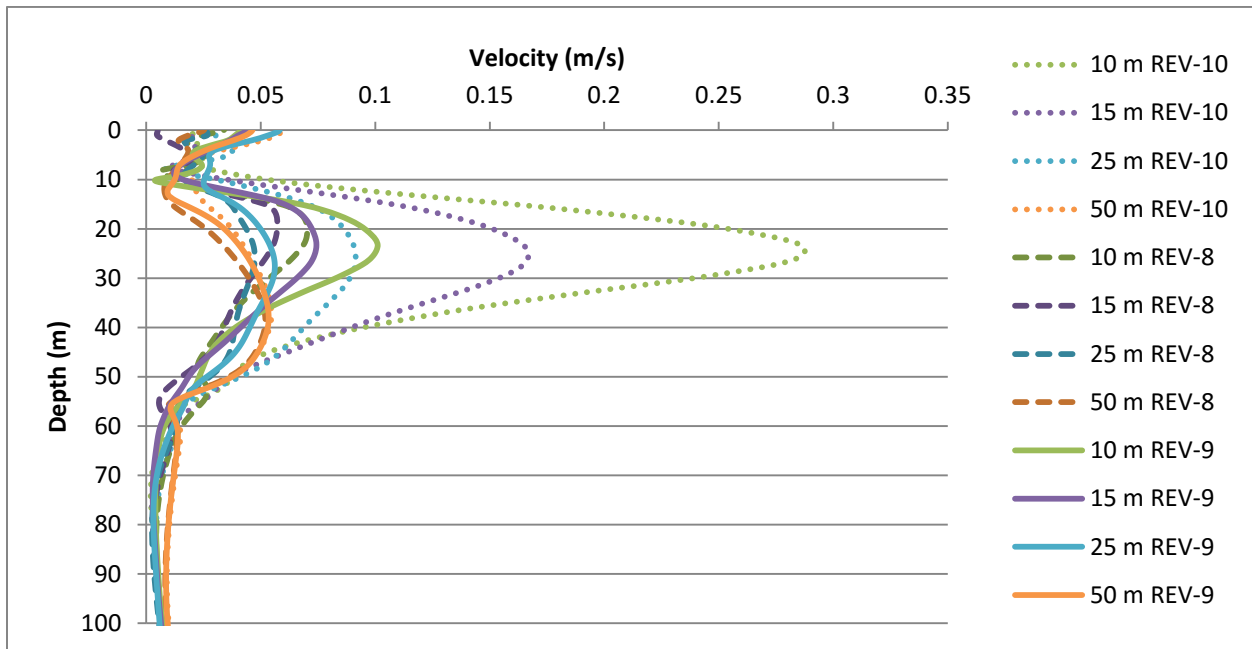


(b)

Figure 39: Velocity profiles upstream of Intake 3 for linear thermal stratification profiles (a) 0 – 50 m upstream; (b) 10 – 50 m upstream.



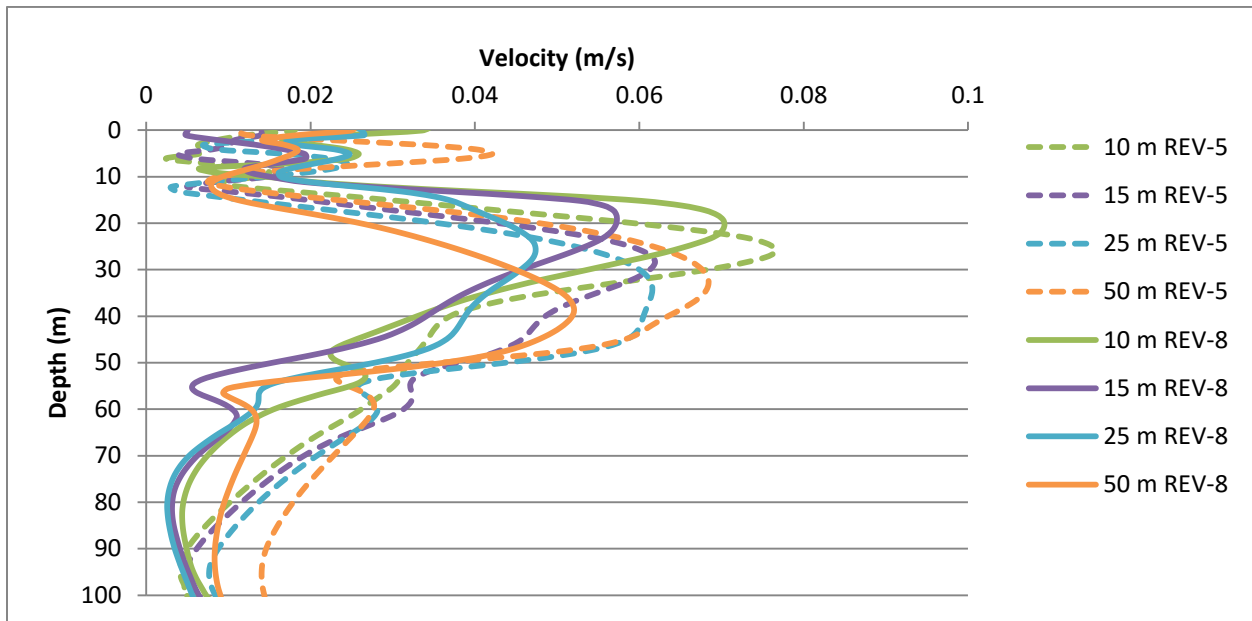
(a)



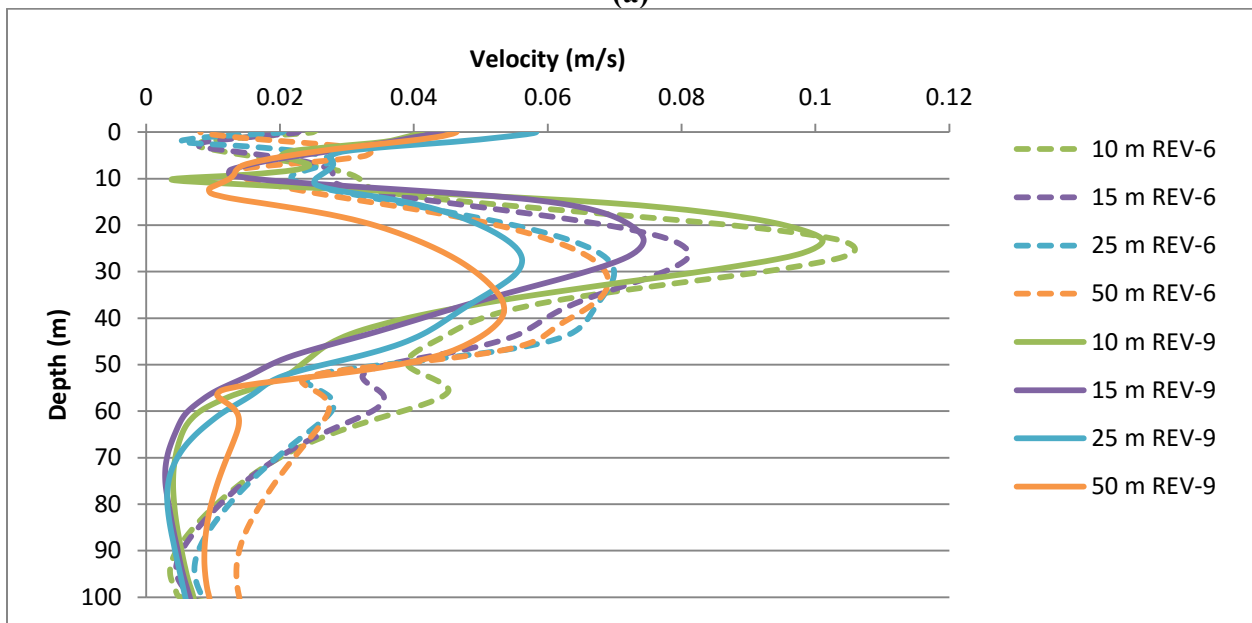
(b)

**Figure 40: Velocity profiles upstream of Intake 3 for discrete thermal stratification profiles (a) 0 – 50 m upstream; (b) 10 – 50 m upstream.**

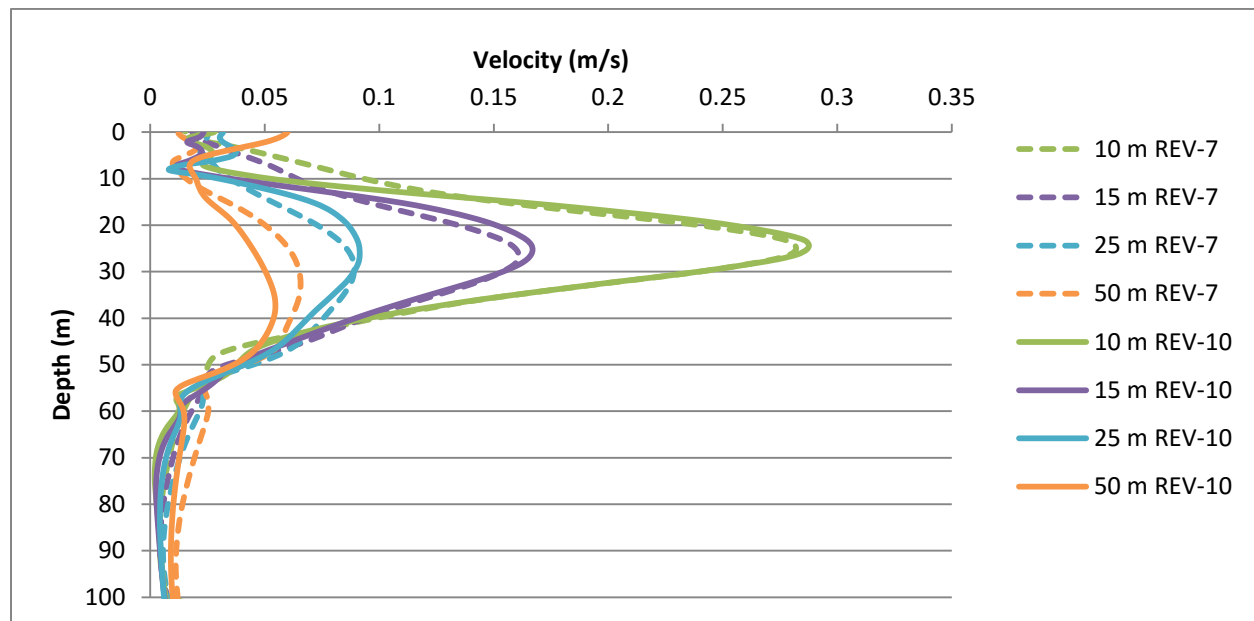
The difference between the linear and discrete thermal stratification scenarios is outlined by Figure 41 (a) for 6 operational intakes, (b) for 4 operational intakes and (c) for a single operational intake. The greatest discrepancies are noted with increased number of operational intakes. When a single unit is operational there is little impact on the upstream flow field. Typically greater peak velocities are notable for the linear stratification profiles and the discrepancies are most notable at distances greater than 15 m upstream of the dam face.



(a)



(b)



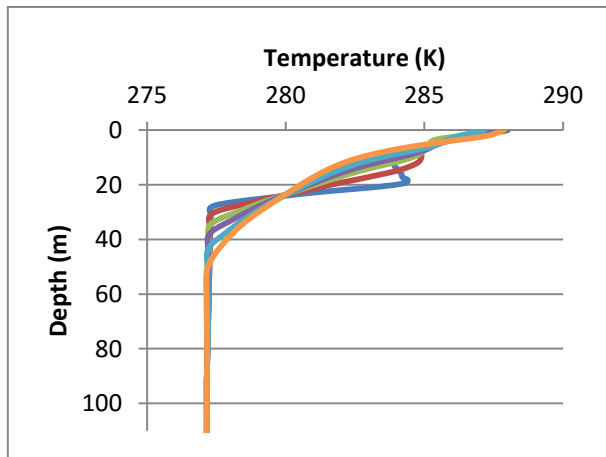
(c)

**Figure 41: Impact of thermal stratification profile on velocity profile upstream of Intake 3 (a) REV-5 and REV-8; (b) REV-6 and REV-9; (c) REV-7 and REV-10.**

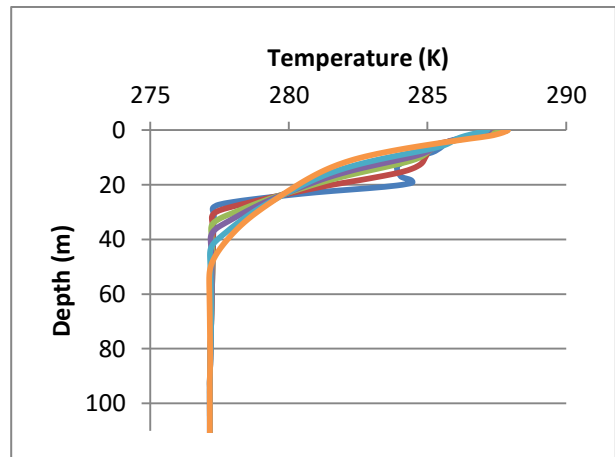
In addition to having an impact on the flow field upstream of the dam, thermal stratification also has an impact on the temperature structure of the forebay as was demonstrated for Mica Dam.

The variation in thermal stratification upstream of Intake 3 at Revelstoke is included for each of the thermal stratification scenarios are includes as Figure 42. REV-2 has been excluded as it is isothermal and does not have any variation in temperature throughout the reservoir. Figure 42 (a), (b) and (c) indicate that there is no substantial difference in the thermal structure of the reservoir when the intakes are operating at maximum discharge. Regardless of the initialization thermal profile, the reservoir thermal stratification tends to become more linear at greater distances upstream of the dam. Similar to Mica, the thermal structure approaches a discrete, two-layer stratification profile as it approaches the dam face. As demonstrated by Figure 42 (f) and (i) this is also the most distinct for the scenarios when all intakes are operational. The

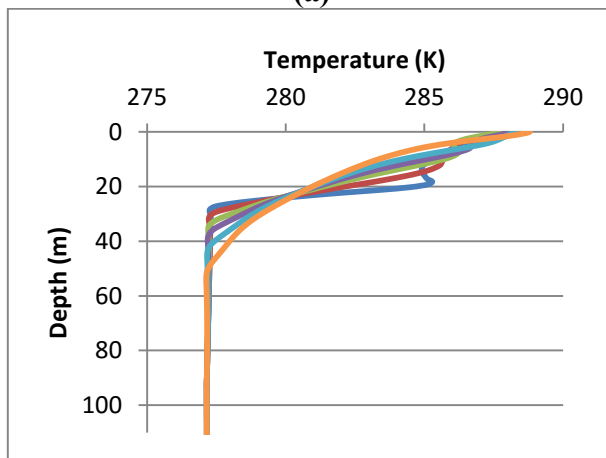
variations in thermal profile upstream of the dam face are less distinct when fewer intakes are operational, despite operating at higher discharges. This indicates that the impact of the dam on the thermal structure of the forebay is most substantially impacted by the number of intakes operational, as opposed to the discharge through each intake.



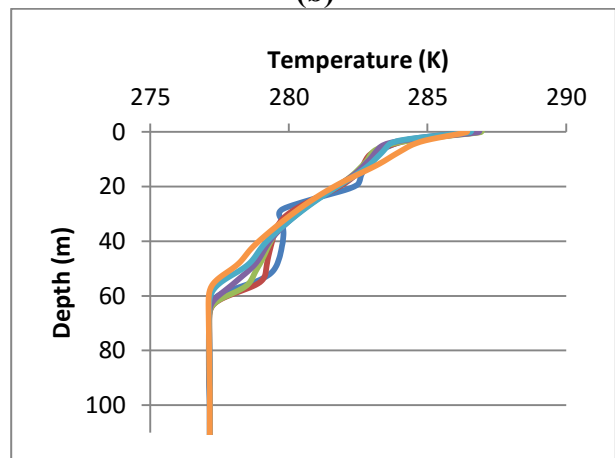
(a)



(b)



(c)



(d)

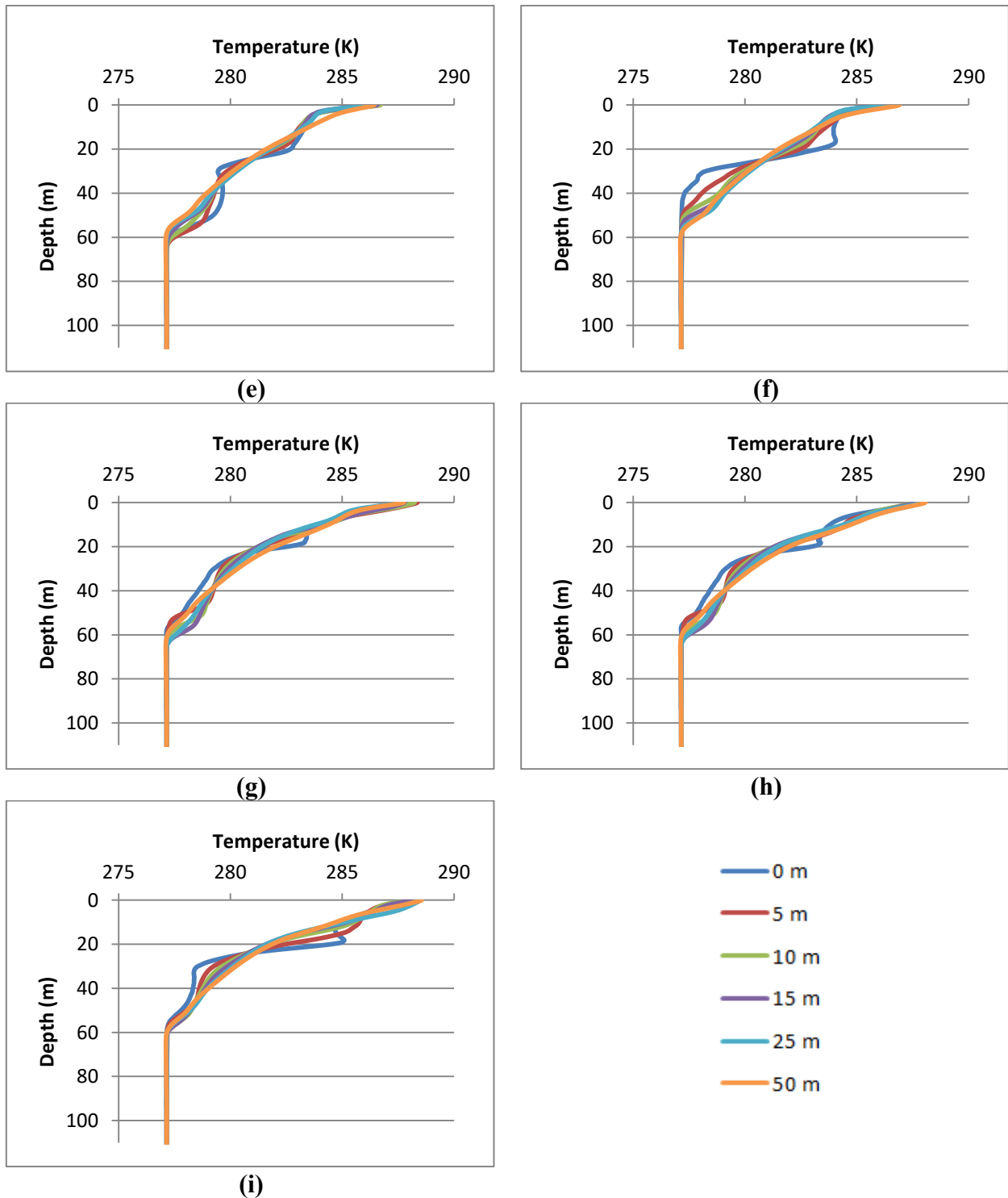


Figure 42: Thermal stratification profiles at varied distance upstream of Intake 3 (a) REV-1; (b) REV-3; (c) REV-4; (d) REV-5; (e) REV-6; (f) REV-7; (g) REV-8; (h) REV-9; (i) REV-10.

#### ***4.4.3 Discharge Temperature***

In addition to impacting the flow field and thermal structure of the forebay upstream of the dam, thermal stratification also results in warmer water being drawn down toward the intakes level. This is demonstrated for the MCA-1 scenario in Figure 34. The discharge temperature through the facility is of importance for assessing fish attraction to the risky zone as well as evaluating the downstream impacts of hydropower operations. This is especially important if spawning grounds are located near the tailrace as the dam discharge temperature may impact incubation timing for eggs. The outlet temperatures that were simulated by the CFD model in each of the Mica scenarios is outlined in Table 7.

**Table 7: Mica Dam discharge temperatures (°C).**

<b>Scenario</b>	<b>Intake 1</b>	<b>Intake 2</b>	<b>Intake 3</b>	<b>Intake 4</b>	<b>Intake 5</b>	<b>Intake 6</b>	<b>Average</b>
<b>MCA-1</b>	7.83	8.00	7.38	7.56	7.82	8.22	7.80
<b>MCA-2</b>	3.98	3.98	3.98	3.98	3.98	3.98	3.98
<b>MCA-3</b>	8.77	9.95	8.43	7.81	7.85	8.63	8.57
<b>MCA-4</b>	3.98	3.98	3.98	3.98	3.98	3.98	3.98
<b>MCA-5</b>	7.82	9.20	7.31	6.84	6.91	7.44	7.59
<b>MCA-6</b>	6.93	8.38	6.27	5.86	5.97	6.73	6.69
<b>MCA-7</b>	8.22	8.81	8.17	7.11			8.08
<b>MCA-8</b>	3.98	3.98	3.98	3.98			3.98
<b>MCA-9</b>			10.30				10.30
<b>MCA-10</b>			3.98				3.98

The discharge temperatures that are simulated by the model again indicate the importance of thermal stratification modelling for hydropower facilities. In all scenarios, water that passes through the facilities when there is thermal stratification present is of greater temperature than the isothermal scenarios. This difference ranges from 2.7 to 6.3 degrees for Mica Dam.

At Mica Dam, the difference in outlet temperature compared to the corresponding isothermal cases is most pronounced when linear stratification is input into the model. In comparing the different stratification profiles the temperature differences are 4.6, 3.6 and 2.7 degrees for linear, hyperbolic and discrete stratification profiles respectively. This suggests that selective withdrawal is most prominent for discrete stratification and is less prominent as the stratification profile is less well developed.

The increase in outlet water temperature was greatest during lower flow scenarios, when a single intake was operational. The temperature difference was also greatest during low pool scenarios, where the water surface is oriented closer to the intakes.

It is also notable that at the Mica facility there is not only a difference between the outlet temperatures between scenarios, but also in the simulated temperatures at each of the outlets. With the complex geometry of the Mica forebay that greatest temperature water is typically withdrawn from Intake 2 (with the exception of MCA-1).

The simulated discharge temperature for each of the Revelstoke scenarios is outlined in Table 8. At Revelstoke Dam, the difference in average outlet temperature ranges from 2.5 to 3.9 degrees compared to the isothermal cases, which is significant, however is smaller than the difference simulated at Mica. As the Revelstoke intakes are oriented in the middle of the water column, the intakes withdraws from a greater proportion of colder underlying water.

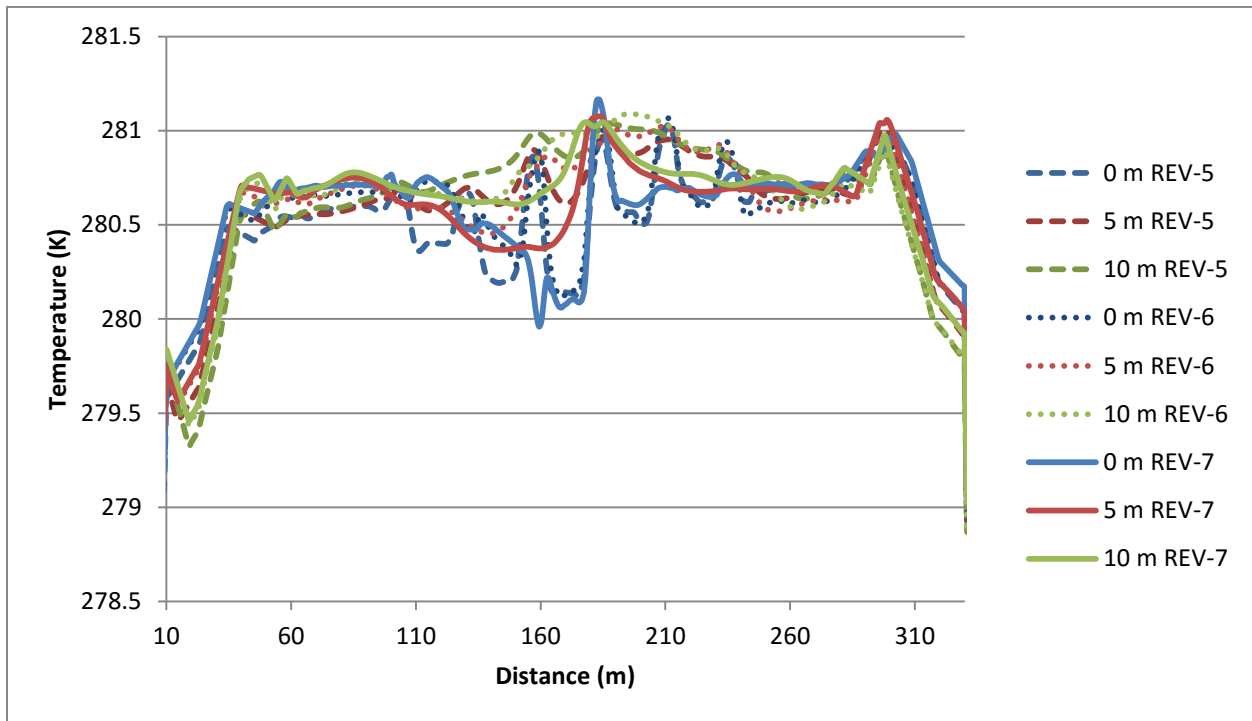
**Table 8: Revelstoke Dam discharge temperatures (°C).**

<b>Scenario</b>	<b>Intake 1</b>	<b>Intake 2</b>	<b>Intake 3</b>	<b>Intake 4</b>	<b>Intake 5</b>	<b>Intake 6</b>	<b>Average</b>
<b>REV-1</b>	6.79	6.58	6.53	6.45	6.43	6.66	6.57
<b>REV-2</b>	3.98	3.98	3.98	3.98	3.98	3.98	3.98
<b>REV-3</b>	6.64	6.40	6.61	6.40	6.24	6.56	6.47
<b>REV-4</b>	7.11	6.69	6.88	6.68	6.51	7.23	6.85
<b>REV-5</b>	7.58	7.66	7.68	7.58	7.45	7.49	7.57
<b>REV-6</b>	7.60	7.69	7.76	7.53			7.65
<b>REV-7</b>			7.73				7.73
<b>REV-8</b>	8.16	7.53	7.38	7.23	7.41	8.26	7.66
<b>REV-9</b>	8.12	7.52	7.44	7.41			7.62
<b>REV-10</b>			7.87				7.87

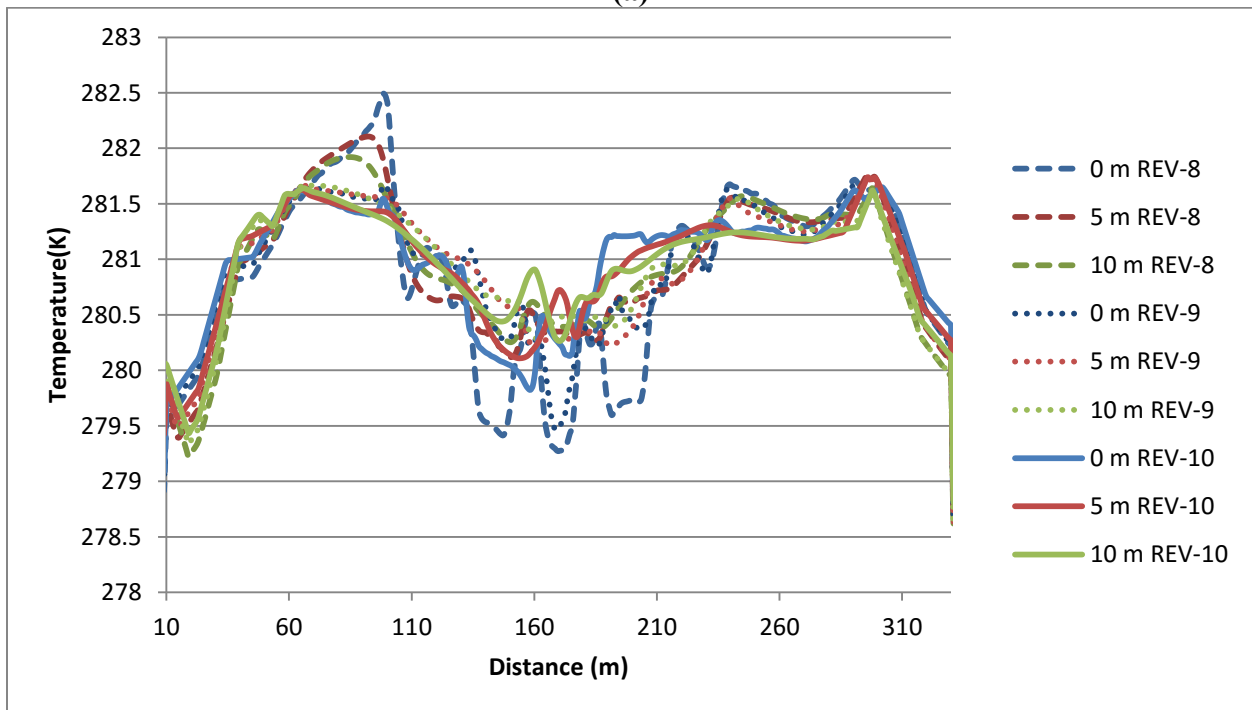
It is notable that, similar to Mica, the highest temperatures were noted when a single intake was operational as opposed to a combination of other intakes. There was not a significant difference in the outlet temperature simulated by the linear and the discrete stratification profiles at Revelstoke.

The variation in temperature upstream of Revelstoke Dam at the intakes elevation is outlined for the linear stratification scenarios as Figure 43 (a) and discrete scenarios as Figure 43 (b). It is notable that for all scenarios the temperature is increased in front of the intakes and that the impacts do not extend laterally across the entire reservoir width. Generally, for the linear scenarios, temperatures were greatest near the centre of the intakes, centered on intakes 3 and 4. In the discrete scenarios, the warmest temperatures were simulated near Intake 1 and 6. The variation in temperature parallel to the dam face at the intakes elevation is included in Figure 44. It is notable that the greatest variation in temperature laterally across the reservoir width is noticed nearest the dam face in all scenarios. Further away from the dam, while there are still minor variations in temperature, the peaks are not substantial.

For the discrete thermal stratification scenarios (REV-4, REV-8, REV-9 and REV-10) the discharge temperature can be estimated based on the ratio of flow from the hypolimnion to the total discharge through the facility ( $Q_2/Q_0$ ). This has been previously studied experimentally by Shammaa and Zhu (2010) and Islam and Zhu (2015). Based on the simulated temperatures at Revelstoke, the  $Q_2/Q_0$  values for each of the four scenarios are 0.76, 0.69, 0.70 and 0.68 respectively. The scenarios studied by Shammaa and Zhu (2010) are fundamentally different than those at Revelstoke Dam as the dam has multiple intakes, therefore the results can only be directly compared for REV-10 where a single intake is operational. In this scenario, a critical height ( $h_c$ ) corresponding to the minimum vertical distance from the intake centre to the thermocline at which no withdrawal from the epilimnion will occur was calculated as 3.9 m based on Craya's (1949) formula. At this depth, the  $Q_2/Q_0$  is calculated theoretically as 0.70 by Shammaa and Zhu (2010) which agrees well with the current simulations. When the intakes are treated as single intakes (without taking into account superposition, the theoretical  $Q_2/Q_0$  values outlined by Shammaa and Zhu (2010) for REV-4, REV-8, REV-9 and REV-10 are 0.70, 0.63, 0.64 and 0.70 respectively. These values agree well with the numerical simulations in this study. Alternatively, if the discharges are lumped together as a single point sink, the theoretical  $Q_2/Q_0$  values for each of the scenarios are 0.62, 0.70, 0.70 and 0.70 respectively. This indicates that this assumption is not valid for simulating multiple point sinks, and does not accurately reflect the flow field upstream of Revelstoke Dam. It also indicates that the intakes are well represented as a series of point sinks. There is little effect of superposition on the outlet temperatures and  $Q_2/Q_0$  values when multiple intakes are operational for the scenarios investigated.



(a)



(b)

**Figure 43: Temperature upstream of dam face (a) Linear stratification scenarios; (b) Discrete stratification scenarios.**

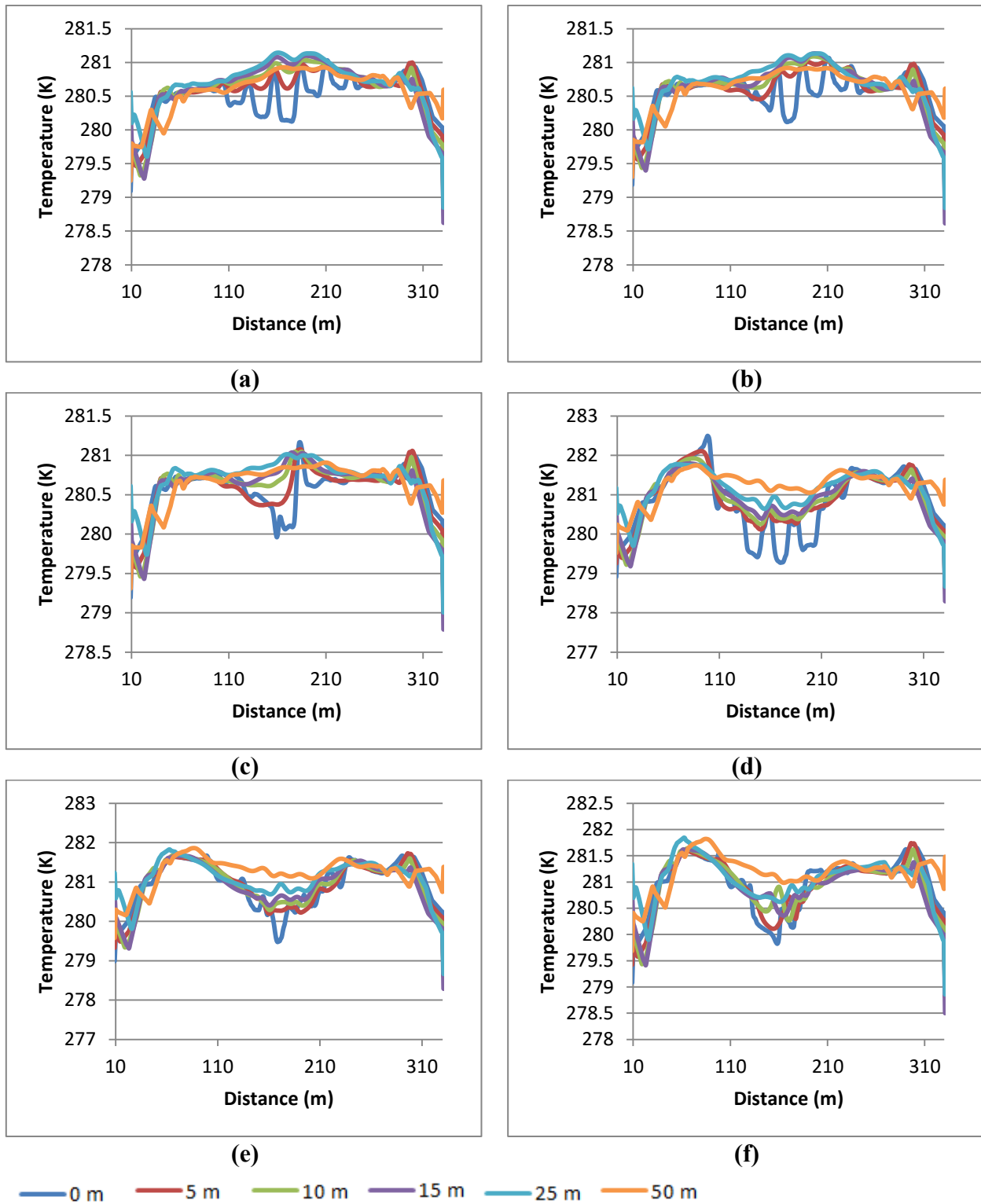


Figure 44: Temperature upstream of dam face (a) REV-5; (b) REV-6; (C) REV-7; (d) REV-8; (e) REV-9; (f) REV-10.

#### ***4.4.4 Fish Entrainment Risk***

To evaluate the potential impact on fish entrainment risk of thermal stratification, the concept of entrainment risk zones as developed in Chapter 3 were evaluated. The entrainment risk zones are outlined by the volume of the reservoir exceeding a given threshold velocity. For the purpose of the current study, threshold volumes of 0.15, 0.25, 0.50 and 1.00 m/s were evaluated. For each of the operational conditions analyzed noted that for the higher threshold velocities there was little impact on entrainment risk zone between isothermal and thermally stratified scenarios. At Mica Dam, the entrainment risk volume increase by including thermal stratification into the model was less than 4 % for the 1.00 m/s threshold. For the 0.50 m/s threshold, the entrainment risk volume was increased by between 12-19 % when thermal stratification was included. For the 0.25 and 0.15 m/s threshold the entrainment risk volume was substantially increased, by between 180-685 % and 410-760 % respectively.

This indicates that the volume of the reservoir that is occupied by velocities exceeding these thresholds is greatly increased during the later summer and fall months. It also demonstrates the importance of including thermal stratification in model simulations when evaluating fish entrainment risk for these time periods. There is little impact on the entrainment risk zone for larger fish, with swimming capabilities exceeding the larger threshold values. Smaller fish, such as juveniles, which have lower threshold swimming capabilities, have greatly increased entrainment risk during thermally stratified scenarios.

The distinct increase in velocity gradient in the vertical direction that is established under thermally stratified scenarios due to surficial water moving at a much lower velocity than the

---

deeper water below the thermocline may act as a deterrent to fish entrainment. Enders et al. (2012) noted that for salmonids, velocity gradients were one of the hydraulic parameters that were detectable by fish in altered flows. As many salmonid species in Kinbasket, including Bull trout and Kokanee, are generally surface oriented fish, detection of increased velocity gradient with respect to depth may induce an evasive response in fish being drawn towards the intakes. It has been previously noted that the majority of entrainment events at Mica Dam only occur during the winter months when the reservoir is isothermal and the vertical velocity gradients are less substantial.

At Revelstoke Dam, a similar analysis was performed comparing scenarios REV-1, REV-3 and REV – 4 to the isothermal scenario (REV-2). For the 1.00 m/s threshold there was a marginal increase in entrainment zone of less than 0.7 % in volume for each of the scenarios. For the 0.50 m/s threshold this was increased to less than 3.5 % in each of the scenarios. There was a more substantial increase for the 0.25 and 0.15 m/s threshold, at 24-28 % and 61-80 % respectively. This is similar to the results obtained for Mica Dam. The entrainment volume for smaller fish (i.e. juvenile fish) and weaker swimmers is greatly increased when thermal stratification is included in the model. The simulated difference in isovolume compared to isothermal conditions at Mica Dam were more substantial than those at Revelstoke.

The impact of thermal stratification on entrainment risk zone was much larger at Mica Dam than at Revelstoke Dam. The proximity of the intakes at Mica Dam (bottom oriented) as opposed to Revelstoke's intakes (mid-water column) to the boundaries of the reservoir results in a much larger impact on entrainment volume for all of the velocity thresholds.

At Revelstoke Dam, the entrainment risk volumes are presented in Table 9. For both the discrete stratification and linear stratification scenarios there was little change to entrainment risk volume by adjusting the flow distribution through the intakes (at the same total discharge) for the 0.15 and 0.25 m/s velocity thresholds. The impact however was substantial for the higher velocity thresholds (0.50 and 1.00 m/s).

**Table 9: Revelstoke Dam entrainment risk volumes (m<sup>3</sup>).**

Scenario	0.15 m/s	0.25 m/s	0.50 m/s	1.00 m/s
<b>REV-1</b>	407964	25380	7568	4149
<b>REV-2</b>	243209	20256	7342	4122
<b>REV-3</b>	391560	25129	7558	4150
<b>REV-4</b>	438304	25860	7595	4150
<b>REV-5</b>	36159	3382	2623	0
<b>REV-6</b>	35982	2806	1999	1477
<b>REV-7</b>	38374	2935	1207	687
<b>REV-8</b>	44843	3392	2631	0
<b>REV-9</b>	44615	2796	2000	1481
<b>REV-10</b>	47204	2971	1212	688

When evaluating fish entrainment risk for a facility the life stage of fish occupying the forebay of the dam must be taken into consideration in hand with the facility operation. At Revelstoke, the thermal stratification of the reservoir has the largest impact on the entrainment zone for juvenile fish with smaller threshold swimming capabilities. The flow distribution is more important for larger fish with larger threshold swimming capabilities. When a single unit is operating alone velocities exceed 2 m/s are present in some location of the reservoir (directly adjacent to the intake). These velocities are strong enough to entrain large fish, despite the volume of the risk zone being relatively small. By splitting discharge between multiple intakes, the peak velocity in the overall reservoir is reduced, which can eliminate hydraulic entrainment risk for large fish

species, such as the endangered White Sturgeon (*Acipenser transmontanus*) (not specifically present in the Mica or Revelstoke Reservoirs, but present at downstream facilities on the Columbia River).

#### **4.5 Conclusions**

In this study, the computational modelling developed in Chapter 3 was extended to evaluate the impact of the upstream thermal regime on the simulated flow field upstream of the dam. In general, similar results were noted at Mica and Revelstoke Dams. The impact of thermal stratification at Revelstoke was less pronounced than at Mica, due to the distance of the sidewalls and the bottom of the reservoir from the intakes. It can be concluded that thermal stratification is particularly important when there are boundaries located adjacent to the intakes and the complex geometry of the Mica forebay enhanced the impact of thermal stratification on the upstream flow field.

The results indicate that under thermally stratified conditions, the draw from the reservoir is restricted to the intakes depth, resulting in higher peak velocities in profiles greater than 10 m upstream of the facility. Thermally stratified flows also results in lower velocities at depths shallower than approximately 1-1.5 times the equivalent diameter of the intakes above the intakes. The peak velocities at the intakes elevation however, were between 1.5 and 2.1 times the peak velocities in an isothermal reservoir at Mica Dam and 0.4 to 1.8 times the peak velocities in and isothermal reservoir at Revelstoke Dam. Under all thermally stratified scenarios the maximum were shifted towards the surface towards the water surface (up to 10 m) when compared to isothermal conditions.

CFD modelling of alternative thermal stratification profiles indicated that reservoirs with a well-established, hyperbolic stratification profile is approximated well as a two-layered, or discrete stratification. In these scenarios, large discharges through Mica Dam resulted in a decrease in thermocline elevation approaching the dam face.

A linearly thermally stratified reservoir, such as Kinbasket Reservoir has a stratification profile that changes in shape approaching the dam face. The thermal structure of the reservoir that was measured to be linear at distances greater than 50 m upstream of the dam, developed a hyperbolic stratification profile at distances within 50 m of the dam face. For reservoirs with linear stratification profiles, such as Kinbasket Reservoir it may not be appropriate to approximate the reservoir using a hyperbolic or discrete stratification function, especially if the temperatures that are simulated by the model are of importance for the study.

For the Revelstoke simulations, where the impact of varying the discharge through each intake while maintaining the same total discharge through the dam was investigated, there was very little impact on varying discharge through the facility in either the linear or discrete thermal stratification scenarios. As anticipated there is slightly lower temperature variation when a single intake is operational (at a higher discharge, such as in scenarios REV-7 and REV-10, however the impact on outlet water temperature is within 0.2 degrees of the outlet temperature with 6 intakes operational (at lower discharge) in both thermal stratification scenarios. This indicates the total discharge, and proximity of the intakes to the thermocline is more important than the flow distribution between the intakes in terms of outlet temperature. The results were compared against the theoretical  $Q_2/Q_0$  values determined by Shammaa and Zhu (2010). These indicated that for the discrete thermal stratification scenarios, the numerical model accurately

represents the ratio of discharge from the hypolimnion to the overall discharges. It also showed that treating each intake as a single point sink and neglecting superposition provides a good approximation of the  $Q_2/Q_0$  ratio, and thus, the outlet temperature, when using the results of Shammaa and Zhu (2010).

The high risk volume for entrainment is greatly increased for smaller and juvenile fish at Revelstoke during the summer months when thermal stratification is present. Changing the distribution of flow through the intakes has little advantage in regards to reducing the entrainment volume for smaller fish. It does however have an impact on the entrainment volume for larger fish with greater swimming capabilities.

It was found that between the four different thermal stratification profiles used in the study, the velocity field generated closely matched for each of scenarios with the exception of the isothermal profile. This indicates that including thermal stratification is important for CFD models of reservoirs in the summer months. As collecting thermal stratification data is both time and cost prohibitive in some cases, the thermal stratification profile can be estimate based on regional meteorological data. Using a predicted thermal stratification profile will provide a better estimate of the reservoirs flow field than using an isothermal assumption. It should however be noted that there were larger discrepancies in the temperature values output in the model for linear, hyperbolic and discrete stratification scenarios. If the specific study requires knowledge of the temperature of the water throughout the forebay, it is recommended that measuring the thermal stratification profile, by thermistor chain, or a conductivity-temperature-depth sensor is completed.

Having knowledge of the thermal behaviour of a reservoir is important to understand upstream fish movement and entrainment risk. It also provides valuable information on the outlet temperature of the dam, which may result in downstream biological impacts and should be taken into account, specifically if the tailrace is located in close proximity to spawning grounds. In the study, it was noted that inclusion of thermally stratification in computational modelling consistently results in increased water temperatures at the outlets. This is most prominent in linearly stratified reservoirs where the phenomenon of selective withdrawal is less well established. As hydropower reservoirs are more likely to develop linear stratification profiles due their operations, it is particularly important to evaluate the impacts of hydropower operations on the downstream water temperatures. The method used in this study to perform CFD simulations including thermal stratification upstream of hydropower facilities is valuable tool for engineers, biologists and managers as it allows for the proactive investigation of the impact of hydropower generation operation on both the hydraulic and thermal structures of upstream and downstream habitat.

#### **4.6 Acknowledgements**

I would like to thank the late Mr. Paul Higgins and Mr. Alf Leake of BC Hydro for providing information used in the completion of this study. Additionally I would like to thank Ms. C. Beth Robertson, Mr. Chris Krath, Mr. Pierre Bourget and Ms. Beth Manson for assistance in the collection of field data. Funding for this research was provided by the Natural Sciences and Engineering Research Council of Canada (NSERC), NSERC Hydronet as well as Engineers Canada and Manulife Financial.

#### 4.7 References

Anohin, V.V., Imberger, J., Romero, J.R., and Ivey, G.N. (2006). “Effect of long internal waves on the quality of water withdrawn from a stratified reservoir.” *Journal of Hydraulic Engineering - ASCE*, 132(11), 1134-1145.

BC Hydro (2006a). “Mica Dam Entrainment Risk Screening”, BC Hydro, Report No. E487.

BC Hydro (2006b). “Revelstoke Dam Entrainment Risk Screening” Report No. E486, Rev. 1.  
Prepared for Generation.

BC Hydro Report. (1997a). “Summary of Water Temperature Monitoring and Studies.”

Bhuyian, F. and Zhum, D.Z. (2009). “Computation Fluid Dynamics Modeling of Flow Pattern Induced by Hydropower Intakes in Revelstoke and Mica Dams”. Report submitted to BC Hydro.

Biosonics (2011). “MCA/REV FESMON#2 Revelstoke Reservoir Kokanee Behaviour and Entrainment Rate Assessment”. Interim Report: 10-87057-002. Submitted to BC Hydro.

Bray, K., Sebastian, D., Weir, T., Pieters, R., Harris, S., Brandt, D., Vidmanic, L. (2013). “Kinbasket and Revelstoke Reservoirs Ecological Productivity and Kokanee Population Monitoring 2008 – 2010 Synthesis Report. BC Hydro Reference No. CLBMON-2 and CLBMON-3.

Caliskan, A. and Elci, S. (2009). “Effects of selective withdrawal on hydrodynamics of a stratified reservoir.” *Water Resources Management*, 23, 1257-1273.

- Casamitjana, X., Serra, T., Colomer, J., Baserba, C., and Perez-Losada, J. (2003). “Effects of the water withdrawal in the stratification patterns of a reservoir.” *Hydrobiologia*, 504, 21-28.
- Craya, A. (1949), “Theoretical research on the flow of nonhomogenous fluids”, *La Houille Blanche*, 4, 44-55.
- Enders, E.C., Gessel, M.H., Anderson, J.J., & Williams, J.G. (2012). “Effects of decelerating and accelerating flows on juvenile salmonid behavior”, *Transactions of the American Fisheries Society*, 141(2), 357-364.
- Fischer, H.B., List, E.J., Koh, R.C.Y., Imberger, J., Brooks, N.H. (1979). “Mixing in Reservoirs.” *Mixing in Inland and Coastal Waters*, Academic Press Inc., San Diego CA. p.150 – 228.
- Islam, M.R. and Zhu, D.Z. (2015). “Selective withdrawal in two-layer stratified flows”, *Journal of Hydraulic Engineering*, 141(7) , 04015009.
- Langford, M.T., Zhu, D.Z., Leake, A. and Cooke, S. (2015). “Hydropower Intake-induced Fish Entrainment Risk Zone Analysis”, submitted to *ASCE Journal of Hydraulic Engineering*.
- Prigo, R.B., Manley, T.O., and Connell, B.S.H. (1995). “Linear, one-dimensional models of the surface and internal standing waves for a long and narrow lake.” *American Journal of Physics*, 64(3), 288-300.

RL&L Environmental (1997). “Hugh L. Keenleyside Dam Water Temperature Monitoring 1996”, RL&L Environmental Services Ltd., Edmonton, AB.

Robertson, C.B. (2012). “Forebay Thermal Dynamics at Hydropower Facilities on the Columbia River System”. M.Sc. Thesis, University of Alberta.

Shammaa, Y. and Zhu, D.Z. (2010). “Experimental study on selective withdrawal in a two-layer reservoir using a temperature-control curtain.” *Journal of Hydraulic Engineering - ASCE*, 136(4), 234-246.

Vidal, J., Casamitjana, X., Colomer, J., Serra, T. (2005). “The internal wave field in Sau reservoir: Observation and modeling of a third vertical mode.” *Limnology and Oceanography - ASLO*, 50(4), 1326-1333.

Wiegand, R.C. and Chamberlain, V. (1987). “Internal waves of the second vertical mode in a stratified lake.” *Limnology and Oceanography - ASLO*, 32(1), 29- 42.

Wood, I. R. (2001). “Extensions to the theory of selective withdrawal.” *J. Fluid Mech.*, 448, 315–333.

## **Chapter 5**

### **Conclusions and Recommendations**

---

#### **5.1 General Conclusions**

Fish entrainment at hydropower facilities has been gaining attention over previous years by both hydropower operators and regulators. The operation of hydropower facilities has an impact on the upstream flow field, thermal structure and erosion and sedimentation patterns in the upstream reservoir. This drastically changes the habitat adjacent to the intakes which may put resident fish at risk of entrainment. This thesis is focused on increasing our knowledge of the flow field induced by hydropower operations and providing methodologies for assessing the hydraulic influence of the facilities both in the field as well as using computational fluid dynamic

modelling. This thesis is specifically focused on the application of this understanding of the flow field and thermal structure developed by operational hydropower facilities to assessing impacts on aquatic habitat. General conclusions for this thesis are summarized below.

Chapter two investigated the impact of hydropower operations on the flow field upstream of a run-of-the-river hydropower development. At Aberfeldie Dam, both a detailed field study and a CFD modelling study were completed. Aberfeldie Dam has a relatively shallow headpond which results in higher velocities than are generally noted at larger facilities that maintain an upstream reservoir. A relatively large scour hole has formed upstream of the dam immediately adjacent to the intakes. The shear stress induced on the bed at this facility is varied seasonally based on the amount of discharge through the headpond. During high discharge during spring freshet, the bed shear stress is increased above the critical shear stress which will erode away the bed. There is a corresponding increase in scour hole size in these conditions. During low flows, when clear water conditions prevail, the bed shear stress is lower than the critical shear stress and sediments will fall out of suspension in-filling the reservoir. It is anticipated that annually the headpond is in dynamic equilibrium and the average bed shear stress across the headpond is approximately 0.8 Pa. The CFD model was used to determine that there is a potential of 0.20 m annual fluctuation in the average bed elevation at this facility based on the simulated bed shear stresses. The scour hole generated by the facility was compared against laboratory measurements for intakes on a flat bed, achieving similar results and indicating the form of the scour hole may not be sensitive to flow field. The scour hole at Aberfeldie Dam includes a refuge zone for fish adjacent to the risky zone. This slow moving, recirculating flow field serves as an attractant to

fish, particularly during the winter. CFD is a promising tool for assessing the impact of developing habitat compensation measures by targeted dredging and/or built-in groins.

Chapter three involved completion of challenging field measurements and CFD modelling at Mica Dam, a high head, high discharge facility on the Columbia River. This particular facility, which impounds a large reservoir for both flood protection and hydropower storage, has a drastically varying water surface elevation of the course of the year. The reservoir is drawn down in the fall and winter and fills during the spring and summer. The flow field induced by the dams operations has significant annual variation with the highest velocities observed at low pool. The bottom orientation of the outlets and adjacent wing walls on the dam face creates a unique scenario where a vortex is formed adjacent above the east-most intake. The velocity field induced by the dam indicates that within 15 m of the dam face, the flow field is best represented as a series of point sinks. Greater than 15 m upstream of the dam, the flow field can be approximated as a line sink. The results generated by the CFD model were compared to those obtained using a potential flow solution. The potential flow solution can be used to identify the distance upstream of the dam where uniformity is achieved for the bottom oriented intakes. The flow field simulated by the CFD model indicated that the turbulent kinetic energy was very low in the forebay and was not likely to serve as a deterrent for resident fish. The high risk volume for entrainment increases exponentially with decreasing threshold swimming capability. As such, weaker swimmers, including small and juvenile fish as well as anguilliform swimmers, are of much higher risk for entrainment than larger, stronger swimmers. When the reservoir is drafting, and the highest entrainment volumes are noted; small fish are at greatest risk of entrainment, while the dam poses very little risk of entrainment to larger fish. These

observations parallel those made by a telemetry study of Bull trout in the forebay. In addition to fish swimming capability, location within the water column, and seasonal use of the forebay play an important role in assessing fish entrainment. Therefore the actual entrainment through hydropower turbines involves both physical hydraulics and behavioral ecology.

Chapter four extended the modelling that was completed in Chapter three to evaluate the impact of seasonal thermal stratification on the flow field and thermal structure of the forebays at Mica Dam and Revelstoke Dam. This chapter investigated the impact of reservoir level, intake orientation with respect to the reservoir bottom, varied thermal stratification profile and operational mode on the physical hydraulics of the forebays and relates it to fish entrainment risk. The inclusion of thermal stratification in the simulations resulted in the discharge being somewhat restricted to the intakes elevation. This resulted in higher peak velocities from 1.5 to 2.1 times higher for bottom oriented outlets and 0.4 to 1.8 times higher for mid-depth oriented outlets for distances greater than 10 m upstream of the dams. In thermally stratified scenarios, the peak velocities at greater than 10 m upstream skewed upwards by up to 10 m towards the water surface when compared to isothermal conditions.

Varying the thermal stratification profile indicated that approximating a well-developed hyperbolic stratification profile as a two-layer discrete profile, as has been done in both laboratory and numerical simulations previously, is a valid assumption. This assumption however, is not valid for linearly stratified reservoirs, especially if temperature is of importance for the study (such as in fisheries studies). For all simulations the inclusion of thermal stratification has a substantial impact on the outlet temperature of discharge through the dam. Despite having a greater depth, this was more prominent at Mica Dam due to the bottom

orientation of the outlets. The discharge temperature through the dam in discrete two-layer stratification scenarios were compared against analytical values that have previously been developed. The proportion of flow from the epilimnion and hypolimnion matched well with previously reported values, validating the use of CFD to investigate selective withdrawal in hydropower reservoirs. The entrainment volume is greatly increased for smaller and juvenile fish when thermal stratification is included in the model (compared to isothermal conditions). Redistributing the discharge through multiple intakes has little impact on the entrainment volume for smaller fish, however does impact the entrainment volume for larger fish with greater swimming capability.

The velocity field generated by the CFD model closely matched for each of the thermal stratification profiles investigated (when compared to isothermal conditions) indicating that it is important to include thermal stratification when modelling reservoirs during summer months. Using a predicted thermal stratification profile, estimated from meteorological conditions, will provide a better estimate of the flow field when compared to using an isothermal assumption. If the temperature structure through the reservoir is of interest for a particular study, measurements of the thermal profile by thermistor chain or conductivity-temperature-depth sensor is recommended as the temperature structure was more sensitive to the thermal profile than the velocity field in this study.

## **5.2 Recommendations for Further Research**

There are numerous opportunities to extend the research that has been developed to further our knowledge about modelling the flow field induced by hydropower facilities, including its impact on bed morphology and fish entrainment risk. Additional opportunities exist to broaden our

understanding of thermally stratified flows and how they can be modelled. Some of these include:

Including morphodynamics in the CFD modelling for run-of-the-river projects to develop a more detailed understanding of how these reservoirs operate on an annual basis. This will provide further information on the dynamics of erosion and sedimentation and bed form deformation which provides valuable information to direct operations and dredging. The analysis of sediment deposition and erosion potential developed in this thesis does not take into account properties such as cohesion. The erodibility of specific sediments based on composition and simulated bed shear stress could be evaluated in more detail.

It was noted that actual fish entrainment is not only a function of the physical hydraulics of the forebay, but also the behavioral ecology of those fish occupying the habitat adjacent to the dams. Combining fish movement, and blood chemistry (indicative of stress) datasets with the knowledge developed in this thesis will provide important information on the hydraulic characteristics that impact fish entrainment and/or avoidance of hydropower outlets.

Using CFD to understand the implication of thermal stratification on the flow field and thermal structure upstream of both point sinks and lines sinks should be studied further. The study that was completed for this thesis strongly indicates that the inclusion of thermal stratification when modelling reservoirs in the late summer and early fall months is necessary.

## References

---

- Amaral, S. V., Hecker, G. E., and Dixon, D. A. (2011). “Designing leading edges of turbine blades to increase fish survival from blade strike,” *EPRI-DOE, Conference on Environmentally-Enhanced Hydropower Turbines*, WA.
- Anohin, V.V., Imberger, J., Romero, J.R., and Ivey, G.N. (2006). “Effect of long internal waves on the quality of water withdrawn from a stratified reservoir.” *Journal of Hydraulic Engineering - ASCE*, 132(11), 1134-1145.
- Atkinson, E. (1996). “The Feasibility of Flushing Sediment from Reservoirs”, Report ID 137. HR Wallingford.
- Barnthouse, L.W. (2013). “Impacts of entrainment and impingement on fish populations: A review of the scientific evidence”. *Environ. Sci. Policy* 31: 149–156. Elsevier Ltd. doi: 10.1016/j.envsci.2013.03.001.
- Basson, G. R., & Olesen, K. W. (1997). “Modelling flood flushing”. *International Water Power & Dam Construction*, 49(6), 40-41.
- BC Hydro (2006). “Fish entrainment risk screening and evaluation methodology”, BC Hydro, Report No. E478.
- BC Hydro (2006). “Mica Dam Entrainment Risk Screening”, BC Hydro, Report No. E487.

BC Hydro (2006). “Revelstoke Dam Entrainment Risk Screening” Report No. E486, Rev. 1.

Prepared for Generation.

BC Hydro Report. (1997). “Summary of Water Temperature Monitoring and Studies.”

Bhuyian, F. and Zhu, D.Z. (2009). “Computation Fluid Dynamics Modeling of Flow Pattern Induced by Hydropower Intakes in Revelstoke and Mica Dams”. Report submitted to BC Hydro.

Biosonics (2011). “MCA/REV FESMON#2 Revelstoke Reservoir Kokanee Behaviour and Entrainment Rate Assessment”. Interim Report: 10-87057-002. Submitted to BC Hydro.

Bray, K. (2010). “Kinbasket and Revelstoke Reservoirs Ecological Productivity Monitoring – Progress Report Year 1.” *Columbia River Project Water Use Plan*, BC Hydro, Revelstoke, B.C.

Bray, K. (2011). “Kinbasket and Revelstoke Reservoirs Ecological Productivity Monitoring – Progress Report Year 2.” *Columbia River Project Water Use Plan*, BC Hydro, Revelstoke, B.C.

Bray, K. (2012). “Kinbasket and Revelstoke Reservoirs Ecological Productivity Monitoring – Progress Report Year 3.” *Columbia River Project Water Use Plan*, BC Hydro, Revelstoke, B.C.

Bray, K., Sebastian, D., Weir, T., Pieters, R., Harris, S., Brandt, D., Vidmanic, L. (2013). “Kinbasket and Revelstoke Reservoirs Ecological Productivity and Kokanee Population

Monitoring 2008 – 2010 Synthesis Report. BC Hydro Reference No. CLBMON-2 and CLBMON-3.

Bryant, D. B., Khan, A. A., & Aziz, N. M. (2008). "Investigation of flow upstream of orifices". *Journal of Hydraulic Engineering*, 134(1), 98-104.

Caliskan, A. and Elci, S. (2009). "Effects of selective withdrawal on hydrodynamics of a stratified reservoir." *Water Resources Management*, 23, 1257-1273.

Casamitjana, X., Serra, T., Colomer, J., Baserba, C., and Perez-Losada, J. (2003). "Effects of the water withdrawal in the stratification patterns of a reservoir." *Hydrobiologia*, 504, 21-28.

CFX (2009). "ANSYS CFX solver theory guide", Release 12.0, ANSYS Inc., PA 15317.

Coutant, C.C., Whitney, R.R. (2000). "Fish behaviour in relation to passage through hydropower turbines: a review". *Transactions of the American Fisheries Society*, 129(2), 351-380.

Craya, A. (1949). "Theoretical research on the flow of nonhomogenous fluids", *La Houille Blanche*, 4, 44-55.

Csiki, S., Rhoads, B.L. (2010). "Hydraulic and Geomorphological Effects of Run-of-the-River Dams." *Progress in Geomorphology*. 34(6). Pages 755-780.

Enders, E.C., Gessel, M.H., Anderson, J.J., & Williams, J.G. (2012). "Effects of decelerating and accelerating flows on juvenile salmonid behavior", *Transactions of the American Fisheries Society*, 141(2), 357-364.

EPRI (1992). Fish entrainment and turbine mortality review and guidelines. Stone & Webster Environmental Service, Boston, Massachusetts. .

Fathi-Moghadam, M., Emamgholizadeh, S., Bina, M., Ghomeshi, M. (2010). “Physical modelling of pressure flushing for desilting of non-cohesive sediment.” *Journal of Hydraulic Research*, 48(4), 509-514.

Fischer, H.B., List, E.J., Koh, R.C.Y., Imberger, J., Brooks, N.H. (1979). “Mixing in Reservoirs.” *Mixing in Inland and Coastal Waters*, Academic Press Inc., San Diego CA. p.150 – 228.

Fraleley, J., Sheppard, B. (2005). “Age, growth, and movements of westslope cutthroat trout, *Oncorhynchus clarki lewisi*, inhabiting the headwaters of a wilderness river”. *Journal of Northwest Science*, 79(1), 12-21.

Francois, M., Vinh, P., and Mora, P. (2000). “Fish friendly kaplan turbine,” "*Proceedings of the 20th IAHR Symposium on Hydraulic Machinery and Systems*", Charlotte, NC, Paper No. ENV-03.

Goodwin, R.A. (2004). “Hydrodynamics and juvenile salmon movement behavior at Lower Granite Dam: decoding the relationship using 3-D space-time (Cel Agent IBM) simulation”. Ph.D. Thesis, Cornell University.

Goodwin, R.A., Nestler, J.M., Anderson, J.J., Weber, L.J., and Loucks, D.P. (2006). “Forecasting 3-D fish movement behavior using a Eulerian–Lagrangian–agent method (ELAM)”. *Ecol. Modell.* 192: 197–223. doi: 10.1016/j.ecolmodel.2005.08.004.

Harvey, H.H., Bothern, C.R. (1972). “Compensatory swimming in the kokanee and sockeye salmon *Oncorhynchus nerka* (Walbaum)”, *Journal of Fish Biology*, 4, 237-247

Huang, B., Zhu., D.Z., Shao, W., Fu, J.J., Rui, J.L. (2014). “Forebay Hydraulics and Fish Entrainment Risk Assessment Upstream of a High Head Dam in China”, *Journal of Hydro-environment Research*, in press, DOI: 10.1016/j.jher.2014.03.002

Google. (2015). Google Maps, <<http://www.maps.google.com>> (August 29, 2015).

Guo, S., Shao, Y., Zhang, T.Q., Zhu, D.Z., Zhang, Y.P. (2013). “Physical modeling on sand erosion around defective sewer pipes under the influence of groundwater”, *Journal of Hydraulic Engineering*, 139(12), 1247–1257.

Islam, M.R. and Zhu, D.Z. (2015). “Selective withdrawal in two-layer stratified flows”, *Journal of Hydraulic Engineering*, 141(7) , 04015009.

Jacobson, P. (2011). “Fish Passage through Turbines: Application of Conventional Hydropower Data to Hydrokinetic Technologies,” Electric Power Research Institute (EPRI), Palo Alto, CA, Final Technical Report No. 1024638.

Johnson, G.E., Dauble, D.D. (2006). “Surface Flow Outlets to Protect Juvenile Salmonids Passing Through Hydropower Dams.” *Reviews in Fisheries Science*, 14(3). Pages 213-244.

Julien, P. (2008). “Erosion and sedimentation”. Cambridge University Press, Cambridge, UK.

Katapodis, C., Gervais, R. (1991). “Ichthyomechanics”. Freshwater Institute, Central and Atlantic Region, Department of Fisheries and Oceans, Winnipeg, MB.

Katapodis, C. (1992). "Introduction to fishway design". Freshwater Institute, Central and Arctic Region, Department of Fisheries and Oceans Canada, Winnipeg, Manitoba. 70 pages.

Katapodis, C., Kells, J.A., Acharya, M. (2001). "Nature-like and conventional fishways: alternative concepts?", *Canadian Water Resources Journal*, 26(2), 211-232.

Katapodis, C., Williams, J.G. (2012). "The development of fish passage research in a historical context". *Ecological Engineering*, 48, 8-18.

Khan, L.A., Wicklein, E.A., Rashid, M., Ebner, L.L., and Richards, N.A. (2004). "Computational fluid dynamics modeling of turbine intake hydraulics at a hydropower plant", *Journal of Hydraulic Research*, 42(1), 61-69.

Khan, L.A., Wicklein, E.A., Rashid, M., Ebner, L.L., and Richards, N.A. (2008). "Case study of an application of a computational fluid dynamics model to the forebay of the Dalles Dam, Oregon.", *Journal of Hydraulic Engineering*, 134(5), 509-519.

Lai, J.-S., & Shen, H. W. (1996). "Flushing sediment through reservoirs". *Journal of Hydraulic Research*, 34(2) , 237-255.

Langford, M.T., Zhu, D.Z., Leake, A. and Cooke, S. (2015). "Hydropower Intake-induced Fish Entrainment Risk Zone Analysis", submitted to *ASCE Journal of Hydraulic Engineering*.

Liu, J., Minami, S., Otsuki, H., Liu, B., & Ashida, K. (2004). "Prediction of concerted sediment flushing". *Journal of Hydraulic Engineering* , 130(11), 1089-1096.

- Marcy, B.C., Jr., A.D. Beck and R.E. Ulanowicz. (1978). Effects and impacts of physical stress on entrained organisms. pp. 135-188. In: J.R. Schubel and B.C. Marcy, Jr., (eds.). *Power Plant Entrainment: A Biological Assessment*. Academic Press, NY.
- Martins, E. G., Gutowsky, L. F., Harrison, P. M., Patterson, D. A., Power, M., Zhu, D. Z., Cooke, S. J. (2013). "Forebay use and entrainment rates of resident adult fish in a large hydropower reservoir". *AQUATIC BIOLOGY*, 19(3), 253-263.
- Martins, E. G., Gutowsky, L. F., Harrison, P. M., Flemming, J. E. M., Jonsen, I. D., Zhu, D. Z., Cooke, S. J. (2014). "Behavioral attributes of turbine entrainment risk for adult resident fish revealed by acoustic telemetry and state-space modeling". *Animal Biotelemetry*, 2(1), 13.
- McPhail, J.D., Troffee, P.M. (1998). "The mountain whitefish (*Prosopium williamsoni*): a potential indicator species for the Fraser system", Department of Zoology, University of British Columbia, Vancouver, BC. Prepared for: Environment Canada, Report No. DOE FRAP 1998-16. 71 pages.
- Mesa, M.G., Welland, L.K., and Zydlewski, G.B. (2004). "Critical swimming speeds of wild bull trout". *Northwest Sci.* 78: 59–65.
- Meselhe, E.A., and Odgaard, A.J. (1998). "3D numerical flow model for fish diversion studies at Wanapum dam", *Journal of Hydraulic Engineering*, 124 (12), 1203-1214.
- Monten, E. (1985). "Fish and Turbines: Fish Injuries During Passage Through Power Station Turbines," Norstedts Tryckeri, Sweden, Report No. 549.

NHC (2005). “Aberfeldie redevelopment project, hydraulic model study, final report”, Northwest Hydraulic Consultants, 2005. Prepared for BC Hydro. 92 pages.

NPP (2005). “Fish entrainment and mortality study, Vol 1, Niagara Power Project”, New York Power Authority.

Powell, D.N, Khan, A. (2012). “Scour upstream of a circular orifice under constant head”.  
*Journal of Hydraulic Research* , 50(1), 28-34.

Powell, D.N., Khan, A. (2015). “Flow Field Upstream of an Orifice under Fixed Bed and Equilibrium Scour Conditions”, *Journal of Hydraulic Engineering*, 141(2), 04014076 1-8

Prigo, R.B., Manley, T.O., and Connell, B.S.H. (1995). “Linear, one-dimensional models of the surface and internal standing waves for a long and narrow lake.” *American Journal of Physics*, 64(3), 288-300.

Rakowski, C.L., Richmond, M.C., Serkowski, J.A., Ebner, L. (2002). “Three dimensional simulation of forebay and turbine intakes flows for the Bonneville project”, *Proc., of HydroVision 2002*, Oregon.

Rakowski, C.L., Richmond, M.C., Serkowski, G.E. Johnson (2006). “Forebay computational fluid dynamics modeling for the Dalles Dam to support behaviour guidance system siting studies”, Pacific Northwest National Laboratory. Richland, WA. 37 pages.

- Rakowski, C.L., Richmond, M.C., Serkowski, (2010). “Bonneville powerhouse 2 3D CFD for the behavioural guidance system”, Pacific Northwest National Laboratory. Richland, WA. 39 pages.
- Rakowski, C.L., Richmond, M.C., Serkowski, (2012). “Bonneville Powerhouse 2 guidance efficiency studies: CFD model of the forebay”, Pacific Northwest National Laboratory. Richland, WA. 104 pages.
- RL&L Environmental (1997). “Hugh L. Keenleyside Dam Water Temperature Monitoring 1996”, RL&L Environmental Services Ltd., Edmonton, AB.
- RL&L (2000). “Resident fish entrainment information review”, RL&L Information Services Ltd.
- Robertson, C.B. (2012). “Forebay Thermal Dynamics at Hydropower Facilities on the Columbia River System”. M.Sc. Thesis, University of Alberta.
- Sale, M. J., Cada, G. F., Rinehart, B. N., Sommers, G. L., Brookshier, P. A., and Flynn, J. V. (2000). “Status of the US Department of Energy’s advanced hydropower turbine systems program,” Proceedings of the 20th IAHR Symposium on Hydraulic Machinery and Systems, Charlotte, NC, Paper No. ENV-01.
- Schilt, C. R. (2007). Developing fish passage and protection at hydropower dams. *Applied Animal Behaviour Science*, 104(3), 295-325.
- Scott WB, Crossman EJ. (1998). Freshwater fishes of Canada. Galt House Publications, Oakville, ON

SEC (2014). "Routine Maintenance Dredging: Aberfeldie Dam, Bull Rive, B.C.", SEC Project No. 003-04.1, 19 pages.

Shammaa, Y., Zhu, D.Z., Rajaratnam, N. (2005). "Flow upstream of orifices and sluice gates." *Journal of Hydraulic Engineering*, 131(2), 127-133

Shammaa, Y. and Zhu, D.Z. (2010). "Experimental study on selective withdrawal in a two-layer reservoir using a temperature-control curtain." *Journal of Hydraulic Engineering - ASCE*, 136(4), 234-246.

Shen, H. W. (1999). Flushing sediment through reservoirs". *Journal of Hydraulic Research*, 37(6), 743-757.

Shields, I.A. (1936). "Application of similarity principle and turbulence research to bed-load movement". Translated by United States Department of Agriculture Soil Conservation Service Cooperative Laboratory, California Institute of Technology, Pasadena, California. By: Ott, W.P. and van Uchelen, J.C. 27 pages.

Solomon, D. J. (1988). "Fish Passage Through Tidal Energy Barrages," Energy Technical Support Unit, Harwell, U.K., Report No. ETSU TID4056.

Soulsby (1997). "Dynamics of marine sands", Thomas Telford Publications, Thomas Telford Services Ltd., Heron Quay, London.

Turnpenny, A. W. H., Clough, S., Hanson, K. P., Ramsey, R., and McEwan, D. (2000). "Risk Assessment for Fish Passage Through Small Low-Head Turbines," Energy Technical Support Unit, Harwell, U.K., Report No. ETSU H/06/00054/REP.

- USDT (2005). “Design of roadside channels with flexible linings”, Federal Highway Administration, United States Department of Transportation. 154 pages.
- Van Esch, B.P.M. (2012). “Fish Injury and Mortality During Passage Through Pumping Stations.” *Journal of Fluids Engineering*. 134(7). (9pages).
- Vidal, J., Casamitjana, X., Colomer, J., Serra, T. (2005). “The internal wave field in Sau reservoir: Observation and modeling of a third vertical mode.” *Limnology and Oceanography - ASLO*, 50(4), 1326-1333.
- Von Raben, K. (1964). “Regarding the Problem of Mutilations of Fishes by Hydraulic Turbines,” *Fisheries Research Board of Canada, Translation Series, No. 448*, [Die Wasserwirtschaft, 4 , 97-100 (1957)].
- Westslope Fisheries Ltd. (2012). BC Hydro Aberfeldie dam fish entrainment strategy Bull River fish entrainment – telemetry study. Prepared for BC Hydro. 94 pages.
- Wicklein, E.A., Khan, L.A., Rashid, M., Deering, M.K., and Nece, R.E. (2002). “A three dimensional computational fluid dynamics model of the forebay of Howard Hanson dam”, Washington, Proc., Hydro Vision 2002, Portland, Oregon.
- Wiegand, R.C. and Chamberlain, V. (1987). “Internal waves of the second vertical mode in a stratified lake.” *Limnology and Oceanography - ASLO*, 32(1), 29- 42.
- Wood, I. R. (2001). “Extensions to the theory of selective withdrawal.” *J. Fluid Mech.*, 448, 315–333.

Xue, W., Huai, W., Li, Z., Zeng, Y., Qian, Z., Yang, Z. (2013). “Numerical simulation of scouring funnel in front of bottom orifice,” *Journal of Hydrodynamics*, 25(3), 471-480.